UNDRAINED CREEP BEHAVIOR
OF ATCHAFALAYA CLAY
FROM CU DIRECT-SIMPLE SHEAR TESTS

by

CHARLES E. WILLIAMS

S.B., Massachusetts Institute of Technology

(1971)

Submitted in partial fulfillment

of the requirements for the degrees of

Master of Science and Civil Engineer

at the

Massachusetts Institute of Technology

May 1973

PART I

Signature of Author.....
Department of Civil Engineering,
May 11, 1973

Certified by.....
Thesis Supervisor

Accepted by.....
Chairman, Departmental Committee on Graduate
Students of the Department of Civil Engineering

ABSTRACT

TITLE: UNDRAINED CREEP BEHAVIOR OF ATCHAFALAYA CLAY FROM CU DIRECT-SIMPLE SHEAR TESTS

by

CHARLES E. WILLIAMS

Submitted to the Department of Civil Engineering on May 11, 1973 in partial fulfillment of the requirements for the degrees of Master of Science and Civil Engineer.

The creep behavior of normally consolidated and over consolidated samples of a highly plastic deltaic clay from the Atchafalaya Basin in Louisiana is investigated in consolidated-undrained direct-simple shear tests. From 49 to 95 percent of the undrained shear strength was applied over a typical period of one week in the stress controlled tests. The results of "single incremental" tests are compared to those in which the sample crept under several successive increments.

The rate process theory and other rheologic models for creep are reviewed and both undrained and drained creep data are summarized in light of the various theories, including those for creep rupture.

For initial shear stress increments below 85 percent of failure, the creep behavior of the clay follows the Singh-Mitchell rate process model after an initial transient pore pressure condition. For additional increments, the creep strain rate is initially very slow, but it changes with log time to eventually converge with the Singh-Mitchell model.

The creep rupture models of Saito and Singh-Mitchell were compared to laboratory creep rupture behavior and found reasonably acceptable for this clay. Creep strengths in terms of applied shear stress for a given consolidation stress were found to be 85 percent of that obtained from

conventional controlled strain $\overline{CK_oU}$DSS tests. This value would probably be lower if the creep process was allowed to continue for longer periods of time (greater than one week) to develop sufficient pore pressures for failure.

Thesis Supervisor: Charles C. Ladd

Title: Professor of Civil Engineering

ACKNOWLEDGEMENTS

The author expresses his sincere gratitude to the following:

Professor Charles C. Ladd, his thesis supervisor, whose guidance and thought provoking comments made this investigation possible;

Dr. Lewis Edgers, who suggested the topic and aided the author in all phases of the investigation;

Ms. Patricia Potter, who typed the manuscript;

The U.S. Army Corps of Engineers, Waterways Experiment Station, Vicksburg, Mississippi, whose financial support made this investigation possible.

TABLE OF CONTENTS

TABLE OF CONTENTS (Cont.)

TABLE OF CONTENTS (Cont.)

LIST OF TABLES

LIST OF FIGURES

LIST OF FIGURES (Cont.)

LIST OF FIGURES (Cont.)

LIST OF FIGURES (Cont.)

I INTRODUCTION

1.1 BACKGROUND

For the past fifty years a steadily increasing volume of water has been diverted from the Mississippi River into the Atchafalaya distributary. This is accomplished by means of a flood levee system within the Atchafalaya basin. Progressive siltation of the southern half of the basin along with the increased capacity requirements for the distributary have made it necessary to raise the flowline within the Atchafalaya floodway by means of levees.

Levee construction within the southern portion of the Atchafalaya Basin Floodway in south-central Louisiana has been in progress for more than thirty years (Kaufman and Weaver, 1967). Construction has proceeded in stages so that the thick deposits of soft alluvial and deltaic foundation clays can consolidate and achieve sufficient strength to support subsequent lifts of fill. This procedure has proved to be very time consuming and unsatisfactory. Moreover, settlements in excess of 10 to 15 feet have made it impossible to attain design heights (20 to 25 feet above the original grade) along

large portions of the floodway. Large lateral movements, thought to be caused by undrained shear deformations, yielding and creep of the soft foundation clays, have been a major contributor to the excessive vertical settlements of the levee crown.

In 1964-65 three extensively instrumented test sections were constructed along the East Atchafalaya Basin Protection Levee (EABPL) (Kaufman and Weaver, 1967; USCE, 1968). Test Section I, with a four foot crown and a height of six feet, had a design factor of safety of 1.1 based on a $\phi = 0$ analysis using UU triaxial compression test data. Test Sections II and III, with a wider crown, a height of ten feet, and wide stabilizing berms, had factors of safety of 1.1 and 1.3 based on similar total stress analyses.

Despite very large berms, both Test Sections II and III experienced very large lateral deformations with a resulting drop in the crest elevation, and for all practical purposes failed. These lateral shear deformations, which continued long after the end of construction, were particularly large between elevations -20 to -40 feet (original ground surface El. = 3-4 ft MSL). These large deformations are considered to be caused by undrained shear, which is the subject of separate investigations, and undrained creep.

Considering the fact that a substantial portion of the zone of large deformations (El. -20 to -40 ft) is approximated by a simple shear stress system, any detailed undrained creep investigation should attempt to duplicate this stress system. The subject of this report is undrained creep behavior of EABPL foundation clays with the direct-simple shear stress system.

1.2 DESCRIPTION OF EABPL FOUNDATION CLAYS

The site of the EABPL construction is composed of sand and gravels overlain by approximately 120 feet of clay which can be divided into three categories (Krinitzsky and Smith, 1969).

(1) Poorly drained backswamp deposit (El. -25 to +2 ft)

Presence of considerable organic matter with several inches to several feet of peat; dark gray to black in color; concretionary matter includes carbonates, sulphides and vivianite; soil is typically CH clay with $W_L = 110 \pm 30$.

(2) Well drained backswamp deposit (El. -120 to -25 ft)

Light to dark brown in color due to oxidation; stratification is absent due to reworking by plant roots; fissures due to dessication are common; soil is typically a CH clay with $W_L = 90 \pm 30$.

(3) Lake deposits

Deposited in shallow fresh water; gray in color mostly highly plastic CH clays with some silt and sand ($W_L = 95 \pm 25$); well defined layering with occasional silt and fine sand layers; presence of shells and carbonate concretions; well developed fractures and slickensides due to shear failures during deposition.

The area, which was originally level at El. +2 ft prior to levee construction, has the net overburden stress profile shown in Fig. 1-1 which was obtained from total weight and pore pressure measurements. Maximum past pressure profiles for offsets from the levee centerline indicate overconsolidated layers at elevations -45 to -65 ft and -70 to -100 ft (Fig. 1-2). These findings are also supported by field vane strengths and water content variations at these depths as shown in Figs. 1-3 and 1-4. These layers are probably overconsolidated due to drying of exposed backswamp deposits.

1.3 SCOPE OF RESEARCH

The experimental program involved obtaining representative samples of the clay in the zone of greatest levee foundation

deformations (El. -20 to -40 ft). A series of standard controlled strain Consolidated-Undrained Direct Simple Shear ($\overline{CK_oU}$ DSS) tests were conducted in order to establish a normalized shear strength versus overconsolidation ratio relationship. Subsequently, a program of constant load undrained creep tests were carried out with the Direct Simple Shear device in order to establish strain and strength relationships with stress, time and OCR.

The Singh-Mitchell Theory (see 2.1a and 2.2b) for creep strains and creep failure and Saito's creep rupture theory (see 2.2a) will be applied to the test results in order to evaluate their validity with the EABPL clay.

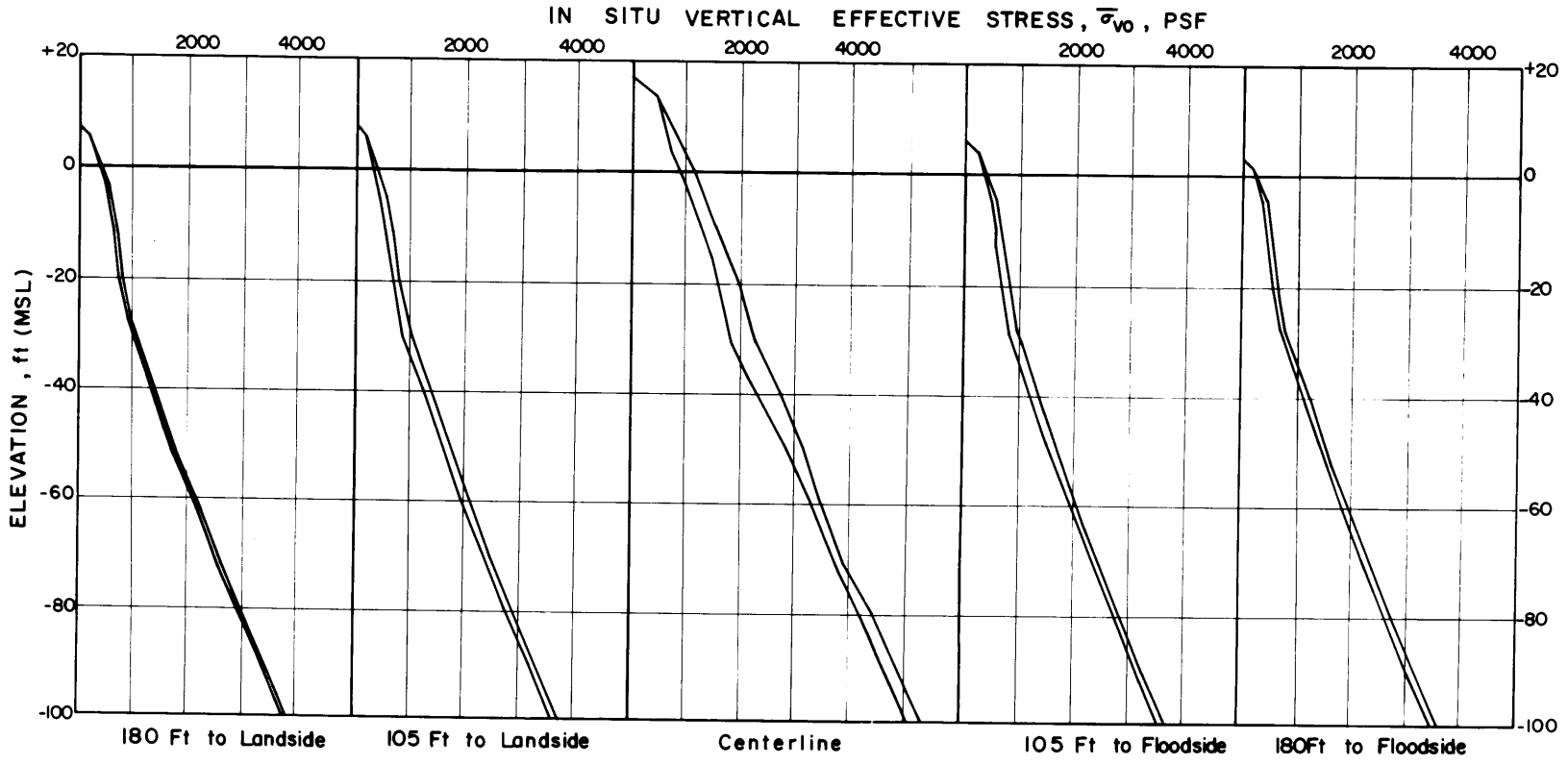

Pre-Construction Effective Vertical Stress Profiles, Test Sections II & III

Figure 1-1

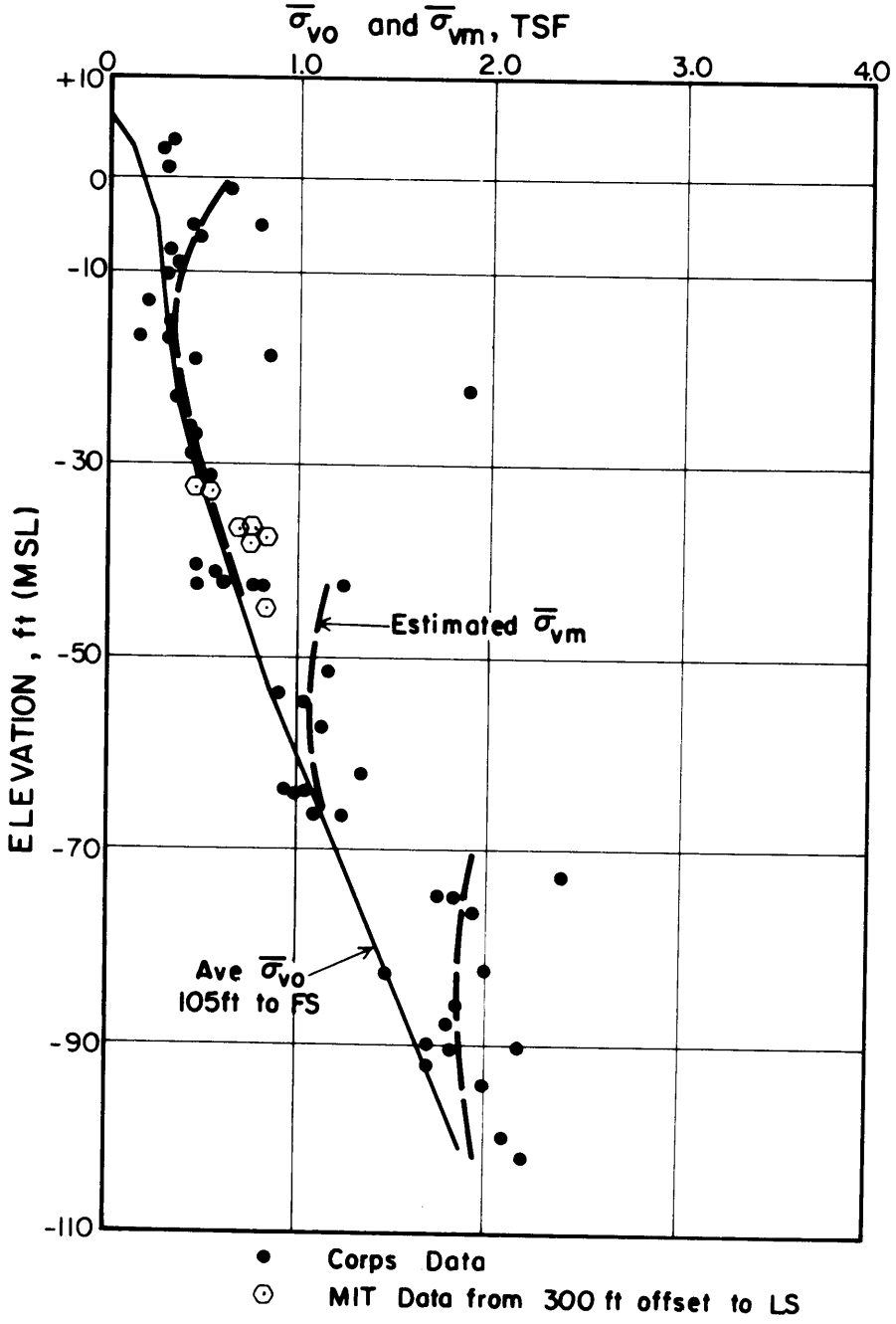

ESTIMATED MAXIMUM PAST PRESSURE, SECTIONS II AND III, 180 FT OFFSETS TO LS AND FS

Figure 1-2

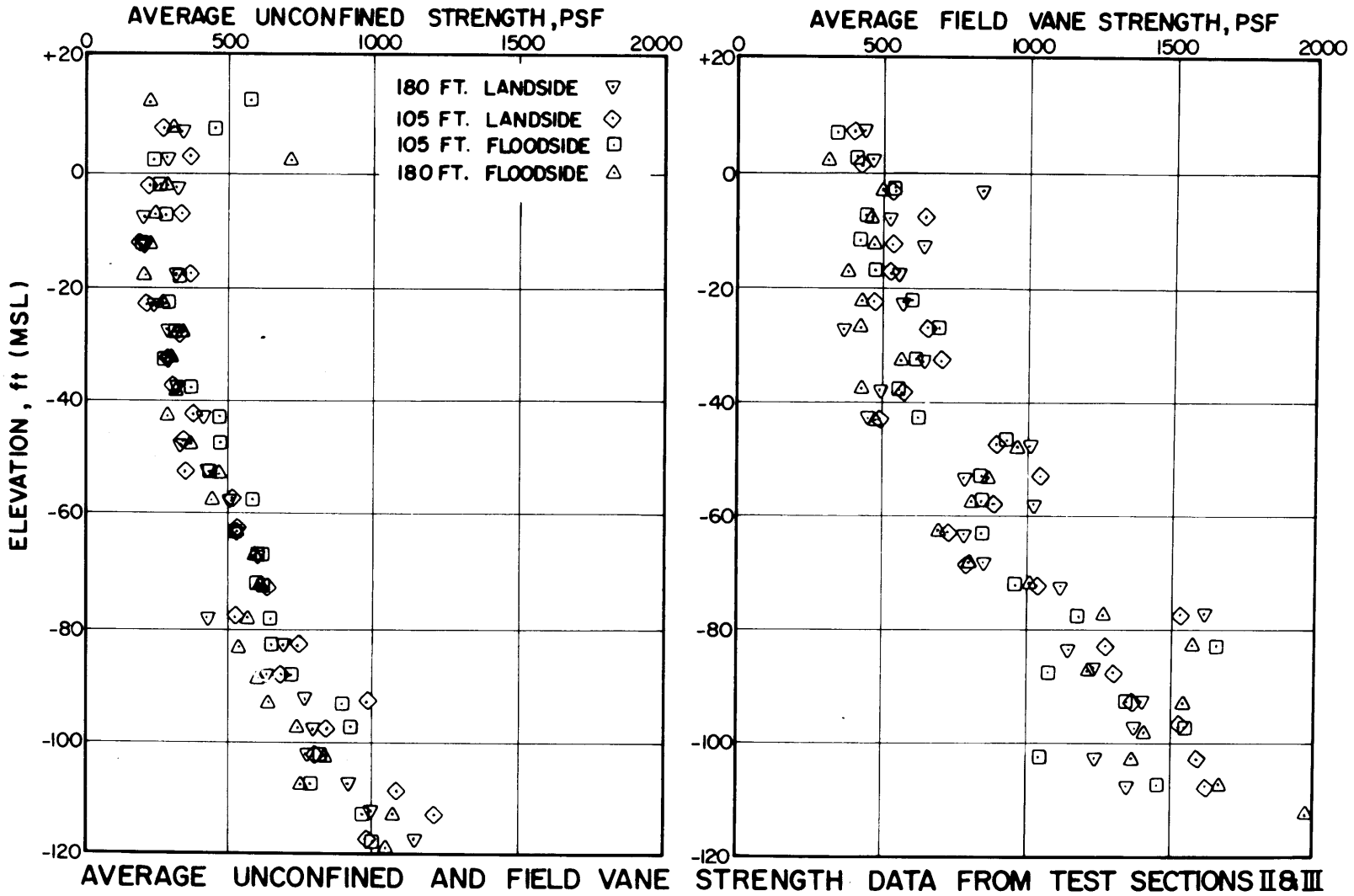
AVERAGE UNCONFINED STRENGTH, PSF
0
500
1000
1500
2000
+20
0
-20
-40
-60
-80
-100
-120
ELEVATION, ft (MSL)
180 FT. LANDSIDE
105 FT. LANDSIDE
105 FT. FLOODSIDE
180 FT. FLOODSIDE
AVERAGE FIELD VANE STRENGTH, PSF
AVERAGE UNCONFINED AND FIELD VANE STRENGTH DATA FROM TEST SECTIONS II & III

Figure 1-3

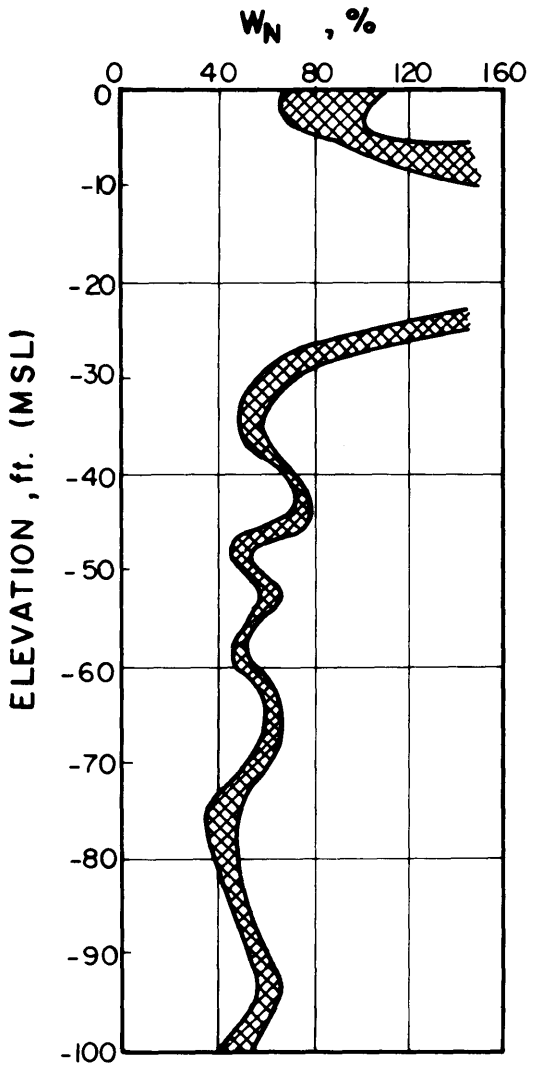

AVERAGE NATURAL WATER CONTENT
PROFILES FOR 105 FT & 180 FT OFFSETS
FOR SECTIONS II & III

Figure 1-4

II REVIEW OF CURRENT LITERATURE

The rate process theory and various rheologic models have been proposed to represent the creep behavior of soils. Creep behavior of particular concern are: strain and strain rate as functions of time, creep rupture (failure) phenomenon, and the effects of strain rate on the shear strength of soils. Several of the more pertinent publications dealing with this subject are reviewed in this section.

2.1 RATE PROCESS CREEP THEORY DEVELOPMENT

(a) Mitchell, Singh, et al

Singh, Mitchell and Campanella (1968) use Fig. 2-1 to describe soil deformations in terms of rate process theory. The theory considers the displacements of flow units as requiring a free energy of activation, ΔF, to surmount the energy barriers as shown in Fig. 2-1. Shear forces in the flow units, f, distort the energy barriers as indicated by curve B and cause preferential flow unit displacements in the direction of shear force. λ represents the distance between successive equilibrium positions and δ, the elastic distortion of the material structure.

The resulting theoretical expression for strain rate is:

$$\dot{\varepsilon} = 2X \frac{kT}{h} \exp\left(\frac{-\Delta F}{RT}\right) \sinh\left(\frac{F\lambda}{2kT}\right) \tag{1}$$

where k = Boltzmann's constant, T = absolute temperature, h = Planck's constant and R = universal gas constant. If $(f\lambda/2kT)$ is greater than one, which is generally the case for stresses sufficient to cause creep in soils, then:

$$\sinh\left(\frac{f\lambda}{2kT}\right) \approx 1/2 \exp\left(f\lambda/2kT\right) \tag{2}$$

and

$$\dot{\varepsilon} = X \frac{kt}{h} \exp\left(\frac{-\Delta F}{RT}\right) \exp\left(\frac{f\lambda}{2kT}\right) \tag{3}$$

"X" is a time and structure dependent parameter which is also dependent on the number of flow units in the direction of deformation and the average component of displacement in the same direction due to a single surmounting of the barrier.

To simplify analysis, Eq. (1) may be written as:

$$\dot{\varepsilon} = K(t)\sinh(\alpha D) \tag{4}$$

in which

$$K(t) = 2X(t) \frac{kT}{h} \exp\left[\frac{-\Delta F(t)}{RT}\right] \tag{4a}$$

and

$$\alpha D = \lambda F/2kT \tag{4b}$$

The authors present consolidated undrained creep data for remolded illite as shown in Fig. 2-2 which conforms to the form of the theoretical log $\dot{\varepsilon}/k$ versus αD relationships. For the range of stresses where the exponential approximation of strain rate is valid, Eq. (4) can be written as:

$$\dot{\varepsilon} = \frac{K(t)}{2} \exp(\alpha D) \tag{5}$$

and "α" can be evaluated from the slope of the straight line sections of the log $\dot{\varepsilon}$ versus D curves where D is the applied deviator stress:

$$\frac{d \log \dot{\varepsilon}}{dD} = \alpha \tag{6}$$

Figure 2-3 presents the typical relationship observed by the authors between log strain rate and log time and indicates that the following expression is possible.

$$\frac{K(t)}{2} = A\left(\frac{t_1}{t}\right)^m \tag{7}$$

where $m = \frac{d \log \dot{\varepsilon}}{d \log t}$ (7a)

and "A" is found by extending the log $\dot{\varepsilon}$ versus D line for t_1 to the value of D = 0 in Fig. 2-2. The resulting modifications yield the following equation for strain rate:

$$\dot{\varepsilon} = A\left(\frac{t_1}{t}\right)^m \exp\ (\alpha D) \tag{8}$$

A and α appear to be dependent on the particular test conditions, such as the stress system, while the authors claim that "m" is a material property which is only slightly influenced by test conditions. They further point out that m can be used as a "creep indicator" since low values of m ($m<1$) are found for clays that exhibit high creep strains, lower strength after creep and creep rupture under sustained loads. Values of m greater than unity are indicative of rapidly decreasing strain rates with time and decreasing $d\varepsilon/d \log t$ under subfailure conditions. The condition where m = 1 implies a constant value of $d\varepsilon/d \log t$ and long term strength equal to short term strength.

Strains are computed by integrating Eq. (8) over time, with knowledge of the strain at a known time; a necessary

condition. The equations for strain are as follows (Singh & Mitchell, 1968):

$$\varepsilon = a + \frac{A}{1-m} e^{\alpha D} (t)^{1-m} \qquad (m \neq 1) \qquad (9a)$$

where

$$a = \varepsilon_1 - \frac{A}{1-m} e^{\alpha D}$$

and

$$\varepsilon = \varepsilon_1 + Ae^{\alpha D} \ln t \qquad (m = 1) \qquad (9b)$$

The authors present laboratory data on London Clay, Osalsa Clay, Illite and San Francisco Bay Mud to support their theory and good agreement appears to be present for stress levels which are 30 to 90 percent of ultimate strength. The theory is rather flexible and can handle cases where strain and log time are either linearly or non-linearly related, which is an improvement over most rheologic models. However, the greatest advantage of this method is the comparative ease with which the creep parameters can be obtained in the laboratory.

This model will be called the Singh-Mitchell rate process model.

(b) Christensen and Wu (1964)

Another form of the rate process theory is presented by Christensen and Wu (1964). Clay deformations are described mathematically by the Kelvin-Maxwell model in Fig. 2-4. The spring K, represents the initial elastic response and the dashpot, the flow process, the spring K_2 models the bond strength at particle contacts which resists soil creep. The combination of springs K_1 and K_2 represent the initial elastic response of the soil.

From this rheologic model, the authors obtain the following expression:

$$u^* = 1 + \frac{1}{A} \ln \tanh \left[Z(t) + \tanh^{-1} \exp(-A)\right]$$

where

$$A = \frac{\sqrt{2}}{3} \alpha D \frac{K_1}{K_1+K_2}$$

$$Z(t) = \frac{1}{2} \alpha\beta \frac{K_1K_2}{K_1+K_2} t$$

$$U^* = \frac{\varepsilon_1-(\varepsilon_1)_o}{(\varepsilon_1)_\infty-(\varepsilon_1)_o} \qquad \text{(dimensionless strain)}$$

and α, β, K_1 and K_2 are soil parameters which can be determined from experimental creep results. $(\varepsilon_1)_o$ is the instantaneous axial strain, ε_1 is the axial strain at time, t, and $(\varepsilon_1)_\infty$ is the axial strain at large times.

The authors assume that creep stops at some large time after load application and a unique $(\varepsilon_1)_\infty$ is reached. Although this assumption may be true for soil with little creep tendency (m > 1 from Singh-Mitchell theory) it is not generally acceptable.

Two major drawbacks of this treatment of the creep process are:

(1) it only applies to soils with low creep potential (m > 1), of which the EABPL clay clearly is not one; and

(2) there are no established relationships between strain rate and time or strain rate and stress level.

(c) Murayama and Shibata (1961)

The authors use the Eyering rate process relationship to model soil creep. The theory is modified to account for a lower restraining resistance at particle bonds, below which movements are elastic and time independent. They arrive at the following:

$$\frac{d\varepsilon b}{dt} = Ab(\sigma-\sigma_o)\ \sinh\left(\frac{B_b\sigma_b}{\sigma-\sigma_o}\right) \qquad (1)$$

where

$$A_b = 2\lambda akT\ \exp\ \left(\frac{-E_o}{kT}\right) \qquad (2)$$

$$B_b = \frac{\lambda}{2bkT}$$

where K = Boltzmann's Constant

T = absolute Temperature

h = Planck's Constant

λ = average distance between unbalanced molecules

n = number of molecules wiht activation per unit length in the direction of stress

N = number of molecules with activation per unit area perpendicular to the direction of stress

σ_o = restraining resistance

E_o = free energy of activation

Strain equations are developed with the aid of a rheologic model as shown in Fig. 2-5 and result in:

$$\varepsilon = \frac{\sigma}{E_1} + \frac{(\sigma-\sigma_o)}{E_2} + \frac{(\sigma-\sigma_o)}{B_2E_2}\ \log\ \frac{A_2}{2}\ B_2E_2t \qquad (4)$$

(where $A_b + B_b$ from Eq. (1) are changed to A_2 and B_2) and:

$$\varepsilon_{t\to\infty} = \frac{\sigma}{E_1} + \frac{(\sigma-\sigma_o)}{E_2} \qquad (5)$$

These equations predict a linear variation of strain with log time, followed by a decrease in slope and the attainment of a constant ultimate value. They also point out that the above relations do not apply when an ultimate stress is reached which brings on failure. From laboratory results from long term anisotropic consolidation tests the authors report that $d\varepsilon/d \log t$ varies linearly with applied stress, which is in agreement with their equations, but in disagreement with Singh and Mitchell who find that $\log (d\varepsilon/dt)$ varies linearly with $\overline{D} = D/D_{max}$. The authors also report that long term undrained strength decreases linearly with the time to failure.

Although their theory development is straight forward and agreement between laboratory data and theory is obtained, the Murayama-Shibata relations do not appear to be as advanced as the work of Singh and Mitchell and therefore are not as useful.

(d) Shibata and Karube (1969)

Shibata and Karube mainly extend the work of Murayama &

Shibata and arrive at the same questionable conclusion that $\dot{\varepsilon}d = d\varepsilon/d \log t$ varies linearly with deviator stress (where $\dot{\varepsilon}d$ is deviatoric strain). While never stating whether they still believe that strain varies linearly with log time, they present the following empirical equation, which is in disagreement with the Singh-Mitchell model:

$$\dot{\varepsilon}_d = \text{Constant} \cdot \exp(B\sigma_d)$$

where B is a stress factor and σ_d is the deviator stress. They maintain that "B" is a function of overconsolidation ratio and that overconsolidated samples yield a steeper slope on a $\dot{\varepsilon}_d$ versus deviator stress plot.

Their most credible work has to do with creep strengths of clays. The authors state that there exists a yield value past which sufficient pore pressures are generated to produce undrained failure, or so-called "creep rupture". This relationship, which was developed completely empirically through laboratory observation, can best be shown by Fig. 2-6.

Although this effort is an improvement over the work of Murayama and Shibata, the same drawbacks still exist

and the equations concerning strain rate are questionable. Their section on creep strength is nevertheless definitely useful.

(e) Barden (1969)

Barden maintains that soil deformation is a function of stress ratio ($\bar{\sigma}_1/\bar{\sigma}_3$ or Singh-Mitchell's D/D_{max}). He separates the volumetric and deviatoric components of creep and by use of rate process and the rheologic models in Fig. 2-7, arrives at the following:

$$\nu = \nu_{FINAL} + \frac{2.3}{K\alpha} \log \left(\frac{\alpha\beta Kt}{2}\right)$$

$$\gamma = \gamma_{FINAL} + \frac{2.3}{G\alpha} \log \left(\frac{\alpha\beta Gt}{2}\right)$$

The volumetric strain and its corresponding equilibrium value are represented by ν and ν_{FINAL} and the shear distortion and its equilibrium value by γ and γ_{FINAL}. The parameters α and β are constants from the rheologic model and can be obtained in the laboratory. The strain rates follow directly from the above equations:

$$d\nu/d(\log t) = 2.3/K\alpha$$

$$d\gamma/d(\log t) = 2.3/G\alpha$$

where $K\alpha$ and $G\alpha$ are functions of the effective stress ratio.

Although Barden's laboratory data are completely from drained tests, he presents the undrained laboratory results of various investigations (including Singh and Mitchell) which in general support his equations.

Although Barden concludes that his theory is acceptable, he points out that during undrained creep, possible build up of pore pressures will change the effective stress ratio and thus, the strain rate. This problem can be bypassed by using the deviator stress. The main drawback of Barden's theory is that K and G are probably as difficult to obtain in the laboratory as E, the undrained Young's modulus.

(f) Bishop and Lovenbury (1969)

Bishop and Lovenbury conducted long term triaxial compression drained creep tests on London and Pancone clay. Using $\bar{D} = (\sigma_1-\sigma_3)/(\sigma_1-\sigma_3)_f$ of 17-98 percent, they conducted the tests until either failure was reached or problems with equipment developed (some of the tests were still in progress after three years).

Axial strain versus log time was approximately linear

for samples that did not fail and plots of log strain rate versus log time were approximately linear (London Clay data was especially good in this respect) as shown in Figs. 2-8 and 2-9. Sudden increases in strain rate at large times or "instabilities" which were accompanied by substantial volume decreases were unexplained although the authors maintain that these decreases were due to fundamental modifications in soil structure and not experimental error.

These excellent laboratory data lend great support to the Singh-Mitchell theory. Log strain rates vary approximately linearly with log time over large time periods and it is demonstrated that creep rupture can occur at stress levels less than full strength. The only real drawback in the paper are the instabilities which are yet to be explained.

2.2 CREEP RUPTURE

(a) Saito, et al (1961, 1965, 1969)

Saito and Vezawa (1961) conducted a series of unconfined and triaxial (CU) compression tests on a number of Japanese soils in an attempt to determine the range of stresses and elapsed times for which slow creep movements generate into failure. On the basis of these tests, the authors claim to have found a unique relationship between creep rupture life (time after loading) and strain rate. This relationship which is linear on a log-log plot is shown in Fig. 2-10 and appears below as:

$$\log tr(\text{min.}) = 2.33 - 0.916 \log \dot{\varepsilon}(1/\text{min.}) \pm 0.59 \qquad (1)$$

They also add that the following is approximately true:

$$\dot{\varepsilon} \cdot tr = 2.14 \qquad (2)$$

Saito (1965) later defines $\dot{\varepsilon}$ as the constant strain rate which develops prior to failure and that tr is the elapsed time from this point to failure. Saito claims that the above relationships apply to all soils (this is obviously the reason for the rather large range for

tr in Eq. (1)). He supports his work with several field cases which are of questionable worth due to the rather arbitrary way in which strain is measured in the field.

In a later paper Saito (1969) concerns himself with the transient creep range which occurs at a time closer to failure than the steady state creep which he had studied previously. From his basic steady state equation, Saito develops a three parameter equation to model transient creep behavior and presents a graphical solution for analyzing field problems.

Saito's work is completely empirical and his claim as to the generality of his equations with regard to soil type is questionable but it is a step in the right direction. The major drawback of his work is that is appears to be of little practical significance. Failure is not indicated until it is actually occuring and by then remedial action is out of the question.

(b) Singh and Mitchell (1969)

The authors deal with the problems of creep rupture and time to failure by modifying their basic equation (Eq. (8) in section 1.21a).

$$\dot{\varepsilon}t = At_1^{m} \exp\ (\alpha D)t^{1-m}$$

Strains at time "t" (for $m \neq 1$) are proportional to $\dot{\varepsilon}t$ at that time as shown below:

$$\varepsilon = C_1 + \frac{\dot{\varepsilon}t}{1-m}$$

where

$$C = \varepsilon_1 - \frac{Ae^{\alpha D}t_1}{1-m}$$

For $m \geq 1$, $\dot{\varepsilon}t$ is constant or decreases linearly on a plot of log $\dot{\varepsilon}t$ versus log t. However, for $m < 1$, $\dot{\varepsilon}t$ increases linearly with a slope of 1 - m until a given value of $\dot{\varepsilon}t$ is reached at which time there is a rapid change to a much greater constant slope as shown in Fig. 2-11. Singh and Mitchell (1969) define the $\dot{\varepsilon}t$ at which this event takes place as indicative of failure conditions. Thus $(\dot{\varepsilon}t)_f$ is independent of stress level and appears to be unique for each soil type. Analytically t_f can be found by:

$$\log_e\ (t_f) = \frac{1}{1-m}\ (C_2 - \alpha D)$$

where

$$C_2 = \log_e (\dot{\varepsilon}t)_f - \log_e (At_1^m)$$

In comparing this method with that of Saito and Vexawa (1961), we find it to be much more attractive. Although Saito and Uezawa also arrive at a unique "$\dot{\varepsilon}t_r$", they weaken its development by making it too general while Singh and Mitchell claim a unique $(\dot{\varepsilon}t)_f$ for each soil. The main advantage is that the Saito relationship is referring to a time just prior to creep rupture (long after $(\dot{\varepsilon}t)_f$ has been reached) and Singh and Mitchell are concerned with a modest change in creep rate long before shear failure which makes it a more valuable indicator and eliminates one of the major drawbacks of the Saito relationship. But most important, the Singh-Mitchell relationship is an extension of a much larger development of a theory for creep in soils and is not merely an empirical tool.

2.3 CREEP STRENGTH

(a) Arulanandan, et al (1971)

The authors conducted a series of undrained triaxial compression creep tests on isotropically consolidated San Francisco Bay Mud in order to prove the Roscoe (1963)

relation:

$$q = \frac{M}{(1-K/\lambda)} \log_e \frac{P_o}{P}$$

where M = slope of failure envelope on p,q plot

p_o = isotropic stress

p = mean normal stress

q = deviator stress

$\lambda = C_c/2.3$ = Compression Index/2.3

$K = C_s/2.3$ = Swell Index/2.3

Stress levels ranged from 30 to 90% of failure stress and loads were maintained for two weeks after which time the unfailed samples were taken to failure.

Results showed that the yield stress was only 60 - 75% of the ultimate strength for all consolidation stresses. Creep stress paths crossed both experimental and Roscoe's (1963) theoretical stress paths. The large pore pressures generated during the test were responsible for this phenomenon. Possible reasons for these pore pressures are:

(1) leaks through membranes and seals;

(2) osmotic pressure due to the salt concentration of San Francisco Bay Mud;

(3) structural rearrangement of particles or a

drainage into micropores from compression of the microstructure, which is comparable to secondary compression in their viewpoint.

The last reason is most likely due to the fact that mercury jackets and a saline cell fluid were used.

Reason three above was further investigated by consolidating samples of San Francisco Bay Mud and Kaolinite for 30 hours and then closing the drainage valve. The results, as shown in Fig. 2-12, indicate that the Bay Mud, with a high secondary compression tendency, generates pore pressures due to the arresting of secondary compression. The Kaolinite, with lower secondary compression tendency, begins to generate pore pressures but "thixotropy" is thought by the authors to eventually dominate the process and pore pressures decrease.

The authors therefore conclude that the arresting of secondary compression during undrained creep generates large pore pressures which can fail samples at deviator stresses much lower than ultimate values as shown in Fig. 2-13.

These results, which tie in well with the creep failure data of Shibata and Karube (1969), Bishop and

Lovenbury (1969), Singh and Mitchell (1969) and Walker (1969) are very useful and their proposed mechanisms may be helpful in explaining such phenomena.

2.4 CONCLUSIONS

Of the various rate process and rheologic models, the Singh-Mitchell treatment appears to be the most attractive. Although this method is of a more empirical nature than some of the others, it is by far the most advanced and unrestrictive. The model parameters can be obtained in the laboratory with relative ease.

Although the Singh-Mitchell treatment of creep rupture appears to be somewhat superior to that of Saito, it must be kept in mind that these two theories apply to two different events in the creep rupture process and both can be evaluated in the laboratory.

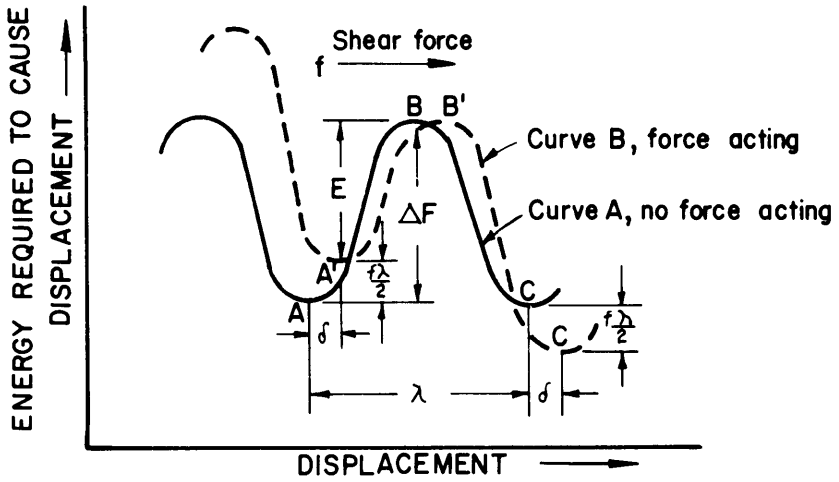

(a) REPRESENTATION OF ENERGY BARRIERS SEPARATING EQUILIBRIUM POSITIONS

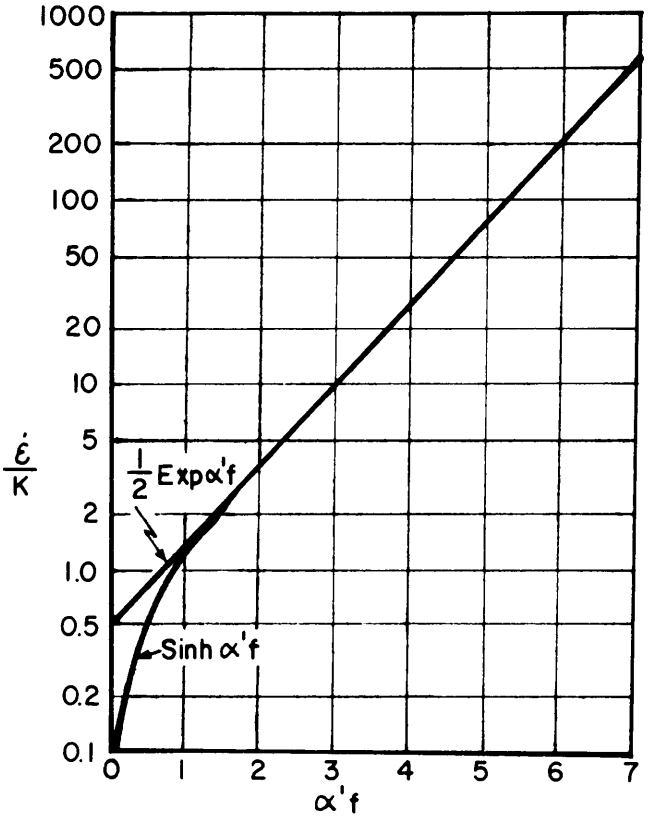

(b) $\dot{\varepsilon}/K$ VERSUS $\alpha'f$ ACCORDING TO HYPERBOLIC SINE AND EXPONENTIAL FUNCTIONS

DERIVATION OF BERKELEY THREE PARAMETER RELATIONSHIP BASED ON RATE PROCESS THEORY (After Mitchell et al, 1968).

Figure 2-1

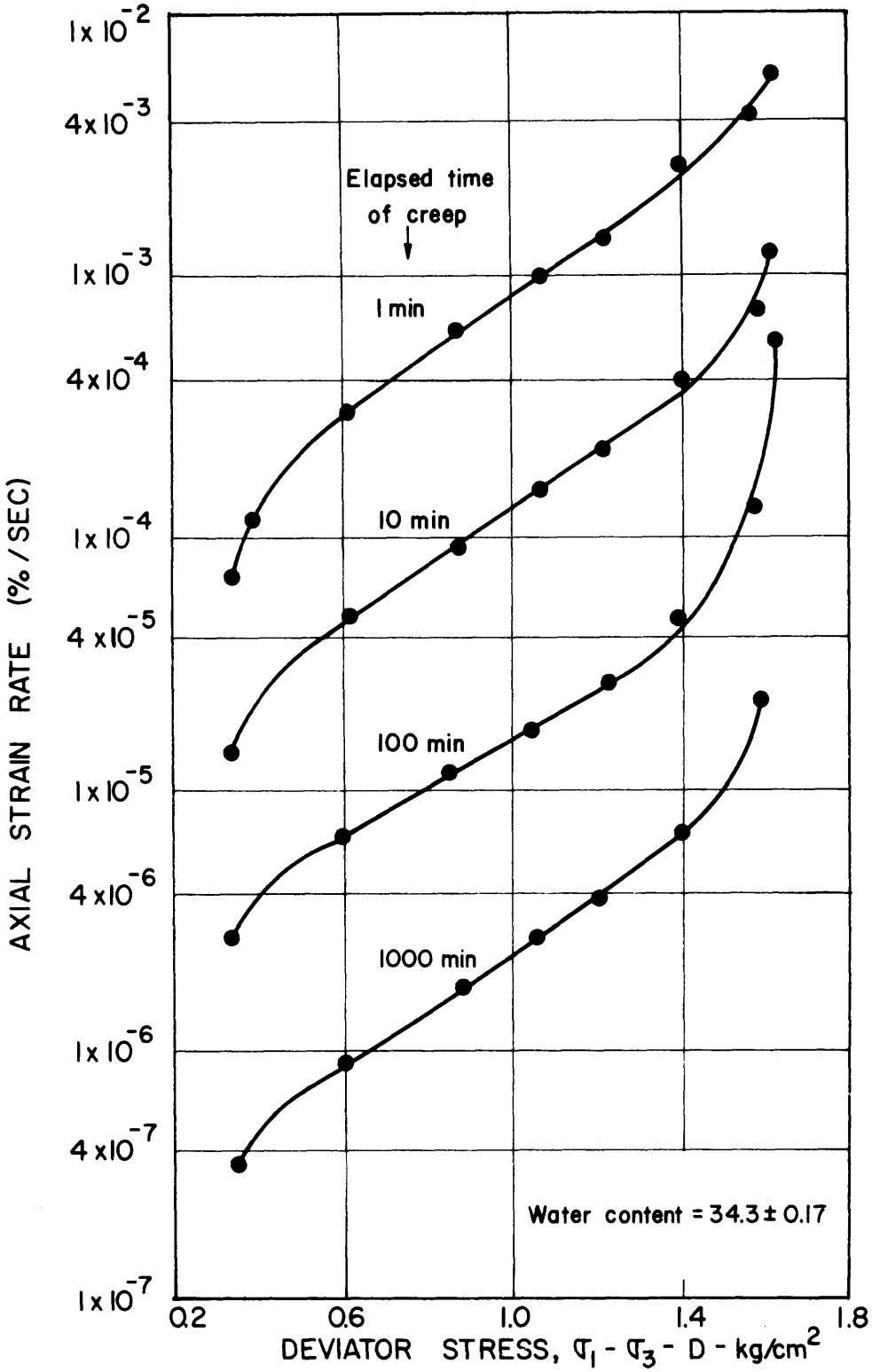

VARIATION OF STRAIN RATE WITH DEVIATOR STRESS FROM $\overline{CIU}$ C CREEP TESTS ON REMOLDED ILLITE (After Singh and Mitchell, 1968)

Figure 2-2

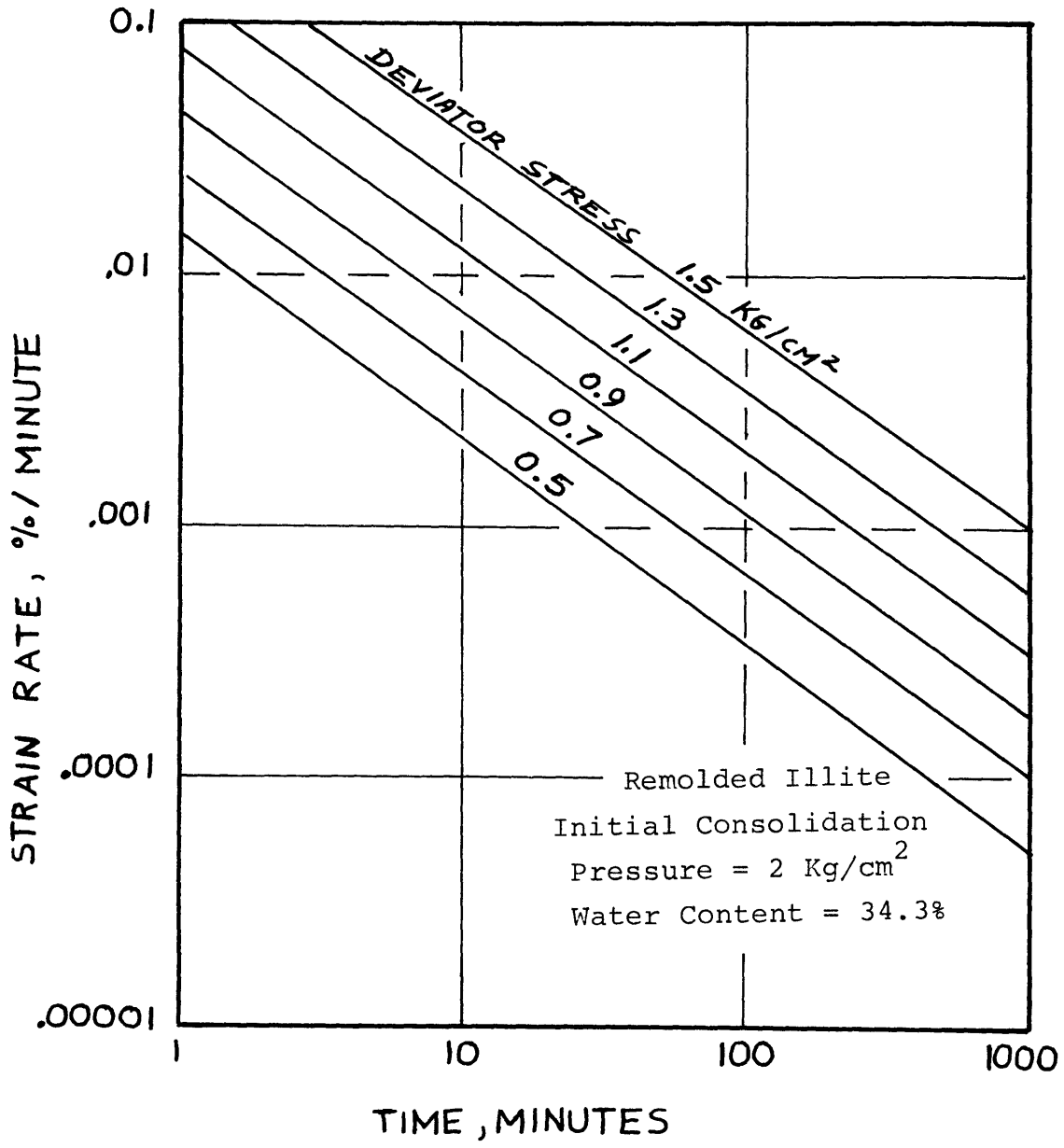

INFLUENCE OF TIME ON STRAIN RATE DURING CREEP OF REMOLDED ILLITE (Mitchell et, al. 1968)

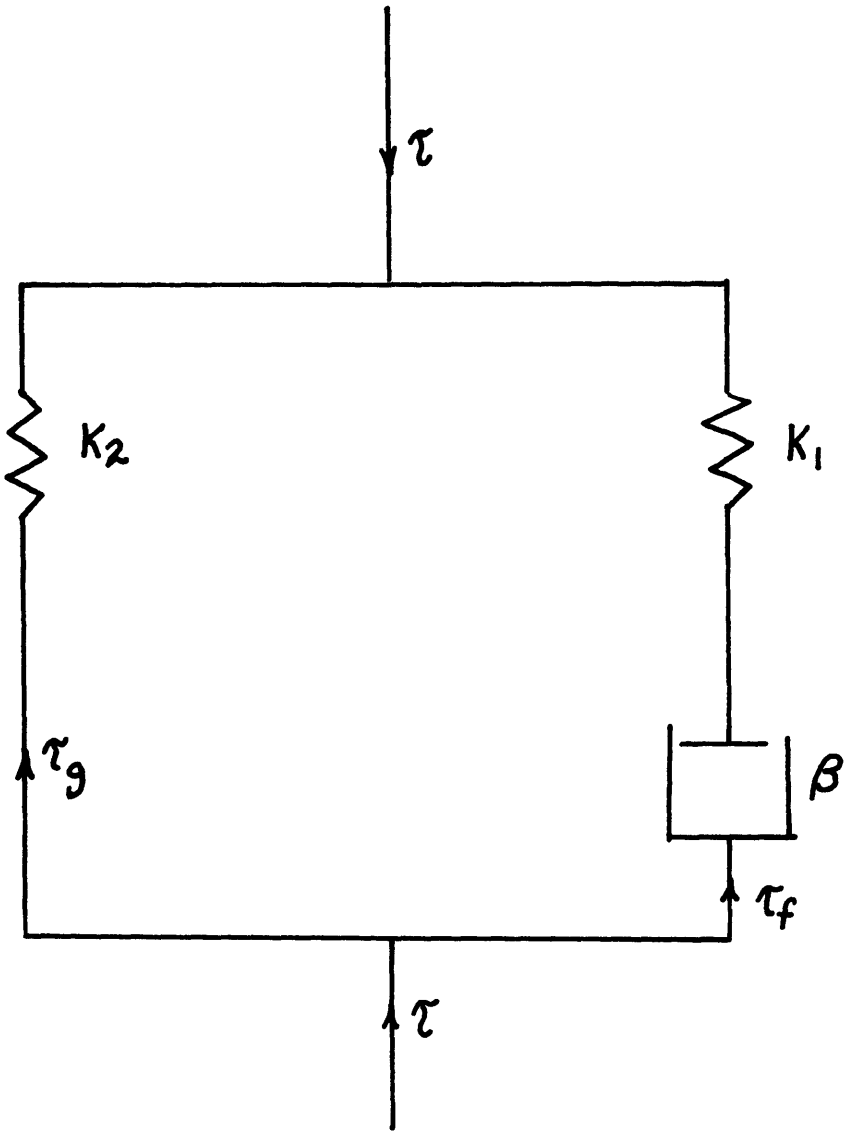

RHEOLOGIC MODEL FOR CHRISTENSEN AND WU(1964)
RATE PROCESS DEVELOPMENT

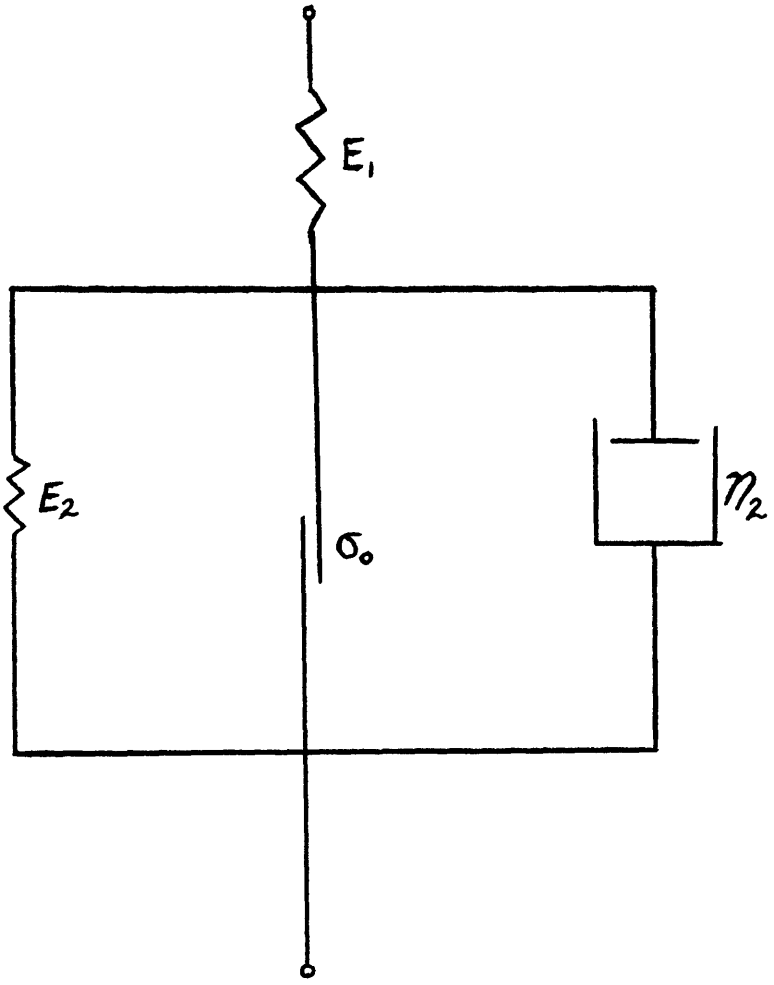

RHEOLOGIC MODEL FOR MURAYAMA AND SHIBATA(1961)
RATE PROCESS THEORY

Figure 2-5

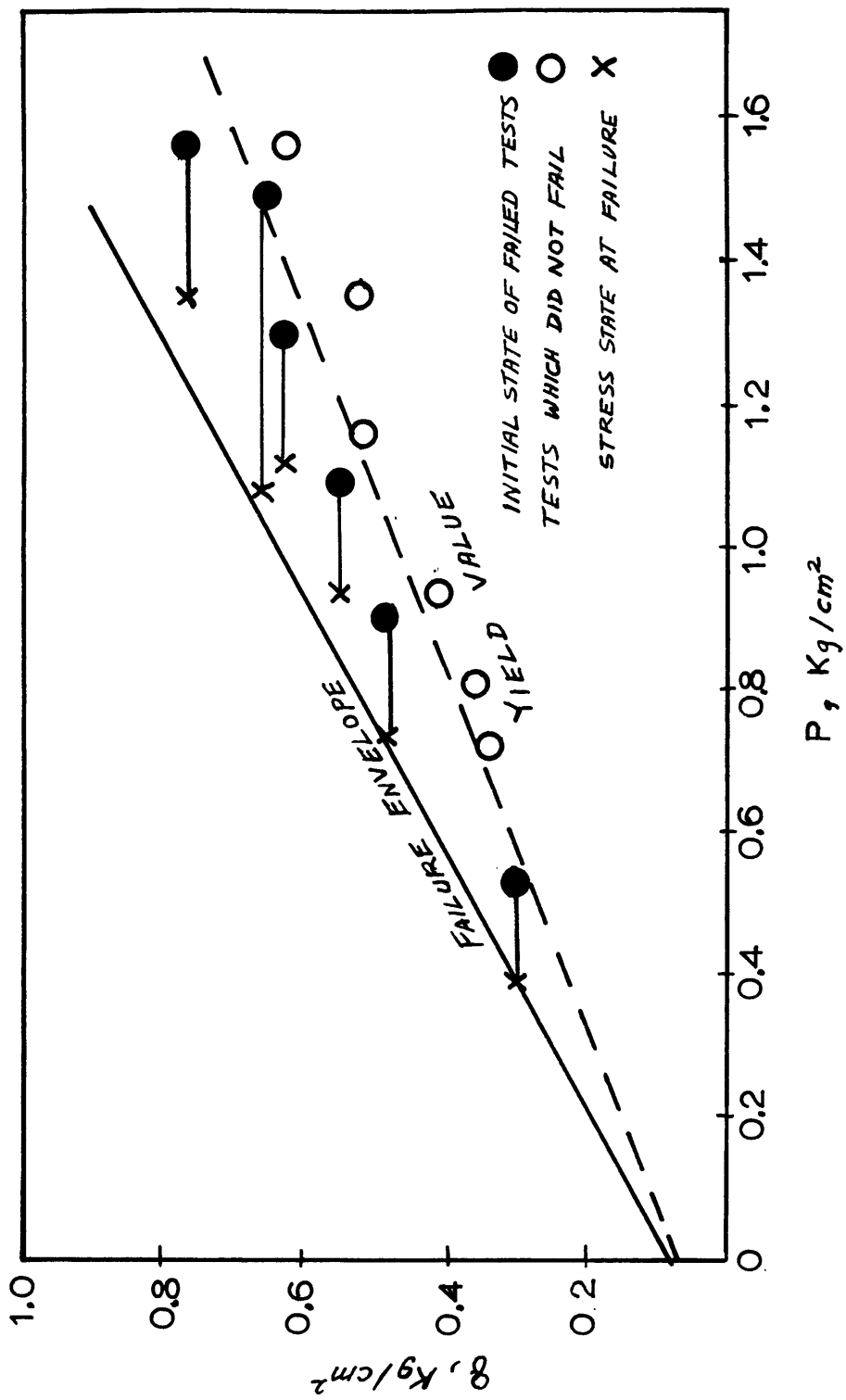

Stress Controlled $\overline{CIUC}$ Tests on N.C. Remolded Clay(After Shibata and Karube, 1969)

Figure 2-6

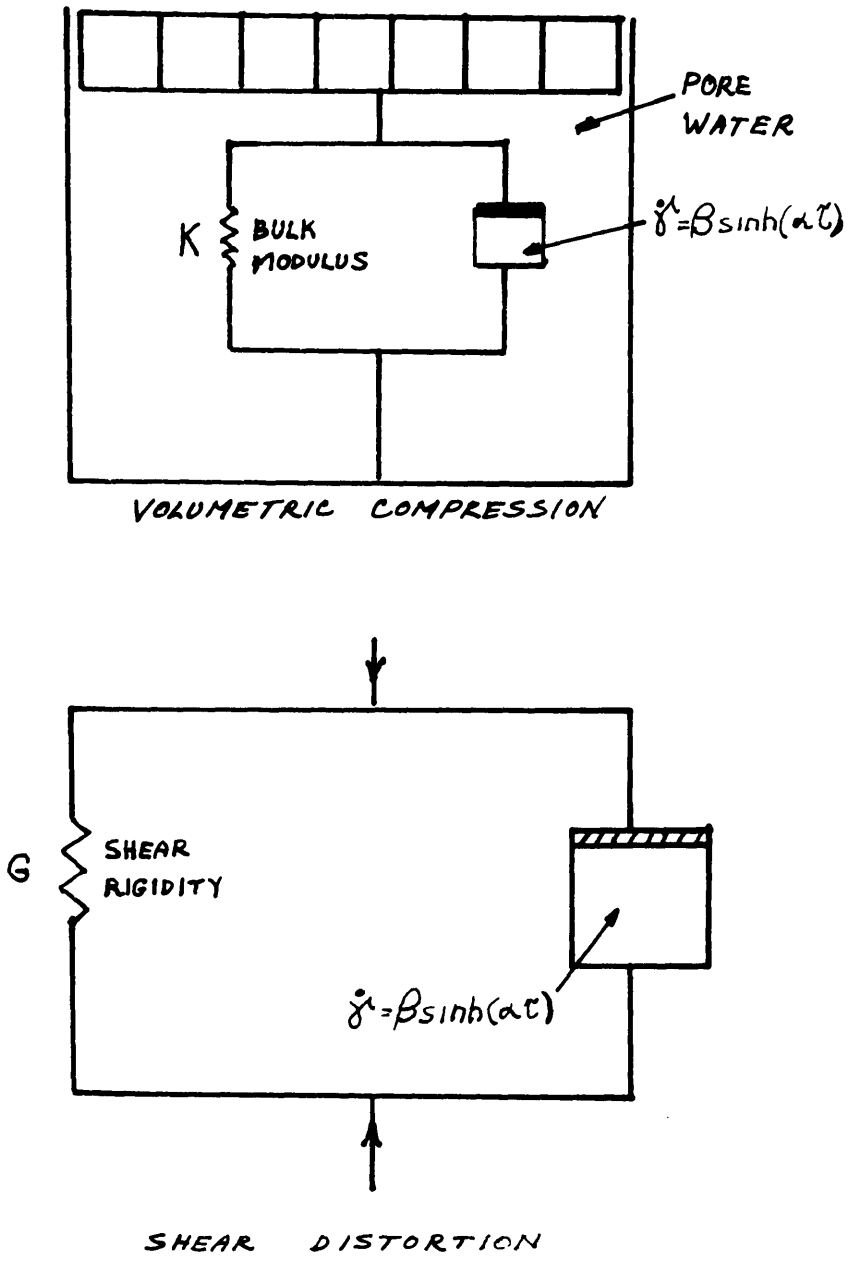

FIGURE 2-7 Barden's Rheologic Model (Barden,1969)

Figure 2-7

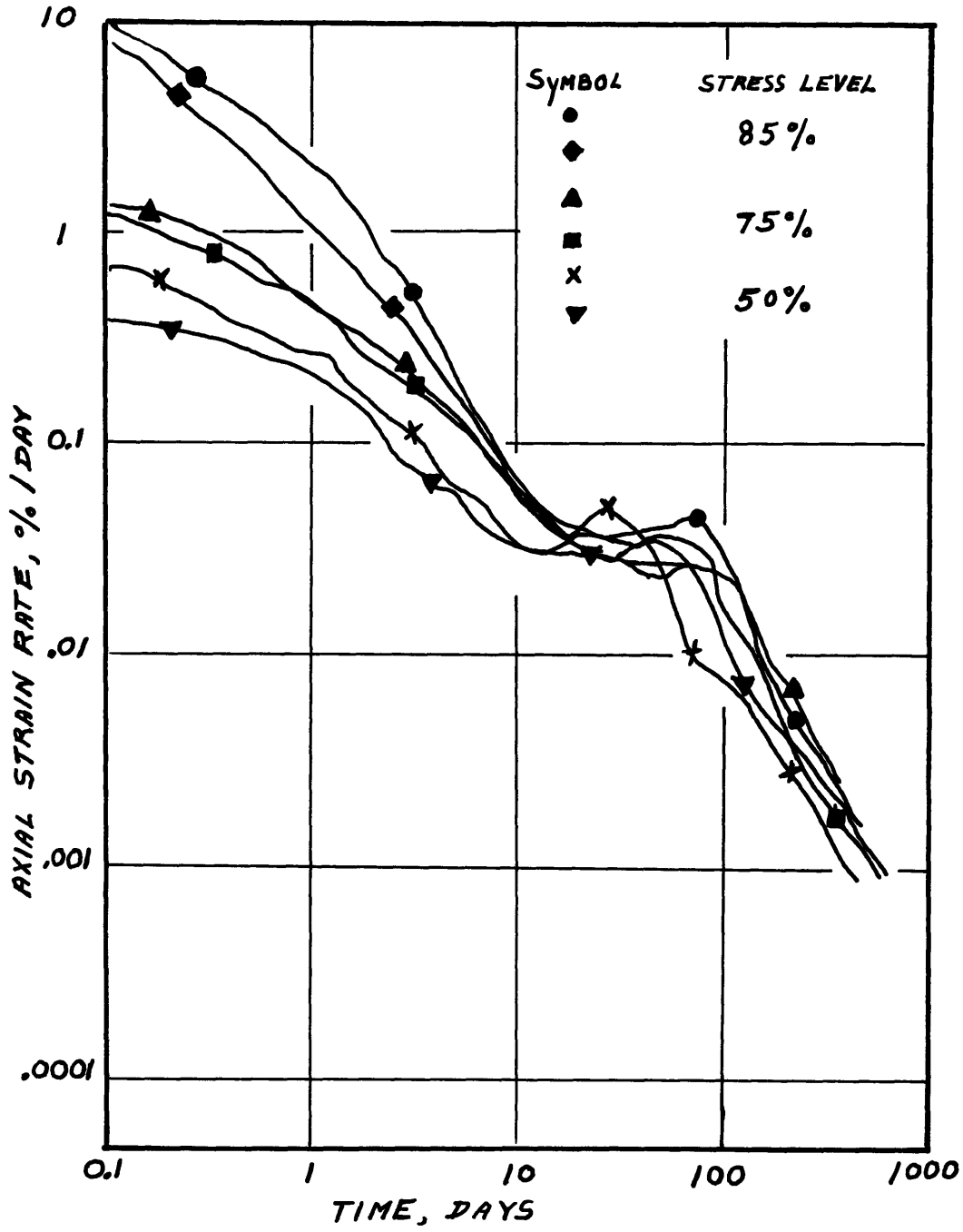

DRAINED TRIAXIAL CREEP RESULTS ON PANCONE CLAY
(Bishop and Lovenbury, 1969)

Figure 2-9

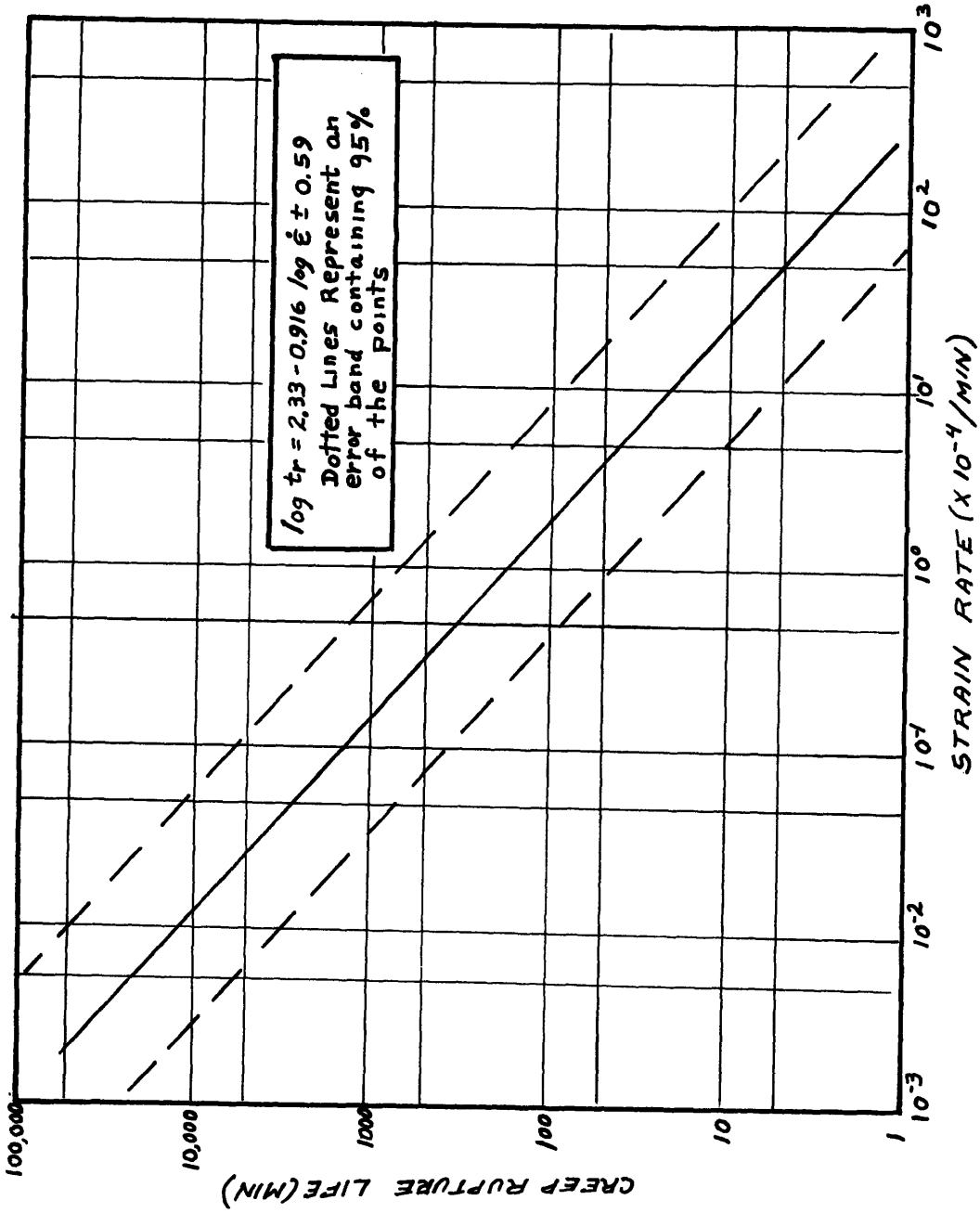

DEMONSTRATION OF THE SAITO CREEP RUPTURE RELATION (after Saito, 1961)

Figure 2-10

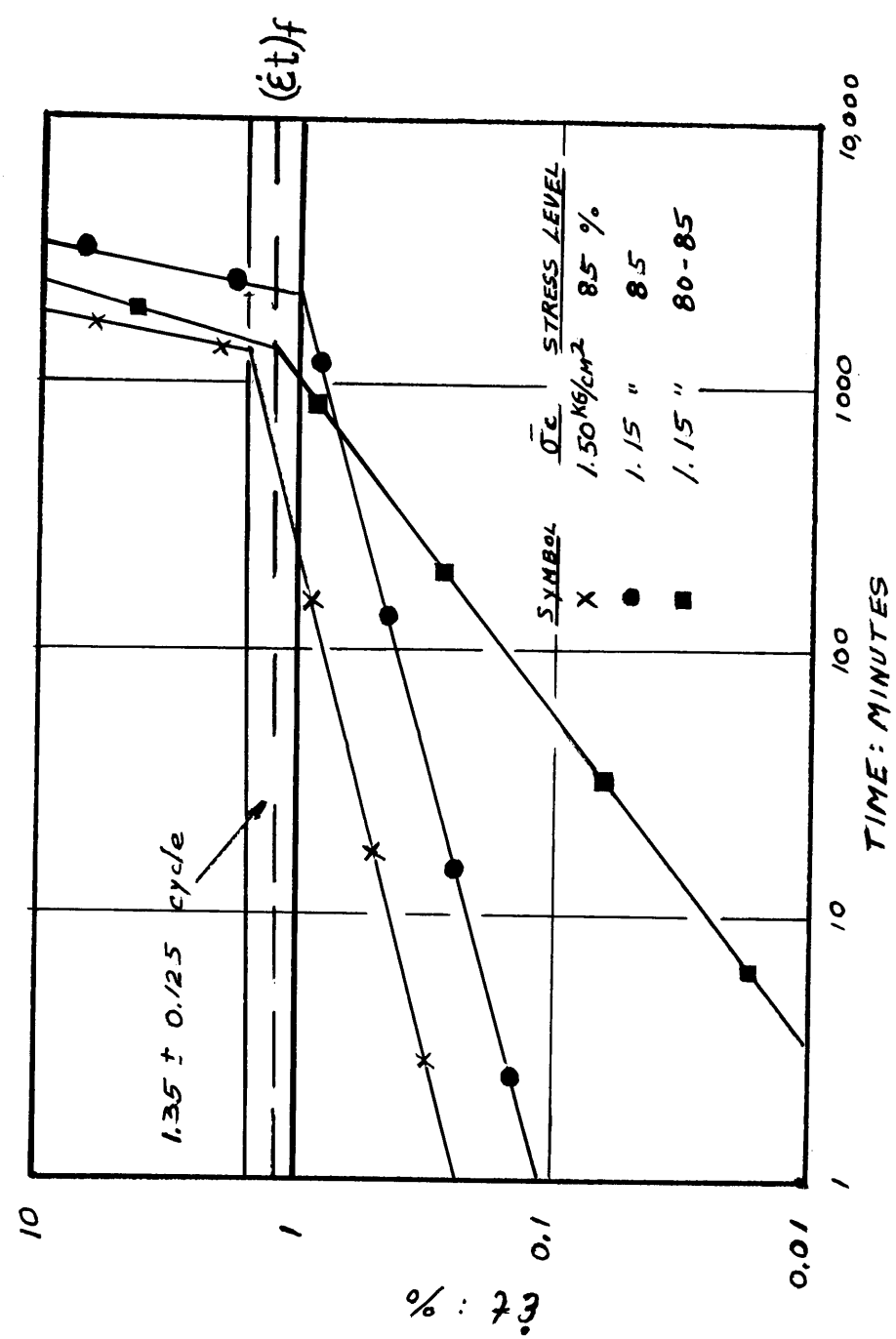

FIGURE 2-11 Singh-Mitchell Creep Rupture Concept (Singh and Mitchell, 1969)

Figure 2-11

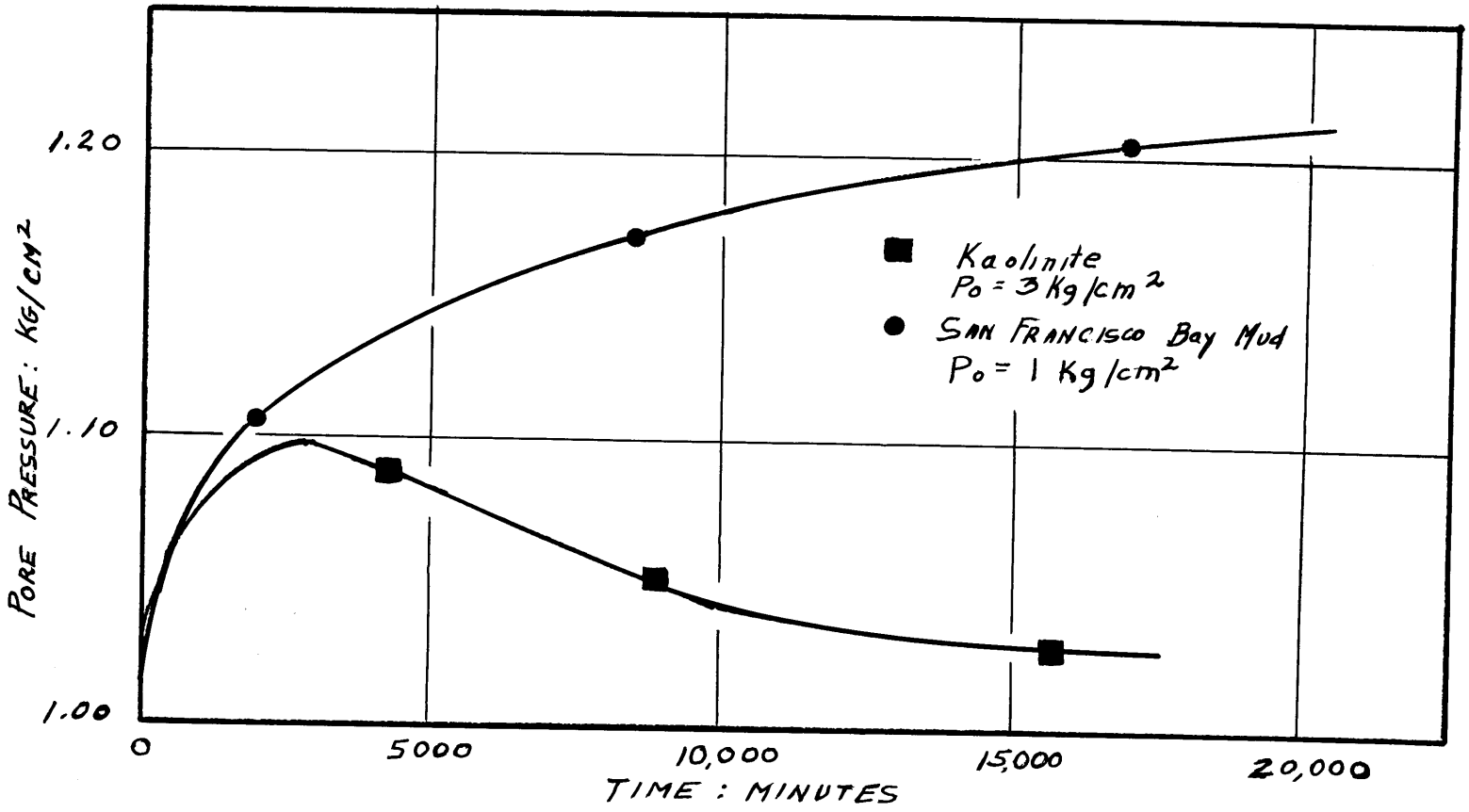

FIGURE 2-12 Influence of Consolidation Conditions on the Pore Pressure Generation of Two Clays(Arulanandan, et. al. 1971)

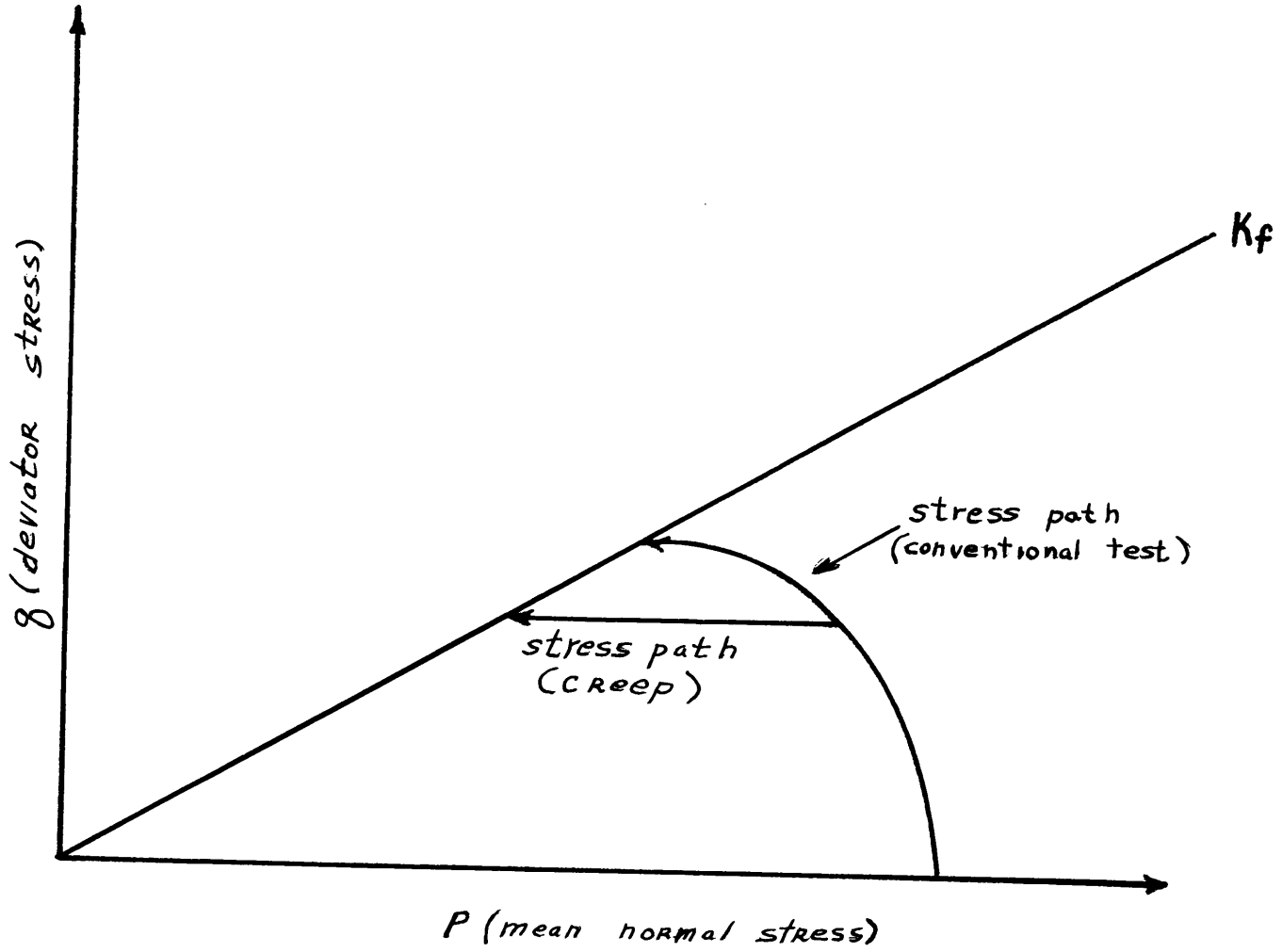

Figure 2-13

FIGURE 2-13 Typical Stress Path to Failure for an Undrained Creep Test on NC Clay

III DESCRIPTION OF EQUIPMENT AND PROCEDURES

3.1 INTRODUCTION

The Direct Simple Shear device used for this investigation was developed by the Norwegian Geotechnical Institute and manufactured by Geonov. It is very similar to the machine used for tests described by Bjerrum and Landva (1966). The primary requirements that the machine satisfies are:

(1) Ability to induce fairly uniform horizontal shear deformations in a cylindrical sample.

(2) Capability of performing drained or constant volume tests.

(3) Ability to keep the upper and lower sample surfaces parallel during testing.

(4) Controlled stress on strain.

(5) Maximum vertical load of 800 kg, horizontal load of 400 kg.

(6) Designed for 50 cm^2 by two cm sample confined in a wire reinforced membrane.

(7) Capability of testing soft clays as well as stiff clays, silt and sand. A method of sample preparation was devised that minimizes sample disturbance.

3.2 SHEAR APPARATUS

The shear apparatus (see Fig. 3-1) is composed of the sample assembly, vertical and horizontal load units and a horizontal load hanger assembly. The sample assembly consists of lower and upper filter caps (16), pedestal (17), and a plastic reservoir for inundating samples during testing.

The vertical load unit consists of the base (18), tower (19), lever arm (12), load gauge (4), piston (20), dial gauge for vertical deflection measurements (6), and lever-arm adjustment (21). The lever-arm has a load magnification ratio of 10 to 1 and is built into a U-formed hanger. A counter weight (22) balances the weight of the load-gauge, piston and sliding box.

The horizontal unit consists of a gearbox (11), proving ring load gauge (10), precision ball-bushing (9) and connection fork (23), and the sliding box (7). The present machine, Model 4, strains the sample by moving the top cap while holding the bottom cap and pedestal stationary. The horizontal load

is transmitted from the horizontal piston through the fork to the sliding box and top cap. The limit of travel is 10 mm in either direction from zero strain.

3.3 SAMPLE PREPARATION

By a system of vertically aligned cutting cylinders, top and bottom caps, pedestal and membrane streching device, the cylindrical sample is mounted in position and confined by the wire reinforced rubber membrane. The procedure is designed to support the sample at all times while minimizing distrubance and is much easier than sample preparation for the triaxial test (see Landva (1964) and Edgers (1967) for more detail).

3.4 TESTING PROCEDURE

For all tests, the sample was installed in the machine and consolidated by dead load increments until the desired consolidation stress was reached. All samples were consolidated to a stress sufficiently greater than the insitu vertical stress so as to minimize the effects of sample disturbance. The reservoir was not filled until $\bar{\sigma}_{vc} = 0.4$ kg/cm^2 was applied in order to avoid swelling. The final increment for normally

consolidated tests and the maximum and final loads for over-consolidated samples were allowed to consolidate for approximately two days in order to develop a constant degree of secondary compression.

For constant volume controlled strain tests, the shear procedure was that described by Edgers (1967).

For controlled stress constant volume creep tests, the horizontal proving ring was removed and the horizontal load was applied by means of the hanger assembly. After consolidation was complete, the lever-arm was connected to the vertical load adjustment screw and the appropriate horizontal load applied to the hanger assembly. The test was started by unclamping the horizontal piston and readings of horizontal strain with time commenced. As in the standard constant volume controlled strain test, the vertical load was adjusted in order to maintain constant sample volume throughout the test. Most of the adjustments occurred in the first two hours and usually only one adjustment per hour was needed thereafter on the first day, and only one or two adjustments per day were needed on subsequent days. The total number of adjustments needed for an average test duration of one week ($\sim$ 10,000 minutes) was on the order of 25. Room temperature during the test was approximately 69°F. Fluctuations of $\pm$ 2°F were common during a 24 hour period.

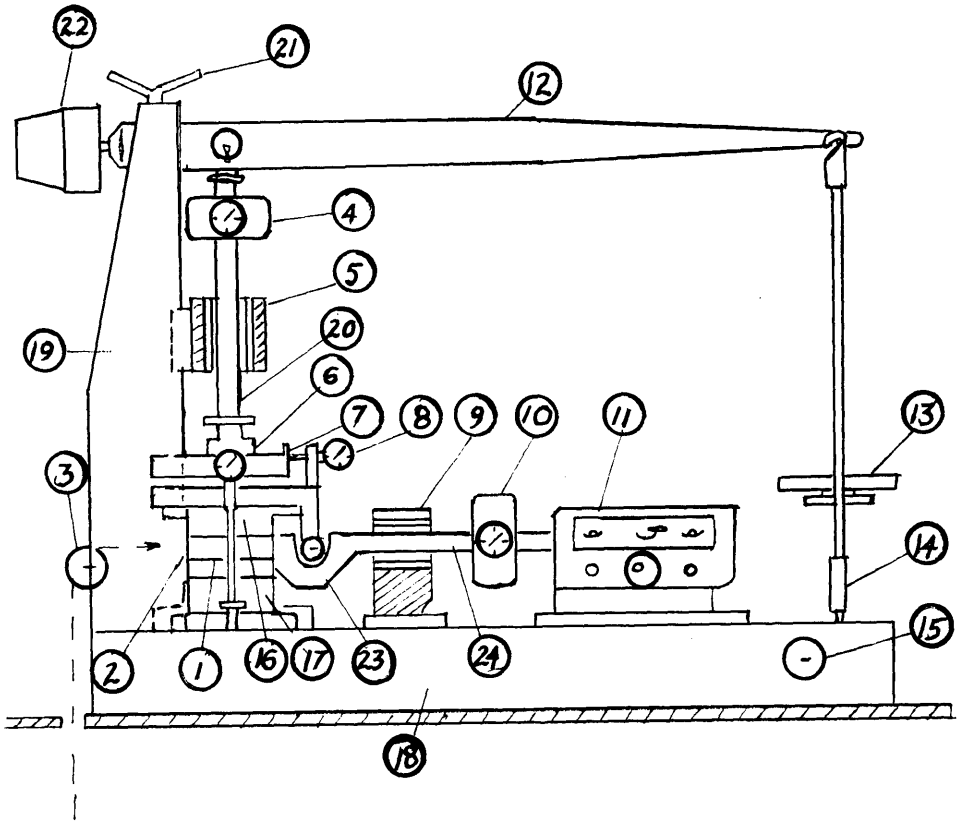

1 Sample 2 Reinforced rubber membrane 3 Wheels for applying dead load 4 Load gauge for vertical load 5 Ball bushing 6 Dial gauges for measurement of vertical deformation 7 Sliding box 8 Dial gauge for measurement of horizontal deformation 9 Ball bushing 10 Load gauge for horizontal force 11 Gear box 12 Lever arm 13 Weights 14-15 Clamping and adjusting mechanism used for constant volume tests 16 Lower and upper filter holders 17 Pedestal 18 Base 19 Tower 20 Vertical piston 21 Adjusting mechanism 22 Counterweight 23 Connection fork 24 Horizontal piston

Fig. 3-1 General Principle of Direct Simple-Shear Apparatus, Model 4 (Edgers, 1967)

Figure 3-1

IV EXPERIMENTAL INVESTIGATION

4.1 SOIL TESTED

The soil for this investigation was obtained from five inch diameter undisturbed fixed piston tube samples obtained from three borings offset approximately 300 feet to the land-side of Test Section III.

Boring No.	Station No.	Offset (ft)	Samples	El. (ft)
94ues	1395+50	310 LS of BL	10A to 13C	-30.5 to -45.8
95ues	1395+45	305 LS of BL	10A to 13C	-30.6 to -45.6
96ues	1395+55	305 LS of BL	10A to 13C	-30.5 to -45.3

Samples used in the investigation ranged in elevations from -35.9 ft to -44.15 ft. Values of $\bar{\sigma}_{vo}$ for this layer, which appears to be either normally consolidated or slightly over consolidated (see Fig. 1-2), range from 0.55 to 0.70 kg/cm^2 according to Foott and Ladd (1972). Consolidation curves for the Direct Simple Shear Tests conducted in the program yielded maximum past pressures in the range of 0.70 to 0.85 kg/cm^2.

Atterberg Limits were conducted on a number of representative samples and the results are shown, along with those obtained by the Army Corps of Engineers, in Fig. 4-1.

A series of constant volume controlled strain direct-simple shear tests were conducted on a number of samples at various overconsolidation ratios.

4.2 TEST PROGRAM

As previously stated, the testing program was conducted to achieve the following:

(1) A relationship between $s_u/\bar{\sigma}_{vc}$ and OCR for $\overline{CK_oU}$ DSS controlled strain tests.

(2) Investigation of the applicability of the Singh-Mitchell Rate Process Theory for EABPL Clay with regards to strain and strain rate as functions of time, stress level and overconsolidation ratio for first load increments.

(3) Investigation of the applicability of the Singh-Mitchell and Saito creep rupture theories for EABPL Clay.

(4) The effect of time on the strength of EABPL Clay.

In addition, the testing program was designed to investigate the behavior of additional load increments with respect to strain and strain rate as functions of time, stress level (applied horizontal shear stress/horizontal shear stress at failure, τ_H/τ_{max}) and overconsolidation ratio. It was hoped that a method could be developed for translating second and third load increment data into the form of initial load performance.

The program designed to achieve these objectives is outlined in Table 4-1 and is basically of two parts: (1) the $\overline{CK_oU}$ DSS controlled strain shear tests, and (2) the controlled stress creep tests. Tests Nos. 2 through 7 were used to develop the $s_u/\bar{\sigma}_{vc}$ versus OCR relationship from which various stress levels for the creep tests can be calculated. The remainder of the program consists of undrained creep tests on normally consolidated and overconsolidated samples in which the number of increments, the stress level and the load duration time serve as variables.

4.3 TEST RESULTS

4.3.1 Controlled Strain Tests

$\overline{CK_oU}$ DSS tests were conducted on seven samples of EABPL Clay. The results are shown in Table 4-2 and Figs. 4-2 to 4-7.

$\overline{CK_oU}$ DSS-1 was lost due to equipment failure and was therefore not tabulated. The normalized shear strength ($s_u/\bar{\sigma}_{vc}$) for normally consolidated samples was very consistent at 0.23. Failure occurred at very high shear strains of 20% and more for normally consolidated samples but this value was somewhat reduced for highly overconsolidated specimens. It was interesting to note that the maximum value of $\tau_H/\bar{\sigma}_v$ occurred simultaneously with the maximum value of τ_H for most of the overconsolidated samples though this was not the case with normally consolidated tests. A plot of normalized shear strength versus log OCR yielded the smooth graph in Fig. 4-7.

4.3.2 Controlled Stress Creep Tests

A summary of the 12 $\overline{CK_oU}$ DSS Creep tests appears in Table 4-3. Appendices B and C contain tabulated test data; strain, log strain rate and log $\dot{\gamma}t$ versus log time curves; stress paths and stress-strain curves for the 12 tests. Summary plots of the data are presented in Chapter 5.

4.3.2.1 Initial Stress Levels

Various shear stress levels were applied to the samples after consolidation was completed. These levels consisted of

50, 65, 73, 80, 85, 90 and 94 percent of failure for normally consolidated samples and 50, 72 and 94 percent for samples with OCR = 2. Samples were allowed to creep for one week (10,000 minutes), except $\overline{CK_oU}$ DSS-12 where $\bar{D} = \tau_H/\tau_{max} = 73\%$ was left on for 40,000 minutes.

4.3.2.2 Additional Shear Increments

Additional higher shear stress levels were applied to samples that did not fail under their initial loadings. These second and third increments were also allowed to creep until either creep failure occurred or a week passed. These loadings are listed in Table 4-3.

4.3.2.3 Creep Failure

Creep failure occurred in 11 of the 12 tests. The first test ($\overline{CK_oU}$ DSS-8) was failed by controlled strain after three shear stress increments had been applied over a three week period. For the remaining tests, creep failure eventually occurred at all applied shear stress levels of 85% or more.

TABLE 4-1: SUMMARY OF SAMPLES FOR TEST PROGRAM

Test No.	Type	Boring	Sample	W_n, %	Elevation, ft
CK_oUDSS-1	Controlled ε	96UES	11B	-	-35.9
CK_oUDSS-2	Controlled ε	96UES	11B	72.2	-36.1
CK_oUDSS-3	Controlled ε	96UES	11B	72.6	-36.2
CK_oUDSS-4	Controlled ε	96UES	11B	76.3	-36.5
CK_oUDSS-5	Controlled ε	96UES	11C	91.7	-36.9
CK_oUDSS-6	Controlled ε	96UES	11C	86.3	-37.1
CK_oUDSS-7	Controlled ε	95UES	10B	78.1	-32.1
CK_oUDSS-8	Creep	94UES	11C	73.8	-36.7
CK_oUDSS-10	Creep	94UES	13C	84.9	-45.0
CK_oUDSS-11	Creep	94UES	13A	27.2	-42.7
CK_oUDSS-12	Creep	94UES	13A	86.7	-42.9
CK_oUDSS-16	Creep	94UES	12C	73.4	-40.5
CK_oUDSS-17	Creep	95UES	13A	79.1	-44.0
CK_oUDSS-18	Creep	95UES	13A	79.2	-44.1
CK_oUDSS-19	Creep	95UES	12D	67.7	-41.2
CK_oUDSS-20	Creep	95UES	12D	80.1	-41.3
CK_oUDSS-21	Creep	95UES	12D	75.1	-41.5
CK_oUDSS-22	Creep	95UES	12D	77.3	-41.6
CK_oUDSS-23	Creep	94UES	10B	79.5	-32.0

SUMMARY OF $\overline{CK_oU}$ DSS TESTS ON EABPL CLAY

TEST	STRESS HISTORY			AT (τ_h) MAXIMUM					AT ($\tau_h/\bar{\sigma}_v$) MAXIMUM					W_N, %	SAMPLE	REMARKS
	OCR	$\bar{\sigma}_{vc}$ / $\bar{\sigma}_{vm}$	t_c (day)	γ (%)	$\dot{\gamma}$ (2)	$\frac{\tau_h}{\bar{\sigma}_{vc}}$	$\frac{\tau_h}{\bar{\sigma}_v}$	$\frac{\tau_h/\bar{\sigma}_v}{\bar{\phi}}$ (3)	γ (%)	$\dot{\gamma}$	$\frac{\tau_h}{\bar{\sigma}_{vc}}$	$\frac{\tau_h}{\bar{\sigma}_v}$	$\frac{\tau_h/\bar{\sigma}_v}{\bar{\phi}}$	W_f, %	EL. ft / $\bar{\sigma}_{vo}$	
2	1.00	3.00 3.00	1.0	18.4	5.5	0.230	0.690 1.725	0.400 21.8	35	20	0.170	0.510 0.840	0.606 31.2	72 ± 41	-36 0.54	$\bar{\phi}_{max}$ too large
3	1.00	1.00 1.00	1.5	22.8	5.5	0.263	0.263 0.489	0.538 28.2	33	5.5	0.225	0.225 0.349	0.645 32.8	72.6 63.7	-36 0.54	$\bar{\phi}_{max}$ too large
4	1.00	2.00 2.00	1.7	21.9	5.5	0.237	0.474 1.197	0.396 21.6	32	5.5	0.206	0.411 0.891	0.461 24.8	76.3 53.9	-36 0.54	
5	2.00	1.00 2.00	0.5 1.8	22.5	5.5	0.434	0.434 0.928	0.468 —	22.5	5.5	0.434	0.434 0.928	0.468 —	91.7 62.1	-37 0.56	
6	4.00	0.50 2.00	1.0 2.2	17.4	5.5	0.750	0.375 0.733	0.511 —	17.4	5.5	0.750	0.375 0.733	0.511 —	86.3 61.4	-37 0.56	
7	8.00	0.375 3.00	1.0 2.0	10	5.5	1.25	0.470 0.723	0.650 —	20±	5.5	0.88	0.33 0.414	0.80 —	78.1 50.9	-32 0.47	Erratic T-3 beyond peak
27	2.00	1.00 2.00	1.7 1.5	20.3	5.5	0.480	0.480 0.990	0.485 —	24.8	5.5	0.463	0.463 0.928	0.500 —	71.6 52.3	-36 0.54	
28	6.00	0.333 2.00	2.0 1.7	12.1	5.5	0.495	0.315 0.583	0.540 —	13.4	5.5	0.935	0.312 0.569	0.548 —	74.7 56.6	-36 0.54	Slippage of top cap

(1) γ = Shear strain

(2) $\dot{\gamma} = d\gamma/dt$ in percent per hour

$\bar{\phi} = \tan^{-1}(\tau_h/\bar{\sigma}_v)$

All stresses in kg/cm^2

Table 4-2

TEST NO.	STRESS LEVEL	γ_o	$\dot{\gamma}_o$	γ_f	$\dot{\gamma}_f$	$(\dot{\gamma}t)_f$	t_f	γ_1	$\dot{\gamma}_1$	t_1	ϕ_o	ϕ_f
$\overline{CK_oU}$DSS-8	0.489	0.654	0.154	2.436	.000034	0.203	7080	(m=.938)		--	7.1°	8.6°
	0.729	2.688	.0984	5.523	.000068	0.524	8595	3.55	.0024	200	12.6°	14.1°
	0.822	5.603	.0123	6.877	.000065	0.627	8310	7.00	.00007	∿10000	15.8°	16.3°
$\overline{CK_oU}$DSS-10	0.729	2.690	1.517	9.187	.000054	0.468	10065	(m=.913)		--	10.8°	14.6°
	0.941	9.653	0.233		FAILURE		?	--	--	--	18.3°	19.7°
$\overline{CK_oU}$DSS-11	0.941	4.804	0.851		FAILURE		?	(m=.738)		--	14.3°	21.7°
$\overline{CK_oU}$DSS-12	0.729	1.720	0.306	7.632	.000018	0.625	40625	(m=.919)		--	10.4°	15.5°
	0.941	7.871	0.122		FAILURE		?	--	--	--	19.7°	21.8°
$\overline{CK_oU}$DSS-16	0.50	0.977	0.154	3.395	.000027	0.246	10050	(m=.937)		--	7.3°	8.9°
	0.65	3.534	.0073	4.837	.000054	0.462	10085	4.40	.00011	3500	11.6°	12.3°
	0.80	4.988	.0107	8.876	.000190	0.940	10063	7.55	.00040	3000	15.1°	16.4°
	0.95	9.053	.0287		FAILURE		1620	--	--	--	19.3°	24.4°
$\overline{CK_oU}$DSS-17	0.941	6.254	0.944		FAILURE		68	(m=.678)		--	21.2°	24.7°
$\overline{CK_oU}$DSS-18	0.72	2.165	0.261	7.759	.000077	0.674	10300	(m=.820)		--	15.3°	17.2°
	0.94	8.119	0.068		FAILURE		?	--	--	--	21.4°	23.3°
$\overline{CK_oU}$DSS-19	0.50	1.358	0.072	2.682	.000024	0.208	10020	(m=.872)		--	11.1°	11.6°
	0.72	2.875	0.030	5.501	.000030	0.495	17260	4.27	.00023	2000	16.4°	17.2°
	0.94	5.791	.0527		FAILURE		2865	--	--	--	21.0°	27.4°

TABLE 4-3: $\overline{CK_oU}$DSS (CREEP) TEST RESULTS - EABPL CLAY

(DESCRIPTION OF PARAMETERS PRESENTED IN TABLE 4-4)

Continued

TEST NO.	STRESS LEVEL	γ_o	$\dot{\gamma}_o$	γ_f	$\dot{\gamma}_f$	$(\dot{\gamma}t)_f$	t_f	γ_1	$\dot{\gamma}_1$	t_1	ϕ_o	ϕ_f
$\overline{CK_oU}$DSS-20	0.90	6.417	1.290		FAILURE		184	(m=.788)		--	19.2°	22.2°
$\overline{CK_oU}$DSS-21	0.85	5.584	1.017		FAILURE		?	(m=.797)		--	15.8°	22.2°
$\overline{CK_oU}$DSS-22	0.80	3.495	0.523	13.78	.000204	1.172	7175	(m=.894)		--	13.3°	17.6°
	0.90	13.848	.0155		FAILURE		?	--	--	--	19.6°	22.3°
$\overline{CK_oU}$DSS-23	.65	1.614	.2514	6.099	.00045	0.385	10080	(m=.924)		--	9.3°	12.5°
	0.80	6.216	.0111	8.866	.000109	0.947	10080	7.90	.00025	35000	15.2°	15.9°
	0.95	9.011	.0259		FAILURE		?	--	--	--	18.7°	23.3°

Continuation of:

TABLE 4-3: $\overline{CK_oU}$DSS (CREEP) TEST RESULTS - EABPL CLAY

(DESCRIPTION OF PARAMETERS PRESENTED IN TABLE 4-4)

TABLE 4-4: DESCRIPTION OF MEASURED TEST PARAMETERS

Stress Level ($\bar{D}_\tau$) = ($\tau_H/\tau_{H\ max}$)

γ_o (Initial Shear Strain, %) = γ @ t = 1 Minute

$\dot{\gamma}_o$ (Initial Strain Rate, %/Min.) = $\dot{\gamma}$ @ t = 1 Minute

γ_f (Final Shear Strain, %) = γ @ t_f

$(\dot{\gamma}t)_f$ (Final Strain Rate X Elapsed Time, %) = $\dot{\gamma}_f$ X t_f

t_f (Final Elapsed Time) = Length of Time the Shear Stress Increment ($\bar{D}\tau$) Was Left on Sample

γ_1 (Steady State Strain) = Strain at Which a Second or Third Load Increment Began to Follow the Singh-Mitchell Theory (See Section 5.2)

$\dot{\gamma}_1$ (Steady State Strain Rate) = Strain Rate at Which a Second or Third Load Increment Began to Follow the Singh-Mitchell Theory

t_1 (Elapsed Time) = Elapsed Time at Which γ_1 and $\dot{\gamma}_1$ Occur

ϕ_o ($\tan^{-1}\ \tau_H/\bar{\sigma}_v$) = ϕ at t = 1 Minute for a Given $\bar{D}\tau$

ϕ_f ($\tan^{-1}\ \tau_H/\bar{\sigma}_v$) = ϕ at t_f

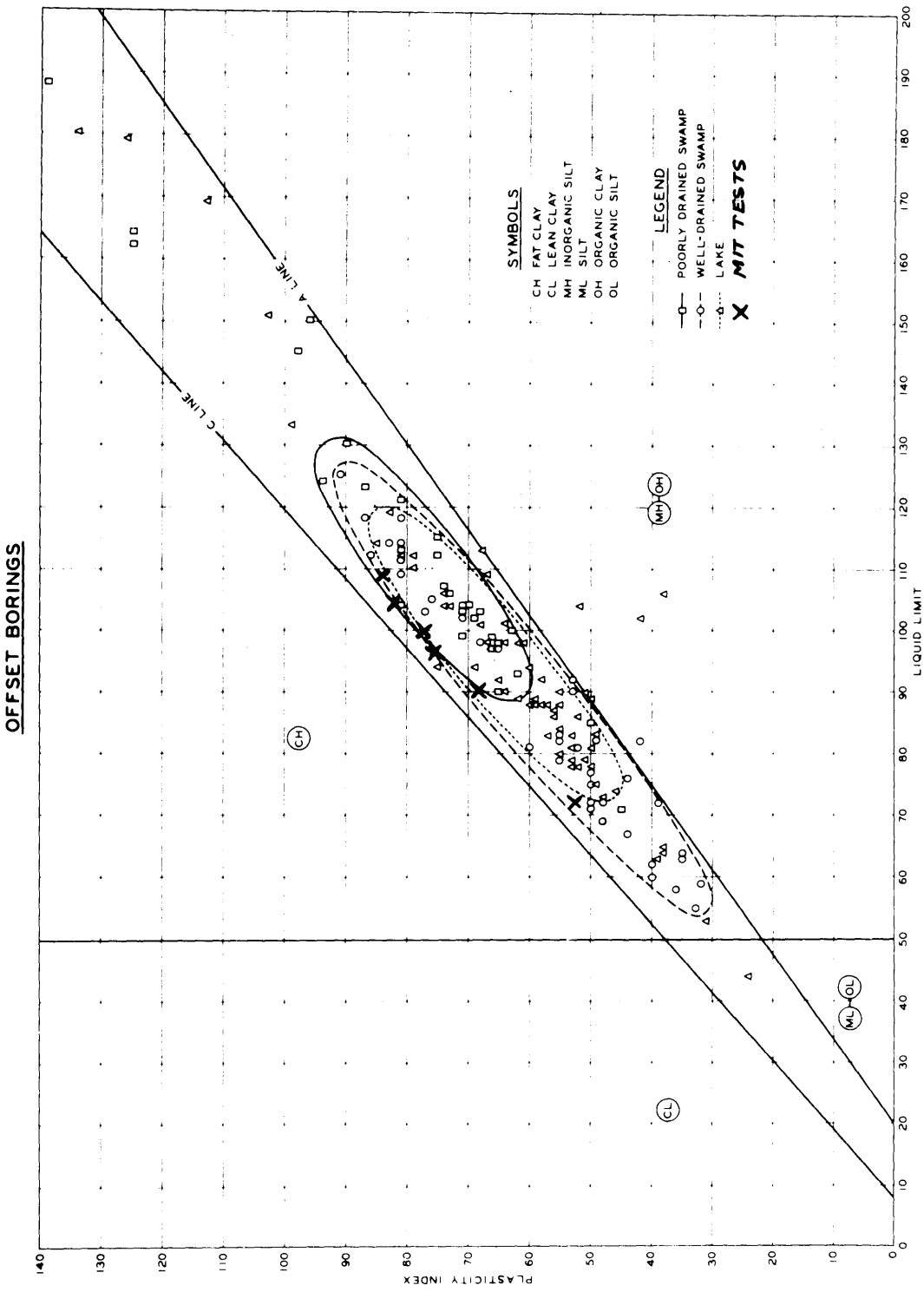

Range in plasticity characteristics of Atchafalaya backswamp materials

Figure 4-1

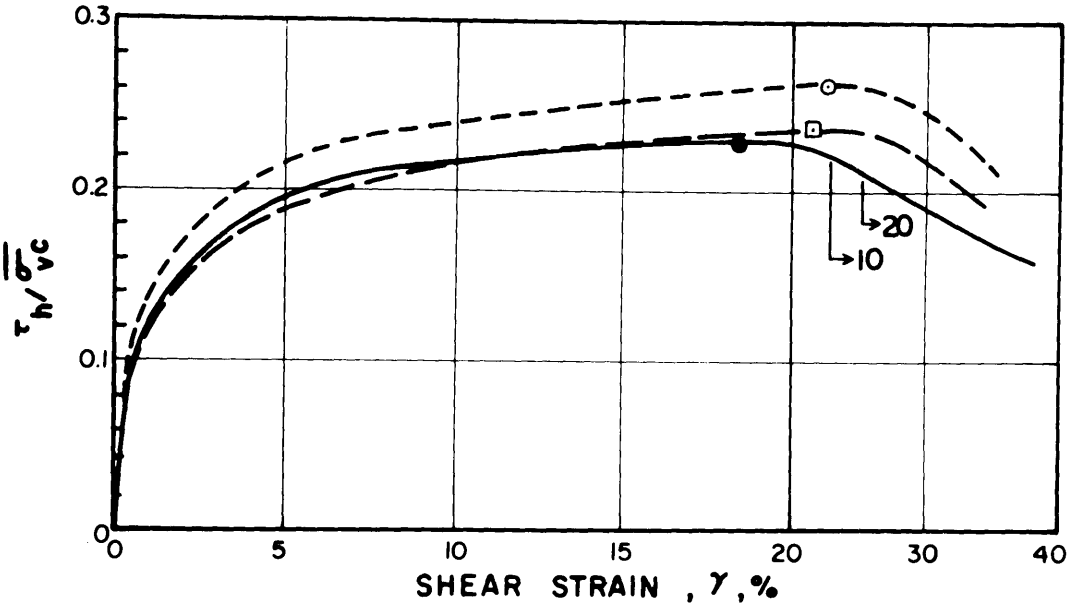

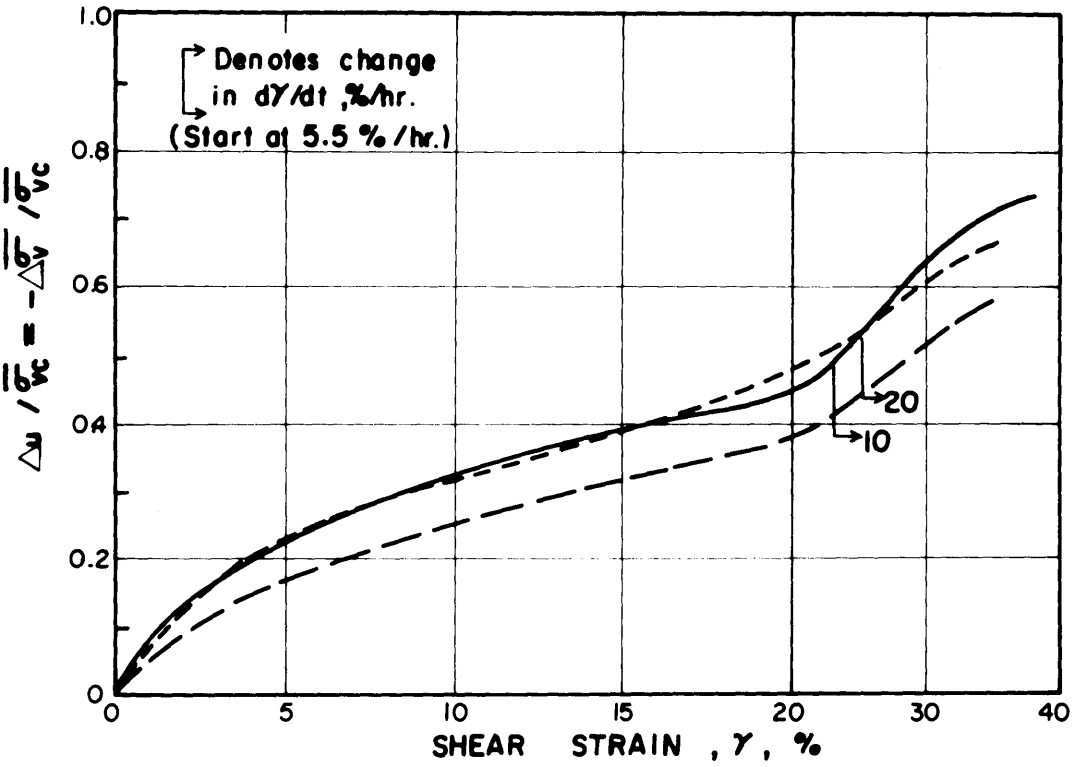

Symbol	No.	W_n %	W_f %	$\bar{\sigma}_{vc}$ TSF	t_c Day	El. ft.
—●—	2	72±	41	3.1	1.0	-36
– –⊙– –	3	72.6	63.7	1.02	1.5	-36
—⊡—	4	76.3	53.9	2.05	1.7	-36

$\overline{CK_oUDSS}$ TESTS ON NORMALLY CONSOLIDATED EABPL CLAY

Figure 4-2

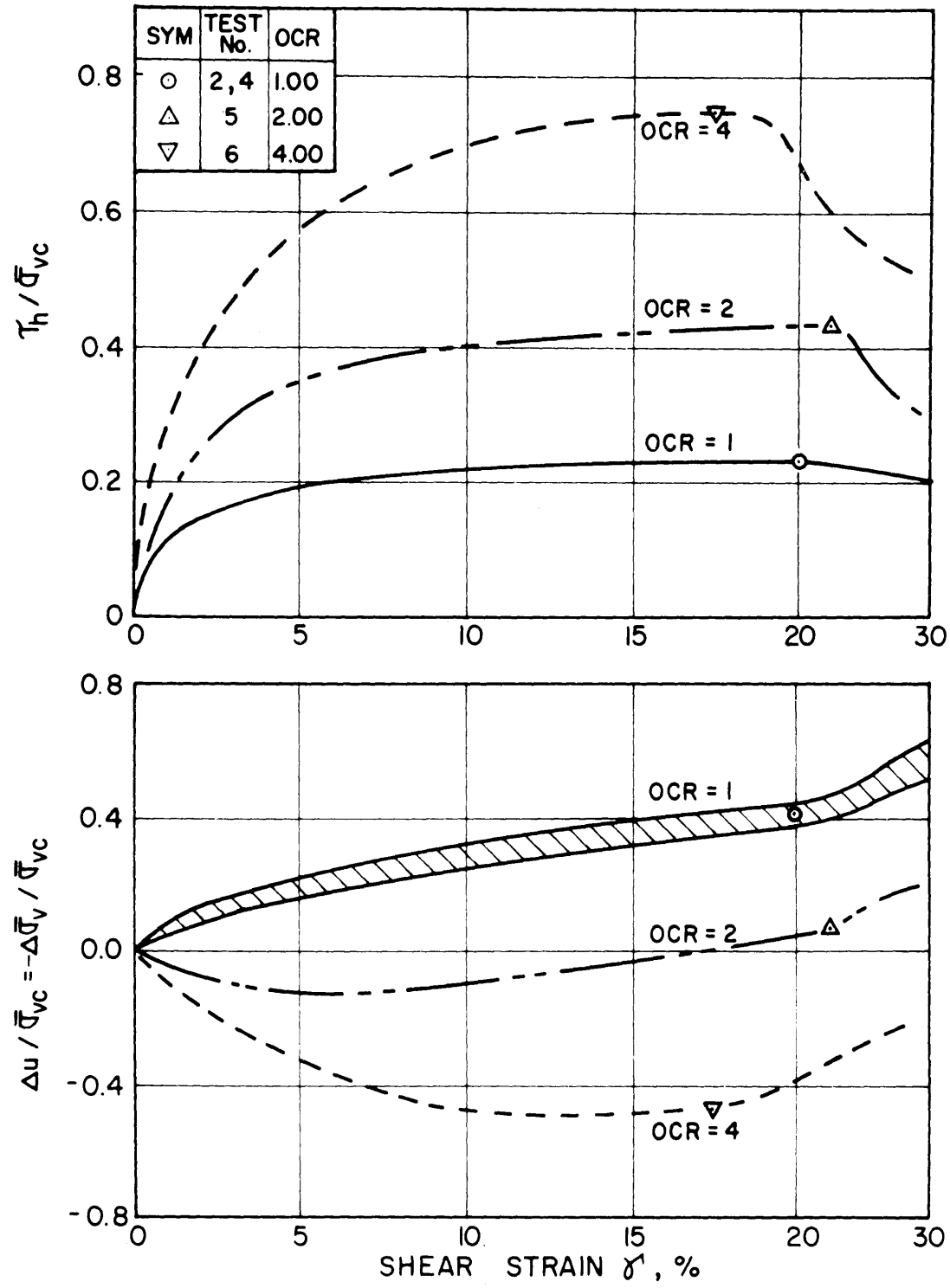

STRESS VS. STRAIN FROM $\overline{CK_0U}$ DSS TESTS ON EABPL CLAY

Figure 4-3

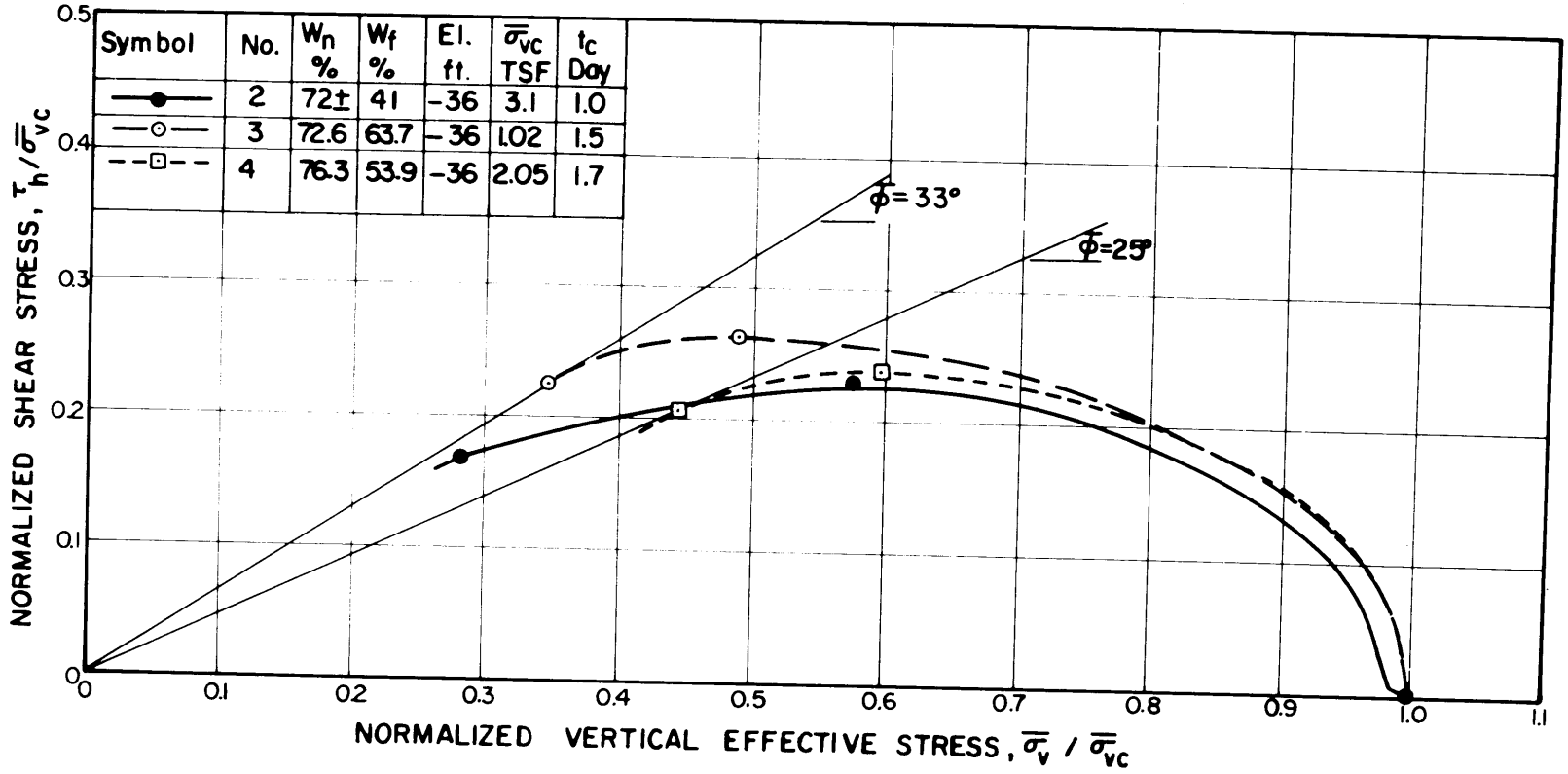

STRESS PATHS FROM $\overline{CK_oUDSS}$ TESTS ON NORMALLY CONSOLIDATED EABPL CLAY

Figure 4-4

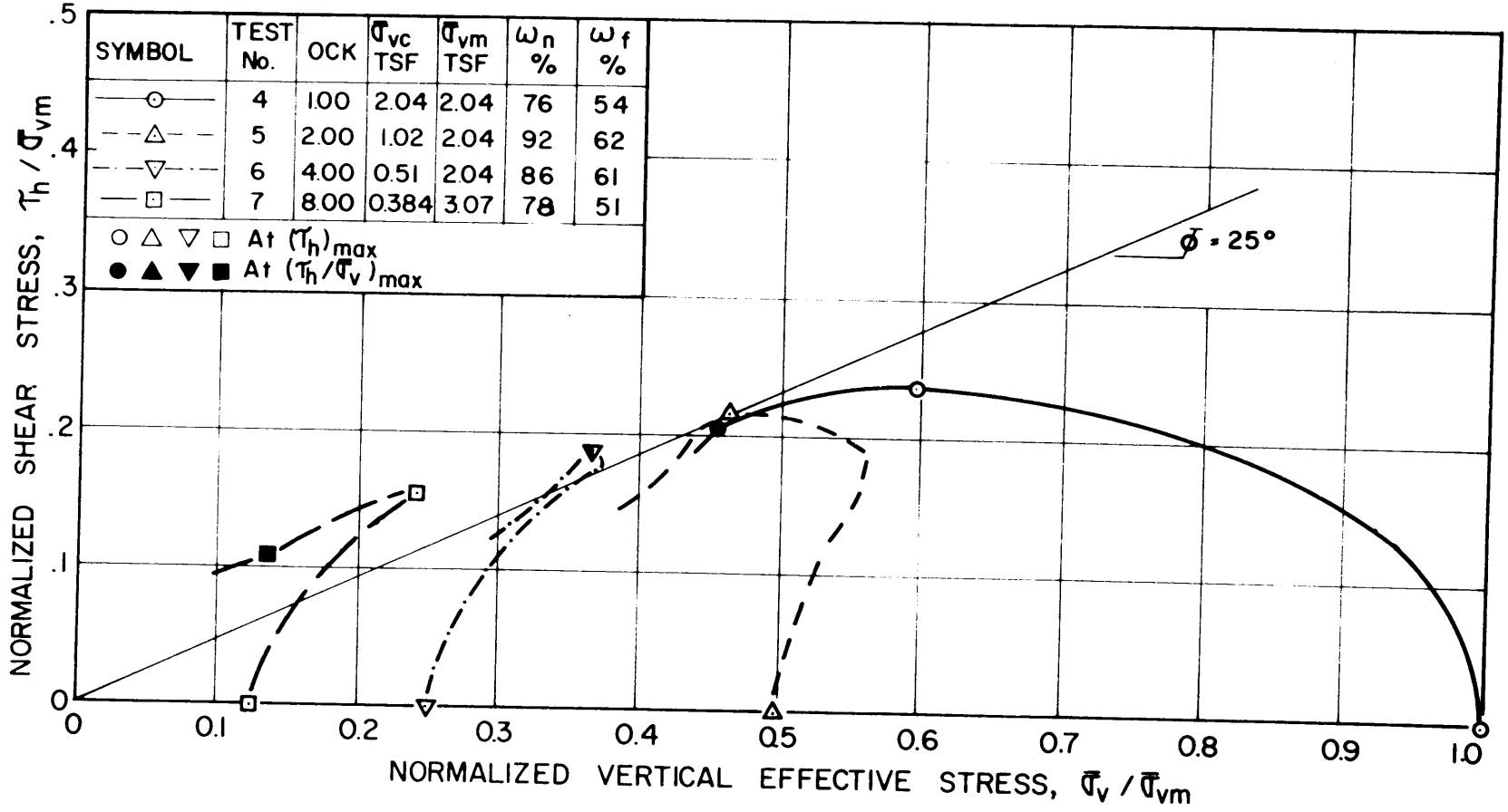

NORMALIZED STRESS PATHS FROM $\overline{CK_oU}$DSS TESTS ON EABPL CLAY

Figure 4-5

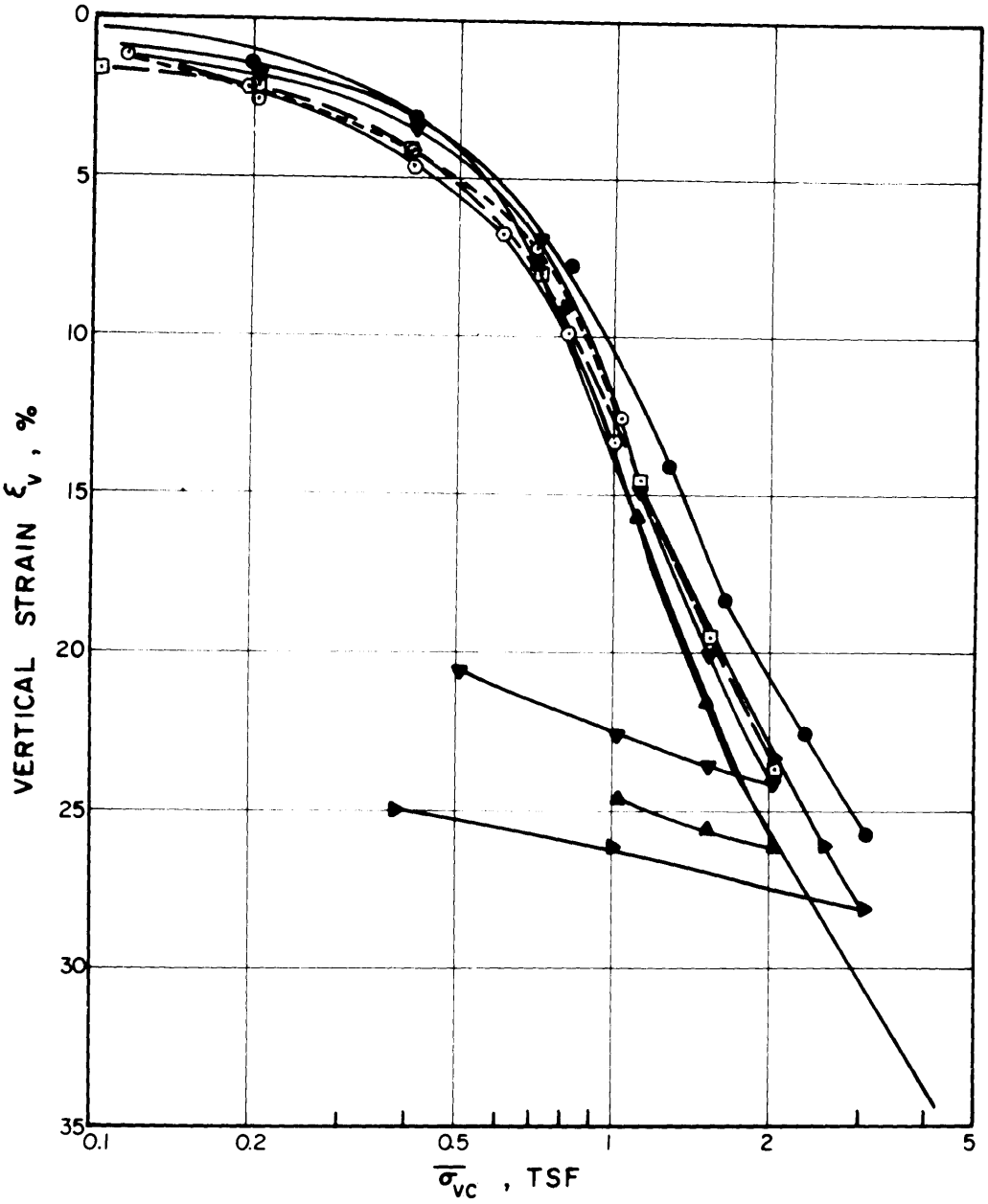

Symbol	No.	W_n,%	El.,ft.
—⊙—	1		
—●—	2	72±	-36
- -⊙- -	3	72.6	-36
—⊡—	4	76.3	-36
—▲—	5	91.7	-37
—▼—	6	86.3	-37
—▶—	7	78.1	-32

COMPRESSION CURVES
$\overline{CK_oUDSS}$ TESTS
EABPL CLAY

Figure 4-6

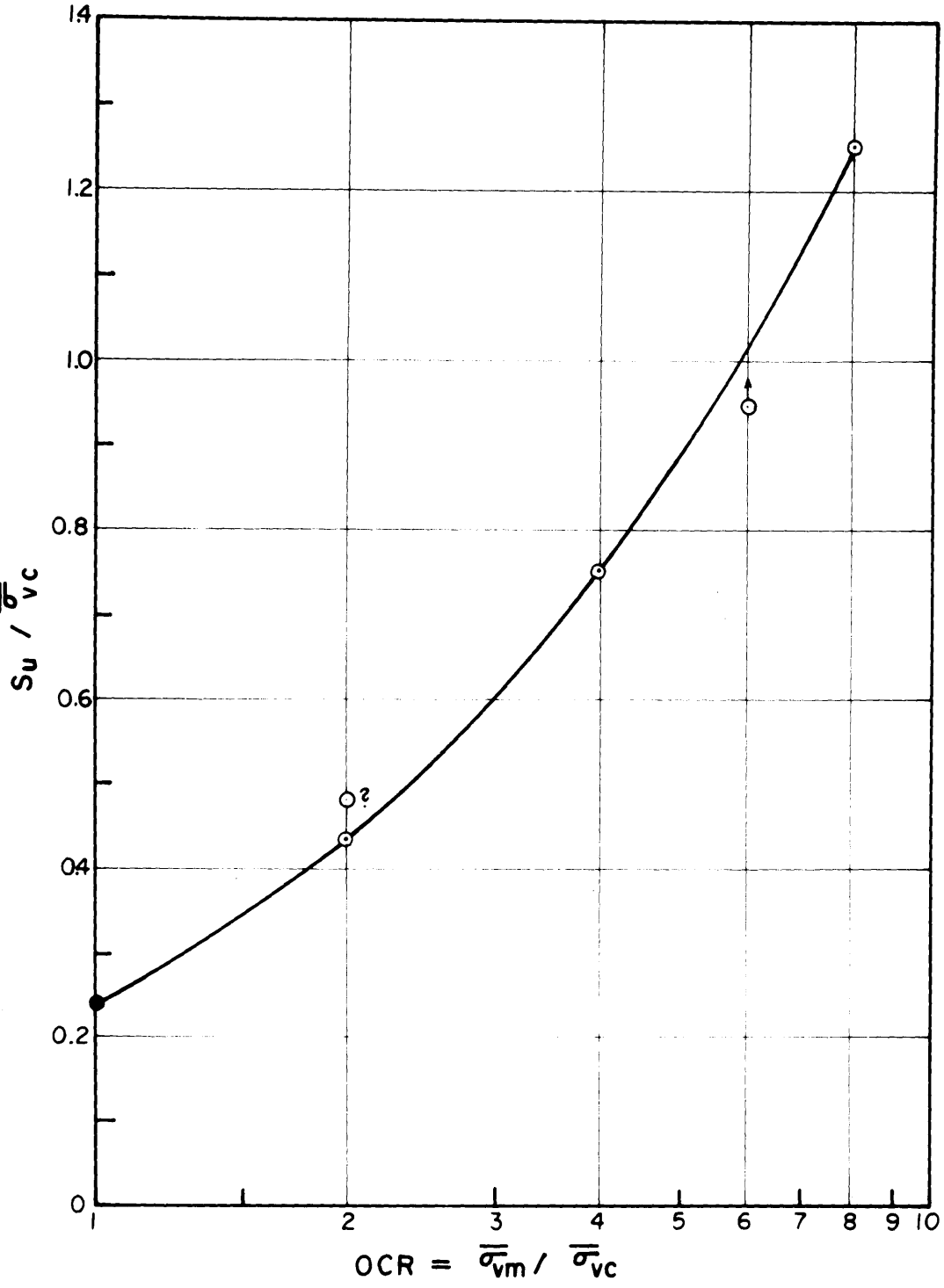

$S_u / \overline{\sigma}_{vc}$ VS OCR FROM $\overline{CK_oU}$ DIRECT — SIMPLE SHEAR TESTS ON EABPL CLAY

Figure 4-7

V DISCUSSION OF TEST RESULTS

5.1 FIRST LOAD INCREMENTS

The term first load increment refers to the first increment of shear stress which is applied to the sample after consolidation is complete. Prior to this process the shear strain is zero. The Singh-Mitchell Rate Process Theory is concerned with the undrained creep that occurs due to this loading.

5.1.1 Normally Consolidated Samples

Results from first loadings on normally consolidated samples are presented in Figures 5-1 through 5-4. Within the first minute of loading there occurred an instantaneous shear strain (γ_o) which can be determined from Figure 5-1. From that point the creep process for stress levels ($\overline{D}_\tau$) of 80 percent or less appeared to follow the linear relationship between log strain rate ($\dot{\gamma}$) and log time which is the basis for the Singh-Mitchell theory (see Fig. 5-2 and 5-3). For stress levels greater than 80 percent, the plots of log strain rate versus log time were initially linear, but the strain

rate then became constant in each case and then increased as the sample creep ruptured. This phenomenon will be covered in detail in a later section.

Unlike the Singh-Mitchell Theory where log-log plots of strain rate versus time yielded parallel lines for the various stress levels (D), EABPL clay yielded straight lines which were divergent with time or in other words, "m" was not constant but a function of stress level, $\overline{D}_\tau$, as shown in Fig. 5-13.

(Note: Singh-Mitchell's $\overline{D}$ refers to the deviator stress ratio in the triaxial test:

$$\frac{\sigma_1 - \sigma_3}{(\sigma_1 - \sigma_3)_f} .$$

Since the deviator stress cannot be determined in the simple shear stress system, $\overline{D}_\tau$ refers to the applied horizontal stress ratio, $\tau_H/\tau_{H\ max}$). Therefore, "m" which is supposedly a constant parameter for a given soil and the index of that soil's creep tendency, is in fact, for EABPL clay, a variable which demonstrates that this clay has greater creep tendencies (decreasing "m") at higher shear stress levels.

Another point which is of interest concerning Fig. 5-2 is the presence of discontinuities in the linear plots which

take place at approximately t = 400 minutes. For all stress levels above 50 percent (except for those that caused failure) the strain rate begins to decrease a few hours after loading at a greater rate than that of the initial log-log plot of strain rate versus time. At approximately t = 400 minutes, a new log-log linear relationship is established which results in a straight line which is "below" the initial line and has a higher value of "m". The sudden application of a shear stress induces positive pore pressures within the sample. The vertical stress is reduced to compensate for this but since C_v is not equal to infinity, time is required before equilibrium returns to the sample. No doubt the average pore pressure in the sample is close to zero (because the sample volume remains constant) but pore pressures within the sample interior are probably greater than zero and those near the edges are negative. The time required for equalization is on the order of 400 minutes, which is approximately the time required for primary consolidation in normally consolidated EABPL clay based on C_v = 0.01 ft^2/day. This value of C_v is within the range recommended by Ladd et al (1972). The hypothesis is further supported by the fact that this phenomenon is only barely noticeable for stress levels ($\overline{D}_\tau$) of 50 percent. As can be seen with the hypothetical stress path in Fig. 5-9, the induced pore pressures for higher stress levels are much greater.

Assuming this hypothesis to be correct, the pore pressures within the sample interior (i.e. on the potential failure plane) decrease the effective vertical stress. Since the shear stress is unaffected by pore pressures, the resultant obliquity (τ_H/σ_v) is greater than that applied and is equal to the obliquity that one would normally obtain from a higher application of $\bar{D}_\tau$. Only when the induced pore pressures are dissipated will the obliquity within the sample and the resultant creep behavior correspond to that level normally associated with the applied $\bar{D}_\tau$.

This situation makes determination of the remaining two parameters in the Singh-Mitchell equation particularly difficult. The two constants (A, $\bar{\alpha}$) are obtained from a plot such as that presented in Fig. 5-4. Since the obliquity at small times (t < 400 minutes) is larger than that normally associated with the applied $\bar{D}_\tau$, the strain rates at small times for a given $\bar{D}_\tau$ are higher than they should be. Since this effect is more marked for larger stress levels, the resulting slope ($\bar{\alpha}$) is too large. A more reasonable result can be obtained by extending the steady state portions of the plots (t > 400 minutes) in Fig. 5-2 back to small times. The resulting data points yield slopes ($\bar{\alpha}$) which are probably more representative of the true soil behavior. As can be seen in Fig. 5-4, all laboratory data points lie above the

modified data for all times except t = 1000 minutes where there is uniform scatter, which is consistent with the hypothesis.

5.1.2 Over Consolidated Samples

Results from first loadings on three over consolidated speciments (OCR = 2) are presented in Figs. 5-5 through 5-8. The creep behavior is essentially that of the Singh-Mitchell Theory, with "m" decreasing with increasing stress level. In contrast with the creep behavior of the normally consolidated specimens, there occurred no discontinuity at t = 400 minutes on the log-log plot of strain rate versus time. The author believes this to be due to the fact that the stress path for OC samples is such that initial pore pressure development is not significant. As a result, "m" remained essentially constant throughout a given test.

It was also found that "m" for any given stress level is significantly less than that for normally consolidated EABPL clay. Inspection of Fig. 5-10 shows that initially the normally consolidated samples exhibit a higher strain rate but that the curves converge with time due to the lower "m" value for the OC samples. At large times the OC samples exhibit greater strain rates.

Initially, for a given value of $\overline{D}_\tau$, the OC sample is closer to the failure envelope (see Fig. 5-11). Nevertheless, the strains obtained at t = 1 minute are essentially equal for the two stress histories (see Fig. 5-17). This is to be expected since Fig. 4-3 shows that equal values of $\overline{D}_\tau$ yield nearly equal values of strain during standard controlled strain $\overline{CK_oU}$DSS tests.

The plot of normalized pore pressure versus shear strain for standard $\overline{CK_oU}$DSS tests in Fig. 4-3 shows that initially two entirely different phenomena occur during the shearing of the NC and OC (OCR = 2) samples. It is only after approximately 6 percent shear strain has occurred that the OC sample begins to develop positive pore pressures (i.e. develop a positive slope in Fig. 4-3) and behave in a manner similar to that of the NC sample. Strangely enough, the plots of the two samples become parallel at this point and failures occur at nearly equal strains. Figure 5-12 is a plot of $\Delta u/\sigma_{vc}$ versus γ for standard $\overline{CK_oU}$DSS tests and $\overline{CK_oU}$DSS creep tests at $\overline{D}_\tau$ = 0.50, 0.72 and 0.94 for NC and OC samples. The author believes that pore pressure generation during undrained shear and creep behavior (i.e. strain rate) are closely linked. Since the NC and OC standard $\overline{CK_oU}$DSS tests behaved quite similarly with regards to stress versus strain, it would appear that one could compare the creep behavior

of NC and OC samples by looking at the amount of pore pressure generation with strain (slope of the curve) relative to that of the standard $\overline{CK_oU}$DSS test for each group (NC and OC). For instance, in the case of $\overline{D}_\tau = 0.50$, the two tests (NC and OC) begin with nearly equal strains at t = 1 minute though the OC sample is at a stress state in terms of effective stress that is closer to failure. Inspection of Fig. 5-12 shows that pore pressure generation for a given strain increment for the NC sample has increased over that of the standard $\overline{CK_oU}$DSS test. At the same time the OC sample shows a significant decrease from that of the standard test. At a later time, the rate of pore pressure increase with strain for the NC sample decreases while that of the OC sample radically increases. As a result, the rate of pore pressure development with strain relative to that of the corresponding standard test is greater for the OC samples. Therefore, the rate of strain rate development is greater for the OC sample though the magnitude of the strain rate may not be greater. Inspection of creep curves for $\overline{D}_\tau = 0.72$ and their positions relative to the standard $\overline{CK_oU}$DSS curves shows a similar phenomenon. On the other hand, the curves for $\overline{D}_\tau = 0.94$ are very similar to their parent curves, the standard $\overline{CK_oU}$DSS test results, but are only displaced to the right. As a result, their creep behavior are very similar. Figure 5-13 shows that the two plots for NC and OC samples tend to

converge at high stress levels, which is what Fig. 5-12 implies. The author realizes that the "m" value for the NC samples was obtained at small times and is therefore not the true value which is representative of the stress level. But it must be kept in mind that the initial unequalized pore pressures developed in the NC sample effected strain rate level to a far greater extent and that "m" was not greatly affected by the phenomenon.

Due to the small amount of data for the OC samples and the difficulty with which good pore pressure data can be obtained in the direct simple shear device, this proposed explanation is mainly conjecture. A similar test program with triaxial equipment would definitely be a great help in evaluating this hypothesis.

Calculation of $\bar{\alpha}$ and A presented little problem though their reliability is questionable due to so little data (three tests). The value for $\bar{\alpha}$ was greater than that obtained from the normally consolidated tests and "A" was somewhat lower (see Fig. 5-8).

5.2 ADDITIONAL LOAD INCREMENTS

For all tests where failure did not occur as a result of the initial shear stress increment, the stress level was increased and creep was allowed to continue.

Examples of this second (or third) load creep behavior are shown in Fig. 5-14 along with results from first load tests for comparison. Other examples can be found in Tests 8, 16, 19 and 23 in Appendix C. In all cases, creep is initially almost nonexistant. The strain rate at small times for a given stress level is much smaller than that of a comparable first load test (same $\overline{D}_\tau$). Apparently, creep from the previous increment has caused a modification in soil structure that results in a more creep resistant sample. After a period of time, the creep process begins to accelerate on a log time scale and the plot of log strain rate versus log time begins to approach that of the first load test for the same $\overline{D}_\tau$ (see Fig. 5-14). At some elapsed time, t_1, this plot intersects the "firstload plot" for that stress level and takes on the log linear behavior of the rate process theory. This is true for both normally consolidated and over consolidated samples.

There does not appear to be any way of expressing this phenomenon in quantitative terms. The values of the initial strain and strain rate as well as the strain, strain rate and elapsed time at which the creep process begins to follow Singh and Mitchell's theory appear to be rather random. No doubt they are dependent on $\Delta\overline{D}_\tau$ as well as the magnitude of the previous increment and its length of duration.

Analysis of this phenomenon was hindered by the lack of data as there were only four tests in which either first or second increments did not cause creep rupture ($D_\tau \leq 0.85$).

5.3 CREEP RUPTURE

Creep rupture is the condition when strain rate increases abruptly and strains become excessive. As can be seen in Figs. 5-1, 5-2, 5-5 and 5-6, this phenomenon occurred for stress levles ($\overline{D}_\tau$) of 85 percent or more.

5.3.1 Singh-Mitchell Creep Rupture Relation

As mentioned in Section 2.2 on creep rupture, Singh and Mitchell define creep rupture as a sudden increase in the slope

of the log $\dot{\gamma}t$ versus log time plot as shown in Fig. 2-11. They claim that the value of $\dot{\gamma}t$ (or $\dot{\varepsilon}t$) at which the change in slope occurs is unique for a given soil.

In the EABPL test program eleven samples were brought to failure through creep rupture. For each case a value of $(\dot{\gamma}t)_f$ (i.e. the point at which there is a sudden increase in slope) was obtained from the appropriate plot by laying off tangents to the two line segements of significantly different slope. For the four tests in which the samples were brought to failure under the initial load increment, a consistent $(\dot{\gamma}t)_f$ of 5.2$\pm$ % was obtained independent of stress level and OCR (see Table 5-1). There occurred only one test ($\overline{CK_oU}$DSS-19) in which a steady state condition was reached by an additional increment just prior to failure (see Fig. 5-15). In all other cases the additional increment which led to failure never attained a strain rate consistent with the Singh-Mitchell Theory before it reached the failure condition. Because of this, the resultant curve of log $\dot{\gamma}t$ versus log time was much too smooth and yielded a value of $(\dot{\gamma}t)_f$ which is much too low as shown by $\overline{CK_oU}$DSS-10 in Table 5-1 and Fig. 5-15. By contrast, the log $\dot{\gamma}t$ versus log time curve for $\overline{CK_oU}$DSS-19 quickly changed slope at t = 500 minutes when steady state was reached and assumed

a "first increment-like" appearance as shown in Fig. 5-15. The resultant $(\dot{\gamma}t)_f$ of 6.0 percent was also consistent with first load increments. All other tests which were failed by additional increment were rejected due to the fact that steady state was not reached prior to failure.

It was interesting to note that the average total strain at $t = t_f$ (see Table 5-1) for the five tests (all those in Table 5-1 excluding $\overline{CK_oU}$DSS-10) was approximately 20 percent which was the average strain at τ_{max} obtained for the controlled strain $\overline{CK_oU}$DSS tests at OCR = 1 and 2. Apparently the occurrence of a unique $(\dot{\gamma}t)_f$ which has units of strain is coincident with a unique undrained γ_f which are 5.2 percent and 20 percent, respectively, for EABPL soil.

5.3.2 Saito's Creep Rupture Relation

As presented in Section 2.2, Saito (1961) has developed an empirical relation for creep rupture. The equation is $\log t_r = 0.50 - 0.916 \log \dot{\varepsilon} \pm 0.59$. The value of ε is the strain rate at which the slope on the log-log plot of strain rate versus time becomes zero (i.e. constant $\dot{\varepsilon}$ with time). This phenomenon can be seen in Fig. 5-2 for values of $\overline{D}_\tau$ greater than 80 percent. The variable "t_r" is the

elapsed time that will occur from the attainment of a constant strain rate to creep rupture ($\dot{\varepsilon} \rightarrow \infty$).

This relation was applied to the eleven EABPL tests and the predicted times to failure compared to those actually obtained in the laboratory (see Table 5-2). In all cases the time to failure fell within the range presented by the Saito relationship, but that range is so large, due to the gererality of the equation, that it is of little use. The $\pm$ 0.59 in Saito's relation represents a time range of more than one log cycle. For short times to failure such as that in $\overline{CK_oU}$DSS-17 this range only constitutes two hours, but at large times to failure of perhaps one to four weeks, a log cycle of 90,000 minutes, or more than two months is the range.

Another major drawback with the Saito relation is that failure is not indicated until it is obvious. By inspection of Fig. 5-1, it can be seen that failure was imminent for all stress levels of 85 percent or more as early as 10 minutes after their application to the sample.

5.3.3 Strength Decrease Due to Creep

Inspection of Table 5-3 shows that stress levels of 85 percent or more caused creep rupture. Since the values of $\bar{\phi}$ at failure were approximately those obtained in conventional undrained direct-simple shear tests, these failures were due to the generation of pore pressure of much greater magnitude than are normally obtained for a given stress level. This process can be seen quite easily by inspection of the creep stress paths in Appendix C. For all stress levels, generation of large pore pressure during creep produced stress conditions which are much closer to failure than are obtained in the conventional $\overline{CK_oU}$DSS test. This phenomenon is particularly marked with the first increment, such as that ($\bar{D}_\tau$ = 0.729) in $\overline{CK_oU}$DSS-10.

These results agree quite well with those obtained by Shibata and Karube (1969), Bishop and Lovenbury (1969), and others. It is interesting to note that the average value of $\bar{\phi}_f$ obtained from the creep tests is consistent with that obtained from standard $\overline{CK_oU}$DSS tests. Apparently the failure envelope for undrained shear of a given soil is unique and independent of the mode of failure (controlled stress or controlled strain). The mechanism of failure must be the same for both cases.

It is difficult to believe the concept of a yield value as presented by Shibata and Karube (1969) (see Fig. 2-6). If one accepts the Singh-Mitchell model, which the author does, then given enough time on a log scale, sufficient strains and pore pressures will be generated to bring about a failure condition for any significant stress level ($D_\tau > 30\%$). The threshold value of 85 percent obtained in this investigation is the minimum stress level at which sufficient pore pressures could be generated to cause creep rupture in a convenient time period (less than a week).

5.4 COMPARISON OF SIMPLE SHEAR STRESS LEVELS WITH TRIAXIAL STRESS LEVELS

The original Singh-Mitchell laboratory investigation which was undertaken as part of their rate process development was conducted with triaxial equipment. Therefore, the Singh-Mitchell definition of $\bar{D}(= \Delta q/\Delta q_F)$ differs from that used in this investigation with the Direct-Simple Shear Device.

For CK_oU Direct-Simple Shear Device:

(Pore Shear Assumption)

From Ladd and Edgers (1971),

$$\frac{q}{\bar{\sigma}_{vc}} = \sqrt{\frac{(1-K_o)^2}{4} + \left(\frac{\tau_H}{\bar{\sigma}_{vc}}\right)^2}$$

$$\text{Tan } \theta_p = \frac{\tau_H/\bar{\sigma}_{vc}}{(1-K_o)/2 + q/\bar{\sigma}_{vc}}$$

$\theta_p = 90° - \alpha$, Fig. 5-18 indicates rotation of principal planes.

For CK_oU Triaxial Compression:

$$q_i = \frac{\bar{\sigma}_{vc}\,(1-K_o)}{2}\ ,\ q_f = \frac{S_u}{\bar{\sigma}_{vc}}\ \bar{\sigma}_{vc}$$

$$\Delta q_f = q_f - q_i = \bar{\sigma}_{vc}\left[\frac{S_u}{\bar{\sigma}_{vc}} - \frac{(1-K_o)}{2}\right]\ ,\ \Delta q = \bar{D}_o \cdot \Delta q_f$$

$$\bar{D} = \frac{q}{q_f} = \frac{q_i + \Delta q}{q_i + \Delta q_f}$$

$$\bar{D} = \frac{\frac{1-K_o}{2} + \bar{D}_o\left[\frac{S_u}{\bar{\sigma}_{vc}} - \frac{1-K_o}{2}\right]}{(S_u/\bar{\sigma}_{vc})}$$

Calculations are shown in Table 5-4.

Though the exact state of stress in the direct-simple shear sample is not known at any time during shear, the

direct shear assumption probably gives one the closest approximation to the actual stress state.

As one can see in Fig. 5-18, the difference in stress states for the triaxial and direct simple shear samples is not extremely large for the ranges of stress level with which the test program was concerned ($\overline{D}_\tau \geq 50\%$). This difference reduces considerably with increasing stress level and OCR.

5.5 USE OF MULTI-INCREMENT TESTING

By utilizing the Singh-Mitchell equations,a series of "first increment" strain-log time curves can be developed from one test. This can be accomplished by applying a series of three or four shear stress increments to one sample and allowing creep to develop for each loading. If each increment (after the first) is allowed to pass through its transient state and begin to behave in the manner predicted by Singh and Mitchell, an "m" value for each stress level ($\overline{D}_\tau$) can be found and plotted as in Fig. 5-13. The various log-log plots of strain rate versus time for the steady state at large times can then be extended back to small times ($t < 400$ minutes), and a plot such as Fig. 5-16 can be

obtained. From these data the parameters "A" and "α" are calculated as in Fig. 5-4. The final data to be obtained are the initial shear strains at t = 1 minute which are shown in Fig. 5-17.

These various parameters can then be used in conjunction with the Singh- Mitchell equation for strains:

$$\gamma_t = \gamma_o - \frac{Ae^{\bar{\alpha}\bar{D}}}{1-m}\left[1 - \left(\frac{t_1}{t}\right)^m t\right]$$

Since the creep parameter "m" is not constant but varies with stress level, $\bar{D}_\tau$, the values of strain rate at a given time become more divergent with time in Fig. 5-4. Although the curved plots at larger times in Fig. 5-4 are no doubt correct, the resulting slopes, $\bar{\alpha}$, do not represent the curves for stress levels greater than 50 percent. In order to obtain representative slopes, a "best-fit" line must be drawn through the data points for t = 10,000 minutes (see dashed line in Fig. 5-4). Such a procedure yields an average value for "$\bar{\alpha}$" of 4.6 which is approximately the value obtained for t = 1 minute.

This resultant parameter modification along with the other creep parameters previously mentioned yielded the theoretical creep strains tabulated in Table 5-5 for

$\overline{D}_\tau$ = 0.50, 0.65, 0.72 and 0.80. The resultant curves are compared with the laboratory strain-log time curves in Fig. 5-19.

The results compare quite well at large times which is the result of the cancellation of two errors.

(1) The initial shear strains (γ_o) are too large due to the fact that they are obtained from second and third increments and not first loadings. The discrepancy can be seen in Fig. 5-17 where the two curves are compared.

(2) The initial creep rate (t < 400 minutes) is too slow. This is due to the fact that for a given stress level, the parameters used to calculate strains are for that increment in the steady state. In the laboratory, the internal obliquity ($\tau_h/\overline{\sigma}_v$) is initially higher than that applied, and therefore, the creep rate is greater.

As a result, the theoretical curves start out too high but lag behind in the first 400 minutes. After that period the two curves are parallel and in most cases, very similar in magnitude.

A further example of this point concerning the initial development of pore pressures can be made by attempting to duplicate a first loading curve with modified data. If one takes the initial shear strain from the first loading condition (γ_o = 1.71%) (see Fig. 5-17) for $\overline{D}_\tau$ = 0.65 and uses the "m" obtained for $\overline{D}_\tau$ = 0.72 for the first 400 minutes and "m" for $\overline{D}_\tau$= 0.65 for the remainder of the time period, one duplicates the first loading curve. These results are shown in Table 5-6.

Since field problems are concerned with strain-log time curves at times much larger than 400 minutes, the multi-increment approach can prove to be quite useful. Strains at much greater times can be calculated from the Singh-Mitchell equation for strain and the initial portion of the curve can be completely ignored by setting $t_1 \geq$ 1000 minutes, which would be a common procedure for field problems.

TABLE 5-1: APPLICATION OF SINGH-MITCHELL CREEP RUPTURE THEORY TO EABPL TEST DATA

TEST NO.	STRESS LEVEL (1)	$(\dot{\gamma}t)_f$: %	t_f: MIN. (2)	γ_f: % (3)	COMMENTS
CUDSS-11	0.941	4.7	580	19+	FIRST INCREMENT
CUDSS-17*	0.941	5.5	55	18.0	FIRST INCREMENT
CUDSS-20	0.90	5.0	130	20.5	FIRST INCREMENT
CUDSS-21	0.85	5.6	1600	26.0	FIRST INCREMENT
CUDSS-19*	0.94	6.0	1400	15.0	THIRD INCREMENT
CUDSS-10	0.941	1.0	410	13.4	SECOND INCREMENT (No Steady State)

(1) (τ_H)applied$/\tau_{H\ max}$

(2) Time when $(\dot{\gamma}t)_f$ occurs

(3) Strain at t_f

* OCR = 2

TABLE 5-2: COMPARISON OF LABORATORY CK_oUDSS CREEP-RUPTURE BEHAVIOR TO SAITO'S CREEP-RUPTURE RELATIONSHIP

TEST NO.	(1) STRESS LEVEL	(2) t_f(MIN)	(3) $\dot{\varepsilon}$(%/MIN)	(4) t_o(MIN)	(5) SAITO'S t_f(MIN)
CUDSS-10	0.941	439-531	0.003	42	(689) 200-2560
CUDSS-11	0.941+	460-893	0.0073	394	(676) 468-1508
CUDSS-12	0.941	1870-2855	0.00163	1030	(2173) 1320-5430
CUDSS-16	0.95	1620	0.00305	75	(713) 239-2553
CUDSS-17*	0.941+	68	0.0805	30	(62) 38-154
CUDSS-18*	0.94	441-1205	0.009	30	(267) 91-950

(1) τ_H applied/τ_{max}

(2) Elapsed Time to Failure

(3) $\dot{\varepsilon}$ = Constant Strain Rate Value Which Occurs Prior to Failure

(4) t_o = Elapsed Time at Which $\dot{\varepsilon}$ Occurs

(5) $t_f = t_o + t_r$, Where $\log t_r = 0.50 - 0.916 \log \dot{\varepsilon} \pm 0.59$, Computed Value is in Parentheses

\+ Initial Increment

* OCR = 2, $\bar{\sigma}_{vm} = 2 kg/cm^2$

TABLE 5-2: COMPARISON OF LABORATORY CK_oUDSS CREEP-RUPTURE BEHAVIOR TO SAITO'S CREEP-RUPTURE RELATIONSHIP (Continued)

TEST NO.	(1) STRESS LEVEL	(2) t_f (MIN)	(3) $\dot{\varepsilon}$ (%/MIN)	(4) t_o (MIN)	(5) SAITO'S t_f (MIN)
CUDSS-19*	0.94	1885-2865	0.00247	810	(1582) 1009-3816
CUDSS-20	0.90+	185	0.0321	105	(179) 124-392
CUDSS-21	0.85+	1974-2574	0.00272	720	(1421) 902-3474
CUDSS-22	0.90	1112-1545	0.0012	100	(1598) 484-5910
CUDSS-23	0.95	780-1580	0.0025	35	(800) 232-3010

(1) τ_H applied/τ_{max}

(2) Elapsed Time to Failure

(3) $\dot{\varepsilon}$ = Constant Strain Rate Value Which Occurs Prior to Failure

(4) t_o = Elapsed Time at Which $\dot{\varepsilon}$ Occurs

(5) $t_f = t_o + t_r$, Where $\log t_r = 0.50 - 0.916 \log \dot{\varepsilon} \pm 0.59$, Computed Value is in Parentheses

\+ Initial Increment

* OCR = 2, $\bar{\sigma}_{vm} = 2 kg/cm^2$

TABLE 5-3: STRENGTH DECREASE DUE TO CREEP

TEST NO.	$\bar{\sigma}_{vc}$	$\bar{\sigma}_{vm}$	LOAD HISTORY	$\bar{\phi}_f=\tan^{-1}(\tau_h/\bar{\sigma}_v)$
(OCR=1)	(kg/cm^2)		(Values of $\bar{D}_\tau$)	
CK_oUDSS-8*	2.0	2.0	0.49,0.73,0.82	20.0
CK_oUDSS-10	2.0	2.0	0.73,0.94	19.75
CK_oUDSS-11	2.0	2.0	0.94	21.7
CK_oUDSS-12	2.0	2.0	0.73,0.94	21.8
CK_oUDSS-16	2.0	2.0	0.50,0.65,0.80,0.95	24.4
CK_oUDSS-20	2.0	2.0	0.90	22.5
CK_oUDSS-21	2.0	2.0	0.85	22.5
CK_oUDSS-22	2.0	2.0	0.80,0.90	22.25
CK_oUDSS-23	2.0	2.0	0.65,0.80,0.95	23.3
			Average	22.0° vs. 21.6°+
(OCR=2)				
CK_oUDSS-17	1.0	2.0	0.94	24.75
CK_oUDSS-18	1.0	2.0	0.72,0.94	23.3
CK_oUDSS-19	1.0	2.0	0.50,0.72,0.94	27.4
			Average	25.1° vs. 25.1°+

* Failed at Controlled Strain

\+ Obtained for Constolled Strain CK_oUDSS Tests on EABPL Clay at $(\tau_h)_{max}$.

TABLE 5-4: RELATIONSHIPS BETWEEN $\bar{D}$, $\bar{D}_o$, $\bar{D}_\tau$ AND ROTATION OF PRINCIPAL PLANES IN $\overline{CK_oU}$ DSS TESTS

EABPL CLAY	$\overline{CK_oU}$ Direct Simple Shear							$\overline{CK_oU}$ Triaxial Compression	
	$\bar{D}_\tau$	$\frac{\tau_h}{\bar{\sigma}_{vc}}$	$\frac{q}{\bar{\sigma}_{vc}}$	$\bar{D}=\frac{q}{q_f}$, %	$\frac{\Delta q}{\bar{\sigma}_{vc}}$	$\bar{D}_o=\frac{\Delta q}{\Delta q_f}$, %	$\alpha^o = 90-\theta_p^o$	$\bar{D}_o$, %	$\bar{D}$, %
OCR=1.0	0	0	0.165	56.3	0	0	90	0	68.8
	50	0.12	0.204	69.8	.039	30.6	72.1	25	76.6
K_o=0.67	75	0.18	0.244	83.2	.079	62.1	66.3	50	84.4
	90	0.216	0.272	93.0	.107	84.1	63.8	65	89.1
$\frac{s_u}{\bar{\sigma}_{vc}}$ =0.24	100	0.24	0.292	100	.127	100	62.4	80	93.8
								90	96.9
								95	98.4
								100	100.0
OCR=2.0	0	0	0.050	11.5	0	0	90	0	11.5
K_o=0.9	25	0.109	0.121	27.6	0.071	18.3	57.6	25	33.6
	50	0.217	0.223	50.9	0.173	44.9	51.5	50	55.8
$\frac{s_u}{\bar{\sigma}_{vc}}$ =0.434	75	0.326	0.329	75.8	0.279	72.5	49.3	65	69.0
	90	0.391	0.394	90.2	0.344	89.0	48.7	80	82.4
	100	0.434	0.437	100	0.387	100	48.3	90	91.3
								95	95.6
								100	100.0
OCR=4.0 K_o=1.0	$\bar{D}_\tau = \bar{D} = \bar{D}_o$, $\alpha = 45^o$							$\bar{D}_o = \bar{D}$	

TABLE 5-5: COMPUTATONS FOR THEORETICAL STRAIN-LOG TIME CURVES

$$\gamma_t = \gamma_o - \frac{Ae^{\bar{\alpha}\bar{D}}}{1-m}\left[1 - \left(\frac{t_1}{t}\right)^m\right] t \quad ; \bar{\alpha} = 4.6,\ A = .014\%/\text{MIN}.$$

$\bar{D}_\tau = 0.05$ $\gamma_o = 0.8\%$ $m = 0.937$

t(MIN)	γ(%)
10	1.152
100	1.547
1000	2.004
10000	2.542

$\bar{D}_\tau = 0.65$ $\gamma_o = 2.1\%$ $m = 0.924$

t(MIN)	γ(%)
10	2.796
100	3.639
1000	4.628
10000	5.811

$\bar{D}_\tau = 0.72$ $\gamma_o = 3.0\%$ $m = 0.915$

t(MIN)	γ(%)
10	4.003
100	5.165
1000	6.608
10000	8.120

$\bar{D}_\tau = 0.80$ $\gamma_o = 4.85\%$ $m = 0.882$

t(MIN)	γ(%)
10	6.318
100	8.246
1000	10.777
10000	14.083

TABLE 5-6: DUPLICATION OF $\overline{D}_\tau$ = 65% STRESS LEVEL

γ_o = 1.71% $\quad \overline{\alpha}$ = 4.6 $\quad$ A = 0.014 $\quad \overline{D}_\tau$ = 0.65

$$\gamma_t = \gamma_o - \frac{Ae^{\overline{\alpha}\overline{D}}}{1-m}\left[1 - \left(\frac{t_1}{t}\right)^m\right] t$$

t	m	γ Theory (%)	γ Lab (%)
1	-	1.71	1.71
10	.915	2.70	2.45
100	.915	3.86	3.75
1000	(.915+.924)/2	5.06	5.05
10000	.924	6.23	6.10

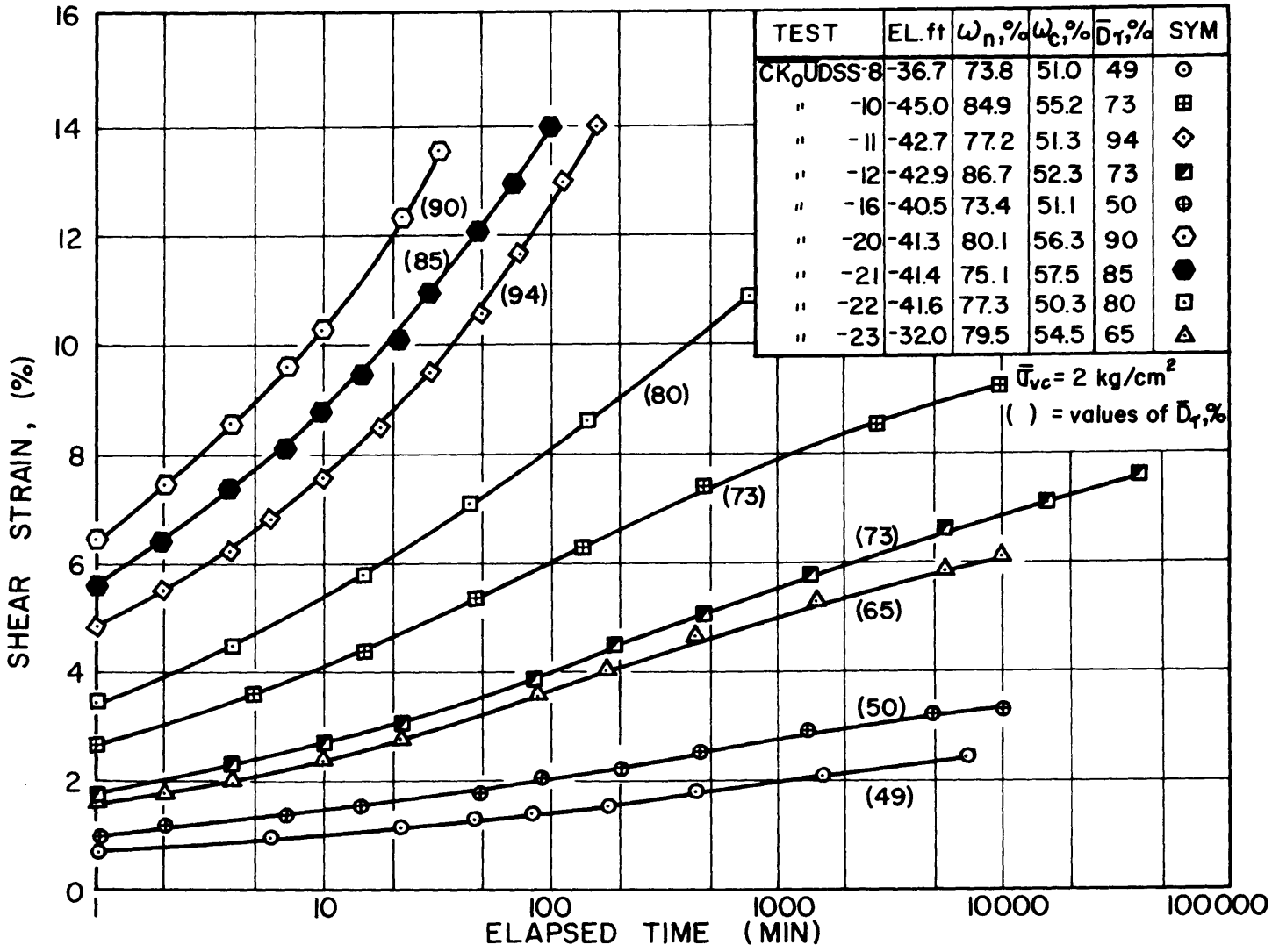

SHEAR STRAIN VS. LOG TIME FROM $\overline{CK_oUDSS}$ CREEP TESTS ON N.C. EABPL CLAY

Figure 5-1

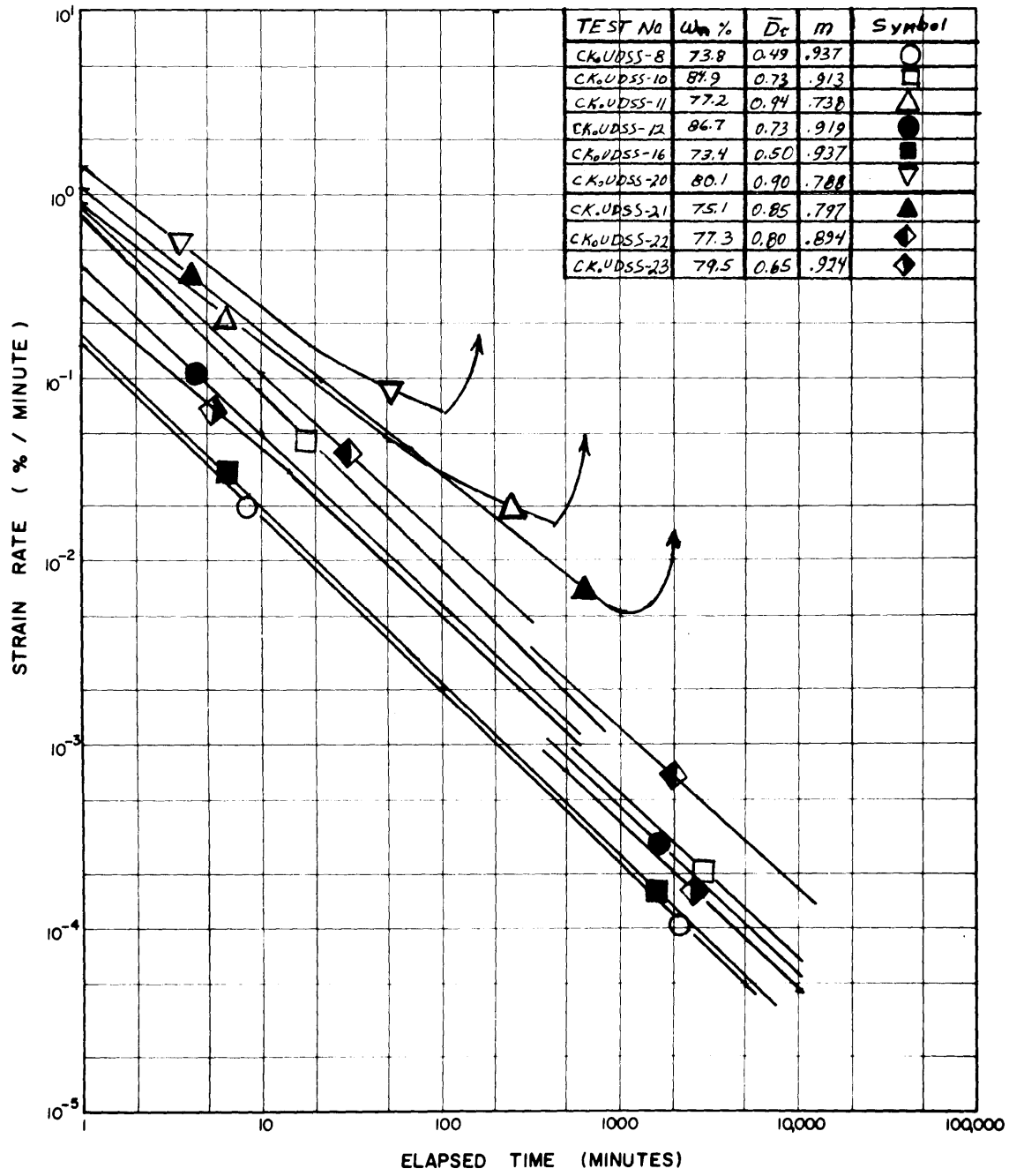

Log Strain Rate vs. Log Time from $\overline{CK_oUDSS}$ Creep Tests on NC EABPL Clay

Figure 5-2

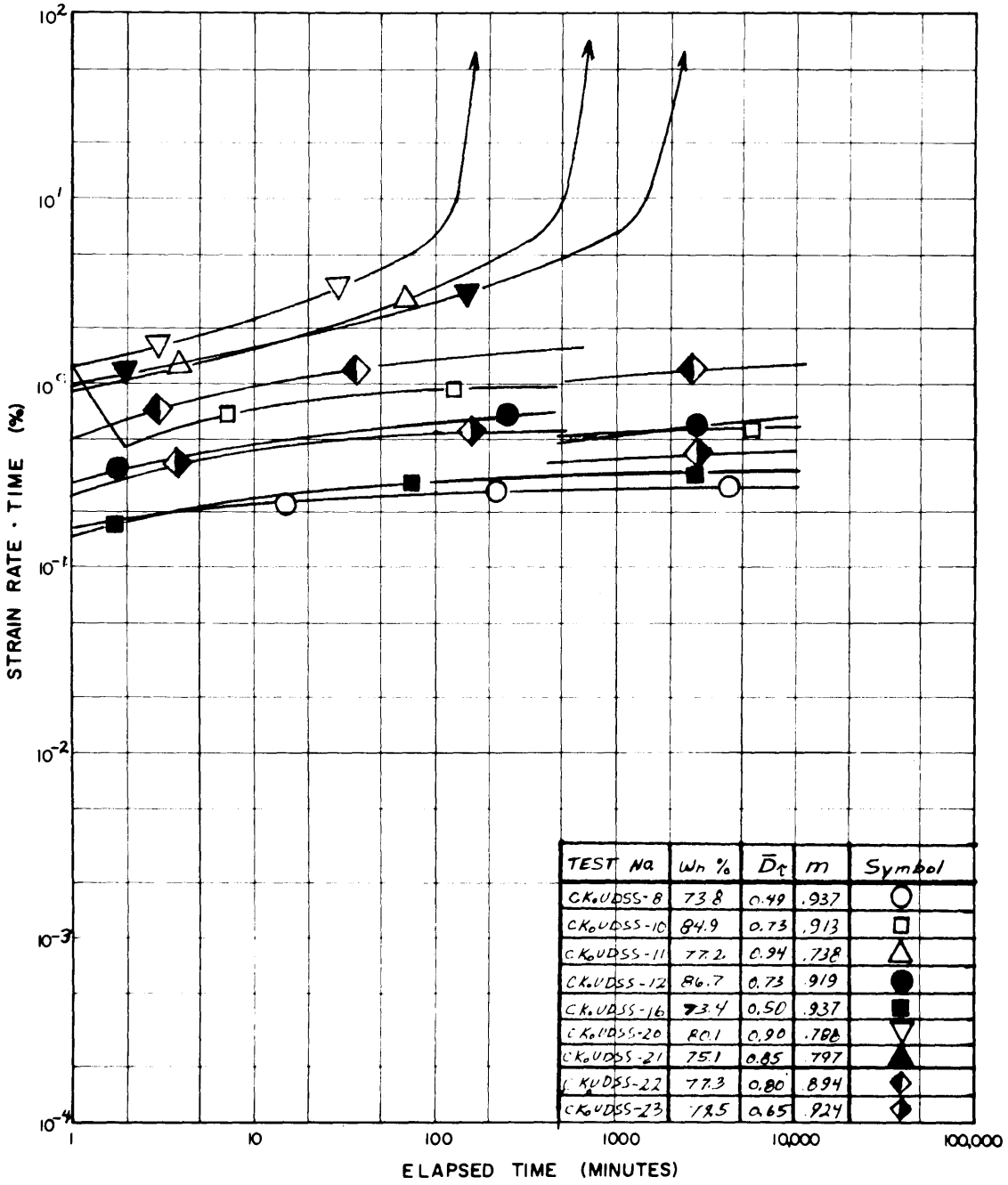

Log (Strain Rate x Time) vs. Log Time from $\overline{CK_oU}$DSS Creep Tests on NC EABPL Clay

Figure 5-3

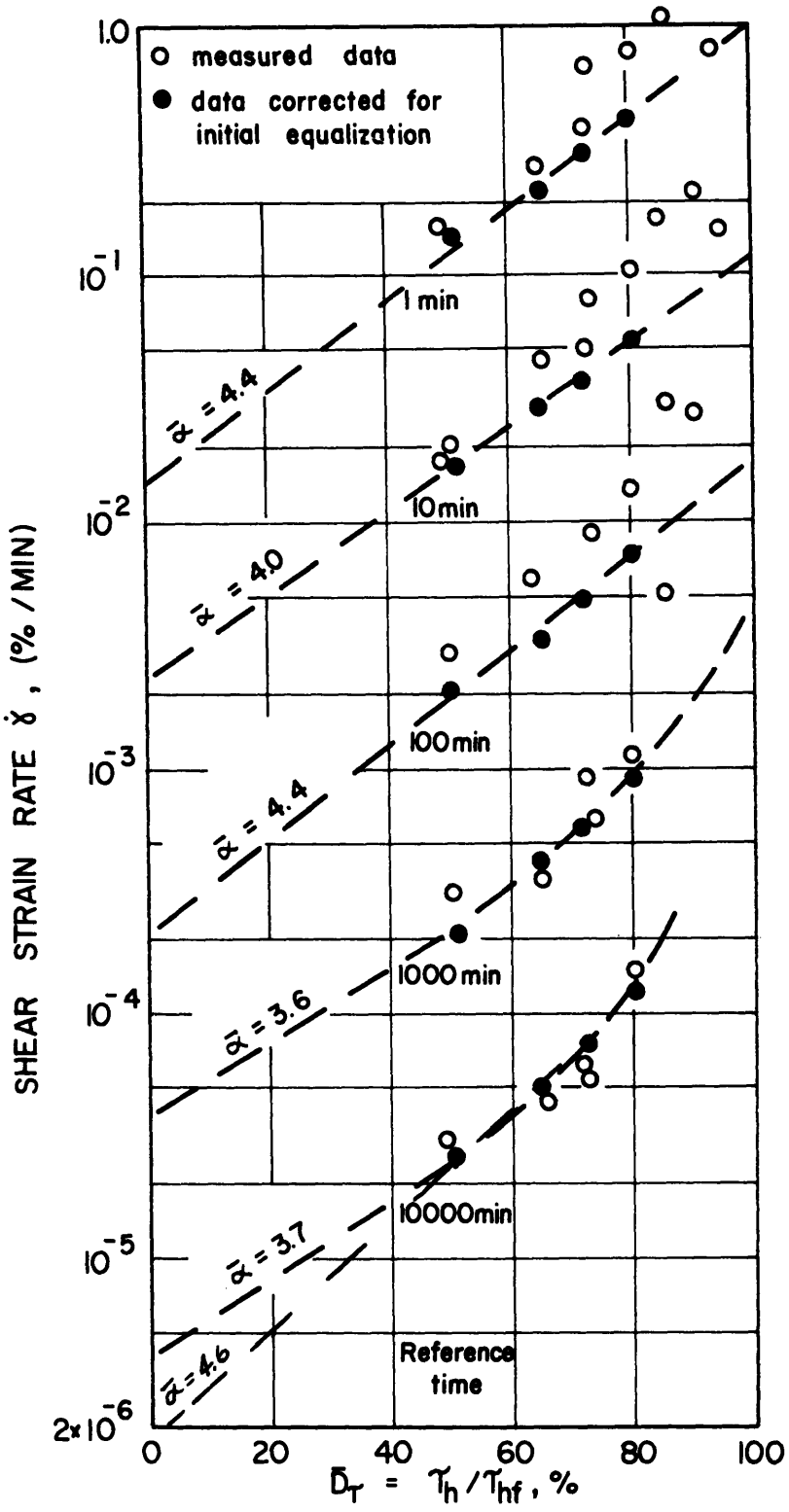

LOG SHEAR STRAIN RATE VS. APPLIED STRESS LEVEL FROM $\overline{CK_0U}$DSS CREEP TESTS ON N.C. EABPL CLAY

Figure 5-4

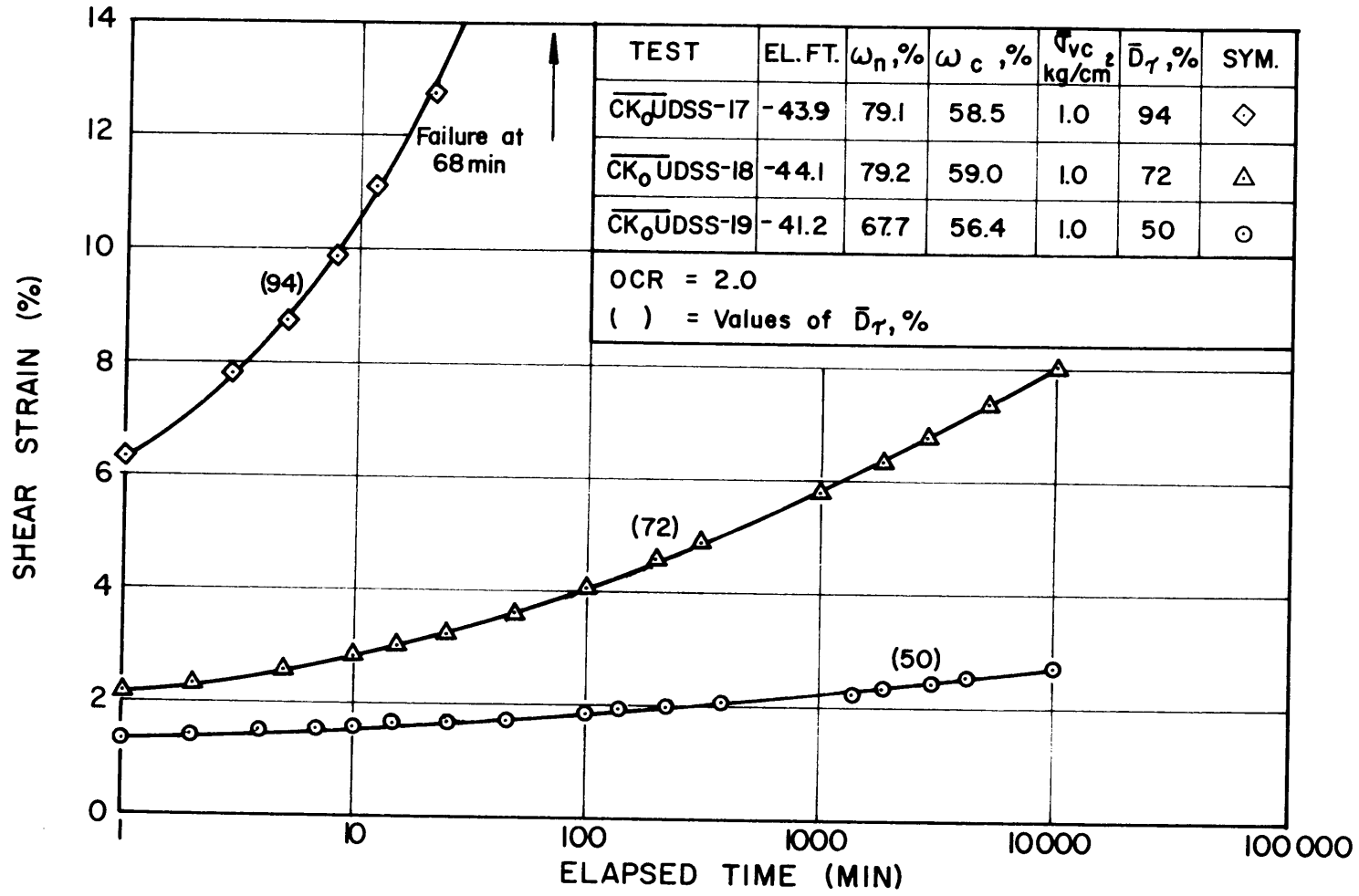

SHEAR - STRAIN VS. LOG TIME FROM $\overline{CK_oU}$DSS CREEP TESTS ON O.C. EABPL CLAY

Figure 5-5

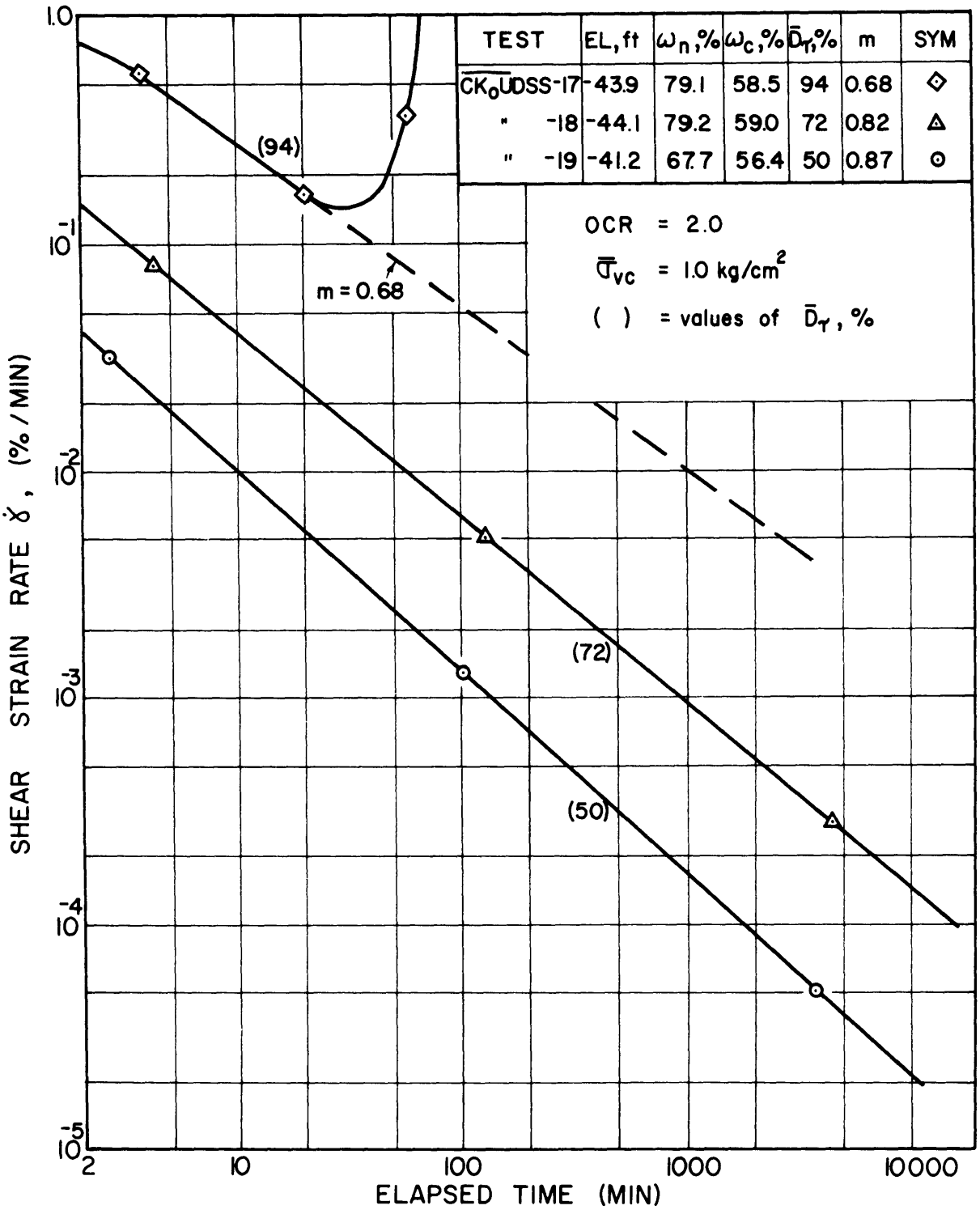

LOG SHEAR STRAIN RATE VS. LOG TIME FROM $\overline{CK_oUDSS}$ CREEP TESTS ON O.C. EABPL CLAY

Figure 5-6

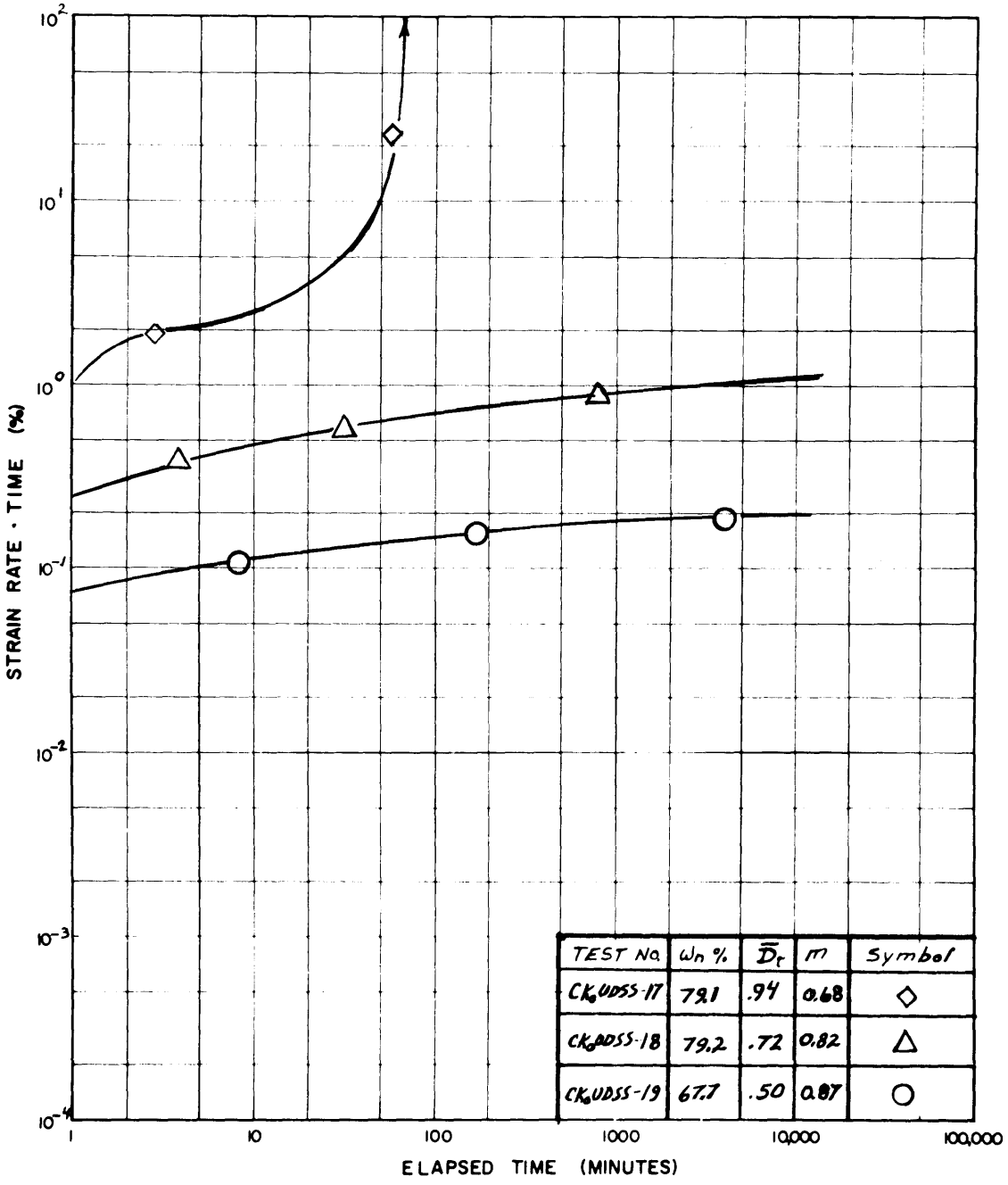

Log (Strain Rate x Time) vs. Log Time from $\overline{CK_oU}$DSS Creep Tests on OC EABPL Clay

Figure 5-7

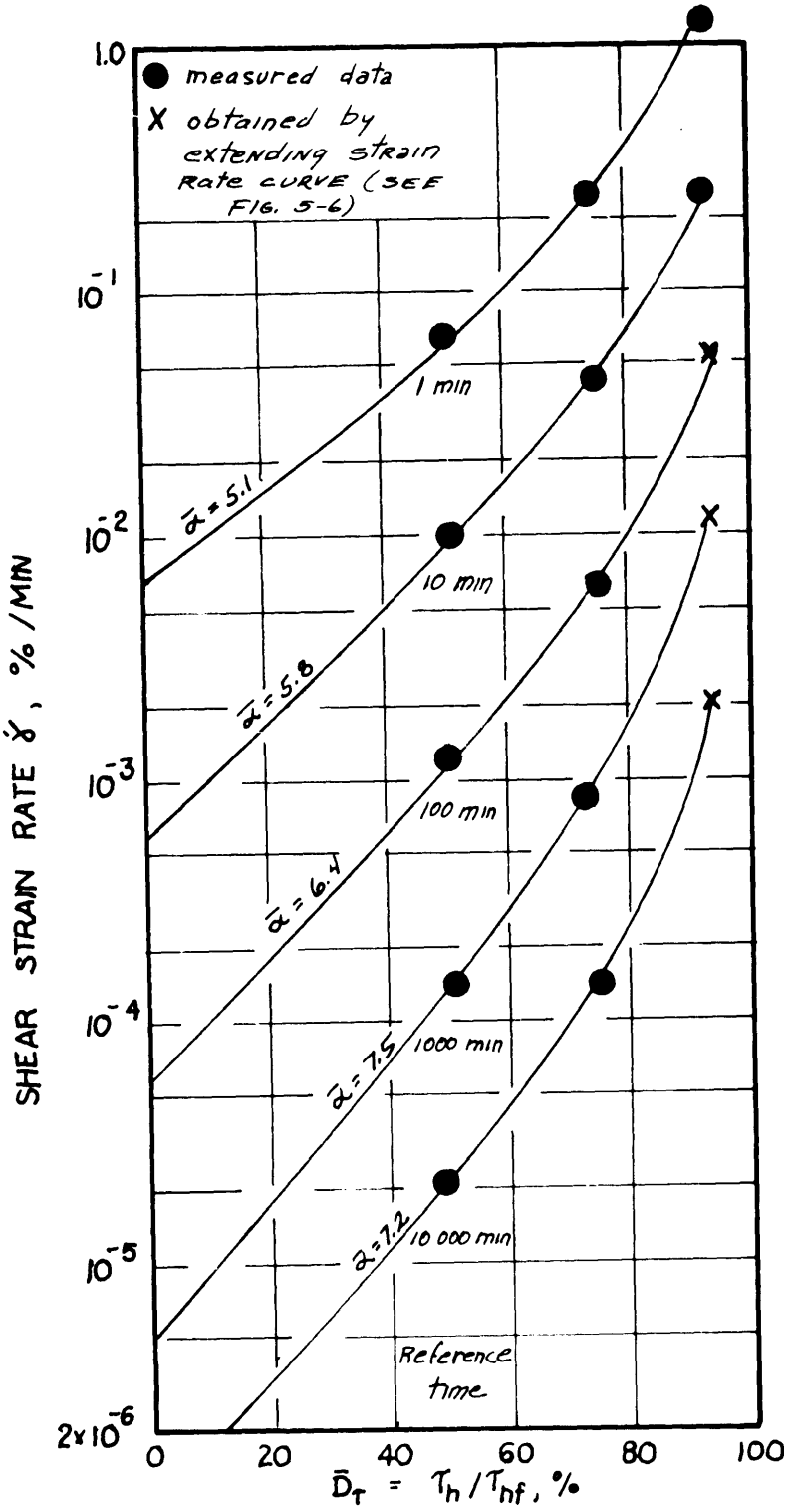

Log Strain Rate vs. Applied Stress Level From $\overline{CK_oU}$DSS Creep Tests on OC EABPL Clay

Figure 5-8

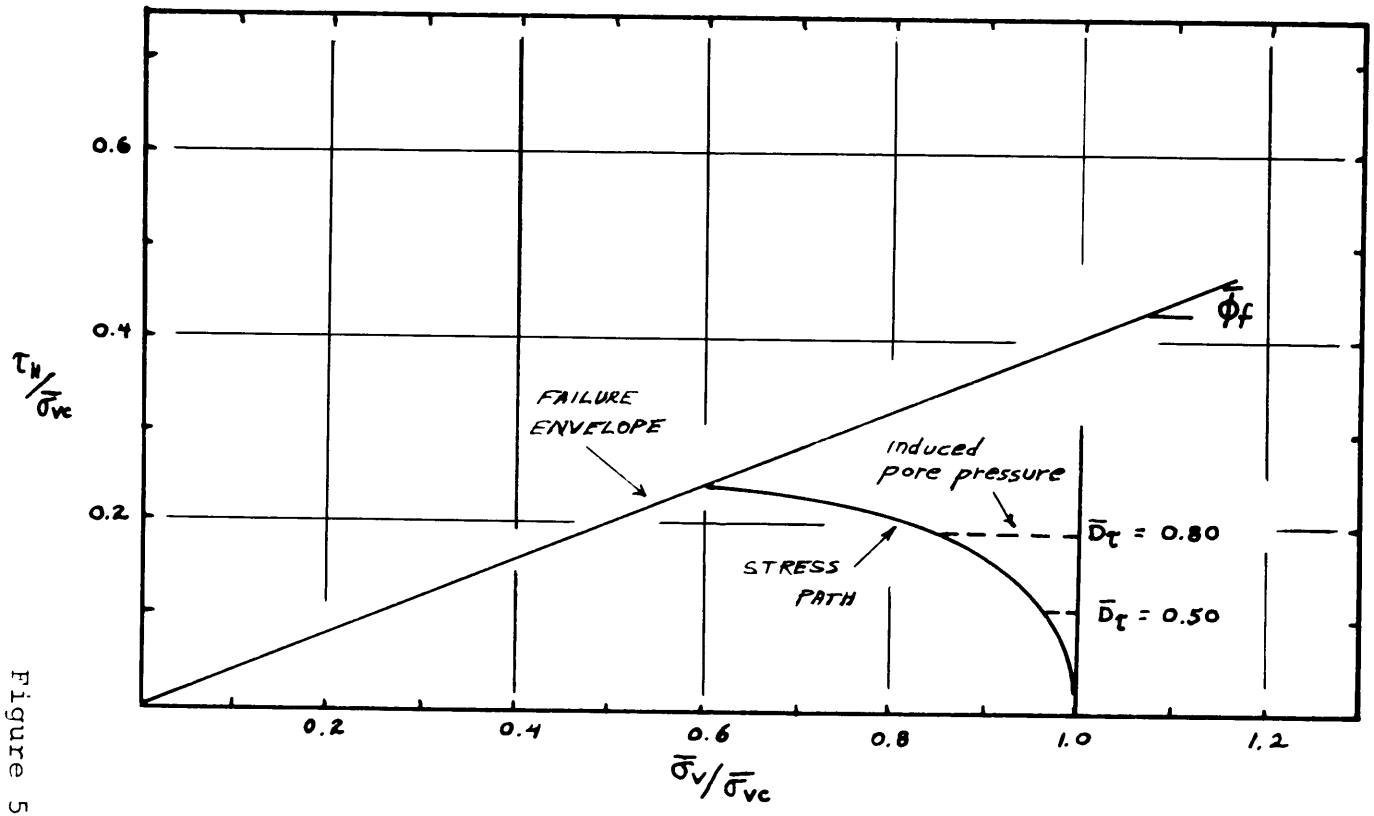

Figure 5-9

Comparison of Induced Pore Pressures for Various Creep Stress Levels

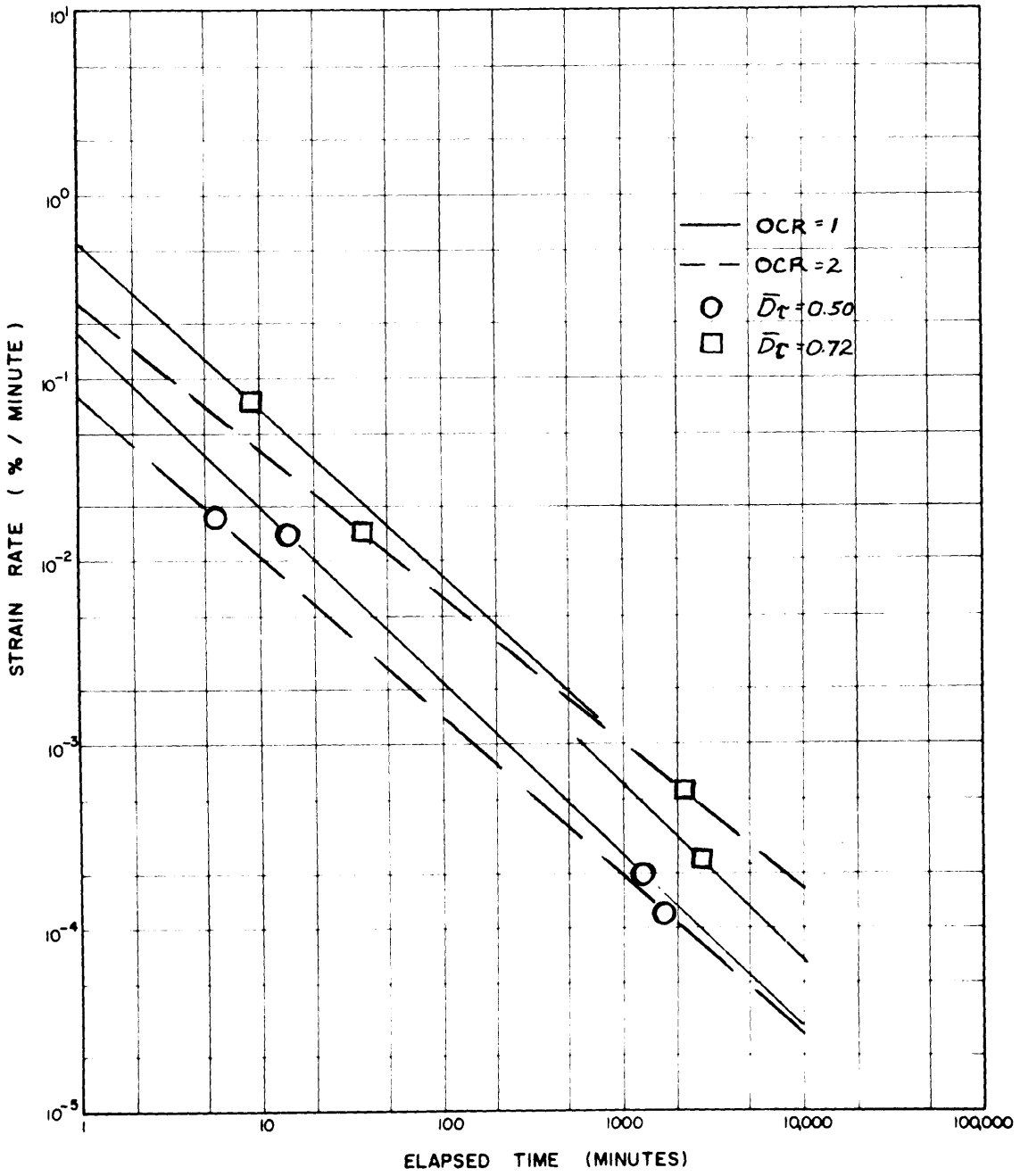

Comparison of Plots of Log Strain Rate Vs. Log Time for NC and OC Samples of FABPL Clay

Figure 5-10

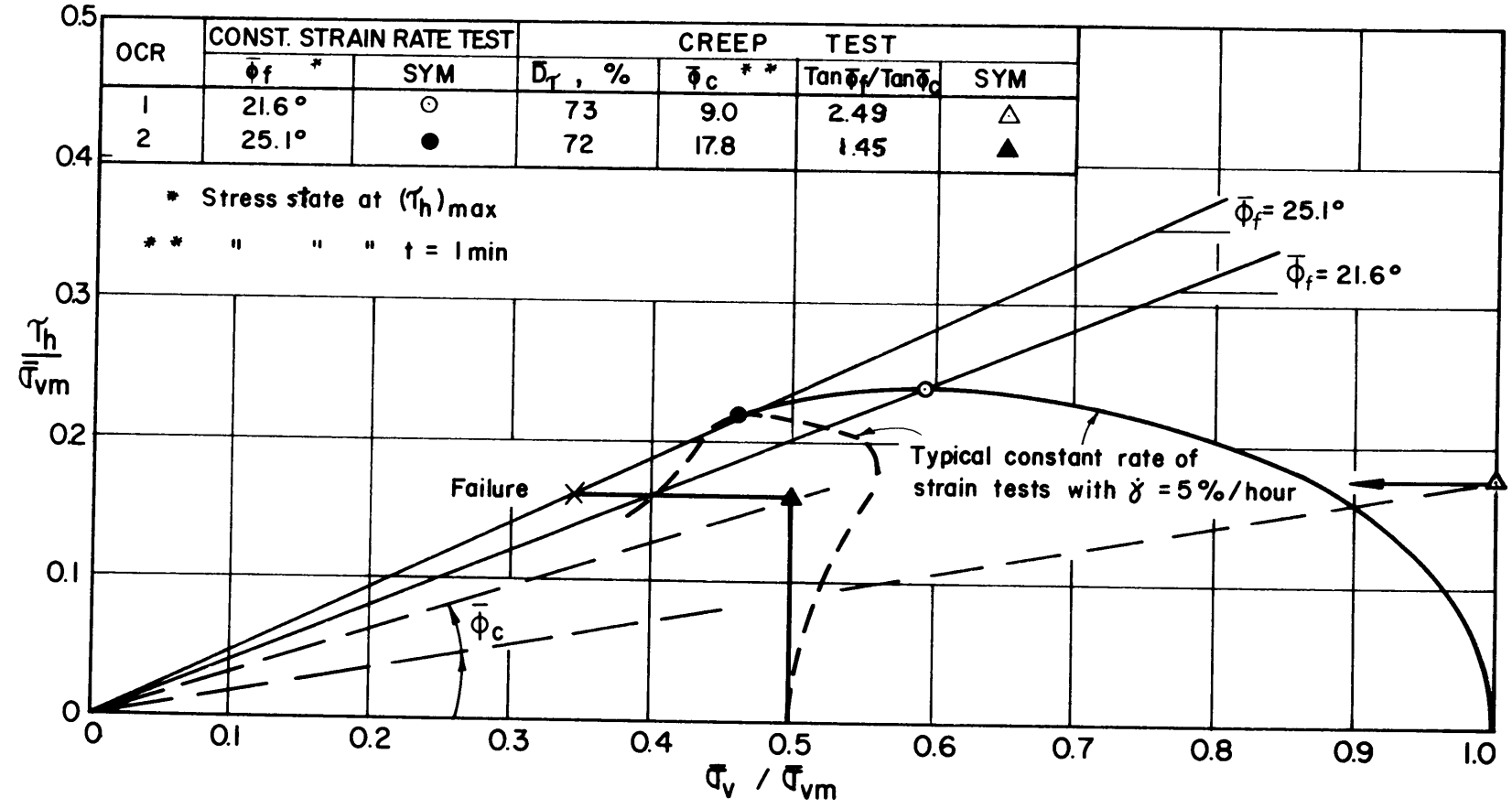

COMPARISON OF STRESS PATHS FROM $\overline{CK_oU}$DSS CREEP TESTS ON N.C. AND O.C. EABPL CLAY

Figure 5-11

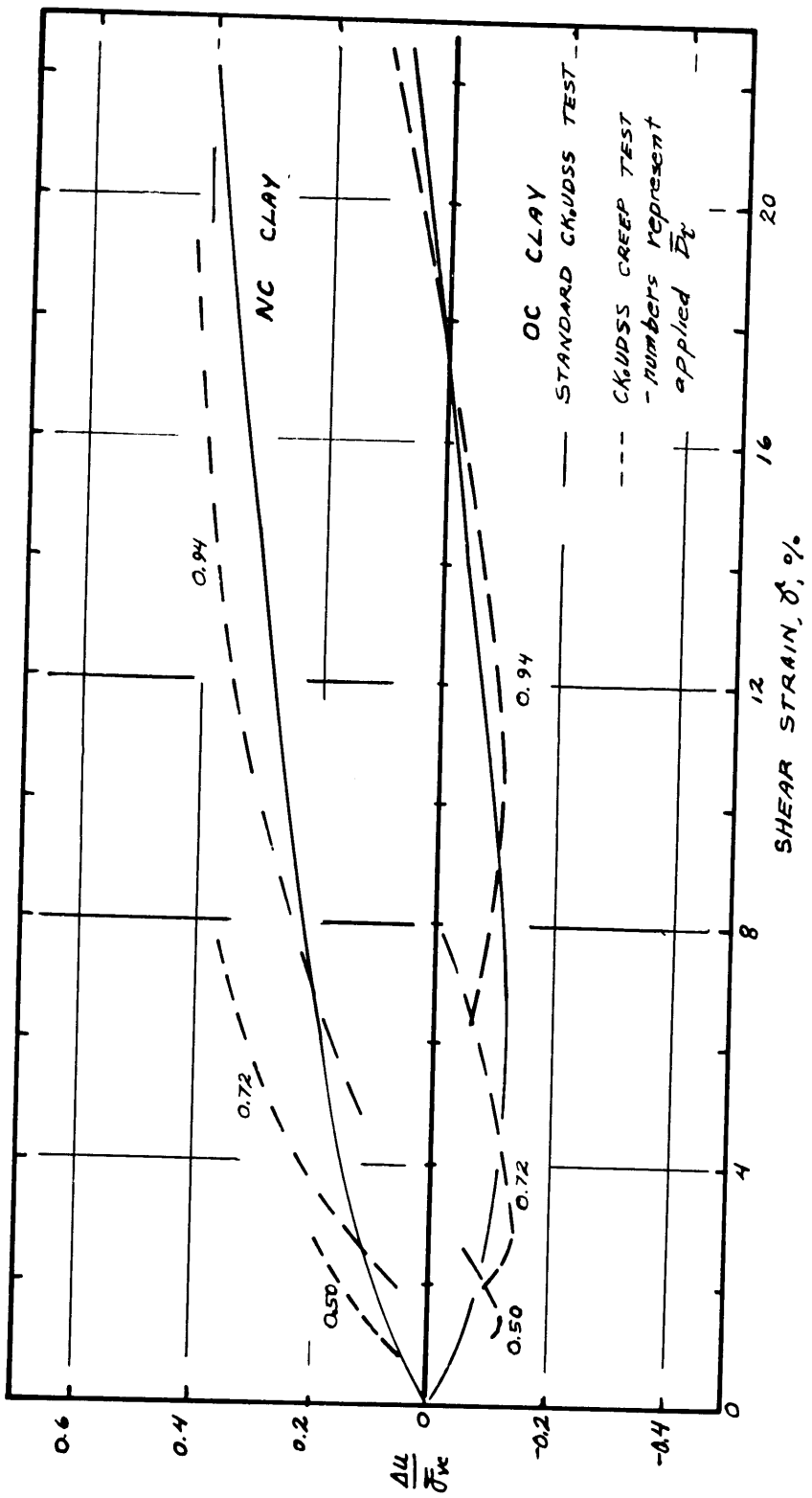

Comparison of Pore Pressure Generation During Creep of NC and OC Samples of EABPL Clay at Various Stress Levels

Figure 5-12

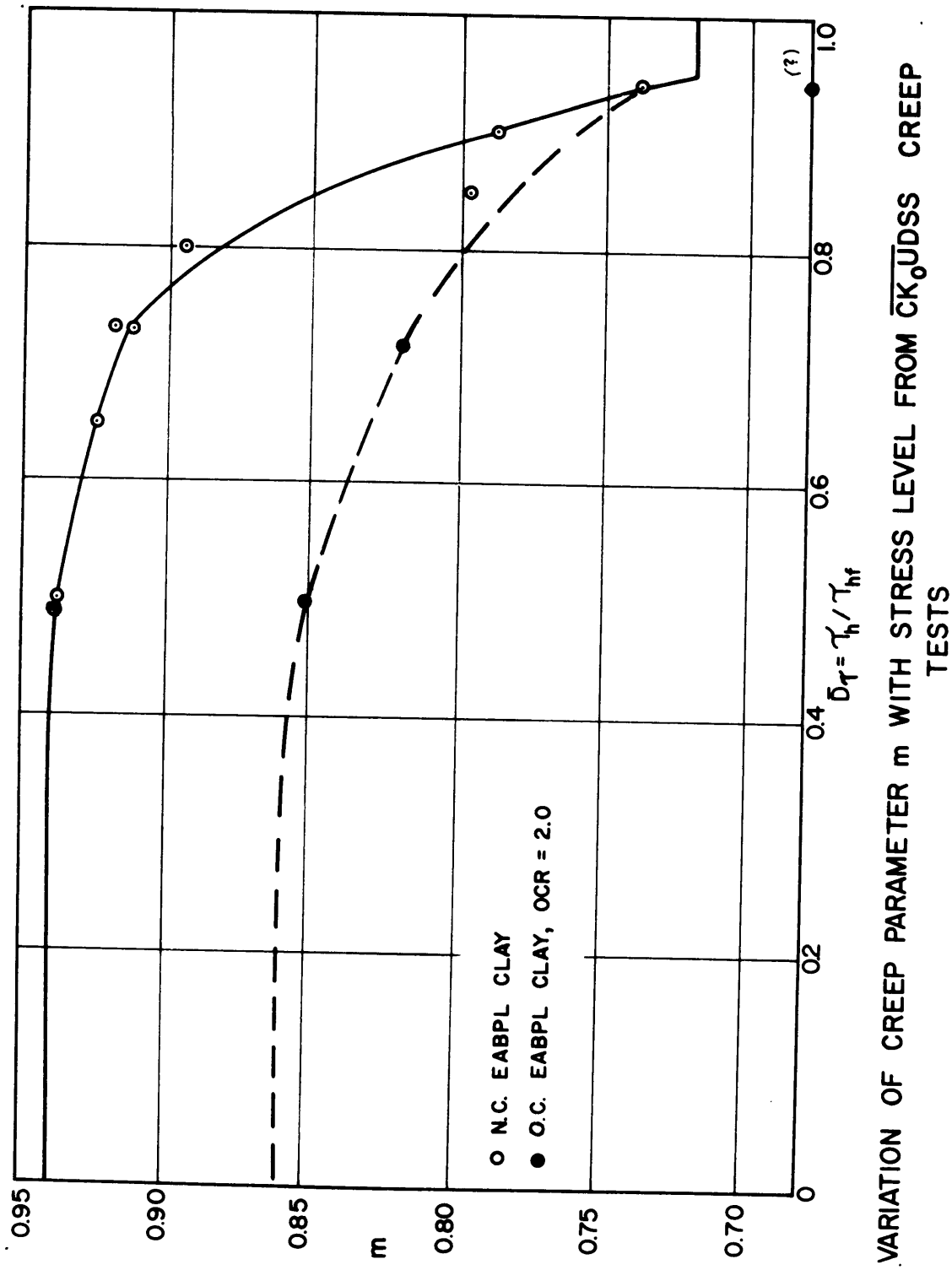
VARIATION OF CREEP PARAMETER m WITH STRESS LEVEL FROM $\overline{CK_0UDSS}$ CREEP TESTS
m
$\delta_\tau = \tau_h / \tau_{hf}$
0.95
0.90
0.85
0.80
0.75
0.70
0
0.2
0.4
0.6
0.8
1.0
(?)
O N.C. EABPL CLAY
● O.C. EABPL CLAY, OCR = 2.0

Figure 5-13

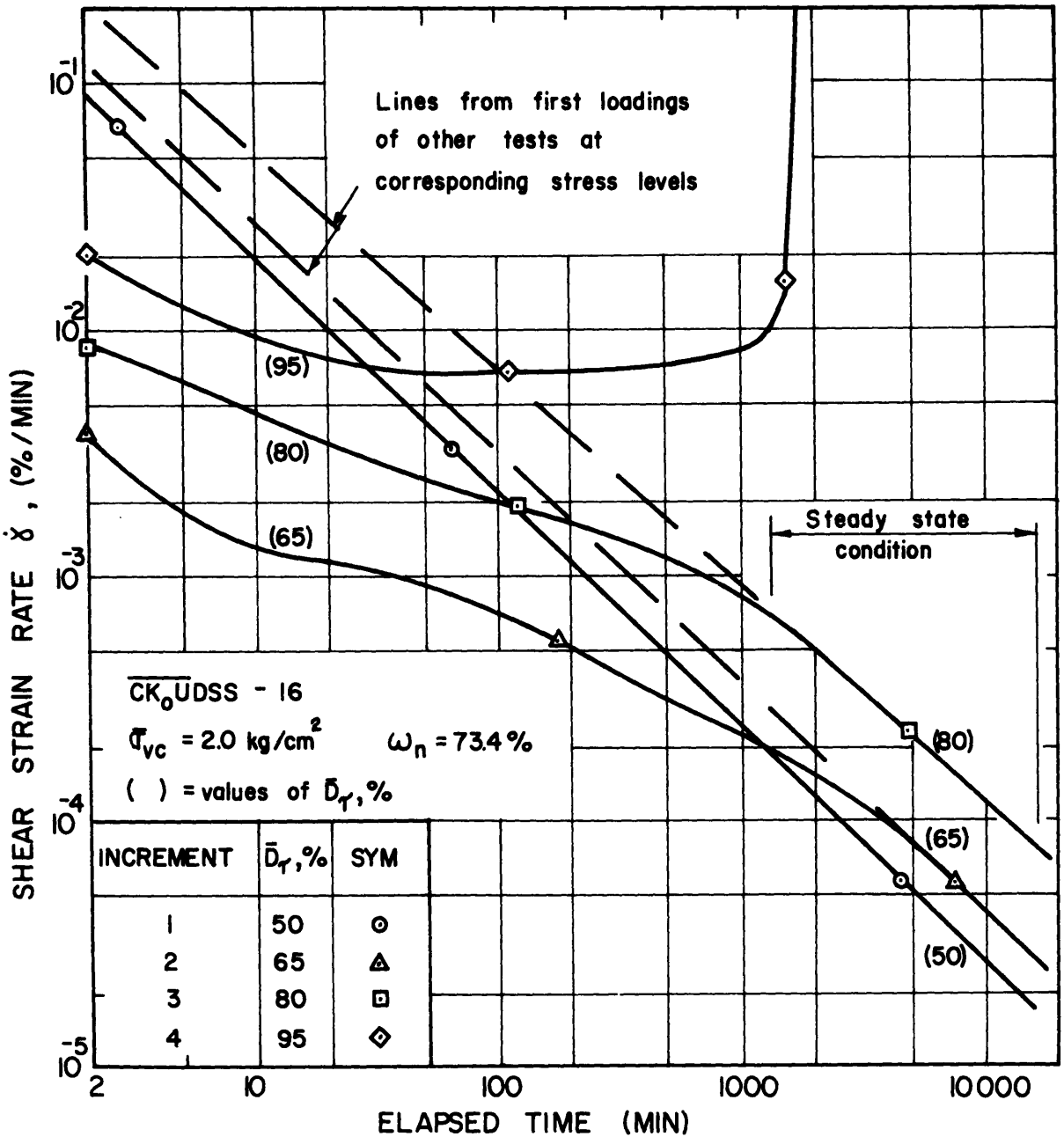

LOG SHEAR STRAIN RATE VS. LOG TIME DURING LATER INCREMENTS FROM $\overline{CK_0U}$DSS CREEP TEST ON N.C. EABPL CLAY

Figure 5-14

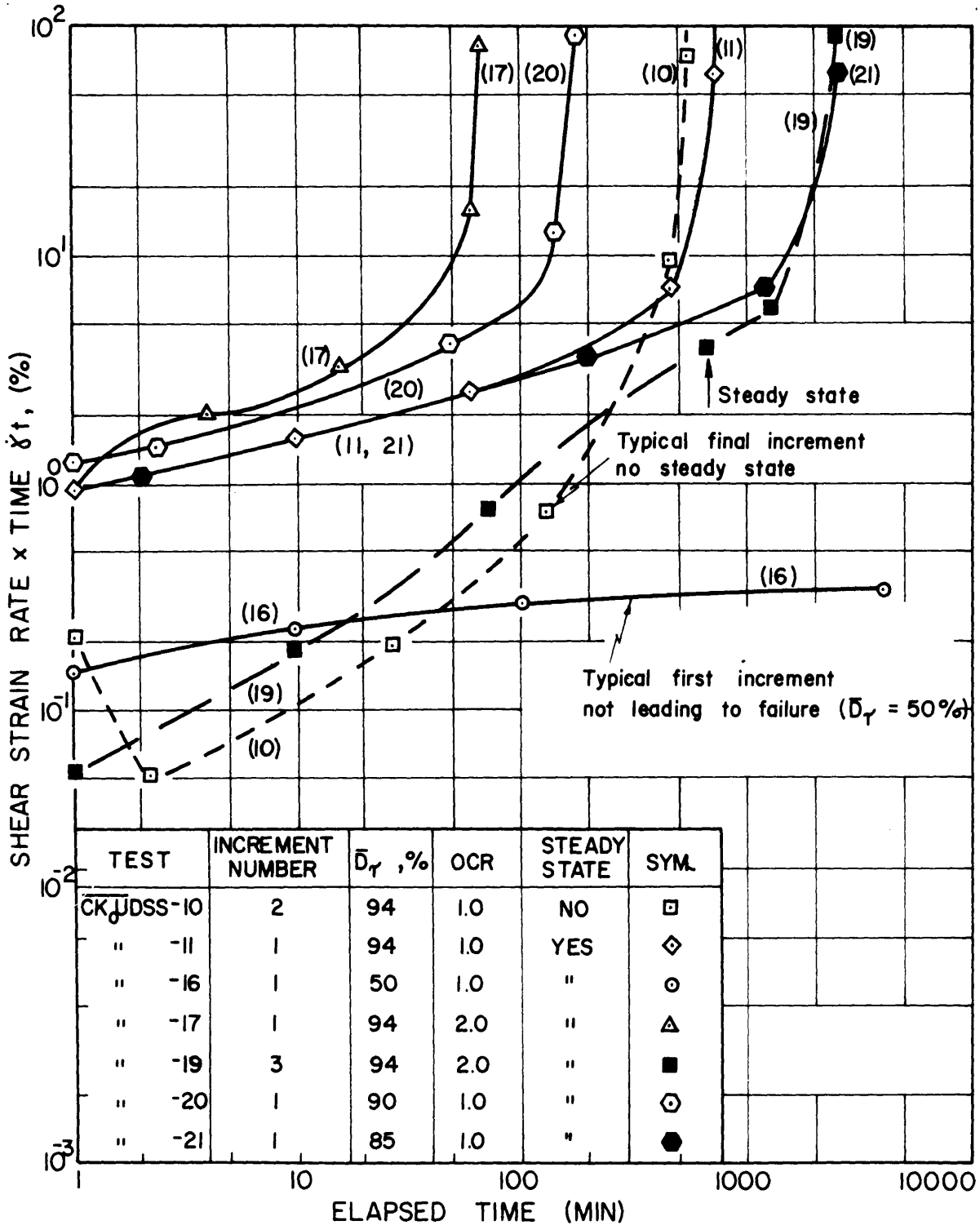

TEST	INCREMENT NUMBER	$\bar{D}_\gamma$, %	OCR	STEADY STATE	SYM.
$\overline{CK_oU}$DSS-10	2	94	1.0	NO	⊡
" -11	1	94	1.0	YES	◇
" -16	1	50	1.0	"	⊙
" -17	1	94	2.0	"	△
" -19	3	94	2.0	"	■
" -20	1	90	1.0	"	⬡
" -21	1	85	1.0	"	⬢

LOG $\dot{\gamma}t$ VS. LOG TIME FROM $\overline{CK_oU}$DSS CREEP TESTS ON EABPL CLAY

Figure 5-15

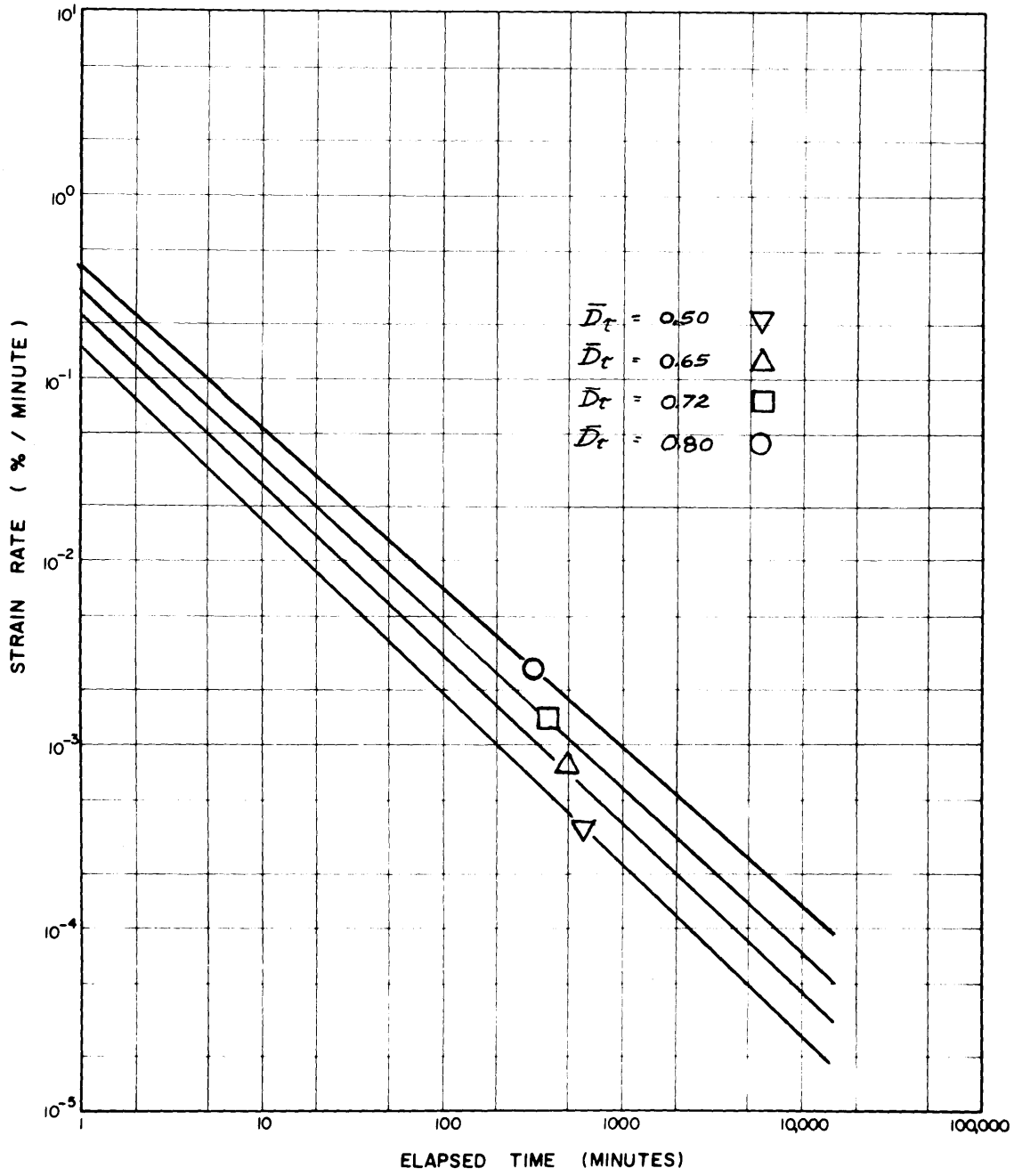

Plot of Log Strain Rate vs. Log Time for Steady State Creep at Various Stress Levels of EARPL Clay

Figure 5-16

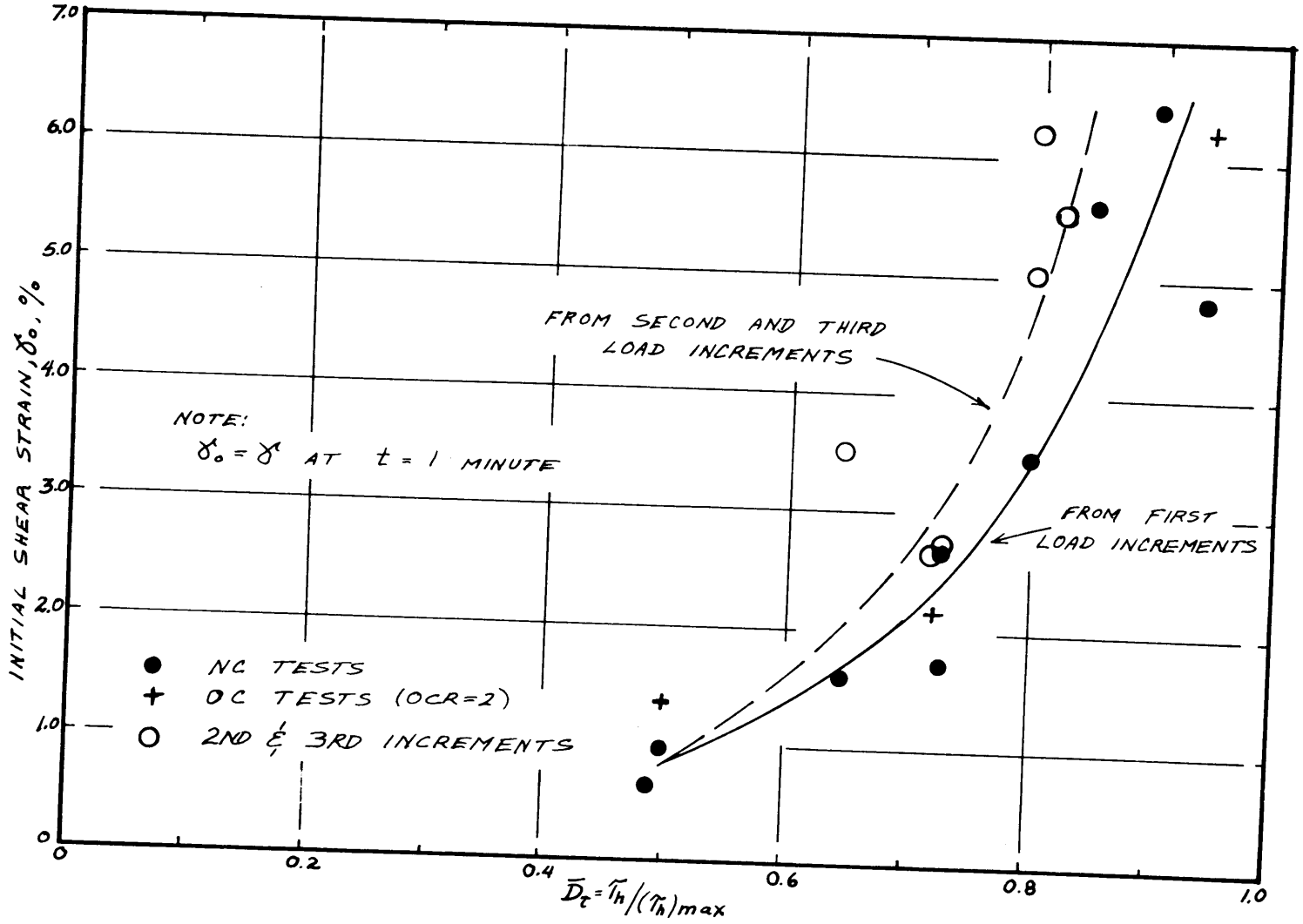

Initial Shear Strain (at t= 1 minute) vs. Applied Stress Level

Figure 5-17

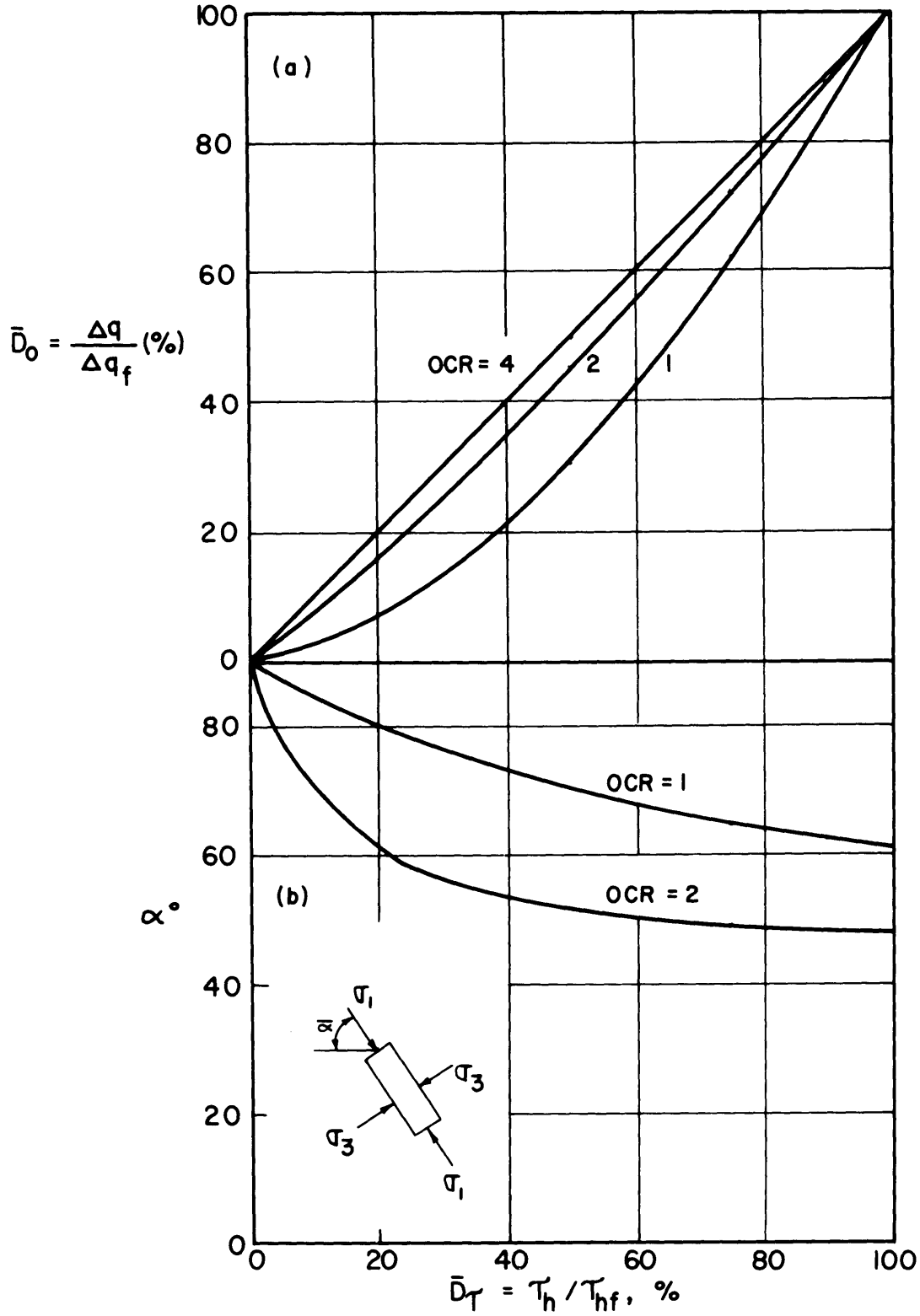

STRESS CONDITIONS IN THE DIRECT SIMPLE SHEAR DEVICE-
ASSUMMED PURE SHEAR

Figure 5-18

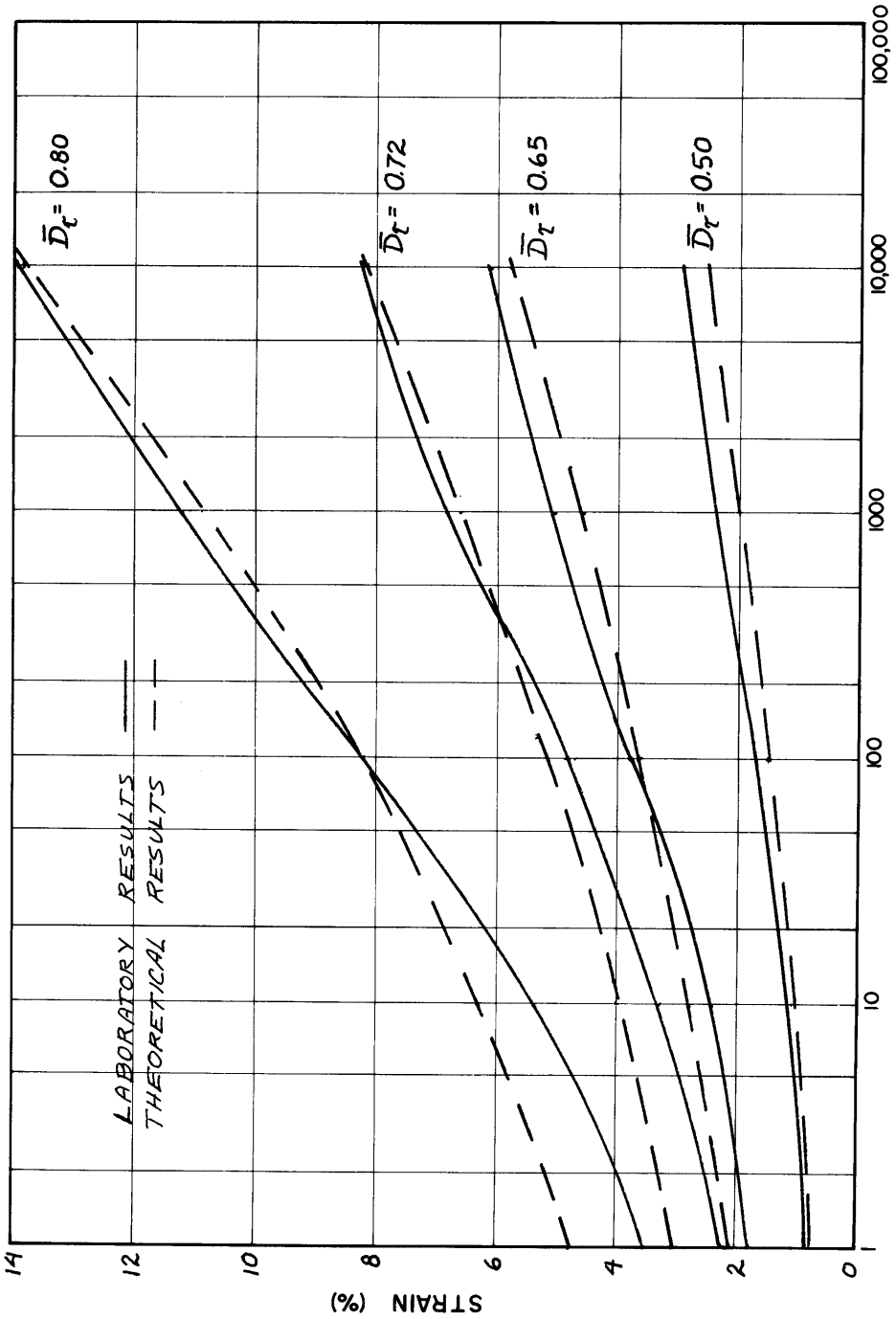

Comparison of Laboratory and Theoretical Creep Curves at Various Stress Levels

Figure 5-19

VI CONCLUSIONS AND RECOMMENDATIONS

6.1 APPARATUS PERFORMANCE

The Geonor Direct Simple Shear Device has proven to be a convenient tool for undrained creep testing. No modifications were necessary as the device is equipped with a "frictionless" load hanger for controlled stress testing. This is contrasted by triaxial creep testing where constant temperature precautions are necessary in order to stabilize pore pressures, and a number of sample area corrections must be made throughout the duration of an increment load to insure the condition of constant stress. On the other hand, all dimensions of the simple shear sample are kept constant during shear and there are no great quantities of water in the system to be affected by temperature. In addition, there are no problems with membrane and equipment leakage as there is with the triaxial device.

While advantageous in many areas, the simplicity of the device also presents a number of problems. The three major drawbacks are:

(1) Lack of knowledge concerning the sample state of stress;

(2) Lack of knowledge concerning sample pore pressures; and

(3) The unsteady state which exists when the initial shear stress increment is applied and the first major adjustment is made on the vertical stress.

6.2 TEST RESULTS

The Singh-Mitchell Rate Process Theory with modifications can be used to model creep behavior for EABPL clay. Results show this clay to have great creep potential ($m < 1.0$). It was found that, contrary to the theory, lines of log $\dot{\gamma}$ vs. log time at various values of $\overline{D}_\tau$ were not parallel (m = constant) but were divergent with time ($m = f(\overline{D}_\tau)$ (see Fig. 5-16). Normally consolidated and over consolidated samples behaved similarly with OC samples more creep susceptible at large times.

Additional load increments (values of $\overline{D}_\tau$) behaved much differently from initial increment behavior. Instead of yielding a linear relation between log $\dot{\gamma}$ and log time; the strain rate initially was much lower than the linear

relationship would yield. With time this new curve would converge with the linear relation and adopt its behavior. Apparently, the previous increment(s) had installed within the sample a greater structural stability than was initially present. The new increment had to overcome this new stability before first increment-like behavior could develop. Unfortunately, no empirical relationships could be developed concerning this initial transient behavior.

It was found that by applying several load increments to one sample, one could reconstruct the equivalent first stress level behavior for each increment applied. This can be accomplished by allowing each increment to pass through the initial transient phase and establish the steady state first increment-like behavior. This established linear relationship between log $\dot{\gamma}$ and log time can then be extended to all times to obtain equivalent first load performance.

It was found that loads of 85 percent or more cause creep rupture. This phenomenon was due to high pore pressure generation rather than a decrease in friction angle, $\bar{\phi}$. This angle (defined as $\bar{\phi} = \tan^{-1}(\tau_h/\bar{\sigma}_v)_{max}$) was essentially the same as that obtained from controlled strain tests.

The creep theories of Saito and Singh-Mitchell were found to be somewhat useful for predicting failure in the laboratory. The Saito relationship was able to yield a time range for failure which included the actual time to failure in all cases. Unfortunately, this time range which covers more than one log cycle of time can be very large and on the order of a week for large times to failure. The Singh-Mitchell Theory was somewhat of an improvement but only applied to first load failures and to those additional increments which achieved steady state creep prior to failure. The average value of $(\dot{\gamma}t)_f$ (the value of $\dot{\gamma}t$ at which there is a sudden increase in slope) was found to be approximately 5.0 percent. For the five cases in which steady state creep existed prior to creep rupture as defined by Singh-Mitchell, failure occurred from 30 to 1700 minutes after attainment of $(\dot{\gamma}t)_f$ = 5.0%. The test with the upper bound time to failure was the lone additional increment test which achieved steady state prior to failure. The Saito time range for this test was 2800 minutes. It was found that the average strain attained prior to failure* in the five tests for which the Singh-Mitchell creep rupture

---

* This strain is defined as that attained when the log-log plot of $\dot{\gamma}t$ vs. time has passed $(\dot{\gamma}t)_f$ and becomes nearly vertical.

theory applied, was 20 percent, which is approximately the average strain at failure for the controlled strain $\overline{CK_oU}$DSS tests. Apparently, the mechanisms which bring about failure under both controlled strain and controlled stress creep are somewhat similar for the strains as well as the obliquity ($\tau_h/\overline{\sigma}_v$) at failure were the same for the two failure modes.

Major drawbacks in the program were:

(1) The inability to ascertain accurate values of $\overline{D}(=\Delta q/\Delta q_f)$ for the various stress levels; and
(2) A great change in creep behavior after approximately 400 minutes of load duration.

The first problem is due to the stress system and made the selection of $\overline{D}_\tau$ for use in the theory's equations a difficult task of questionable success. The second problem, the author believes, has to do with pore pressure equalization in the sample. The rapid application of shear stress increases pore pressures within the sample. Reduction of vertical stress maintains the sample volume and the average sample pore pressure is in equilibrium with the sample stresses. Unfortunately, pore pressures at the sample edges, which can dissipate more quickly than those on the potential

failure plane, are now too low and those near the center are too high. Sample deformations which are more strongly governed by the stress state within the interior of the sample (i.e. on the potential failure plane) are proceeding at an accelerated rate. Therefore, the linear log strain rate versus log time relation for an applied stress level, $\overline{D}_\tau$, is too high as the obliquity ($\tau_h/\overline{\sigma}_v$) within the sample is greater than that which would normally result from the applied stress level, $\overline{D}_\tau$. Only after these excess pore pressures dissipate does the linear creep rate relation drop down to that level which is representative of the applied stress, $\overline{D}_\tau$. All data obtained prior to this event is misleading and presently of little value.

6.3 RECOMMENDATIONS

The two major problems encountered during this investigation were concerned with a lack of knowledge of the stress state within the sample and measurement and dissipation of initial pore pressures within the sample.

The first problem has been the object of considerable effort with little resulting success and the author has

no suggestions for improving the situation. The second consideration can either be handled by measuring this transient excess pore pressure or eliminating it. Measurement would indeed be difficult and at this time not practical. Elimination appears to be the only reasonable recourse. This can be accomplished by either applying a desired stress level in smaller increments over a time period within which a major portion of these excess pore pressures could dissipate or else loading the sample by means of controlled strain until the desired stress level is reached. After transferring the proving ring load to the hanger assembly, the creep test could be commenced. Unfortunately, the data obtained during the execution of these two techniques is also of little use so one accomplishes nothing. Apparently, the best procedure is to ignore all data obtained prior to t = 400 minutes.

Other aspects of the program which need further investigation are the effects of OCR on creep behavior, long term testing (t > 1 month) and creep rupture behavior. Any program designed to investigate these problems could be very useful.

VII REFERENCES

1. Arulanandan, K.; Shen, C.K.; and Young, R.B. (1971), "Undrained Creep Behavior of a Coastal Organic Silty Clay". Geotechnique, Vol. 21, N8.4, pp. 359-395.

2. Bishop, A. and Lovenbury, A., (1969), "Creep Characteristics of Two Undisturbed Clays". The Seventh Intl. Conf. of SMFE, Vol. , pp. 29-37.

3. Bjerrum, L. and Landva, A. (1966), "Direct Simple Shear Tests on a Norwegian Quick Clay". Geotechnique Vol. XVI, No. 1, pp. 1-20.

4. Brooker, E.W. and Ireland, H.). (1965), "Earth Pressure at Rest Related to Stress History". Canadian Geotechnical Journal, Vol. 2, No. 1, pp. 1-15.

5. Christensen, R.W. and Wu, T.H. (1964), "Analysis of Clay Deformation as a Rate Process". ASCE JSMFD, Vol. 90, No. SM6, pp. 125-156.

6. Edgers, L. (1967), "The Effect of Simple Shear Stress System on the Strength of Saturated Clay". M.S. Thesis, Dept. of Civil Engineering, M.I.T.

7. Edgers, L. (1973), "Undrained Creep of a Soft Foundation Clay". Ph.D. Thesis, Dept. of Civil Engineering, M.I.T.

8. Fisk, H.N.; Kolb, C.R.; and Wilbert, L.J. (1952), "Geological Investigation of the Atchafalaya Basin and the Problem of Mississippi River Diversion". U.S. Army Engineer Waterways Experiment Station, Vicksburg, Mississippi.

9. Foott, R. and Ladd, C.C. (1972), "Prediction of End of Construction Undrained Deformations of Atchafalaya Levee Foundation Clays". M.I.T. Dept. of Civil Engineering, Research Report R72-27.

10. Kaufman, R.I. and Weaver, F.J. (1967), "Stability of Atchafalaya Levees". ASCE, JSMFD, Vol. 93, SM4, pp. 157-176.

11. Kolb, C.R. and Shockley, W.G. (1959), "Engineering Geology of the Mississippi Valley", Trans. of the ASCE, Vol. 124, pp. 633-645.

12. Krinitzsky, E.L. and Smith, F.L. (1969), "Geology of Backswamp Deposits in the Atchafalaya Basin, Louisiana", U.S. Army Engineer Waterways Experiment Station, Tech. Rept. S-69-8, Vicksburg, MS.

13. Ladd, C.C.; Williams, C.E.; Connell, D.H. and Edgers, L. (1972), "Engineering Properties of Soft Foundation Clays at Two South Louisiana Levee Sites". M.I.T. Dept. of Civil Eng. Res. Rept. R72-26.

14. Laing Barden, "Time Dependent Deformations of Normally Consolidated Clays and Peats". ASCE, JSMFD, Vol. 95, No. SM1, Jan. 1969, pp. 1-31.

15. Landva, A. (1964), "Equipment for Cutting and Mounting Undisturbed Specimens of Clay in Testing Devices". NGI Publication No. 56, pp. 1-5.

16. Mitchell, J.K.; Campanella, R.G.; and Singh, A. (1968), "Soil Creep as a Rate Process". ASCE, JSMFD, Vol. 94, No. SM1, Jan. 1968, pp. 231-253.

17. Mitchell, J.K., Singh, A. and Campanella, R.G. (1969), "Bonding, Effective Stresses, and Strength of Soils". ASCE, JSMFD, Vol. 95, No. SM5, pp. 1219-1246.

18. Murayama, S. and Shibata, T. (1961), "Rheological Properties of Clays", Proceedings of the 5th Interntl. Conf. on Soil Mech. and Fdn. Engr., Paris, Vol. 6, pp. 269-273.

19. Shibata, T. and Karube, D. (1969), "Creep Rate and Creep Strength of Clays". The 7th Intl. Conf. on SMFE, Vol. 1, pp. 361-367.

20. Singh, A. and Mitchell, J.K. "General Stress-Strain Time Function for Soils". ASCE, JSMFD, Vol. 94, No. SM1, Jan. 1968, pp. 21-46.

21. Singh, A. and Mitchell, J.K. (1969), "Creep Potential and Creep Rupture of Soils". The 7th ICSMFE, Vol. 1, pp. 379-384.

22. Saito, M. and Vezawa, H. (1961), "Failure of Soil Due to Creep", The 5th ICSMFE, Vol. 1, pp. 315-318.

23. Saito, M. (1965), "Forecasting the Time of Occurrence of a Slope Failure". The 6th ICSMFE, Vol. II, pp. 537-541.

24. Saito, M. (1969), "Forecasting Time of Slope Failure by Tertiary Creep". The 7th ICSMFE, Vol. II, pp. 677-683.

25. USCE (1968), "Interim Report on Field Tests of Levee Construction, Test Sections I, II and III, EABPL, Atchafalaya Basin Floodway, La.". Dept. of the Army, New Orleans District, Corps of Engineers, New Orleans, Louisiana.

26. Walker, L.K. (1969), "Undrained Creep in a Sensitive Clay", Geotechnique, Vol. 19, No. 4, pp. 515-529.

27. Watt, B.J. (1969), "Analysis of Viscous Behavior in Undrained Soils", Sc.D. Thesis, Department of Civil Engineering, M.I.T.

APPENDIX A

LIST OF SYMBOLS

Note: Suffix f indicates a failure condition.

Prefix Δ indicates a change.

A bar over a stress indicates an effective stress.

Stresses

q	$(\sigma_v - \sigma_h)/2$ or $(\sigma_1 - \sigma_3)/2$
$\bar{p}$	$(\bar{\sigma}_v + \bar{\sigma}_h)/2 = (\bar{\sigma}_1 + \bar{\sigma}_3)/2$
u	Pore Water Pressure
σ_h	Horizontal Stress
σ_v	Vertical Stress
σ_1	Major Principal Stress
σ_3	Minor Principal Stress
$\bar{\sigma}_{hc}$, $\bar{\sigma}_{vc}$	$\bar{\sigma}_h$, $\bar{\sigma}_v$ at Consolidation
$\bar{\sigma}_{vo}$	Initial In Situ Vertical Effective Stress
$\bar{\sigma}_{vm}$	Maximum Past Pressure
τ	Shear Stress
τ_{max}	Maximum Shear Stress

Stress Ratios

$\bar{D}$	q/q_f
$\bar{D}_o$	$\Delta q/\Delta q_f$
$\bar{D}_\tau$	τ_h/τ_{hf} in the Direct-Simple Shear Test
K	$\bar{\sigma}_h/\bar{\sigma}_v$ or $\bar{\sigma}_{hc}/\bar{\sigma}_{vc}$
OCR	Overconsolidation Ratio = $\bar{\sigma}_{vm}/\bar{\sigma}_{vo}$ or $\bar{\sigma}_{vm}/\bar{\sigma}_{vc}$

Strains

ε	Linear Strain
γ	Shear Strain

Strength Parameters and Stress Strain "Constants"

E_u	Young's Secant Modulus for Undrained Loading in Terms of Total Stress from an Undrained Shear Test
s_u	Undrained Shear Strength
$\bar{\phi}_u$, $\bar{\phi}$, $\bar{\phi}_f$	$\tan^{-1}(\tau/\bar{\sigma}_v)$ at τ_f in the Direct-Simple Shear Test
$\bar{\phi}_{max}$	$\bar{\phi}$ at $(\tau/\bar{\sigma}_v)_{max}$
$\bar{\phi}_c$	$\bar{\phi}$ at Creep Rupture

Strain Rate and Creep Parameters

$\dot{\varepsilon}$	Strain Rate = $d\varepsilon/dt$
$\dot{\gamma}$	Shear Strain Rate
t_r	Time to Rupture
t_f	Time to Failure
t_o	Time at Which Strain Rate Becomes Constant Prior to the Development of Creep Rupture
A	Creep Parameters in Singh-Mitchell Relationship See Section 2.1
D	
$\bar{D}$ (or $\bar{D}_o$, $\bar{D}_\tau$)	
D_{max}	
m	
α	
$\bar{\alpha}$	
ε_1, γ_1	
t	
t_1	

LIST OF SYMBOLS (Cont.)

The following symbols are used in the derivation of the Singh-Mitchell relationship from rate process theory.

f	Shear Force Acting on a Flow Unit
h	Planck's Constant = 6.624×10^{-27} erg - sec^{-1}
K	$2 \times \frac{kT}{h} \exp\left(-\frac{\Delta F}{RT}\right)$
k	Boltzmann's Constant = 1.38×10^{-16} erg $^{o}K^{-1}$
R	Universal Gas Constant = 1.98 cal $^{o}K^{-1}$ $mole^{-1}$
S	Number of Flow Units
T	Absolute Temperature, ^{o}K
t_1	Reference Time
X	Parameter Relating Activation Frequency to Strain Rate
α	$\frac{\lambda}{4SkT}$
α'	$\frac{\lambda}{2kT}$
ΔF	Free Energy of Activation, Calories per mole
λ	Distance Between Equilibrium Positions of Flow Units

Miscellaneous

C_c	Virgin Compression Index
C_r	Recompression Index
CR	Compression Ratio = $C_c/(1 + e_o)$
c_v	Coefficient of Consolidation = $k_v/(m_v\gamma_w)$
e	Void Ratio or Napierian Base 2.7183
e_o	Initial Void Ratio
k	Coefficient of Permeability
log	Log to Base 10
N.C.	Normally Consolidated
O.C.	Overconsolidated
t	Time
w	Water Content
w_n	Natural Water Content
P.I.	Plasticity Index
L.I.	Liquidity Index

APPENDIX B

TABULATED TEST RESULTS

$\overline{CK_oU}$DSS – CREEP TEST

SOIL DESCRIPTION EABPL CLAY
BORING No. 94 UES
SAMPLE No. 11C
ELEVATION -36.7 FT
INITIAL ω_N 73.8 %

TEST No. $\overline{CK_oU}$DSS-8
DATE 10-21-71
CONDUCTED BY CEW
$\bar{\sigma}_{vc}$ (KG/CM^2) 2.0
OCR 1.0
PRETEST Ht.(MM) 21.379

DATE/TIME	VERTICAL PROVING RING	VERT. STRESS	γ (%)	$\dot{\gamma}$(%/MIN)	$\dot{\gamma}t$(%)	ELAPSED TIME (MINUTES)	APPLIED $\overline{D}_\tau$ (PER CENT)
10-2-71 10:00	3057.6	2.0	0	——	——	0	48.9 (.235 Kg/cm^2)
	3005	1.89	.645	.1538	.1538	1	
	2994		.923	.0220	.1320	6	
	2986		1.107	.00915	.2013	22	
	2961	1.80	1.298	.00439	.2065	47	
	2961		1.384	.00229	.1943	85	
	2945		1.476	.00185	.2306	125	
	2945		1.568	.000938	.1735	185	
	2928	1.73	1.784	.000660	.2992	453	
	2918		1.882	.000250	.1651	660	
	2893		2.091	.000139	.2331	1680	
	2893		2.171	.0000810	.2225	2745	
	2876	1.62	2.220	.0000641	.2099	3275	
	2876		2.264	.0000805	.3367	4185	
	2860		2.325	.0000929	.4251	4575	
	2859	1.59	2.344	.0000586	.2956	5046	
	2850		2.387	.0000577	.3244	5625	
	2848		2.399	.0000338	.2031	6005	
	2846	1.56	2.436	——	——	7080	
10-7-71 8:30	2846	1.56	2.436	——	——	0	72.9 (.350 Kg/cm^2)
	2846		2.688	.09843	.09843	1	
	2846		2.731	.01846	.0554	3	
	2846		2.780	.01406	.0843	6	
	2846		2.829	.01093	.1093	10	
	2846		2.879	.00681	.1022	15	
	2846		3.020	.00567	.2153	38	

$\overline{D}_\tau = \tau$ (APPLIED) / τ MAX.

DATE/TIME	VERTICAL PROVING RING	VERT. STRESS	γ (%)	$\dot{\gamma}$ (%/MIN)	$\dot{\gamma}t$ (%)	ELAPSED TIME (MINUTES)	APPLIED $\bar{D}_\tau$ (PER CENT)
	2842		3.094	.00360	.1909	53	
	2837		3.420	.00292	.4353	149	
	2832		3.561	.00214	.4547	213	
	2825	1.52	3.678	.00197	.5308	270	
	2821		3.752	.00166	.5141	310	
	2819		3.869	.00144	.5526	385	
	2816		3.967	.00125	.5748	460	
	2811	1.49	4.023	.000916	.4654	508	
	2811		4.269	.000631	.4980	729	
	2811		4.582	.000519	.7240	1395	
	2780.5		4.724	.000355	.6096	1715	
	2790	1.44	4.871	.000211	.4672	2210	
	2785		4.988	.000182	.5092	2800	
	2784		5.056	.000137	.4408	3225	
	2782		5.185	.000119	.5040	4240	
	2777	1.42	5.333	.0000785	.4556	5805	
	2771		5.425	.0000760	.5439	7155	
	2765	1.393	5.523	—	—	8595	
10-13-71 1300							
	2765	1.393	5.523	—	—	0	82.2 (.395 Kg/cm²)
	2765		603	.01231	.01231	1	
	2765		610	.00219	.01316	6	
	2765		634	.00226	.03399	15	
	2765		653	.00106	.02643	25	
	2765		671	.000671	.03355	50	
			690	.000614	.04914	80	
			714	.000332	.03979	120	
			733	.000263	.05527	210	
			979	.000269	.3027	1125	
			6.034	.000288	.3836	1330	
			6.071	.000246	.3552	1445	
			6.102	.000226	.3623	1605	
			6.126	.000184	.3105	1690	
	2769	1.40	6.278	.000173	.4444	2565	

DATE/TIME	VERTICAL PROVING RING	VERT. STRESS	γ (%)	$\dot{\gamma}$ (%/MIN)	$\dot{\gamma}t$ (%)	ELAPSED TIME (MINUTES)	APPLIED $\bar{D}_T$ (PER CENT)
	2760		6.325	.000226	.6554	2897	
	2760		6.366	.000147	.4355	2956	
	2761	1.38	6.538	.000127	.5433	4275	
	2761		6.581	.0000946	.4398	4650	
	2759.5		6.667	.0000946	.5336	5640	
	2757.5		6.704	.0000928	.5523	5950	
	2750	1.36	6.784	.0000909	.6269	6900	
	2747		6.872	.0000654	.4779	7805	
	2744	1.349	6.877	—	—	8310	
	* SAMPLE IS SHEARED BY CONTROLLED STRAIN						

$\overline{CK_oU}$DSS – CREEP TEST

SOIL DESCRIPTION EABPL CLAY
BORING No. 94 VES
SAMPLE No. 13C
ELEVATION -45 FT
INITIAL ω_N 84.9%

TEST No. $\overline{CK_oU}$DSS-10
DATE 12-3-71
CONDUCTED BY CEW
$\bar{\sigma}_{vc}$ (KG/CM^2) 2.0
OCR 1.0
PRETEST Ht.(MM) 21.501

DATE/TIME	VERTICAL PROVING RING	VERT. STRESS	γ (%)	$\dot{\gamma}$(%/MIN)	$\dot{\gamma}_c$(%)	ELAPSED TIME (MINUTES)	APPLIED $\overline{D}_\tau$ (PER CENT)
11-24-71 755	3057.6	2.0	0	——	——	0	72.9% (.350 Kg/cm^2)
	3057.6		2.690	1.5167	1.5167	1	
	3052		3.033	.2285	.4570	2	
	2975	1.83	3.604	.1406	.7028	5	
	2900	1.67	4.017	.07860	.7074	9	
	2883	1.64	4.390	.05150	.7725	15	
	2883		4.687	.03650	.8026	22	
	2883		4.937	.02828	.8484	30	
	2883		5.083	.02328	.8382	36	
	2883		5.240	.02079	.8938	43	
	2883		5.374	.01746	.8723	50	
	2878	1.62	5.537	.01514	.9081	60	
	2865		5.676	.01276	.8933	70	
	2852		5.868	.00991	.8523	86	
	2850	1.57	6.142	.00777	.9085	117	
	2848		6.288	.00653	.9144	140	
	2847		6.410	.00618	.9771	158	
	2846	1.56	6.489	.00488	.8391	172	
	2840		6.590	.00447	.8716	195	
	2796	1.46	6.998	.00309	.9254	299	
	2797		7.468	.000766	.3997	522	
	2774		8.104	.000676	.9436	1395	
	2795		8.197	.000355	.5739	1615	
	2794		8.273	.000245	.4578	1870	
	2789		8.494	.000246	.6956	2828	
	2750	1.36	8.616	.000166	.5409	3266	
	2751		8.756	.000129	.5687	4410	

$\overline{D}_\tau = \tau$ (APPLIED) / τ MAX.

DATE/TIME	VERTICAL PROVING RING	VERT. STRESS	γ (%)	$\dot{\gamma}$ (%/MIN)	$\dot{\gamma}_t$ (%)	ELAPSED TIME (MINUTES)	APPLIED $\bar{D}_\tau$ (PER CENT)
	2751	1.36	8.779	.0001375	.6228	4530	
	2753		8.843	.000125	.6285	5045	
	2760		9.030	.0000572	.4097	7165	
	2760		9.105	.0000546	.4680	8635	
	2741	1.343	9.187	—	—	10 065	
12-1-71 741	2741	1.343	9.187	—	—	0	94.1 % (.452 Kg/cm^2)
	2744		9.653	.2329	.2329	1	
	2744		9.676	.02328	.04655	2	
	2745		9.746	.01746	.08729	5	
	2755	1.37	9.798	.01270	.1143	9	
	2755		9.885	.00941	.1505	16	
	2764		9.926	.00685	.1508	22	
	2763		10.002	.00705	.2326	33	
	2763	1.39	10.054	.00617	.2528	41	
	2762		10.107	.00613	.3063	50	
	2768		10.171	.00582	.3492	60	
	2760	1.38	10.252	.00603	.4523	75	
	2755		10.340	.006017	.5295	88	
	2755		10.433	.00582	.6112	105	
	2755		10.619	.00629	.8564	136	
	2752		11.050	.00694	1.409	203	
	2735	1.33	11.487	.00824	2.152	261	
	2723		11.981	.01065	3.366	316	
	2700		12.924	.01287	5.098	396	
	2700		13.565	—	—	439	
	2700	1.258	FAILURE			531	

$\overline{CK_oU}$DSS – CREEP TEST

SOIL DESCRIPTION EABPL CLAY
BORING No. 94UES
SAMPLE No. 13A
ELEVATION -42.7 FT
INITIAL ω_N 77.2 %

TEST No. $\overline{CK_oU}$DSS-11
DATE 12-10-71
CONDUCTED BY CEW
$\overline{\sigma}_{vc}$ (KG/CM^2) 2.0
OCR 1.0
PRETEST Ht.(MM) 25.316

DATE/TIME	VERTICAL PROVING RING	VERT. STRESS	γ (%)	$\dot{\gamma}$(%/MIN)	$\dot{\gamma}t$(%)	ELAPSED TIME (MINUTES)	APPLIED $\overline{D}_\tau$ (PER CENT)
12-10-71 816	3057.6	2.0	0	—	—	0	94.1 % (.452 Kg/cm^2)
	3057.6		4.204	4.804	2.402	0.5	
	2950	1.776	4.804	0.851	0.851	1	
	2918	1.71	5.480	0.487	0.974	2	
	2852	1.57	6.266	.3253	1.301	4	
	2852		6.781	.2085	1.251	6	
	2817	1.50	7.517	.1583	1.583	10	
	2800	1.47	8.047	.1189	1.664	14	
	2786		8.468	.1001	1.802	18	
	2775	1.41	8.948	.08675	1.995	23	
	2771		9.509	.0692	2.076	30	
	2755	1.37	10.124	.0526	2.145	40	
	2746		10.635	.0468	2.386	51	
	2745		11.060	.0427	2.565	60	
	2737	1.33	11.661	.0365	2.736	75	
	2730		12.191	.0301	2.743	91	
	2703		12.987	.0270	3.216	119	
	2687	1.23	13.407	.0243	3.300	136	
	2681		13.787	.0250	3.804	152	
	2659		14.058	.0218	3.535	162	
	2660	1.18	15.424	.0184	4.184	227	
	2678		16.270	.01530	4.310	282	
	2660		17.976	.01460	5.749	394	
	2635		18.867	—	—	760	
12-10-71 2309	2640	1.134	FAILURE			893	

$\overline{D}_\tau = \tau$ (APPLIED) / τ MAX.

$\overline{CK_oU}$DSS – CREEP TEST

SOIL DESCRIPTION EABPL CLAY
BORING No. 94UES
SAMPLE No. 13A
ELEVATION -42.9 FT
INITIAL ω_N 86.7%

TEST No. $\overline{CK_oU}$DSS-12
DATE 12-28-71
CONDUCTED BY CEW
$\bar{\sigma}_{vc}$ (KG/CM^2) 2.0
OCR 1.0
PRETEST Ht.(MM) 24.849

DATE/TIME	VERTICAL PROVING RING	VERT. STRESS	γ (%)	$\dot{\gamma}$(%/MIN)	$\dot{\gamma}t$(%)	ELAPSED TIME (MINUTES)	APPLIED $\overline{D_\tau}$ (PER CENT)
1-2-72 800	3057.6	2.0	0	——	——	0	72.9% (.350 Kg/cm^2)
	3057.6		1.495	1.7198	0.8599	0.5	
	3057.6		1.720	0.3057	0.3057	1	
	3015	1.91	1.954	0.1711	.3423	2	
	2960	1.80	2.233	0.1037	.4148	4	
	2909		2.473	.06813	.4769	7	
	2895	1.66	2.642	.04541	.4541	10	
	2894		2.881	.03365	.5383	16	
	2900		3.046	.02421	.5327	22	
	2898		3.220	.01911	.5733	30	
	2893		3.390	.01570	.6280	40	
	2880	1.62	3.534	.01196	.5982	50	
	2866		3.689	.00954	.6203	65	
	2857		3.868	.00690	.5866	85	
	2850	1.57	4.137	.00508	.6604	130	
	2820		4.402	.00363	.6900	190	
	2820		4.646	.00272	.7333	270	
	2814	1.49	4.795	.00191	.6403	335	
	2813		5.015	.00155	.7188	463	
	2797	1.46	5.174	.000789	.4565	579	
	2774		5.758	.000608	.8544	1405	
	2754		5.932	.000301	.5501	1825	
	2741	1.34	6.186	.000243	.6870	2827	
	2741		6.420	.000139	.6000	4310	
	2737	1.33	6.575	.0000808	.4630	5730	
	2729		6.680	.0000683	.4909	7192	
	2718	1.295	6.774	.0000556	.4807	8651	

$\overline{D_\tau} = \tau$ (APPLIED) / τ MAX.

DATE/TIME	VERTICAL PROVING RING	VERT. STRESS	γ (%)	$\dot{\gamma}$ (%/MIN)	$\dot{\gamma}_t$ (%)	ELAPSED TIME (MINUTES)	APPLIED $\bar{D}_\tau$ (PER CENT)
	2719		6.839	.0000507	.5100	10 063	
	2706		7.093	.0000351	.5573	15 892	
	2709		7.238	.0000264	.5734	21 703	
	2693		7.447	.0000193	.5874	30 405	
	2701	1.260	7.632	.0000140	.5688	40 625	
1-31-72 750	2701	1.260	7.632	———	———	0	94.1%
	2701		7871	.12215	.12215	1	(.452 Kg/cm^2)
	2701		7.881	.01248	.0250	2	
	2701		7.921	.01059	.0529	5	
	2701		7.966	.00598	.0598	10	
	2701		7.981	.00432	.0648	15	
	2701		8.031	.00439	.1097	25	
	2701		8.090	.00385	.1539	40	
	2701		8.165	.00336	.2018	60	
	2701		8.225	.00277	.2216	80	
	2701	1.26	8.290	.00277	.2908	105	
	2701		8.350	.00282	.3522	125	
	2701		8.484	.00286	.4973	174	
	2701		8.564	.00268	.5368	200	
	2701		8.718	.00289	.7513	260	
	2701		8.923	.00307	1.0123	330	
	2697		9.122	.00300	1.1861	395	
	2697		9.461	.00313	1.5764	504	
	2694		9.815	.00317	1.9679	621	
	2664	1.18	10.309	.00145	3.338	750	
	2644		11.021	.00450	4.051	900	
	2655		11.565	.00326	3.357	1030	
	2674	1.20	12.716	.00328	4.555	1390	
	2629		13.609	.00482	7.710	1600	
	2635	1.12	13.828	.00438	7.230	1650	
	2636		14.296	.00439	7.713	1757	
	2625		14.601	.004500	8.216	1826	
2-[illegible]-72	2635	1.124	14.805	———	———	1870	
2-2-72 725	FAILURE					2855	

$\overline{CK_oU}$DSS – CREEP TEST

SOIL DESCRIPTION EABPL CLAY
BORING No. 94 VES
SAMPLE No. 12C
ELEVATION -40.5 FT
INITIAL ω_N 73.4 %

TEST No. $\overline{CK_oU}$DSS-16
DATE 3-15-72
CONDUCTED BY CEW
$\bar{\sigma}_{vc}$ (KG/CM^2) 2.0
OCR 1.0
PRETEST Ht.(MM) 24.173

DATE/TIME	VERTICAL PROVING RING	VERT. STRESS	γ (%)	$\dot{\gamma}$(%/MIN)	$\dot{\gamma}t$(%)	ELAPSED TIME (MINUTES)	APPLIED $\overline{D}_\tau$ (PER CENT)
3-21-72 735	3057.6	2.0	0	——	——	0	50 % (.24 Kg/cm^2)
	3057.6		0.885	0.976	0.488	0.5	
	3057.6		0.976	0.154	0.154	1	
	3000	1.88	1.116	0.077	0.154	2	
	2989		1.207	.0364	0.146	4	
	2981		1.298	.0285	.1995	7	
	2981		1.378	.0194	.1938	10	
	2981		1.453	.0143	.2150	15	
	2981		1.593	.0113	.2825	25	
	2970	1.82	1.679	.0023	.2548	35	
	2962		1.779	.00563	.2813	50	
	2956		1.904	.00453	.3400	75	
	2942		1.979	.00307	.2913	95	
	2933	1.74	2.134	.00237	.3551	150	
	2933		2.242	.00137	.2812	206	
	2915		2.462	.00107	.4167	390	
	2905		2.526	.000705	.3328	472	
	2902	1.67	2.585	.000567	.3205	565	
	2884		2.724	.000351	.2881	821	
	2884	1.64	2.885	.000222	.3150	1420	
	2871		2.960	.000153	.2892	1885	
	2865		3.030	.000116	.2755	2365	
	2860	1.59	3.073	.000111	.3163	2855	
	2855		3.143	.000085	.2871	3385	
	2850	1.57	3.196	.000057	.2431	4305	
	2847		3.228	.000049	.2403	4890	
	2847		3.277	.000044	.2597	5953	

$\overline{D}_\tau = \tau$ (APPLIED) / τ MAX.

DATE/TIME	VERTICAL PROVING RING	VERT. STRESS	γ (%)	$\dot{\gamma}$ (%/MIN)	$\dot{\gamma}_t$ (%)	ELAPSED TIME (MINUTES)	APPLIED $\bar{D}_\tau$ (PER CENT)
	2839	1.55	3.325	.0000321	.2381	7419	
	2841		3.357	.0000362	.3131	8645	
	2832	1.531	3.395	—	—	10 050	
3-28-72 720	2832	1.531	3.395	—	—	0	65%
	2827		3.529	0.1390	.0695	0.50	(.312 Kg/cm²)
	2827		3.534	.00733	.0073	1	
	2827		3.540	.00367	.0073	2	
	2834		3.545	.00200	.0080	4	
	2838		3.550	.00268	.0187	7	
	2838		3.566	.00250	.0300	12	
	2838	1.54	3.583	.00117	.0235	20	
	2838		3.593	.000568	.01986	35	
	2838		3.604	.000896	.05106	57	
	2836		3.636	.000780	.0648	83	
	2830		3.700	.000542	.0975	180	
	2830		3.759	.000461	.1428	310	
	2828		3.829	.000288	.1323	460	
	2825	1.52	4.081	.000274	.3913	1430	
	2811		4.172	.000257	.4413	1715	
	2808		4.248	.000139	.2898	2079	
	2808		4.333	.000114	.3278	2870	
	2808	1.48	4.408	.000106	.3683	3480	
	2807.5		4.505	.0000785	.3528	4495	
	2806		4.585	.0000657	.3768	5740	
	2795		4.682	.0000632	.4545	7190	
	2792		4.768	.0000535	.4623	8635	
	2785	1.434	4.837	—	—	10 085	
4-4-72 732	2785	1.434	4.837	—	—	0	80%
	2785		4.977	0.1510	.0755	0.50	(.384 Kg/cm²)
	2785		4.988	0.0107	.0107	1	
	2785		4.993	.00867	.0173	2	
	2780		5.014	.00860	.0344	4	

DATE/TIME	VERTICAL PROVING RING	VERT. STRESS	γ (%)	$\dot{\gamma}$ (%/MIN)	$\dot{\gamma}t$ (%)	ELAPSED TIME (MINUTES)	APPLIED D_τ (PER CENT)
	2780		5.036	.00550	.0385	7	
	2780	1.42	5.047	.00540	.0590	10	
	2780		5.090	.00343	.0629	16	
	2780		5.106	.00256	.0639	25	
	2780		5.202	.00259	.1552	60	
	2784		5.256	.00223	.1854	83	
	2783		5.336	.00188	.2256	120	
	2783		5.476	.00173	.3457	200	
	2782		5.578	.00145	.3757	260	
	2782		5.765	.00131	.5238	400	
	2772	1.41	6.001	.000898	.5237	583	
	2769		6.693	.000772	1.1062	1433	
	2755		6.881	.000500	0.9154	1723	
	2752		7.551	.000432	1.3155	3048	
	2745	1.35	7.959	.000278	1.2027	4320	
	2738		8.356	.000192	1.1377	5938	
	2725		8.634	.000133	1.0447	7843	
	2720		8.715	.000109	0.9404	8633	
	2721	1.302	8.876	—	—	10063	
4-11-72 725	2721	1.302	8.876	—	—	0	95%
	2716		9.031	0.1770	.0885	0.5	(.456 Kg/cm^2)
	2716		9.053	0.0287	.0287	1	
	2716		9.074	.0197	.0393	2	
	2708		9.112	.0172	.0688	4	
	2708		9.160	.0120	.0840	7	
	2712		9.208	.00867	.1040	12	
	2720	1.30	9.273	.00744	.1488	20	
	2720		9.342	.00697	.2090	30	
	2720		9.482	.00669	.3344	50	
	2718		9.643	.00611	.4579	75	
	2717		9.830	.00616	.6596	107	
	2716		10.093	.00623	.9216	148	
	2714	1.29	10.571	.00638	1.4412	226	

DATE/TIME	VERTICAL PROVING RING	VERT. STRESS	γ (%)	$\dot{\gamma}$ (%/MIN)	$\dot{\gamma}_{(t)}$ (%)	ELAPSED TIME (MINUTES)	APPLIED $\bar{D}_T$ (PER CENT)
	2710		10.871	.00697	1.8819	270	
	2708		11.268	.00696	2.269	326	
	2703		11.713	.00710	2.778	391	
	2695	1.25	12.120	.00731	3.259	446	
	2695		12.378	.00710	3.423	482	
	2693		12.823	.00680	3.726	545	
	2678	1.21	14.046	.00750	5.442	726	
	2678		19.532	.00831	11.970	1440	
	2600	1.05	20.862	.01532	23.690	1546	
	2577	1.004	21.999	—	—	1601	
4-12-72 1025		FAILURE				1620	

$\overline{CK_oU}$DSS – CREEP TEST

SOIL DESCRIPTION EABPL CLAY
BORING No. 95UES
SAMPLE No. 13A
ELEVATION -44.0 FT
INITIAL ω_N 79.1%

TEST No. $\overline{CK_oU}$DSS-17
DATE 5-11-72
CONDUCTED BY CEW
$\overline{\sigma_{vc}}$ (KG/CM^2) 1.0
OCR 2.0
PRETEST Ht.(MM) 23.589

DATE/TIME	VERTICAL PROVING RING	VERT. STRESS	γ (%)	$\dot{\gamma}$(%/MIN)	$\dot{\gamma}t$(%)	ELAPSED TIME (MINUTES)	APPLIED $\overline{D_\tau}$ (PER CENT)
5-10-72 745	2575	1.0	0	—	—	0	94.1% (.414 Kg/cm^2)
	2575		5,443	6.254	3.127	0.5	
	2575		6,254	0.944	0.944	1	
	2602	1.056	7.803	0.628	1.884	3	
	2611		8.766	0.4176	2.088	5	
	2611		9.891	0.3251	2.601	8	
	2614		11.042	0.2174	2.609	12	
	2625	1.103	12.717	0.1886	3.792	21	
	2611		14.292	0.1614	4.841	30	
	2592	1.035	16.589	0.1605	7.222	45	
	2583		19.107	0.2571	15.428	60	
	2560	0.969	22.503	—	—	68	
	2522	0.890	FAILURE			68+	

$\overline{D_\tau} = \tau$ (APPLIED) / τ MAX.

$\overline{CK_oU}$DSS – CREEP TEST

SOIL DESCRIPTION EABPL CLAY
BORING No. 9SVES
SAMPLE No. 13A
ELEVATION -44.15 FT
INITIAL ω_N 79.2%

TEST No. $\overline{CK_oU}$DSS-18
DATE 5-15-72
CONDUCTED BY CEW
$\bar{\sigma}_{vc}$ (KG/CM^2) 1.0
OCR 2.0
PRETEST Ht.(MM) 23.614

DATE/TIME	VERTICAL PROVING RING	VERT. STRESS	γ (%)	$\dot{\gamma}$(%/MIN)	$\dot{\gamma}t$(%)	ELAPSED TIME (MINUTES)	APPLIED $\overline{D_\tau}$ (PER CENT)
5-22-72 740	2575	1.0	0	—	—	0	72% (.317 Kg/cm^2)
	2610		1.952	2.101	1.050	0.50	
	2622	1.10	2.101	0.243	.243	1	
	2633		2.316	0.144	.2870	2	
	2645	1.14	2.676	.0837	.4183	5	
	2639		2.902	.0457	.4110	9	
	2633		3.133	.0268	.4026	15	
	2627		3.331	.0183	.4564	25	
	2630		3.589	.0138	.5528	40	
	2623		3.815	.0096	.5740	60	
	2620		3.982	.0075	.6052	81	
	2622	1.10	4.121	.0060	.6089	101	
	2622		4.229	.0045	.5485	122	
	2622		4.342	.00437	.6563	150	
	2621		4.535	.00379	.7283	192	
	2629.5	1.113	4.793	.00269	.7226	269	
	2629		4.879	.00183	.5848	320	
	2618		5.062	.00194	.8073	416	
	2613		5.298	.00146	.7836	536	
	2613	1.08	5.658	.000817	.6735	824	
	2615		6.029	.000610	.8646	1430	
	2607		6.727	.000350	1.0131	2900	
	2585	1.02	7.087	.000210	.9370	4460	
	2565		7.308	.000180	.9970	5860	
	2581.5		7.566	.000210	1.4686	7175	
	2571		7.711	.000150	1.2880	8705	
	2580	1.010	8.028	—	—	10300	

$\overline{D_\tau} = \tau$ (APPLIED) / τ MAX.

DATE/TIME	VERTICAL PROVING RING	VERT. STRESS	γ (%)	$\dot{\gamma}$ (%/MIN)	$\dot{\gamma}t$ (%)	ELAPSED TIME (MINUTES)	APPLIED $\bar{D}_\tau$ (PER CENT)
5-29-72 1125	2580	1.010	7.759	———	———	0	94% (.414 Kg/cm²)
	2580		8.071	.3600	.1800	0.50	
	2580		8.119	.0680	.0680	1	
	2580		8.173	.0418	.0835	2	
	2588		8.286	.0329	.1644	5	
	2597		8.436	.0258	.2580	10	
	2596	1.04	8.544	.0219	.3287	15	
	2588		8.699	.0207	.4560	22	
	2585		8.855	.0180	.5400	30	
	2592		9.113	.0186	.8390	45	
	2590	1.03	9.414	.0187	1.122	60	
	2584		11.171	.0186	2.882	155	
	2584		11.553	.0189	3.305	175	
	2572		13.154	.0187	4.863	260	
	2570	0.99	14.078	.0188	5.829	310	
	2565		15.034	.0189	6.799	360	
	2554		15.986	.0199	8.182	411	
	2551	.9503	16.646	———	———	441	
5-30-72 720		FAILURE				1205	

$\overline{CK_oU}$DSS – CREEP TEST

SOIL DESCRIPTION EABPL CLAY
BORING No. 95 UES
SAMPLE No. 12D
ELEVATION -41.2 FT
INITIAL ω_N 67.7%

TEST No. $\overline{CK_oU}$DSS-19
DATE 5-31-72
CONDUCTED BY CEW
$\overline{\sigma_{vc}}$ (KG/CM^2) 1.0
OCR 2.0
PRETEST Ht.(MM) 21.920

DATE/TIME	VERTICAL PROVING RING	VERT. STRESS	γ (%)	$\dot{\gamma}$(%/MIN)	$\dot{\gamma}t$(%)	ELAPSED TIME (MINUTES)	APPLIED $\overline{D_\tau}$ (PER CENT)
6-7-72 810	2575	1.0	0	—	—	0	50% (.220 Kg/cm^2)
	2635		1.307	1.358	0.679	0.50	
	2635	1.12	1.358	.0720	.0720	1	
	2658		1.415	.0379	.0759	2	
	2666	1.19	1.472	.0216	.0864	4	
	2625		1.523	.0132	.0924	7	
	2623	1.10	1.551	.00925	.0925	10	
	2628		1.597	.00644	.0966	15	
	2629	1.111	1.654	.00397	.1031	26	
	2620		1.716	.00283	.1272	45	
	2618		1.784	.00196	.1414	72	
	2618		1.824	.00143	.1426	100	
	2618		1.881	.000962	.1346	140	
	2619		1.949	.000651	.1497	230	
	2622	1.10	2.034	.000243	.0912	375	
	2618		2.228	.000180	.2471	1375	
	2612		2.273	.000110	.1872	1705	
	2612		2.284	.000077	.1451	1885	
	2610	1.07	2.375	.000096	.2909	3030	
	2620		2.512	.000072	.3072	4260	
	2607		2.569	.0000351	.2008	5720	
	2604		2.614	.0000302	.2166	7165	
	2605		2.660	.0000238	.2079	8730	
	2605	1.062	2.682	—	—	10 020	
6-14-72 720	2605	1.062	2.682	—	—	0	72% (.317 Kg/cm^2)
	2605		2.853	0.1930	.0965	0.50	

$\overline{D_\tau} = \tau$ (APPLIED) / τ MAX.

DATE/TIME	VERTICAL PROVING RING	VERT. STRESS	γ (%)	$\dot{\gamma}$ (%/MIN.)	$\dot{\gamma}_t$ (%)	ELAPSED TIME (MINUTES)	APPLIED $\overline{D}_\tau$ (PER CENT)
	2600	1.05	2.875	.0300	.0300	1	
	2600		2.898	.0247	.0493	2	
	2592		2.949	.0136	.0544	4	
	2592		2.966	.00850	.0595	7	
	2600		3.000	.00578	.0577	10	
	2604		3.018	.00420	.0672	16	
	2605	1.06	3.063	.00352	.0879	25	
	2607		3.120	.00253	.1140	45	
	2606		3.177	.00205	.1438	70	
	2606		3.233	.00151	.1511	100	
	2607	1.07	3.381	.00133	.2720	205	
	2607		3.432	.000977	.2442	250	
	2608		3.591	.000588	.2470	420	
	2602		4.120	.000493	.6999	1420	
	2603		4.217	.000331	.5598	1690	
	2604		4.279	.000241	.4577	1900	
	2602		4.535	.000175	.5262	3010	
	2596		4.779	.000123	.5838	4760	
	2592	1.035	4.933	.0000969	.6060	6255	
	2583		5.029	.0000778	.5712	7340	
	2584		5.126	.0000657	.5740	8735	
	2585		5.285	.0000486	.5644	11 605	
	2581	1.012	5.427	.0000363	.5368	14 785	
	2582	1.01	5.501	—	—	17 260	
5-26-72 725	2582	1.01	5.501	—	—	0	94% (.414 Kg/cm²)
	2578		5.251	.2900	.1450	0.5	
	2578		5.791	.0527	.0527	1	
	2581		5.830	.0340	.0680	2	
	2584		5.893	.0262	.1048	4	
	2585		5.961	.0198	.1388	7	
	2588	1.03	6.012	.0150	.1500	10	
	2588		6.081	.0152	.2280	15	
	2593		6.240	.0130	.3243	25	

DATE/TIME	VERTICAL PROVING RING	VERT. STRESS	γ (%)	$\dot{\gamma}$ (%/MIN)	$\dot{\gamma}_t$ (%)	ELAPSED TIME (MINUTES)	APPLIED $\bar{D}_\tau$ (PER CENT)
	2585	1.02	6.535	.0115	.5740	50	
	2585		6.814	.0106	.7972	75	
	2587		7.109	.0101	1.050	104	
	2580		7.450	.00980	1.353	138	
	2580		8.001	.00925	1.803	195	
	2578		8.467	.00831	2.062	248	
	2569	0.99	9.331	.00778	2.762	355	
	2562		9.945	.00691	3.024	438	
	2564		10.712	.00630	3.494	555	
	2550		11.519	.00608	4.185	688	
	2540		12.263	.00493	3.990	810	
	2500	0.84	15.179	.00498	7.125	1431	
	2503		16.361	.00559	9.122	1633	
	2494		17.162	.00543	9.702	1786	
	2488		17.730	—	—	1885	
5-28-72 710	2473	0.789	FAILURE			2865	

$\overline{CK_oU}$DSS – CREEP TEST

SOIL DESCRIPTION EABPL CLAY
BORING No. 95UES
SAMPLE No. 12D
ELEVATION -41.3 FT
INITIAL ω_N 80.1%

TEST No. $\overline{CK_oU}$DSS-20
DATE 7-17-72
CONDUCTED BY CEW
$\overline{\sigma_{vc}}$ (KG/CM^2) 2.0
OCR 1.0
PRETEST Ht.(MM) 24.638

DATE/TIME	VERTICAL PROVING RING	VERT. STRESS	γ (%)	$\dot{\gamma}$(%/MIN)	$\dot{\gamma}t$(%)	ELAPSED TIME (MINUTES)	APPLIED $\overline{D_\tau}$ (PER CENT)
7-14-72 800	3057.6	2.0	0	—	—	0	90% (.432 Kg/cm^2)
	3030	1.94	5.478	6.417	3.209	0.5	
	2990	1.86	6.417	1.290	1.290	1	
	2955	1.785	7.413	.7163	1.433	2	
	2850	1.57	8.566	.4394	1.758	4	
	2810		9.610	.2948	2.064	7	
	2780	1.42	10.335	.2133	2.133	10	
	2755		11.316	.1718	2.576	15	
	2740	1.34	12.396	.1338	2.943	22	
	2725		13.590	.1019	3.261	32	
	2691	1.240	15.249	.0858	4.291	50	
	2660		16.851	.07105	4.974	70	
	2657	1.17	19.157	.06417	6.739	105	
	2615	1.08	20.445	.06433	8.106	126	
	2617		21.859	.09545	14.031	147	
	2602	1.056	25.981	—	—	184	
		FAILURE				185	

$\overline{D_\tau} = \tau$ (APPLIED) / τ MAX.

$\overline{CK_oU}$DSS – CREEP TEST

SOIL DESCRIPTION EABPL CLAY
BORING No. 95 UES
SAMPLE No. 12D
ELEVATION -41.45 FT
INITIAL ω_N 75.1%

TEST No. $\overline{CK_oU}$DSS-21
DATE 7-24-72
CONDUCTED BY CEW
$\bar{\sigma}_{vc}$ (KG/CM^2) 2.0
OCR 1.0
PRETEST Ht.(MM) 22.700

DATE/TIME	VERTICAL PROVING RING	VERT. STRESS	γ (%)	$\dot{\gamma}$(%/MIN)	$\dot{\gamma}t$(%)	ELAPSED TIME (MINUTES)	APPLIED $\overline{D_\tau}$ (PER CENT)
7-30-72 906	3057.6	2.0	0	—	—	0	85% (.408 Kg/cm^2)
	3000	1.88	4.893	5.584	2.792	0.5	
	2958	1.79	5.584	1.017	1.017	1	
	2900	1.67	6.419	.5813	1.163	2	
	2870		7.328	.3534	1.414	4	
	2830		8.186	.2447	1.713	7	
	2800	1.465	8.796	.1684	1.684	10	
	2790		9.533	.1218	1.828	15	
	2787	1.438	10.268	.0940	2.068	22	
	2787		10.943	.0675	2.024	30	
	2761		12.147	.0510	2.548	50	
	2740	1.34	12.981	.0359	2.514	70	
	2732		13.943	.0282	2.821	100	
	2718		14.956	.0219	3.071	140	
	2700	1.26	15.917	.0144	2.737	190	
	2660		18.254	.0120	4.420	369	
	2670		19.331	.00917	4.355	475	
	2651	1.17	20.143	.00752	4.323	575	
	2648		21.173	.00543	3.912	720	
	2601		25.278	.00541	8.220	1520	
	2598		26.797	.00747	13.143	1760	
	2575	1.000	28.668	—	—	1974	
8-1-72 400		FAILURE					

$\overline{D_\tau} = \tau$ (APPLIED) / τ MAX.

$\overline{CK_oU}$DSS – CREEP TEST

SOIL DESCRIPTION EABPL CLAY
BORING No. 95 UES
SAMPLE No. 12D
ELEVATION -41.6 FT
INITIAL ω_N 77.3%

TEST No. $\overline{CK_oU}$DSS-22
DATE 8-14-72
CONDUCTED BY CEW
$\overline{\sigma_{vc}}$ (KG/CM^2) 2.0
OCR 1.0
PRETEST Ht.(MM) 22.073

DATE/TIME	VERTICAL PROVING RING	VERT. STRESS	γ (%)	$\dot{\gamma}$(%/MIN)	$\dot{\gamma}t$(%)	ELAPSED TIME (MINUTES)	APPLIED $\overline{D_\tau}$ (PER CENT)
8-20-72 730	3057.6	2.0	0	———	———	0	80% (.384 Kg/cm^2)
	2930		3.169	3,4948	1.7474	0.5	
	2900	1.67	3.495	.5234	.5234	1	
	2882	1.635	3.954	.3315	.6629	2	
	2882		4.489	.2105	.8420	4	
	2878		5.007	.1444	1.0108	7	
	2871		5.356	.09522	0.952	10	
	2862		5.768	.07172	1.0758	15	
	2845	1.57	6.216	.05350	1.177	22	
	2830		6.571	.03767	1.130	30	
	2826		7.083	.01935	.8707	45	
	2816		7.635	.01829	1.280	70	
	2800		8.089	.01256	1.256	100	
	2787	1.44	8.653	.00877	1.324	151	
	2766		9.141	.00613	1.348	220	
	2761		9.566	.00465	1.396	300	
	2757		9.932	.00352	1.372	390	
	2751		10.252	.00251	1.243	495	
	2737	1.34	10.874	.00159	1.220	765	
	2700	1.26	11.735	.00113	1.604	1425	
	2710		12.107	.000643	1.196	1860	
	2691		12.677	.000427	1.2349	2890	
	2683		13.235	.000290	1.3061	4500	
	2676		13.502	.000204	1.1718	5735	
8-25-72 705	2674	1.205	13.781	———	———	7175	
	2674	1.205	13.781	———	———	0	90% (.432 Kg/cm^2)

$\overline{D_\tau} = \tau$ (APPLIED) / τ MAX.

DATE/TIME	VERTICAL PROVING RING	VERT. STRESS	γ (%)	$\dot{\gamma}$ (%/MIN)	$\dot{\gamma}t$ (%)	ELAPSED TIME (MINUTES)	APPLIED $\bar{D}_T$ (PER CENT)
	2674		13.804	.0674	.0337	0.5	
	2670		13.848	.0155	.0155	1	
	2670		13.863	.0126	.0252	2	
	2670		13.886	.00581	.0233	4	
	2670	1.20	13.909	.00436	.0436	10	
	2671		13.956	.00419	.0837	20	
	2672		14.014	.00299	.1050	35	
	2672		14.177	.00250	.2350	94	
	2673	1.20	14.427	.00250	.4990	200	
	2673		14.654	.00257	.7330	285	
	2673		14.828	.00239	.8520	356	
	2673		15.072	.00250	1.148	460	
	2673		15.288	.00277	1.496	540	
	2670	1.20	15.782	.00286	2.045	716	
	2670		15.945	.00279	2.146	770	
	2670		16.183	.00274	2.357	860	
	2665		16.468	.00284	2.732	961	
	2650	1.16	16.701	.00350	3.652	1042	
	2635		16.997	—	—	1112	
	2602	1.056	FAILURE			1545	

$\overline{CK_oU}$DSS – CREEP TEST

SOIL DESCRIPTION EABPL CLAY
BORING No. 94VES
SAMPLE No. 10B
ELEVATION -32.0 FT
INITIAL ω_N 79.5%

TEST No. $\overline{CK_oU}$DSS-23
DATE 9-3-72
CONDUCTED BY CEW
$\bar{\sigma}_{vc}$ (KG/CM^2) 2.0
OCR 1.0
PRETEST Ht.(MM) 23.343

DATE/TIME	VERTICAL PROVING RING	VERT. STRESS	γ (%)	$\dot{\gamma}$(%/MIN)	$\dot{\gamma}t$(%)	ELAPSED TIME (MINUTES)	APPLIED $\overline{D_\tau}$ (PER CENT)
9-8-72 725	30516	2.0	0	——	——	0	65% (.312 Kg/cm^2)
	3035		1.4417	1.6136	.8068	0.5	
	3015	1.91	1.6136	.2514	.2514	1	
	2999		1.8188	.1516	.3031	2	
	2980		2.0683	.09759	.3904	4	
	2955	1.79	2.3068	.06839	.4787	7	
	2939		2.479	.04505	.4505	10	
	2925		2.667	.03280	.4920	15	
	2919	1.71	2.872	.02476	.5447	22	
	2912		3.039	.01687	.5061	30	
	2904		3.261	.01293	.5819	45	
	2902	1.67	3.427	.00879	.5274	60	
	28995		3.665	.00635	.5779	91	
	2872		3.904	.00474	.6393	135	
	2868		4.087	.00324	.5837	180	
	2855		4.286	.00232	.5875	253	
	2848		4.458	.00172	.5854	340	
	2842	1.55	4.614	.00102	.4518	443	
	28315		4.991	.000630	.5432	862	
	2785		5.307	.000279	.4300	1543	
4-10-72 1315	2796		5.6504	.000186	.5994	3230	
	2794		5.6782	.000106	.3771	3545	
	2801	1.47	5.7003	.000108	.3996	3699	
	2790		5.7613	.000106	.4562	4315	
	2783		5.8113	.0000853	.4050	4748	
	2783		5.8833	.0000729	.4189	5745	
	2785	1.43	5.9277	.0000662	.4197	6345	

$\overline{D_\tau} = \tau$ (APPLIED) / τ MAX.

DATE/TIME	VERTICAL PROVING RING	VERT. STRESS	γ (%)	$\dot{\gamma}$ (%/MIN.)	$\dot{\gamma}_t$ (%)	ELAPSED TIME (MINUTES)	APPLIED $\bar{D}_\tau$ (PER CENT)
	2781		5.9776	.0000534	.3852	7170	
	2780		5.9942	.0000486	.3750	7715	
	2780		6.0386	.0000445	.3855	8655	
	2775	1.414	6.0996	——	——	10 080	
	2775	1.414	6.0996	——	——	0	80%
	2765		6.2105	0.1165	.05822	0.5	(.384 Kg/cm²)
	2762		6.2160	.01109	.01109	1	
	2762		6.2271	.00924	.01848	2	
	2763		6.2438	.00665	.02661	4	
	2763		6.2604	.00462	.03255	7	
	2768		6.2715	.00299	.02986	10	
	2770	1.41	6.2992	.00178	.03584	20	
	2772		6.3214	.00136	.05169	38	
	2771		6.3713	.00125	.09141	73	
	2771		6.4378	.00113	.1781	131	
	2772		6.4767	.00101	.1570	156	
	2772		6.5487	.000948	.2181	230	
	2772		6.6097	.000848	.2629	310	
	2772		6.6929	.000766	.3063	400	
	2773		6.7705	.000675	.3508	520	
	2772		6.8704	.000641	.4251	663	
	2773		6.9757	.000529	.4447	840	
	2768		7.3306	.000366	.5180	1578	
	2759		7.4526	.000357	.6759	1893	
	2760		7.6134	.000289	.6850	2370	
	2758		7.7798	.000247	.7492	2035	
	2752	1.365	7.9849	.000241	.9328	3875	
	2747		8.0903	.000201	.8683	4325	
	2747		8.2622	.000160	.8412	5256	
	2750		8.3287	.000154	.8848	5760	
	2742		8.4341	.000148	.9460	6375	
	2741		8.5394	.000120	.8617	7180	
	2744	1.35	8.7113	.000109	.9471	8685	

DATE/TIME	VERTICAL PROVING RING	VERT. STRESS	γ (%)	$\dot{\gamma}$ (%/MIN)	$\dot{\gamma}_t$ (%)	ELAPSED TIME (MINUTES)	APPLIED $\bar{D}_\tau$ (PER CENT)
9-22-72 730	2743	1.347	8.8666	———	———	10 080	
740	2743	1.347	8.8666	———	———	0	95%
	2746		8.9941	.1442	.07208	0.5	(.456 Kg/cm^2)
	2746		9.0108	.02588	.02588	1	
	2746		9.0329	.01294	.02588	2	
	2746		9.0496	.01109	.04436	4	
	2746	1.35	9.0884	.00924	.06470	7	
	2746		9.1050	.00762	.07624	10	
	2746		9.1494	.006932	.10398	15	
	2748		9.1882	.00555	.1220	22	
	2748		9.2437	.00530	.1697	32	
	2748		9.3102	.00495	.2228	45	
	2748		9.3823	.00504	.3025	60	
	2748	1.358	9.4765	.00532	.4147	78	
	2748		9.7704	.00567	.7535	133	
	2748		9.8978	.00646	1.0985	170	
	2748		10.591	.00665	1.730	260	
	2726	1.31	11.029	.00710	2.306	325	
	2713		11.783	.00789	3.377	428	
	2650	1.16	12.410	.00925	4.627	500	
	2604		13.264	.01669	9.817	588	
	2604	1.06	17.001	———	———	775	
			FAILURE				

APPENDIX C

PLOTS OF $\overline{CK_oU}$DSS CREEP TESTS

Note: Lines with symbols represent the test being plotted. The remaining curve is the stress-strain curve for the corresponding (NC or OC) controlled strain $\overline{CK_oU}$DSS test.

Note: Curved stress path is that of the corresponding $\overline{CK_oU}$DSS controlled strain test. The remaining stress path is that of the creep test.

$\overline{\phi}_{max} = \tan^{-1}(\tau/\overline{\sigma}_v)_{max}$ from controlled strain $\overline{CK_oU}$DSS test

$\overline{\phi}_u = \tan^{-1}(\tau/\overline{\sigma}_v)$ at τ_{max} from controlled strain $\overline{CK_oU}$DSS test

$\overline{\phi}_c = \tan^{-1}(\tau/\overline{\sigma}_v)$ at creep rupture

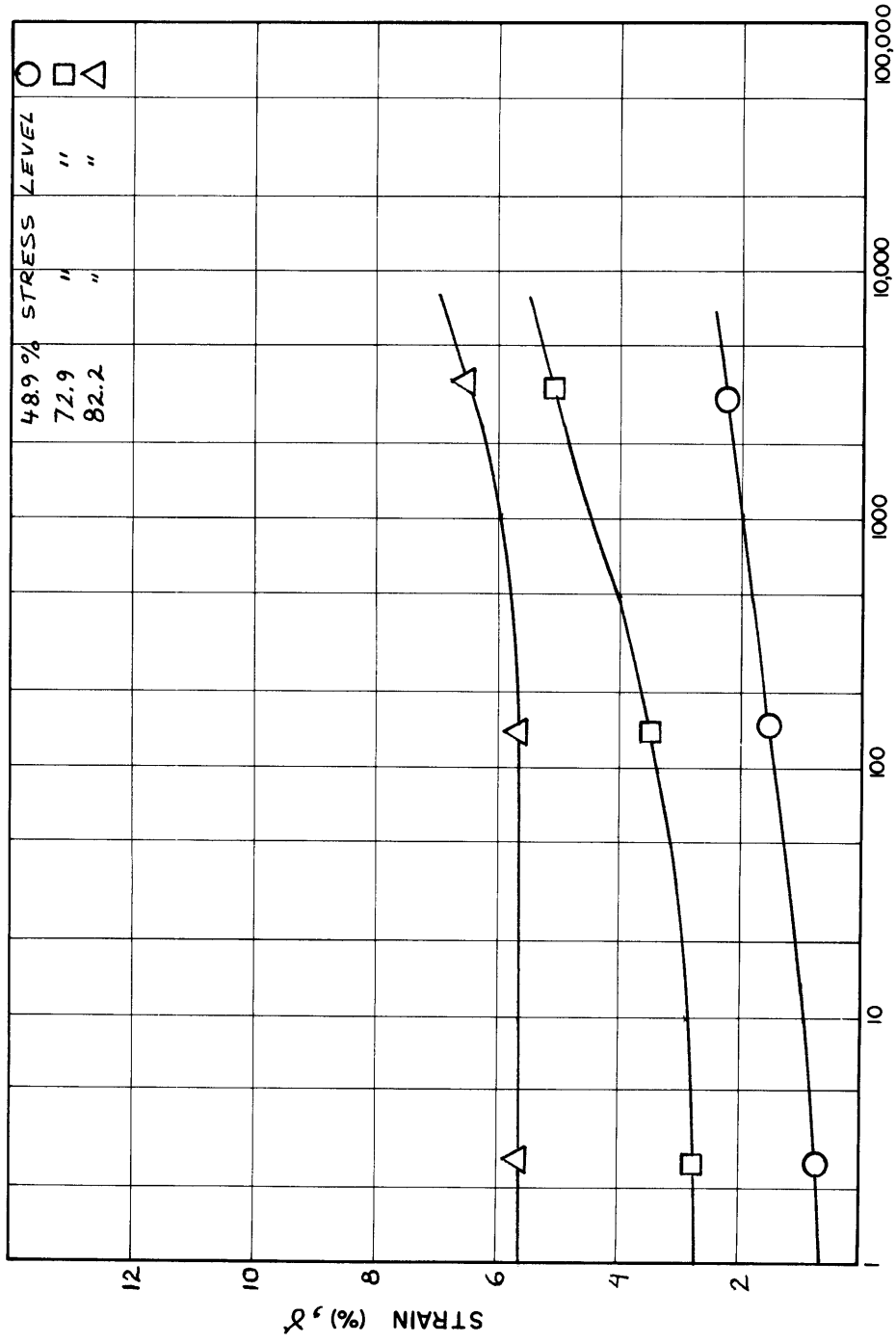

C1: STRAIN VS. LOG TIME, $\overline{\sigma}_o$ UDSS-8

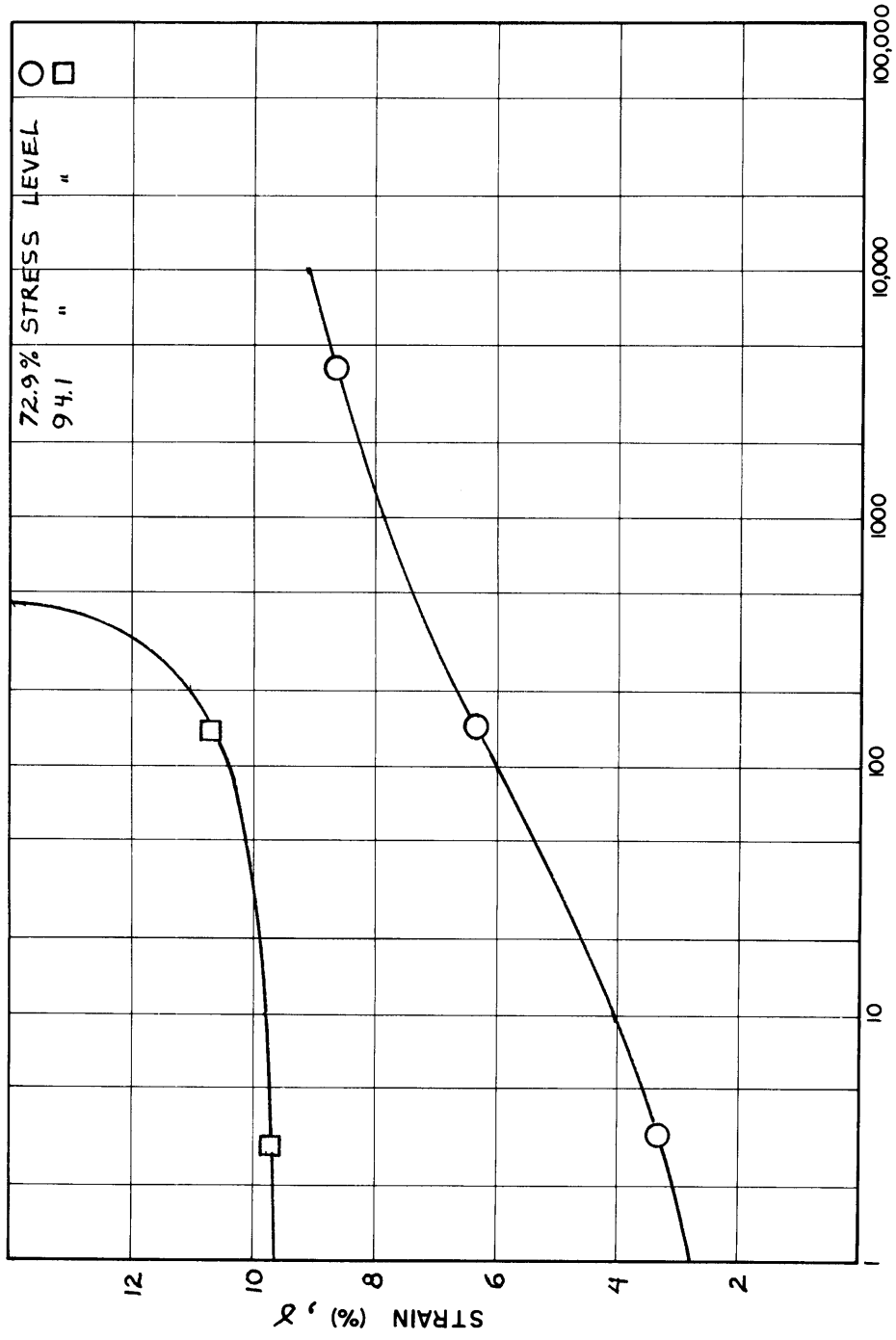

C2: STRAIN VS. LOG TIME, $\overline{CK_o}$UDSS-10

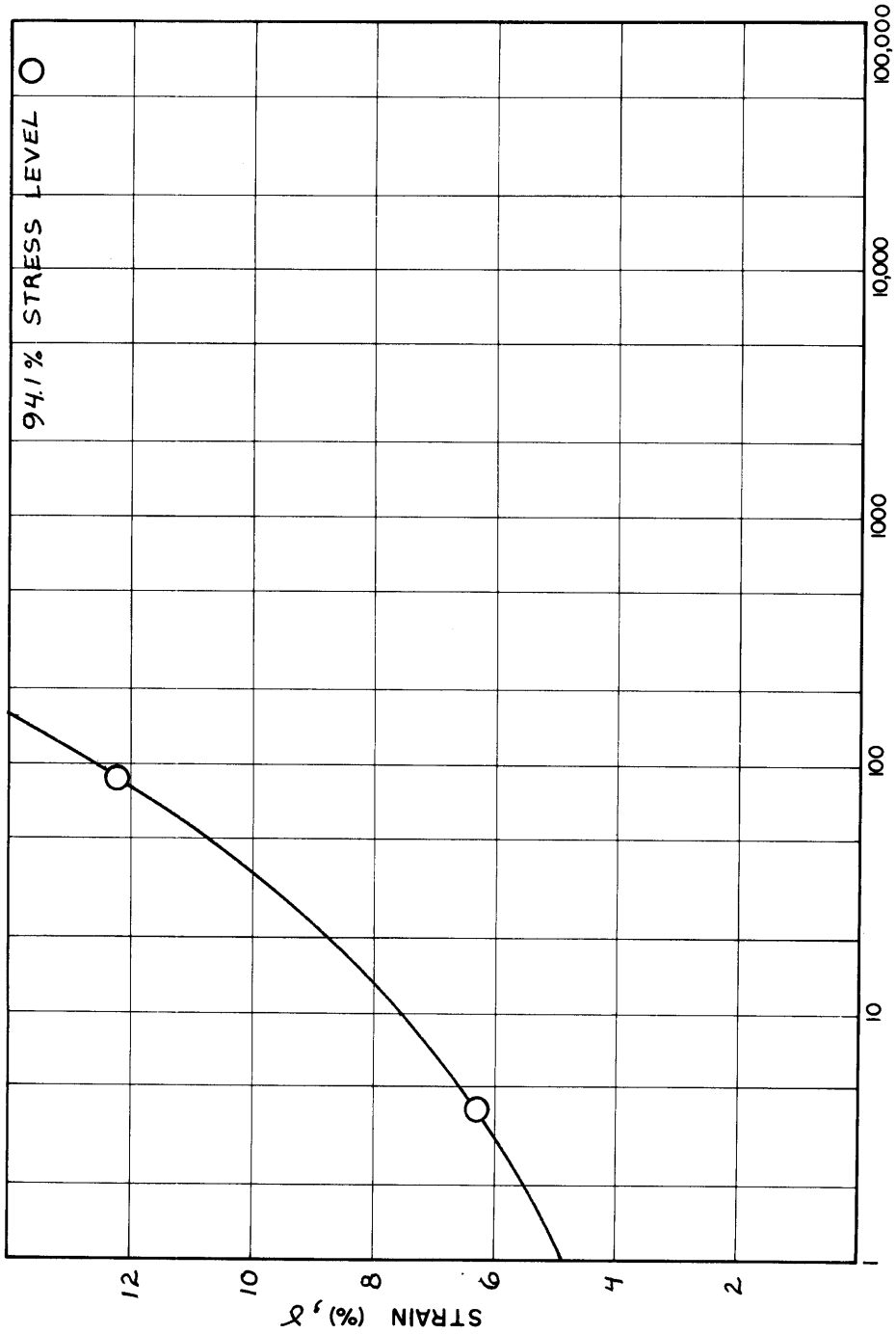

C3: STRAIN VS. LOG TIME, $\overline{CK_o}$UDSS-11

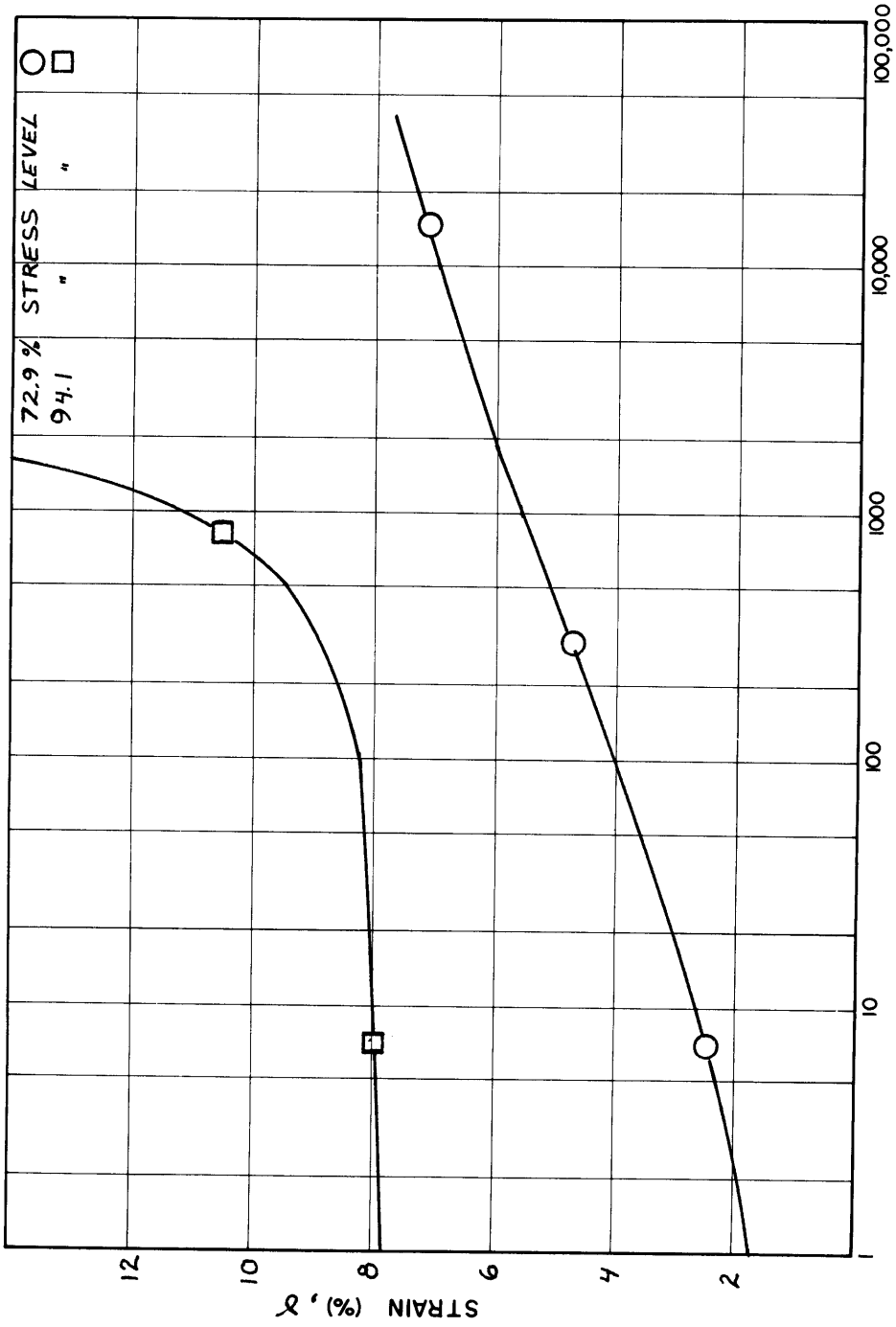

C4: STRAIN VS. LOG TIME, $\overline{CK_O}$UDSS-12

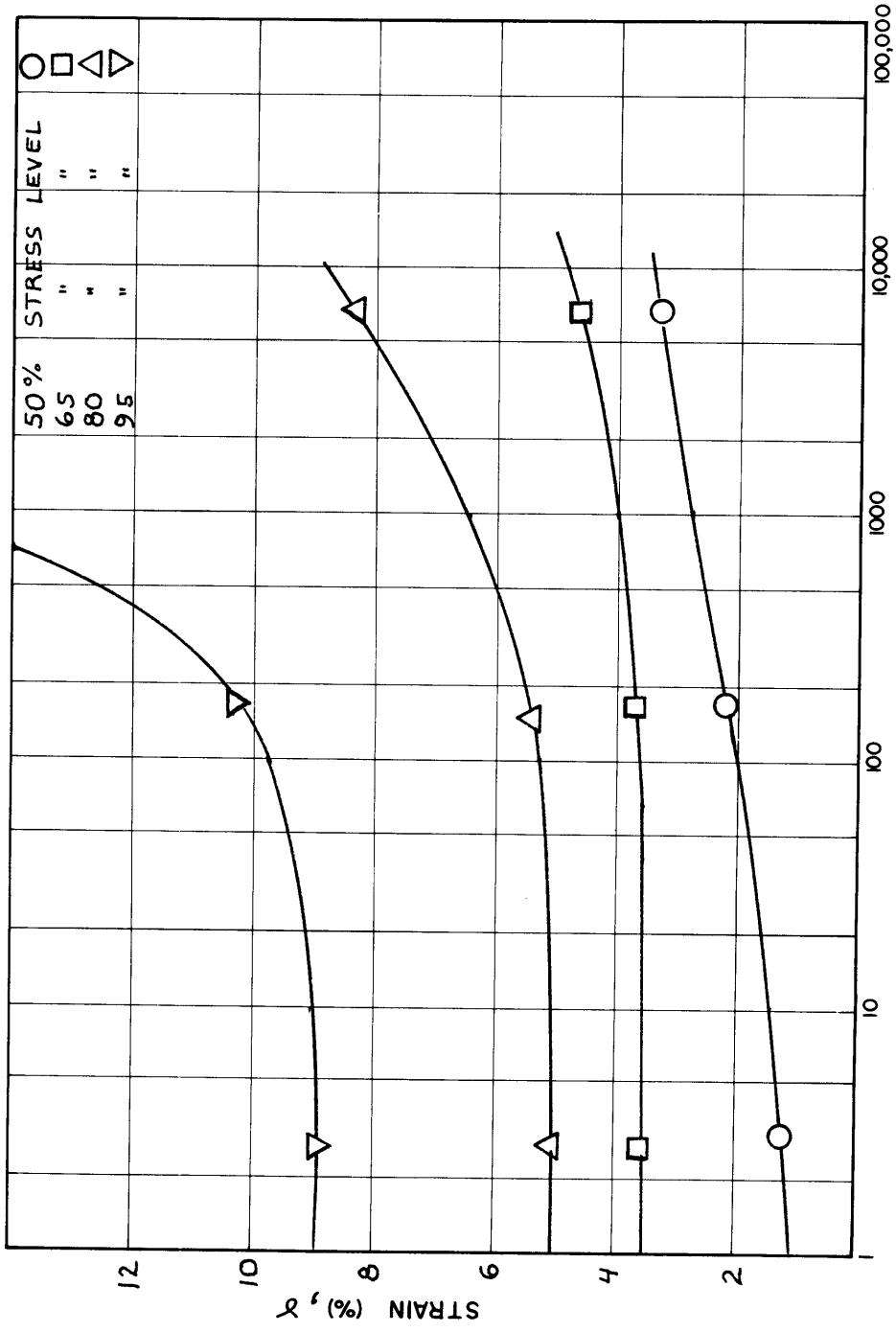

C5: STRAIN VS. LOG TIME, $\overline{CK_o}$UDSS-16

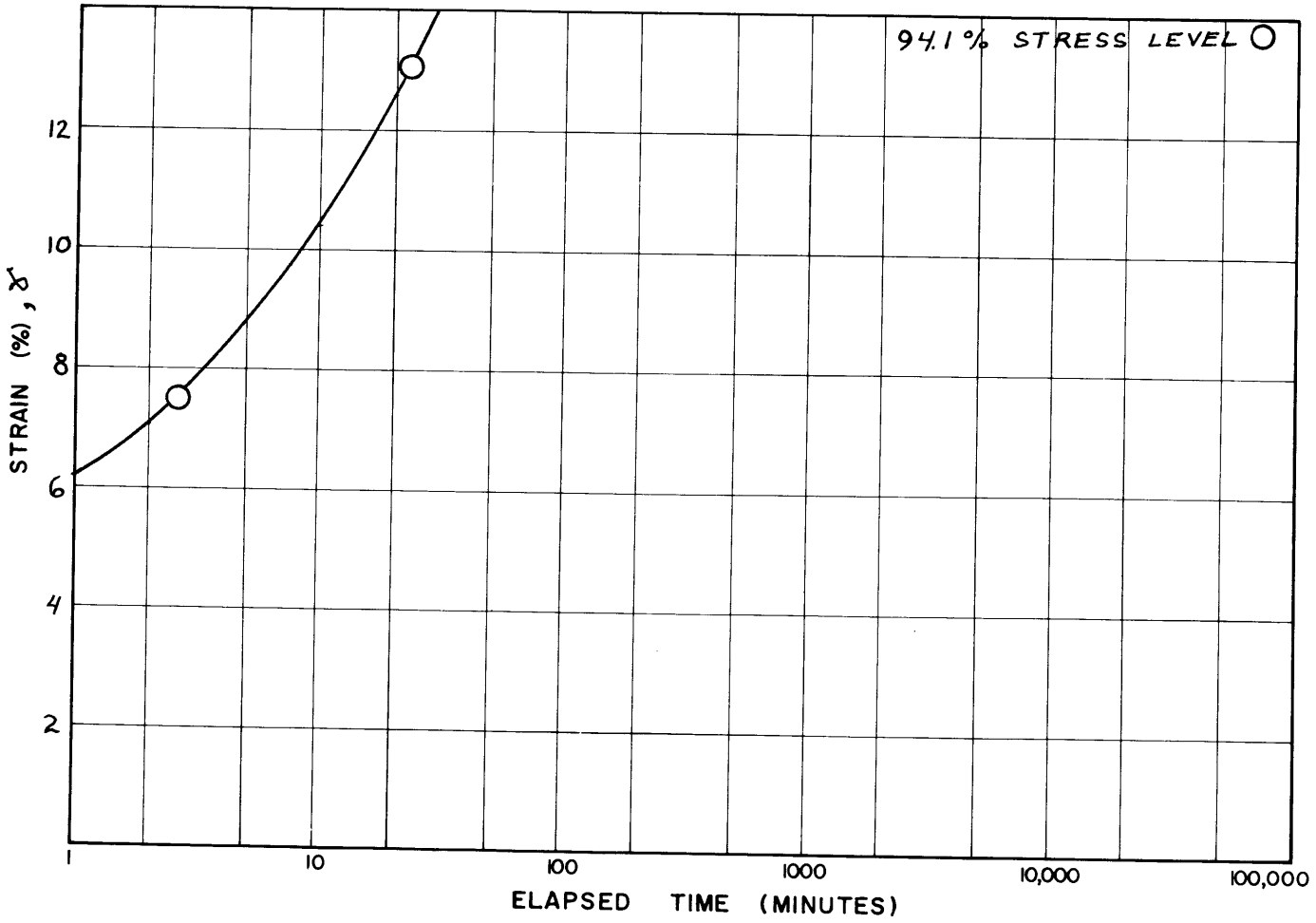

C6: STRAIN VS. LOG TIME, $\overline{CK_oU}$DSS-17

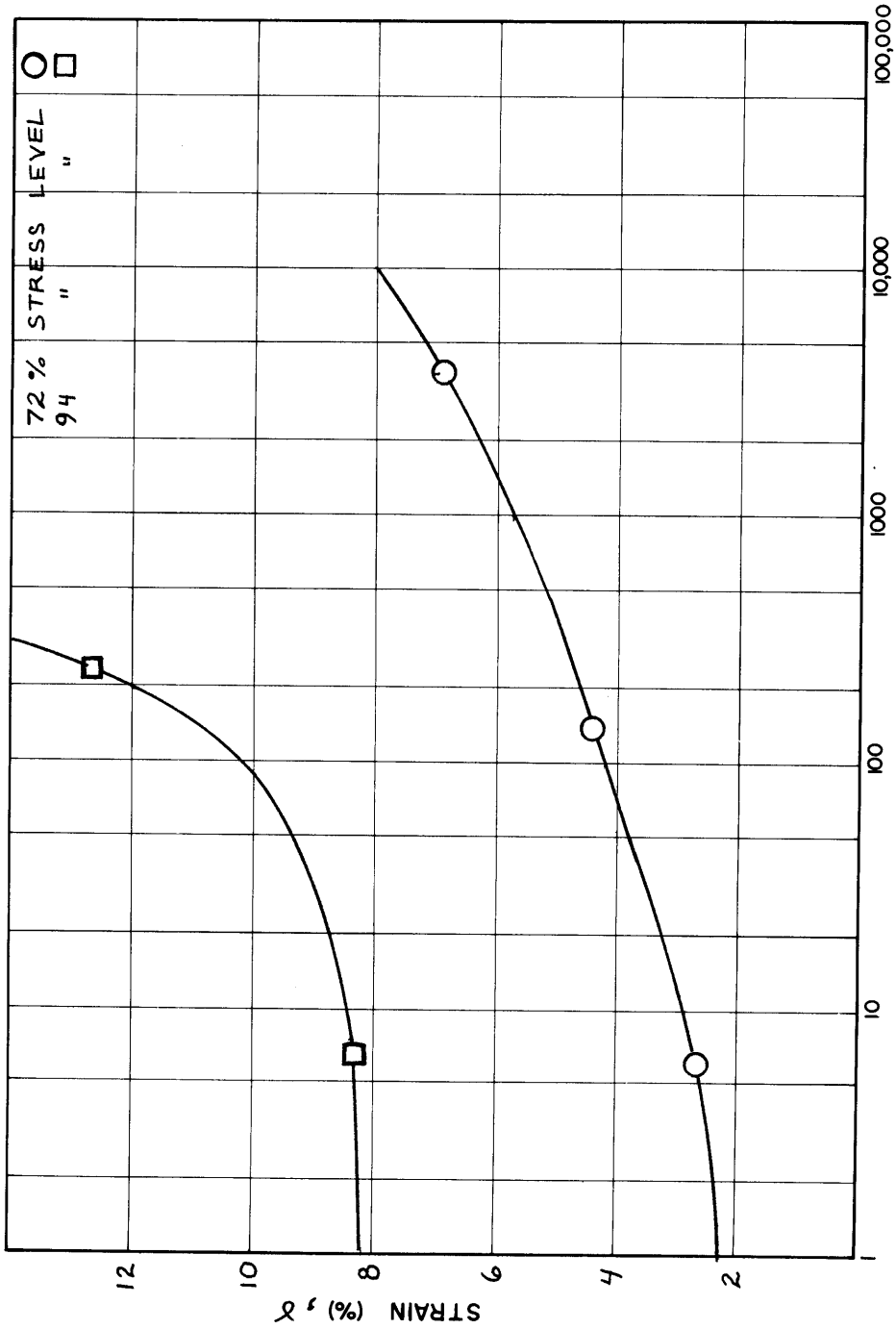

C7: STRAIN VS. LOG TIME, $\overline{CK_o}$UDSS-18

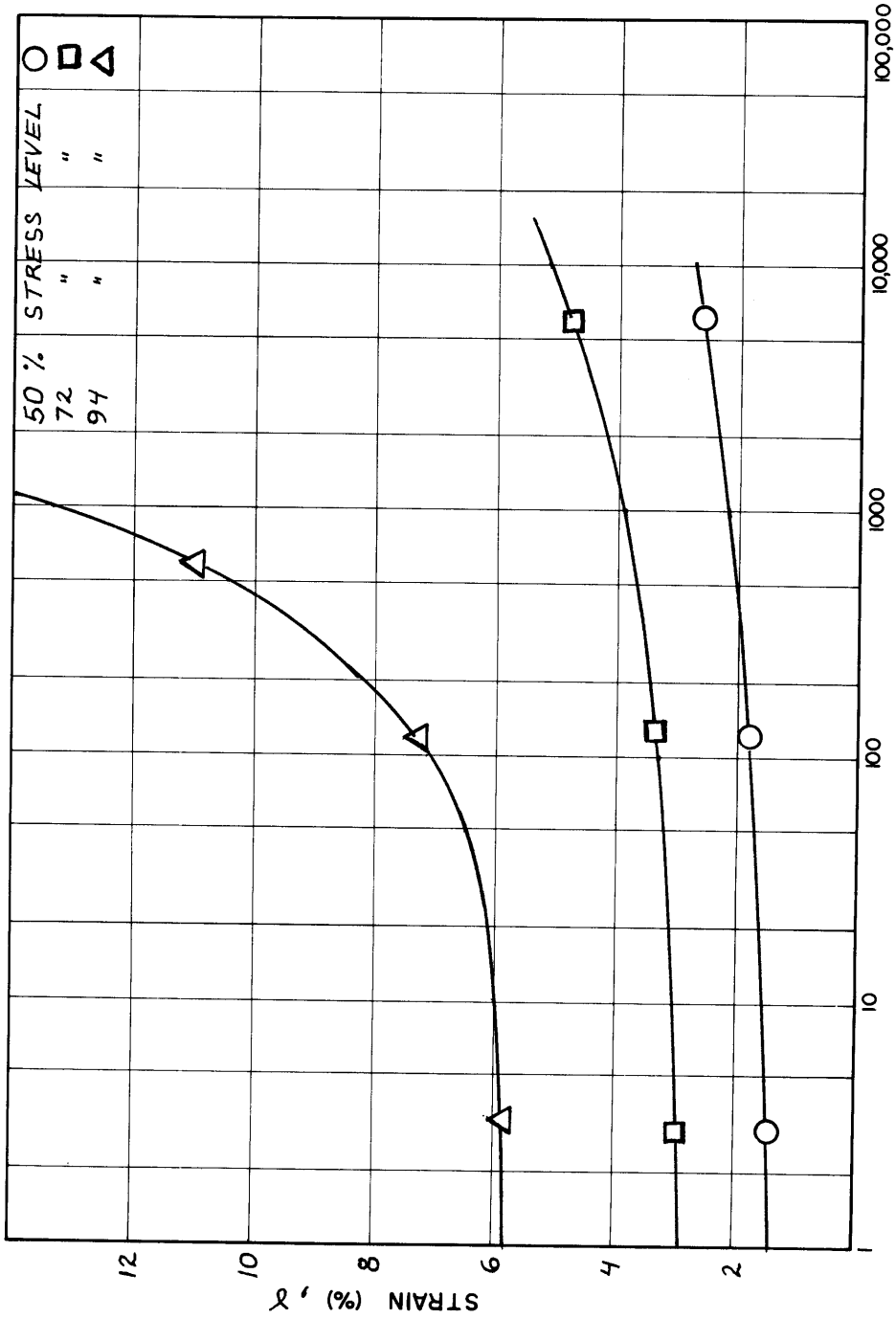

C8: STRAIN VS. LOG TIME, $\overline{CK_oU}$DSS-19

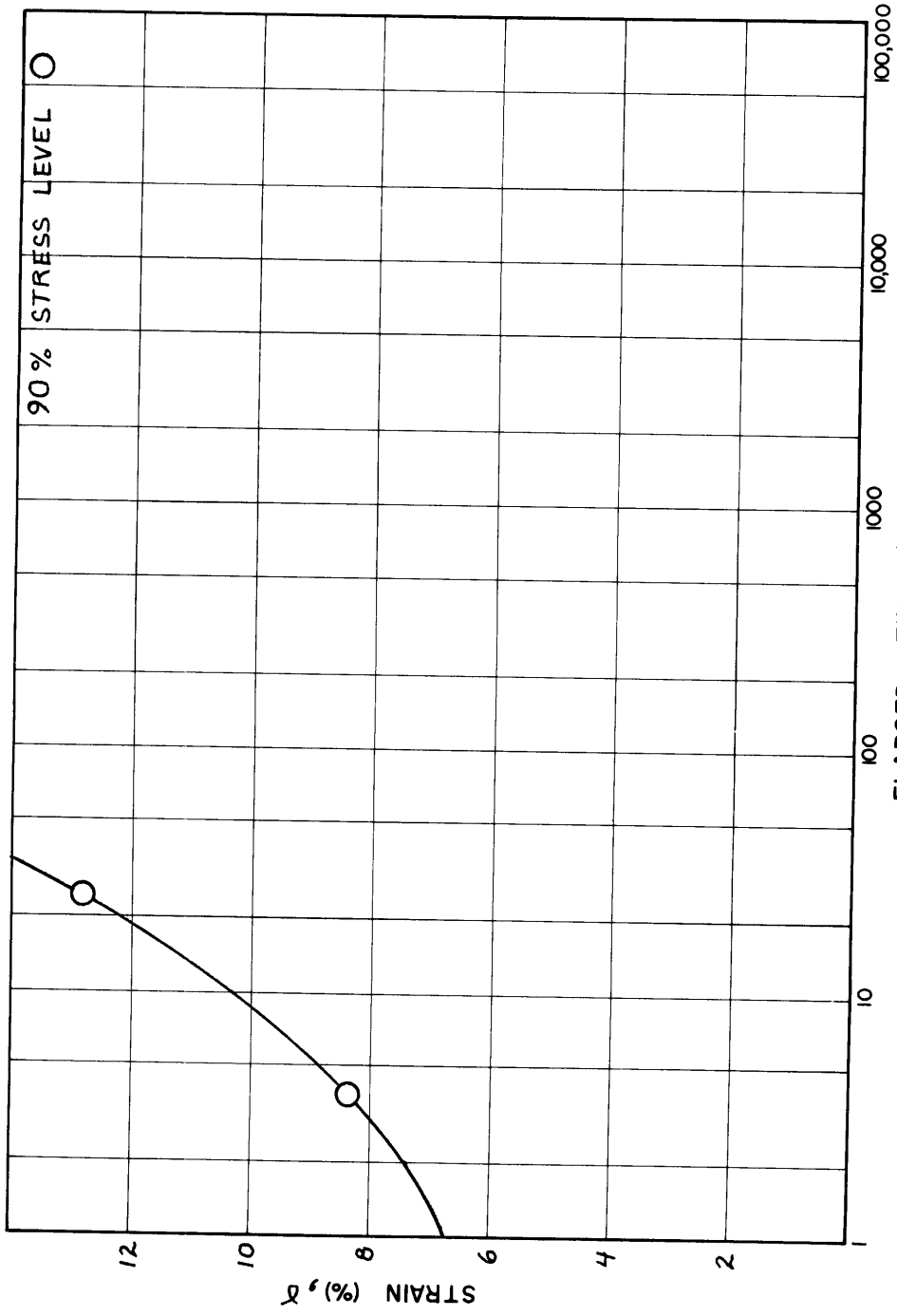

C9: STRAIN VS. LOG TIME, $\overline{CK_o}$UDSS-20

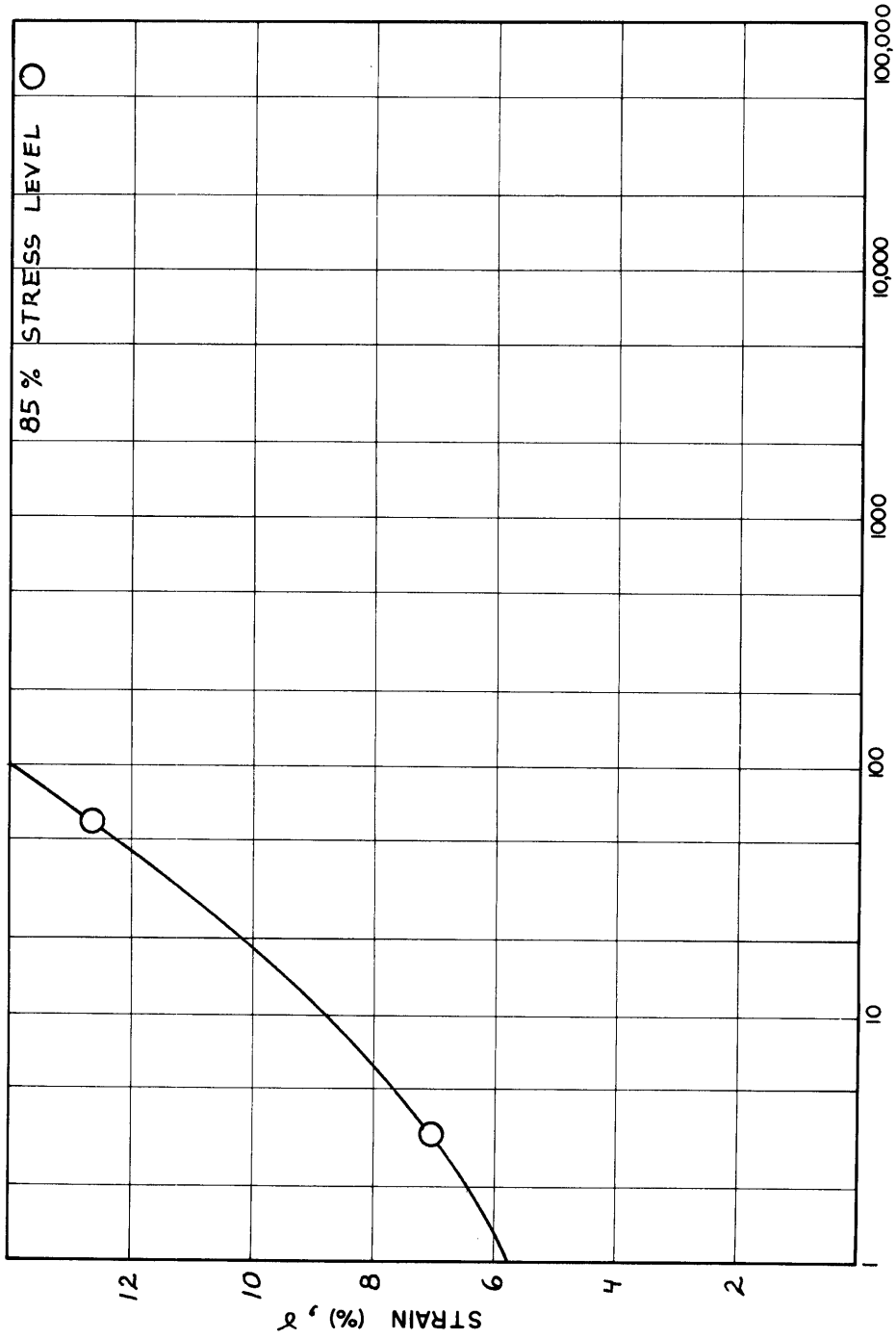

C10: STRAIN VS. LOG TIME, $\overline{CK_o UDSS}$-21

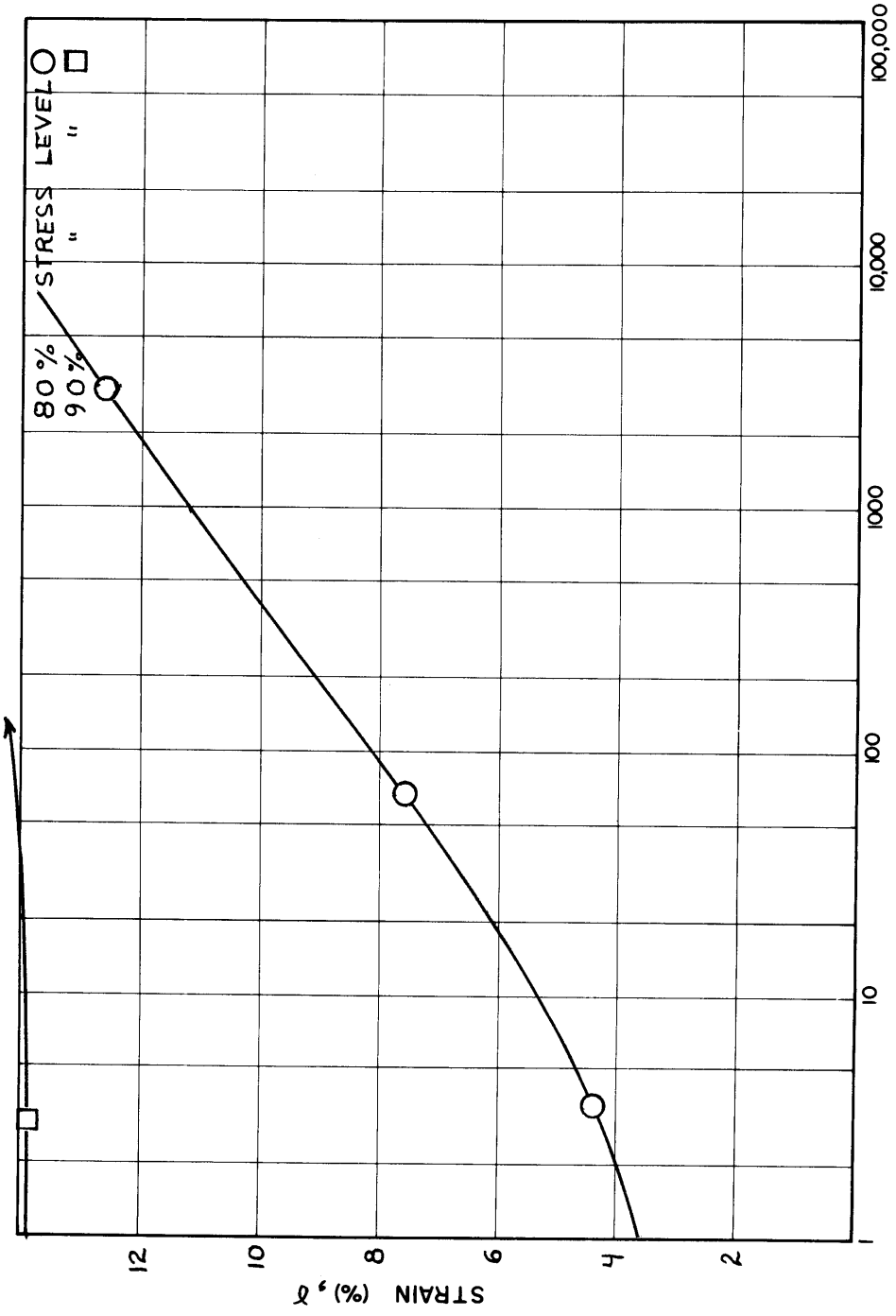

C11: STRAIN VS. LOG TIME, $\overline{CK_o}$ UDSS-22

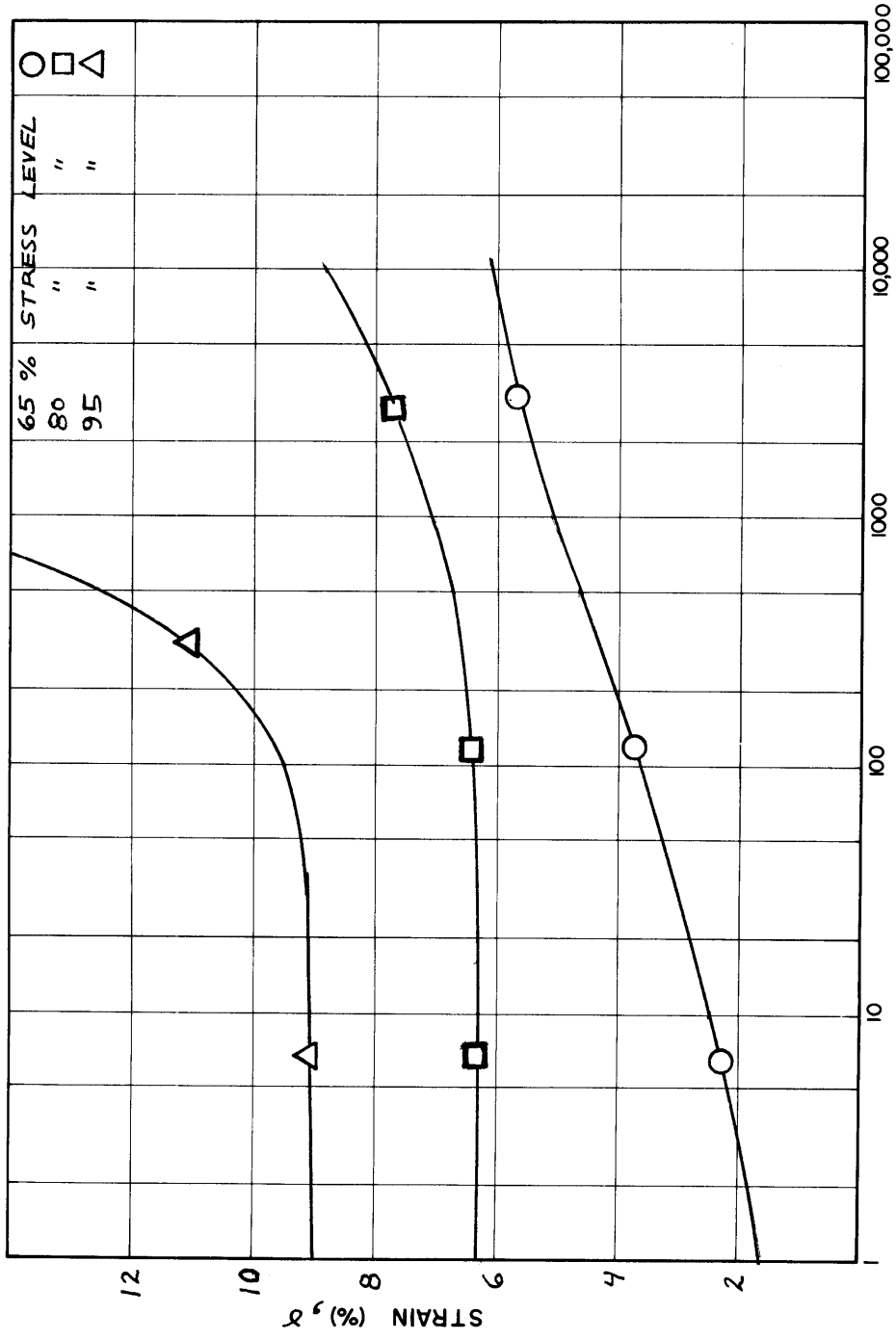

C12: STRAIN VS. LOG TIME, $\overline{CK_o UDSS}$-23

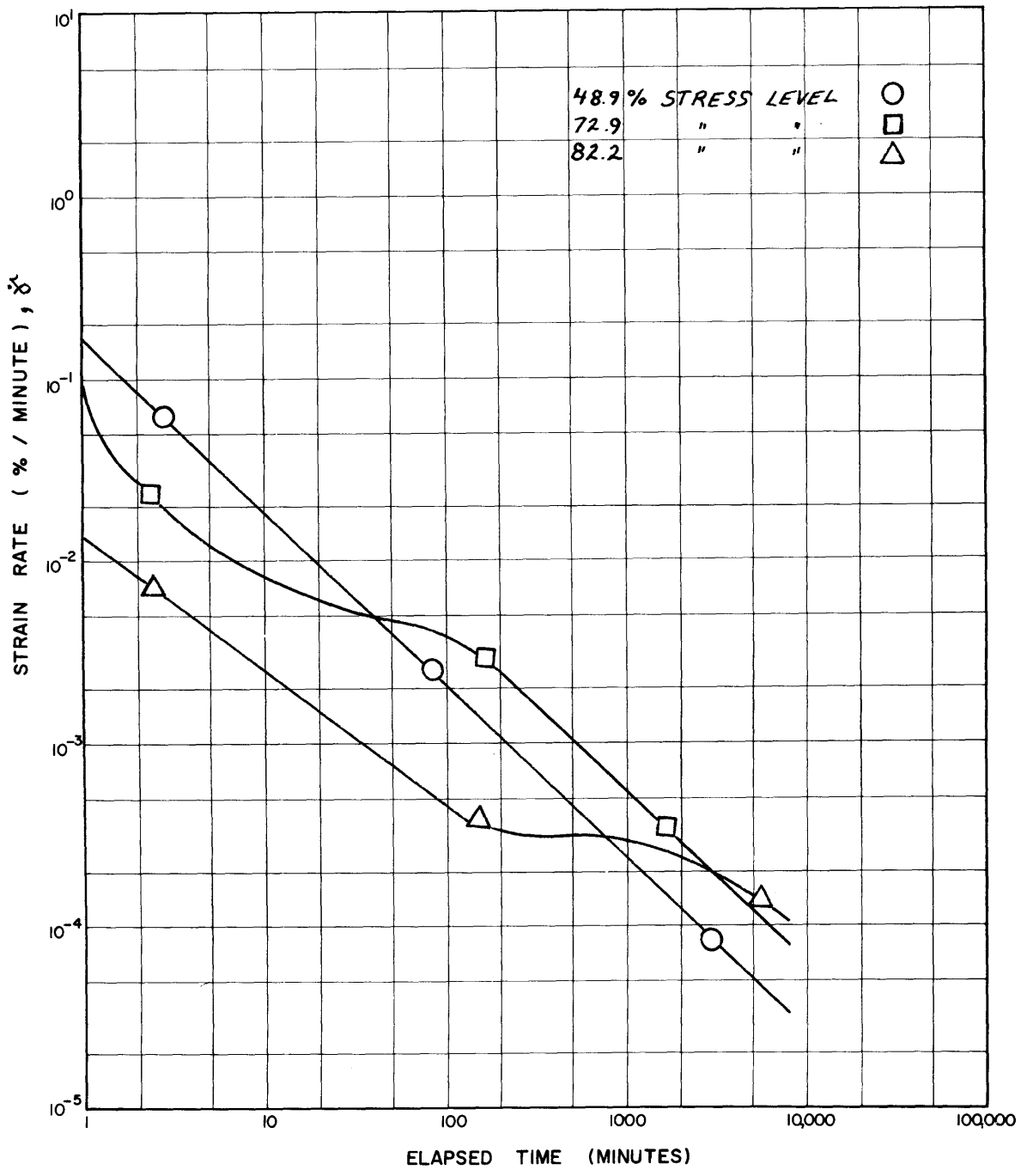

C13: LOG STRAIN RATE VS. LOG TIME, $\overline{CK_oU}$DSS-8

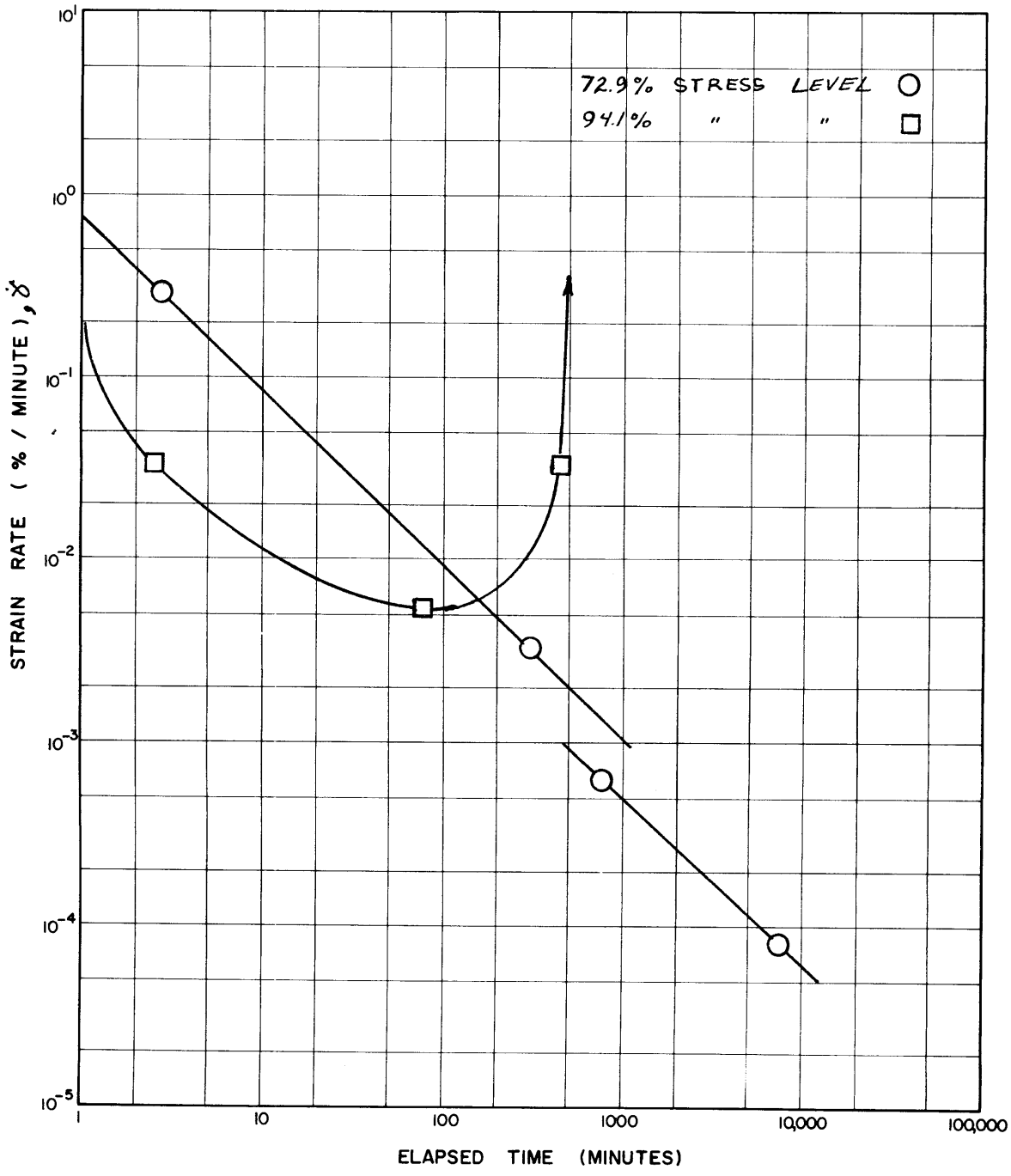

C14: LOG STRAIN RATE VS. LOG TIME, $\overline{CK_oU}$DSS-10

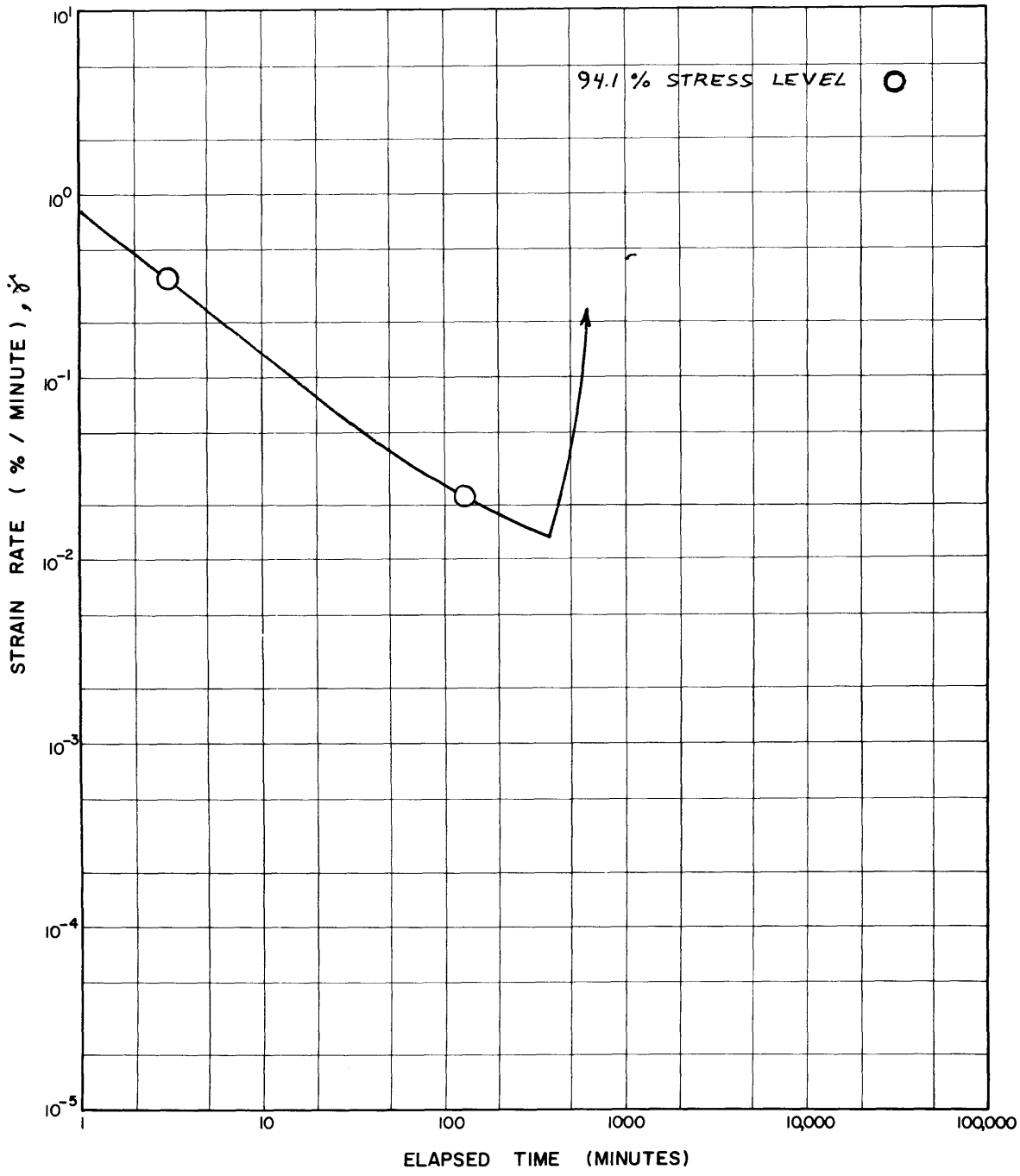

C15: LOG STRAIN RATE VS. LOG TIME, $\overline{CK_oU}$DSS-11

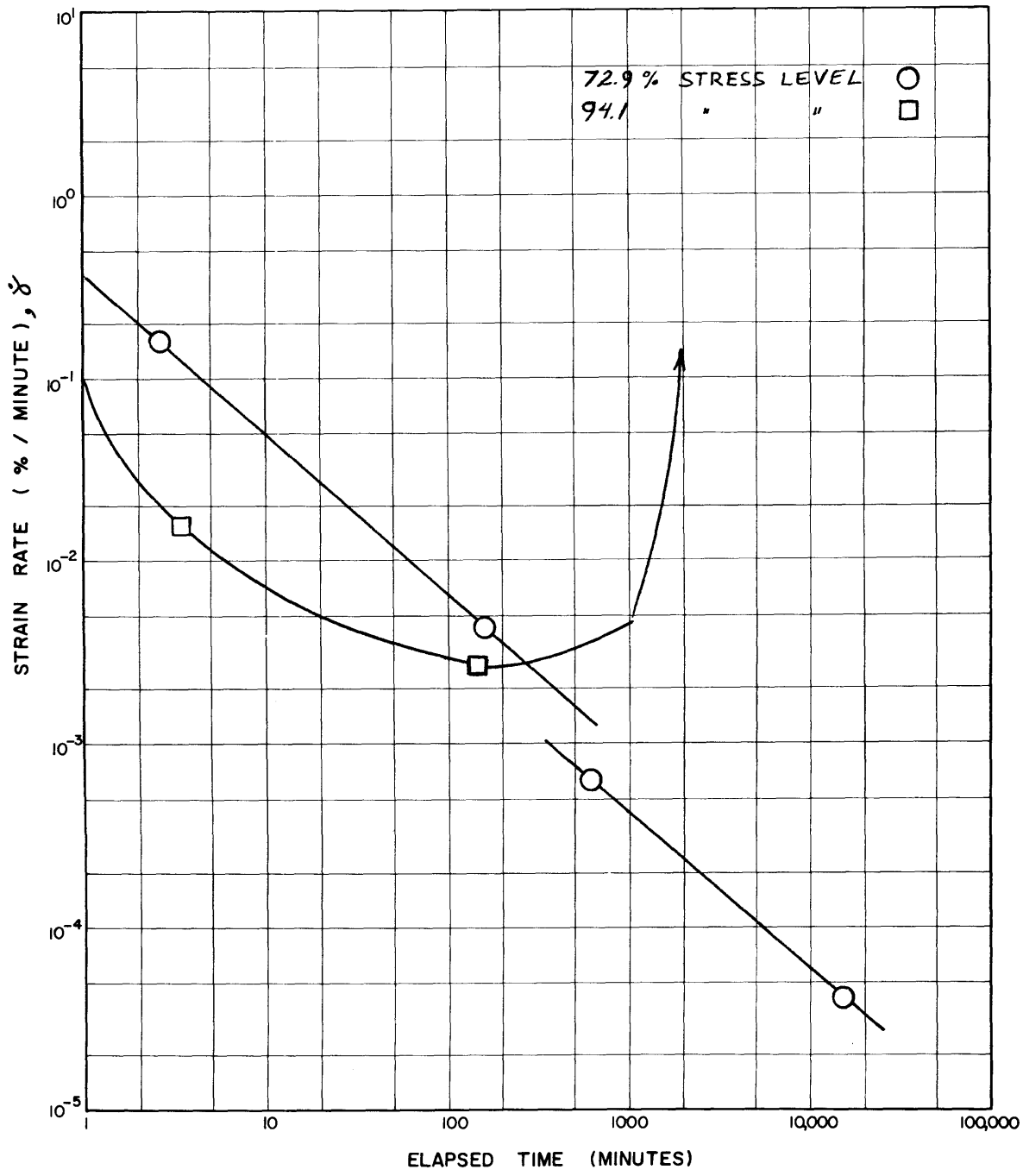

C16: LOG STRAIN RATE VS. LOG TIME, $\overline{CK_oU}$DSS-12

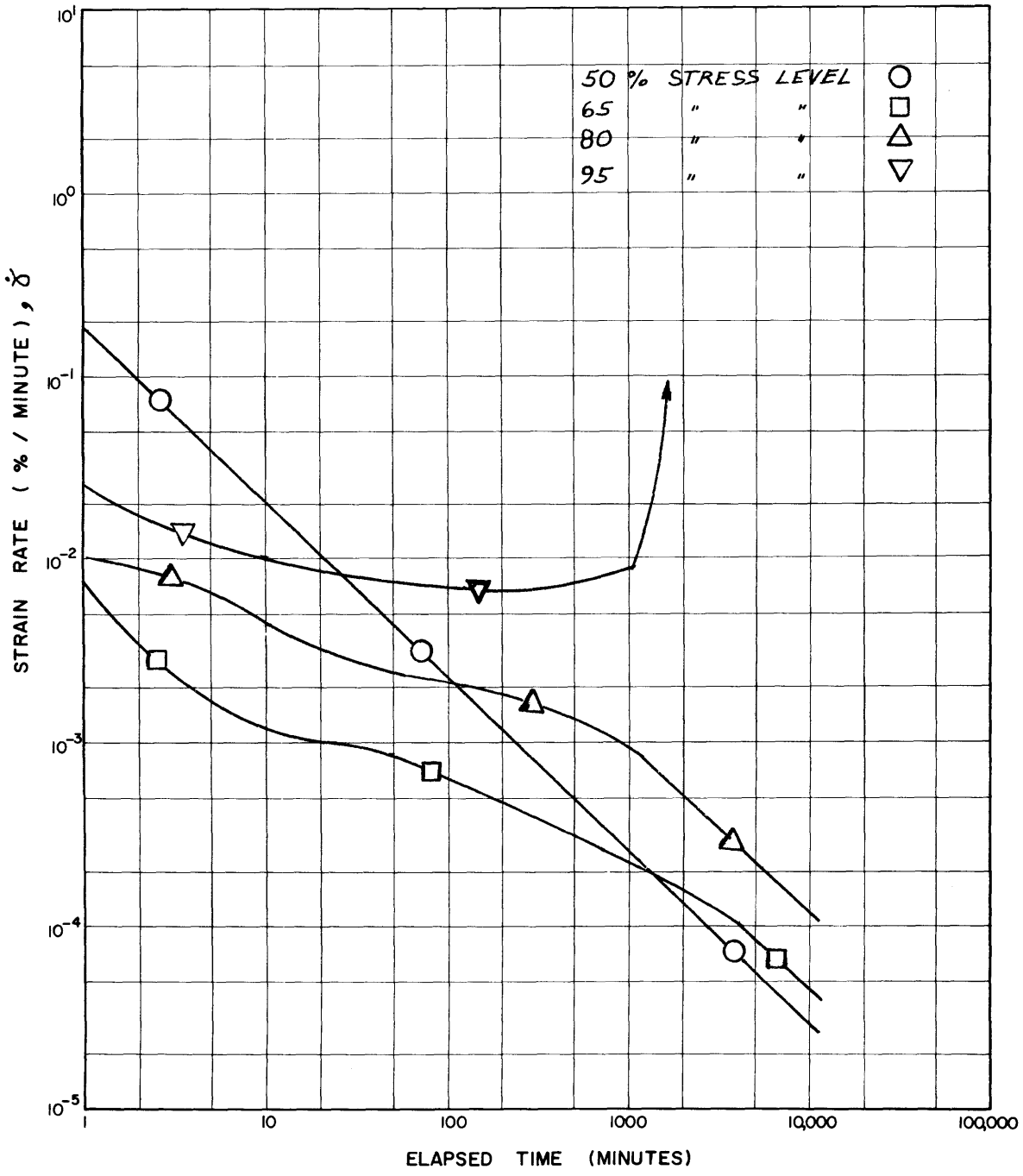

C17: LOG STRAIN RATE VS. LOG TIME, $\overline{CK_oU}$DSS-16

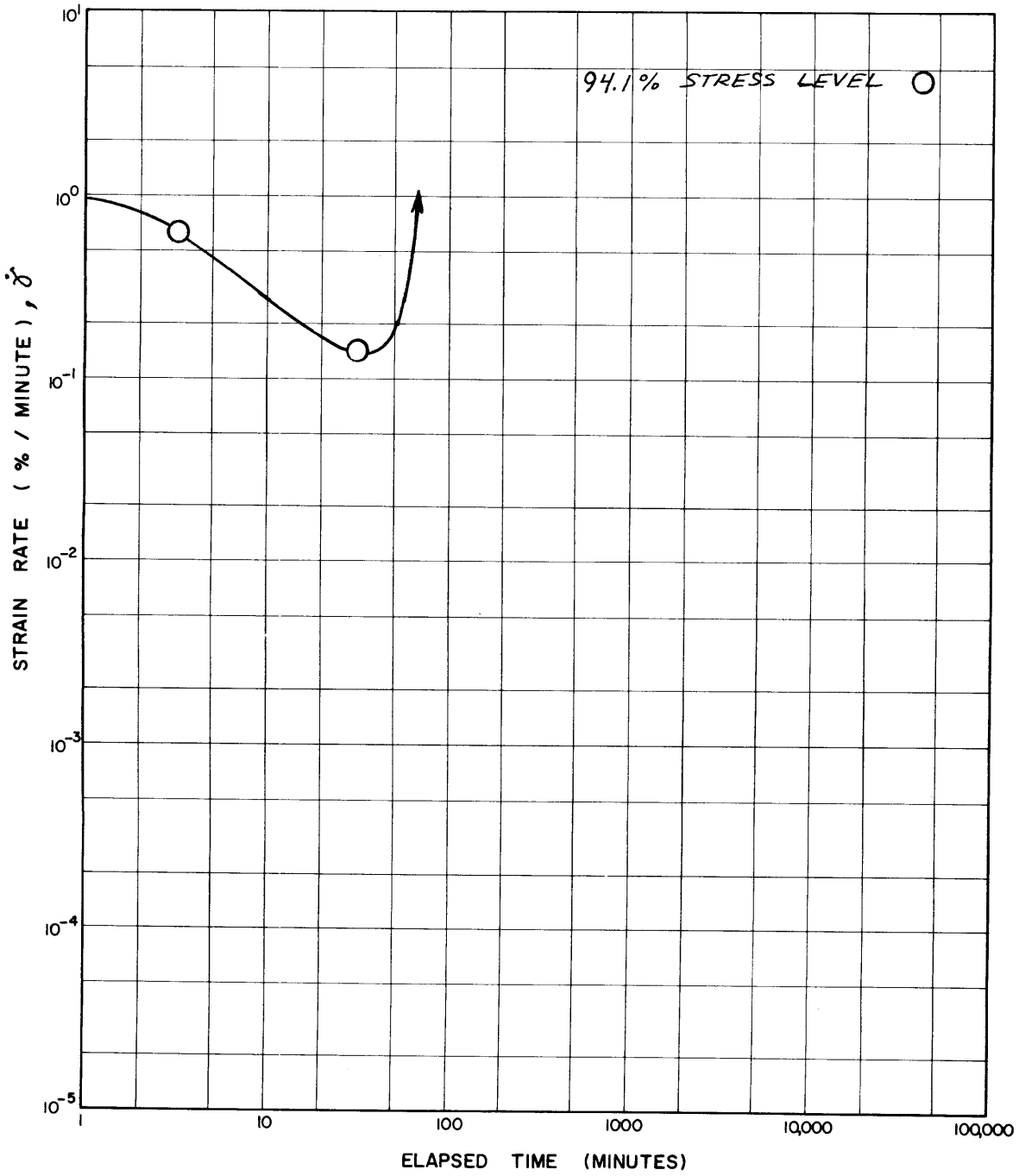

C18: LOG STRAIN RATE VS. LOG TIME, $\overline{CK_oU}$DSS-17

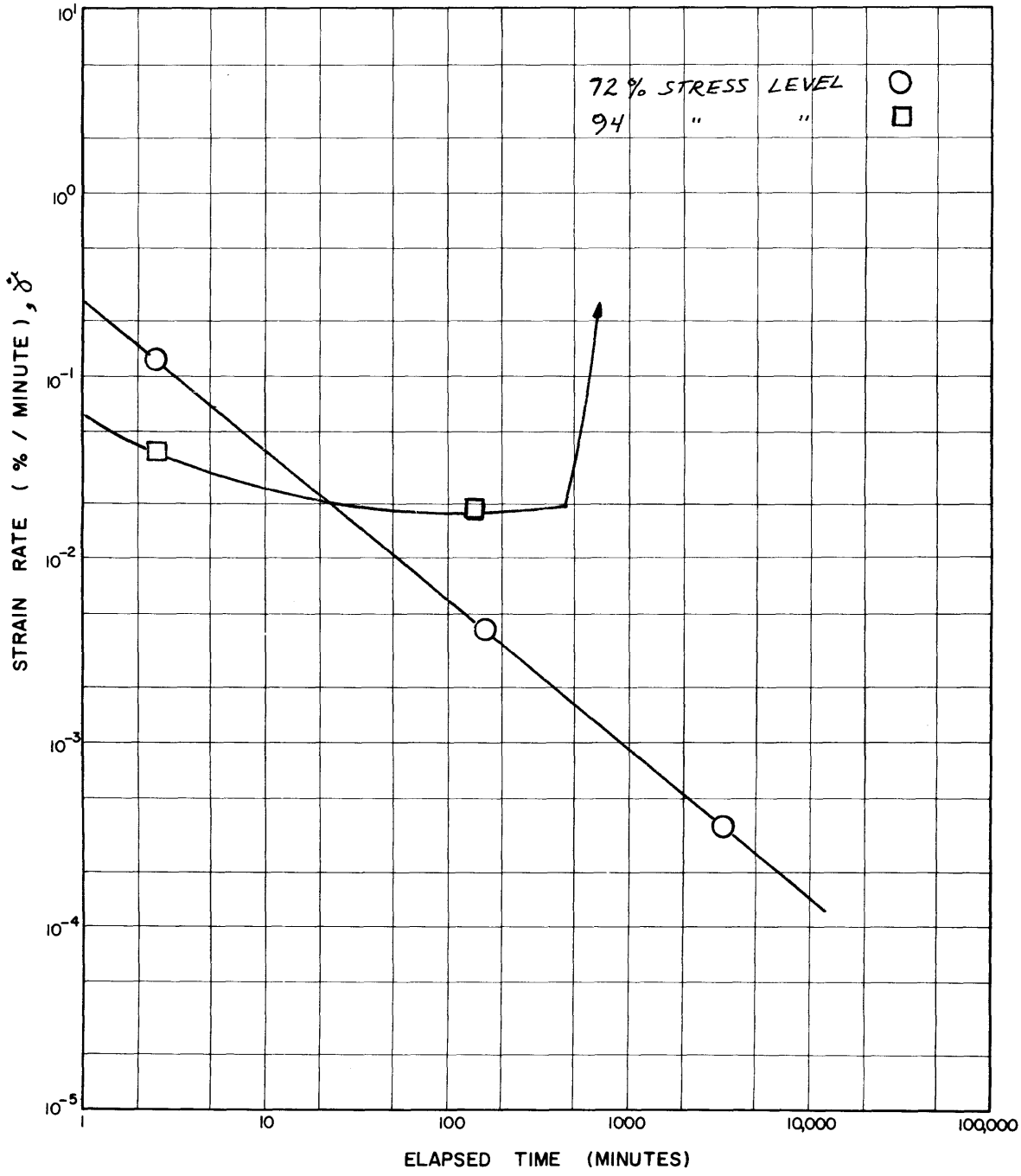

C19: LOG STRAIN RATE VS. LOG TIME, $\overline{CK_oU}$DSS-18

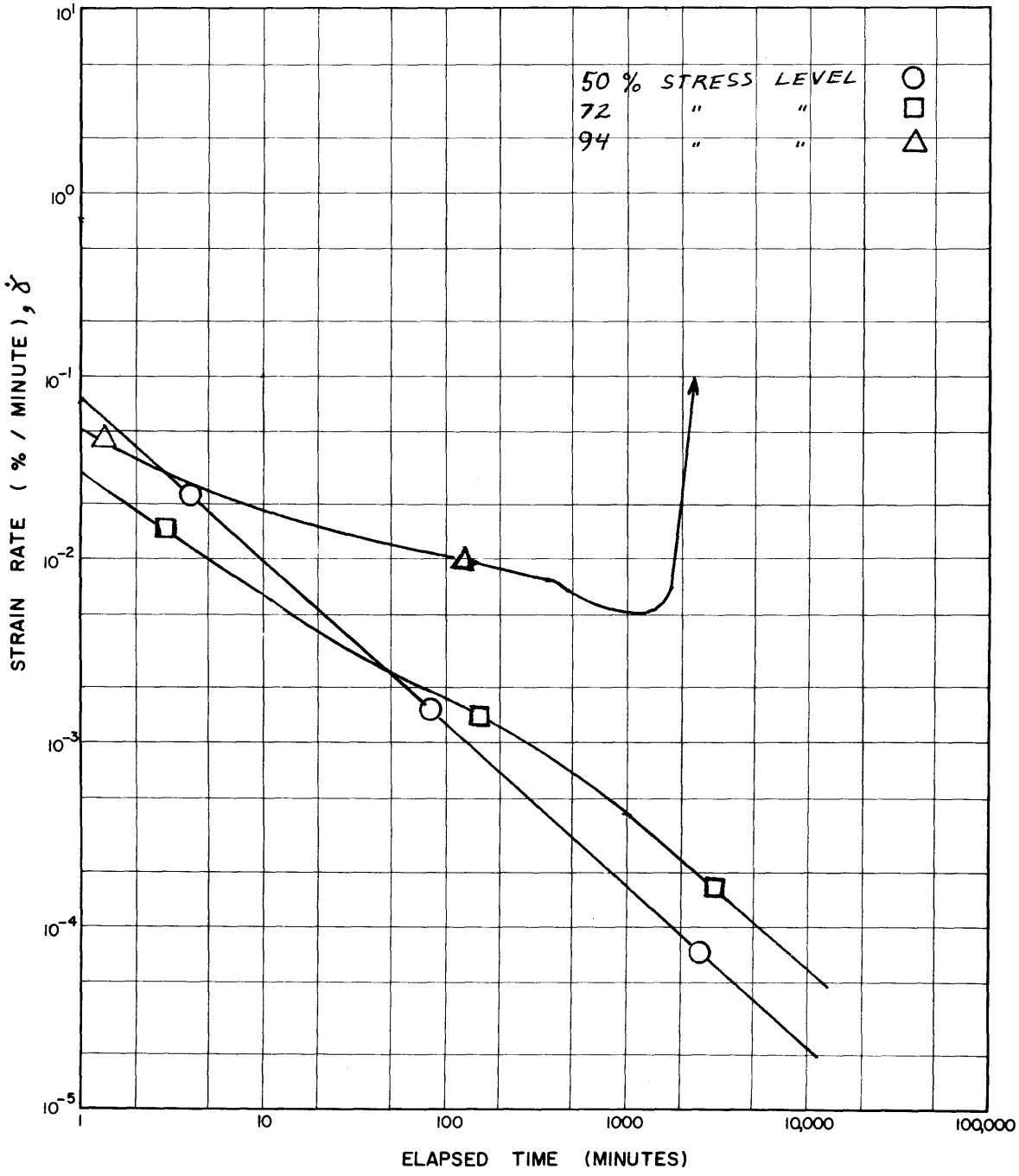

C20: LOG STRAIN RATE VS. LOG TIME, $\overline{CK_oU}$DSS-19

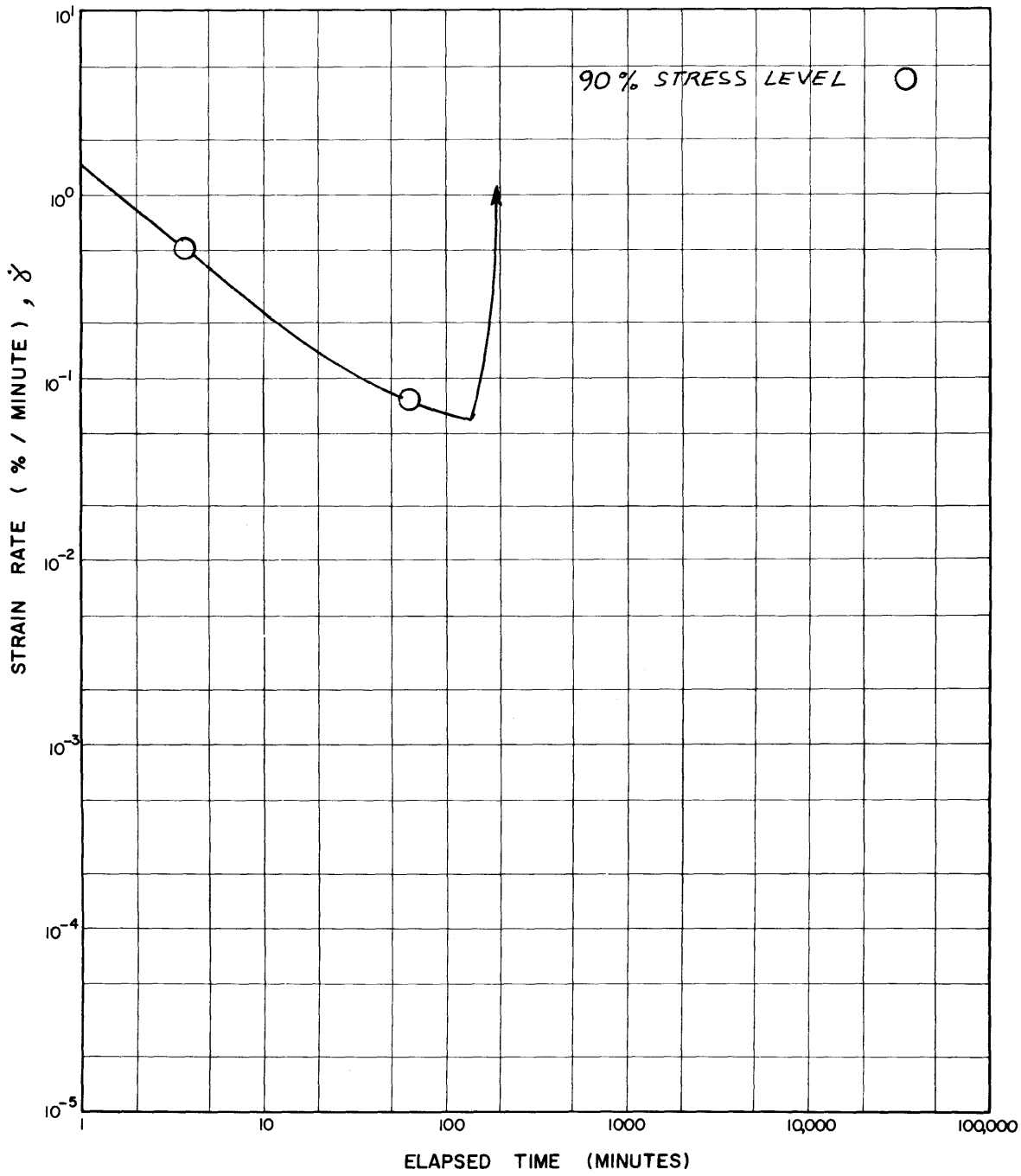

C21: LOG STRAIN RATE VS. LOG TIME, $\overline{CK_oU}$DSS-20

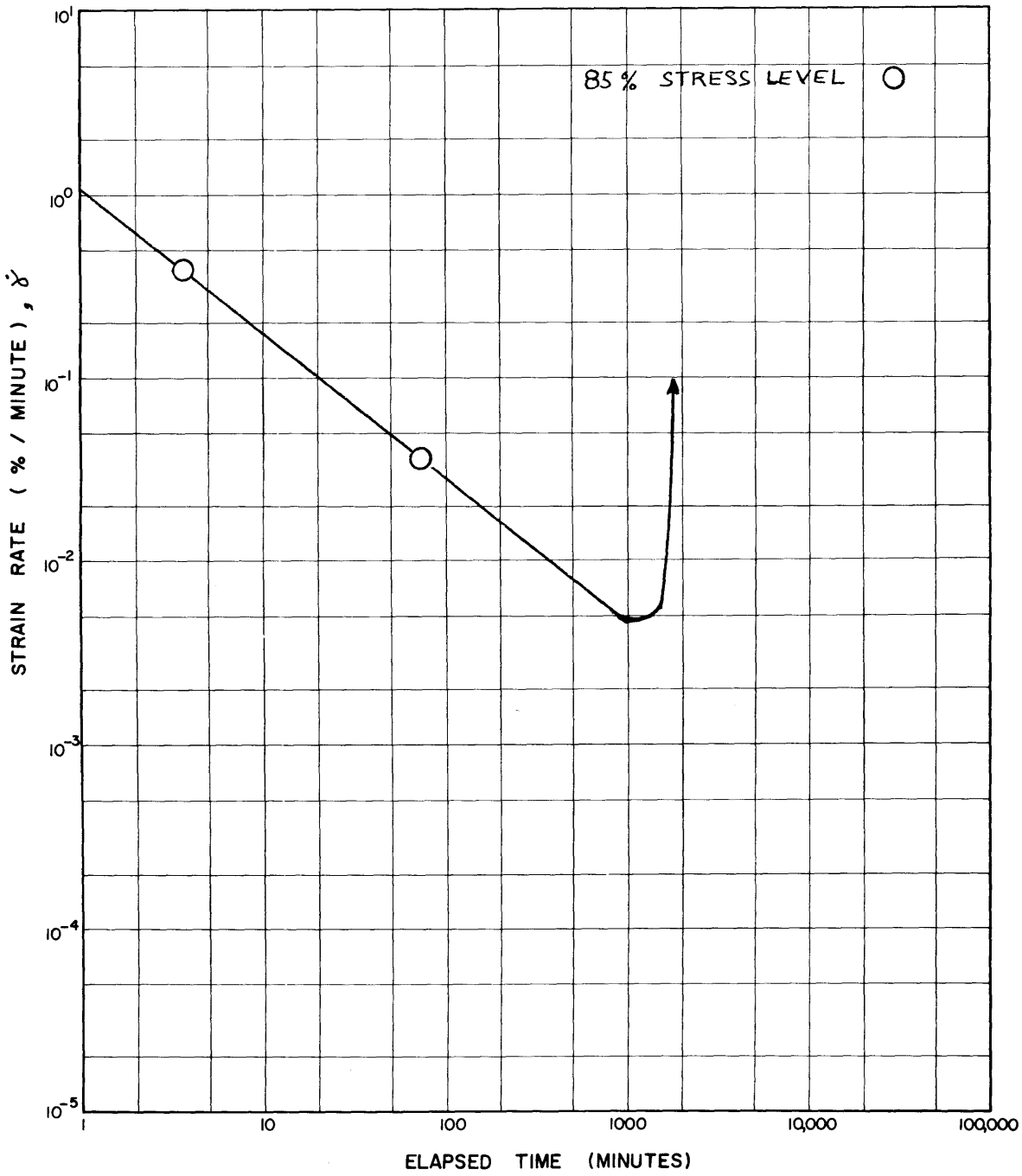

C22: LOG STRAIN RATE VS. LOG TIME, $\overline{CK_oU}$DSS-21

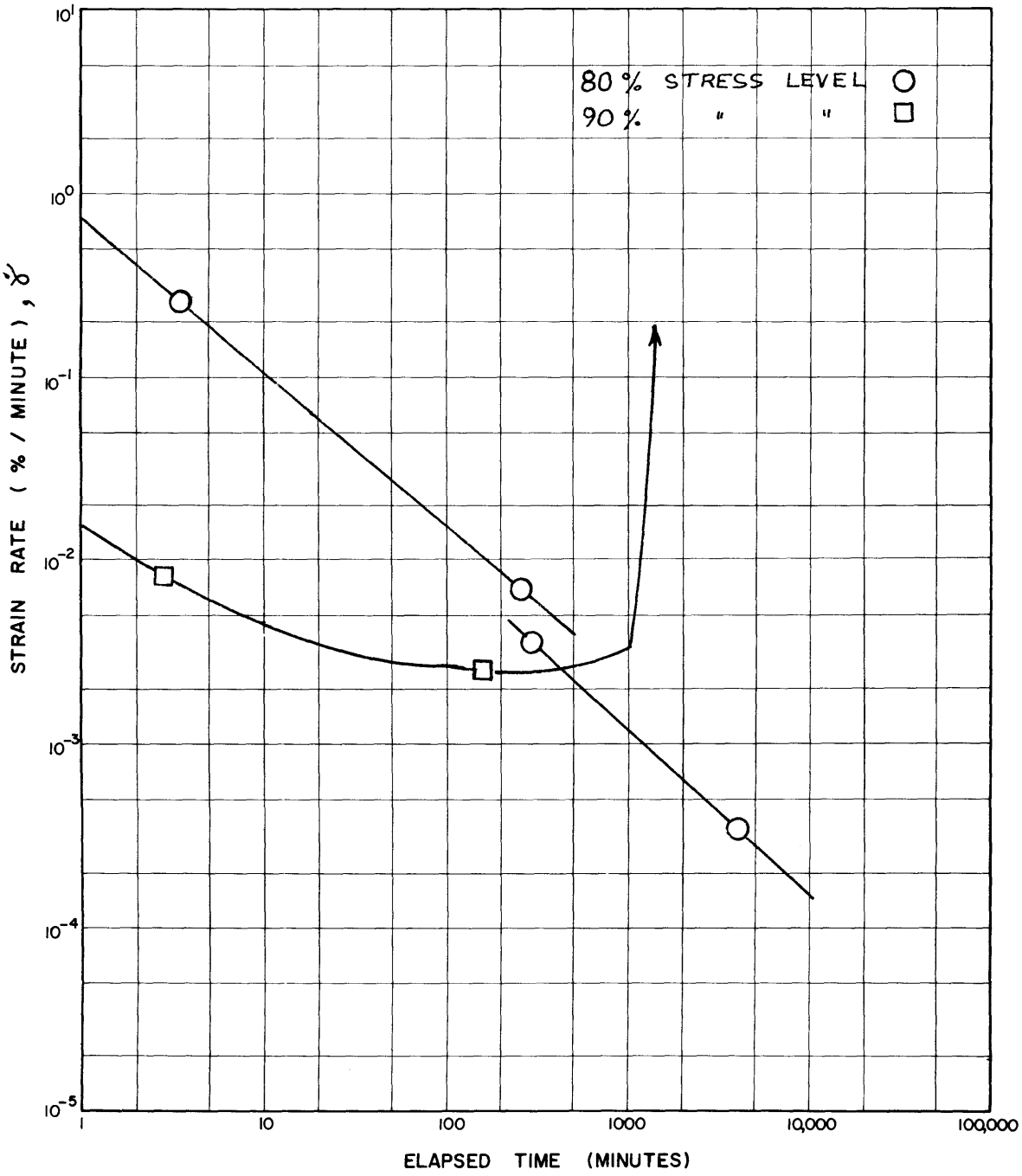

C23: LOG STRAIN RATE VS. LOG TIME, $\overline{CK_oU}$DSS-22

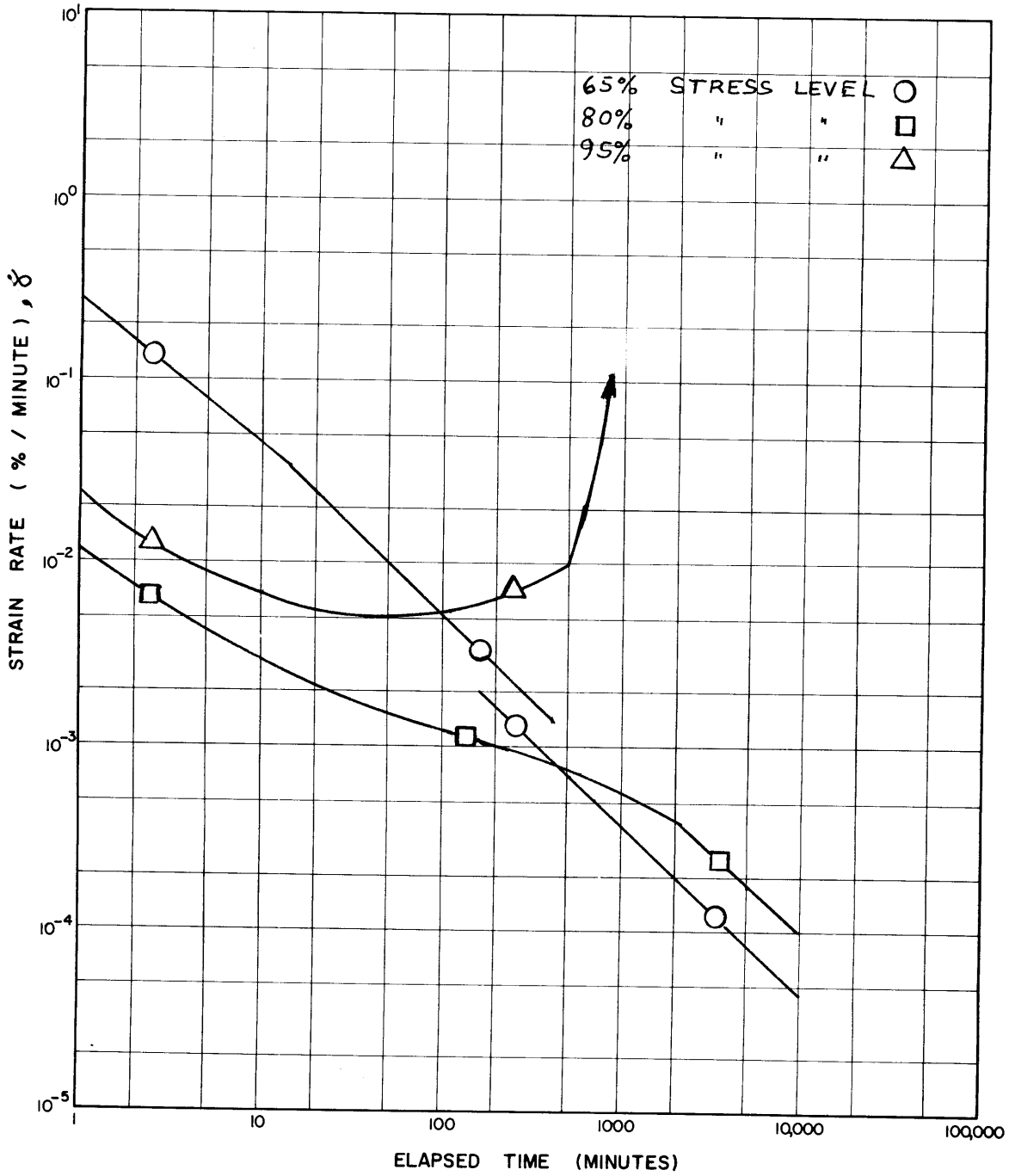

C24: LOG STRAIN RATE VS. LOG TIME, $\overline{CK_oU}$DSS-23

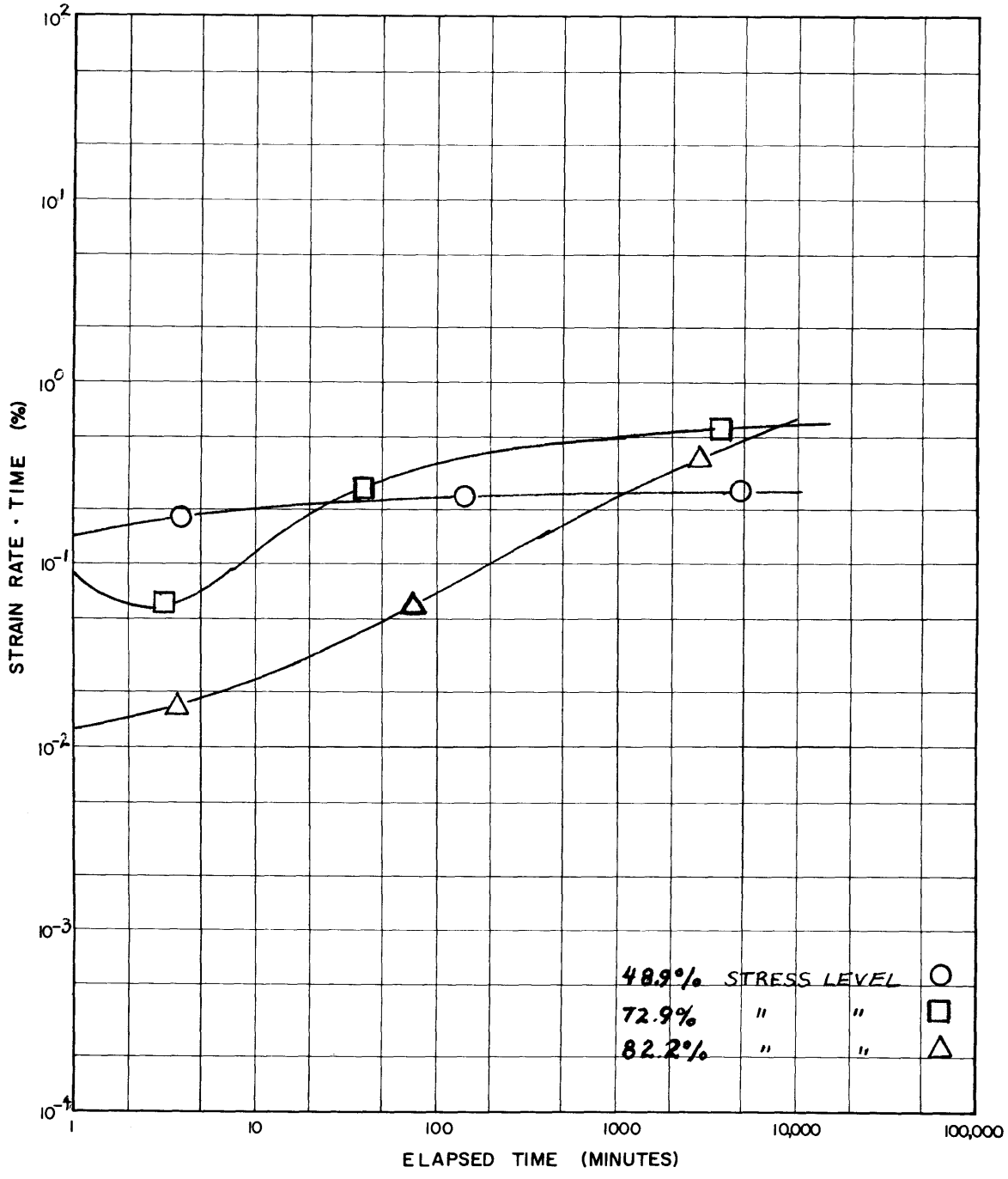

C25: LOG (STRAIN RATE X TIME) VS. LOG TIME, $\overline{CK_o}$UDSS-8

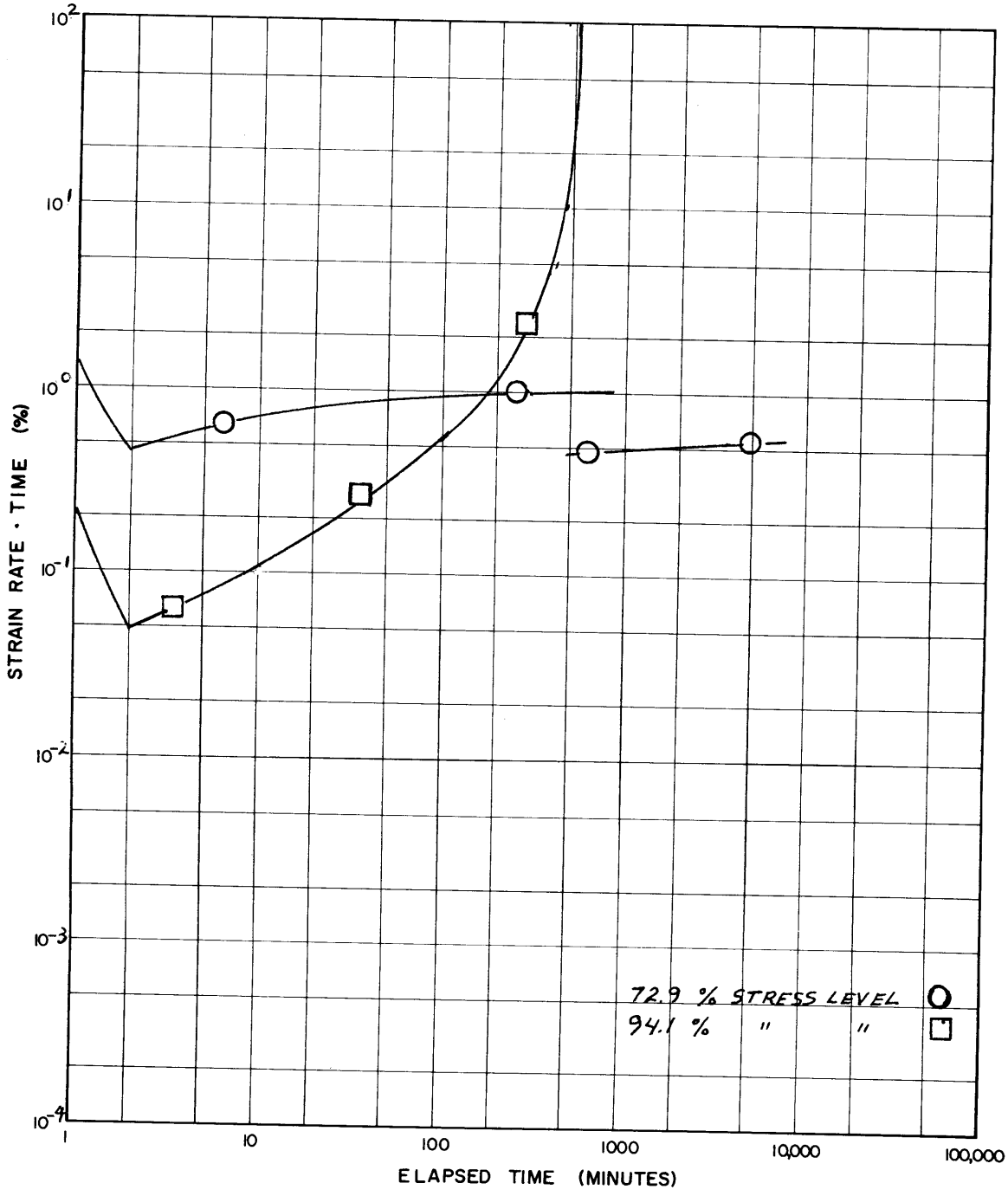

C26: LOG (STRAIN RATE X TIME) VS. LOG TIME, $\overline{CK_o}$UDSS-10

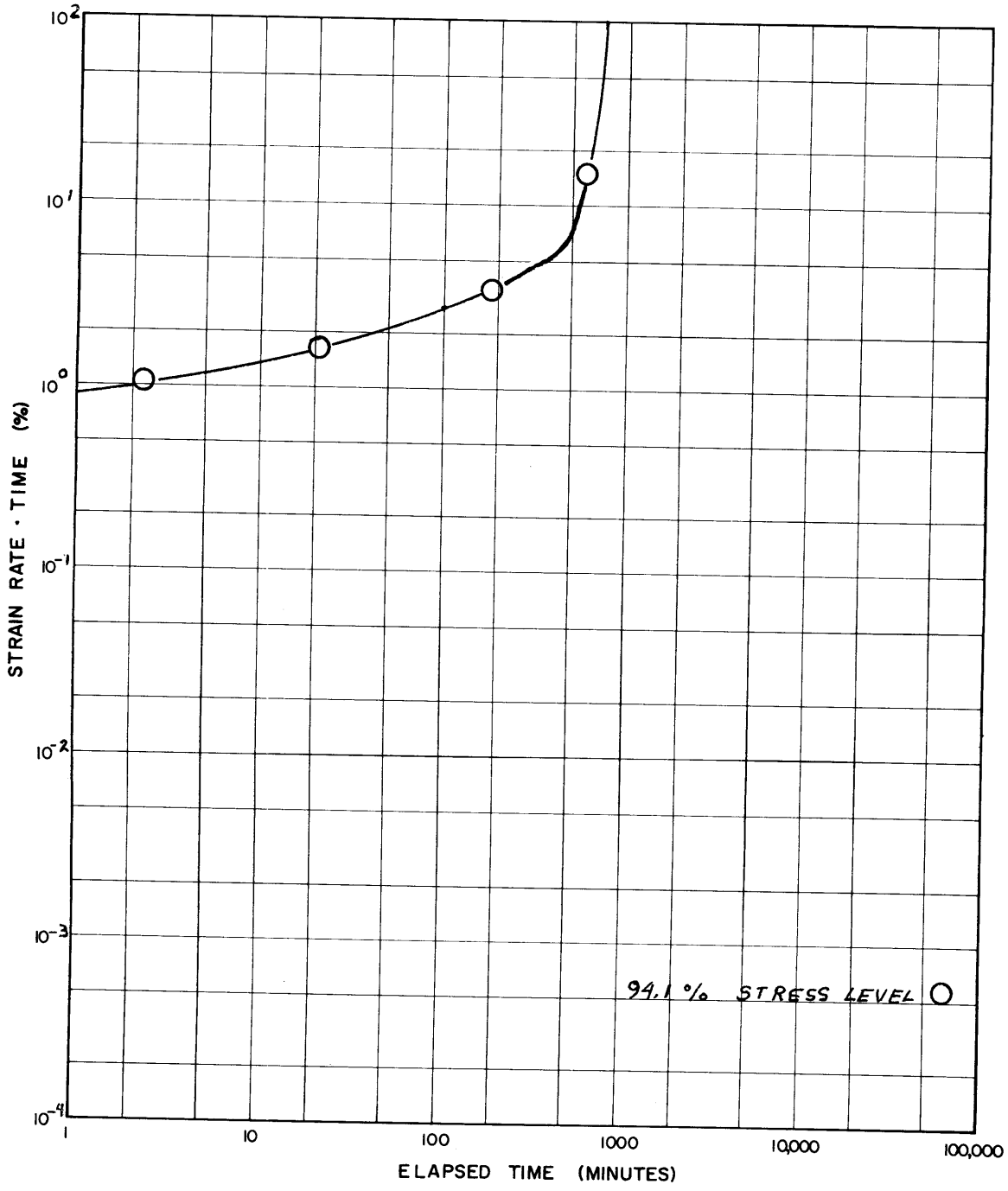

C27: LOG (STRAIN RATE X TIME) VS. LOG TIME, $\overline{CK_o}$UDSS-11

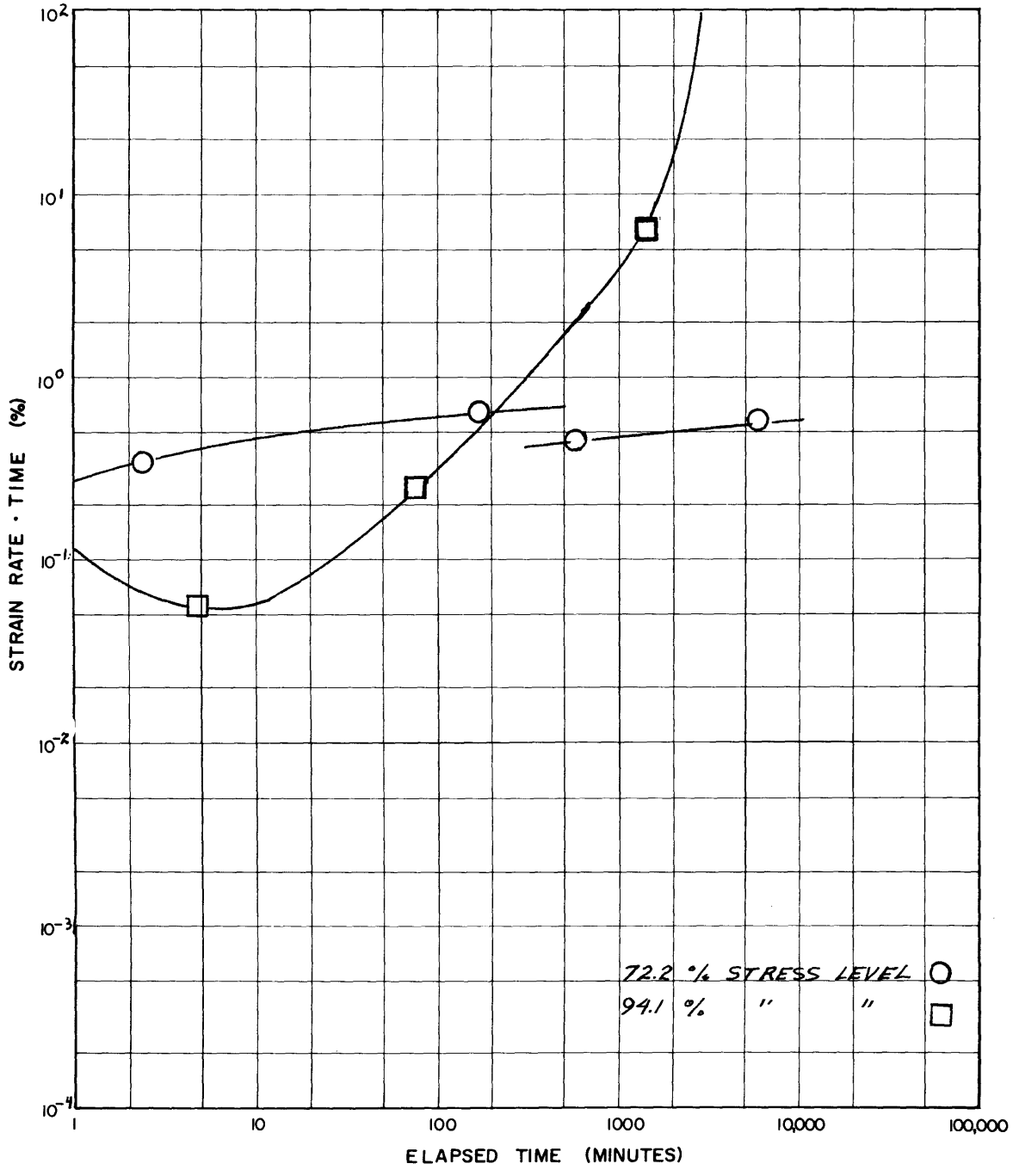

C28: LOG(STRAIN RATE X TIME) VS. LOG TIME, $\overline{CK_o}$UDSS-12

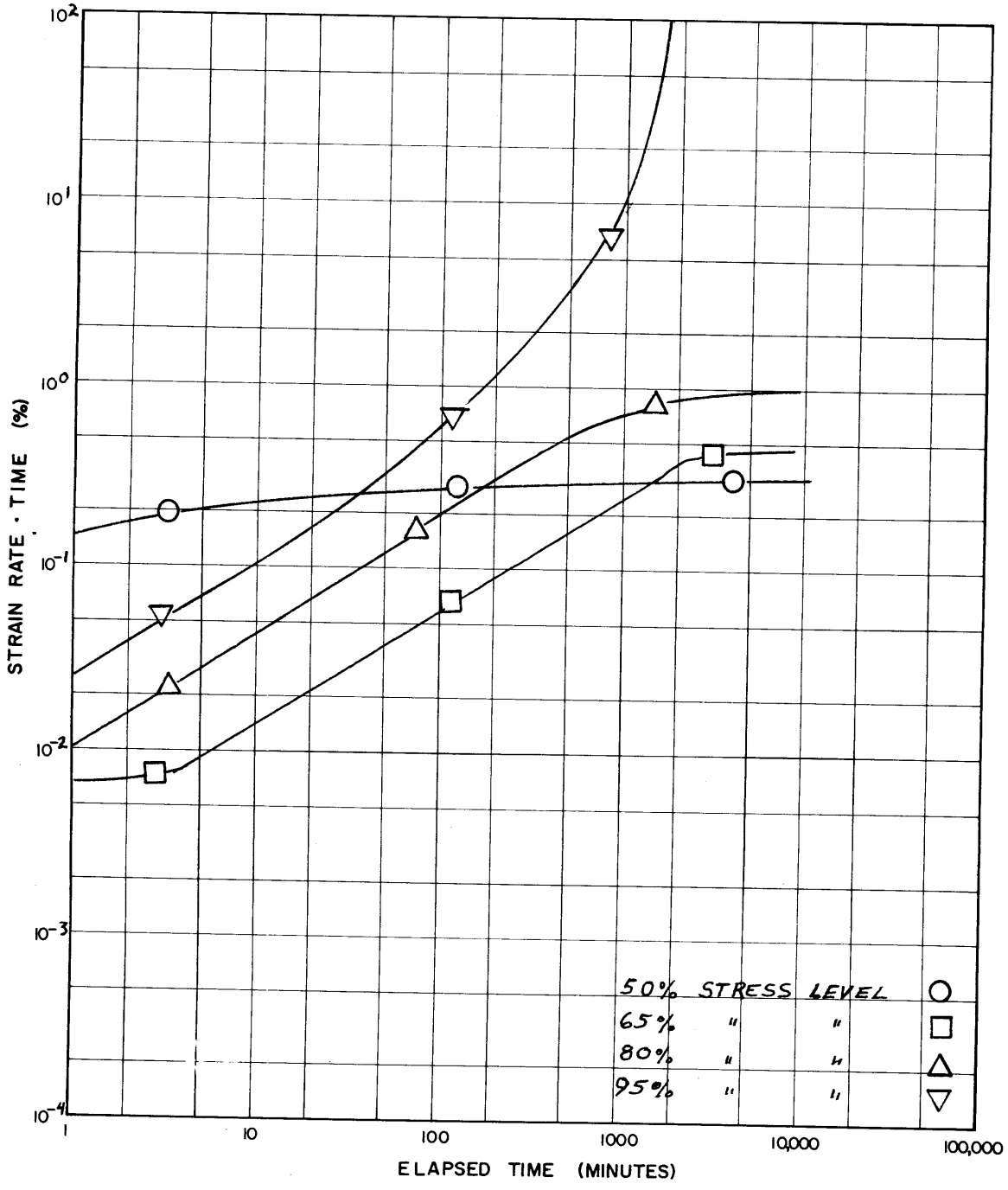

C29: LOG(STRAIN RATE X TIME) VS. LOG TIME, $\overline{CK_o}$UDSS-16

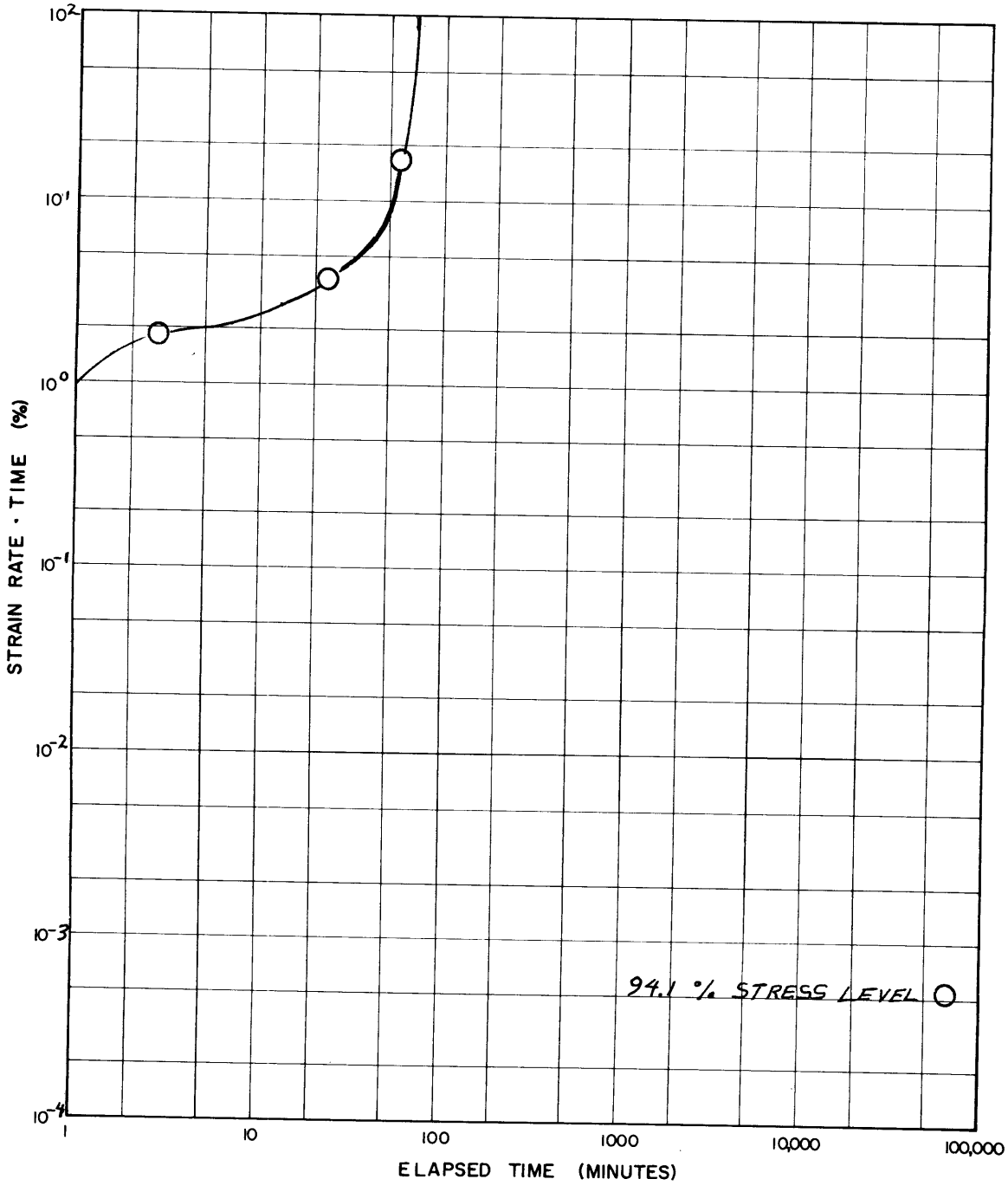

C30: LOG(STRAIN RATE X TIME) VS. LOG TIME, $\overline{CK_o}$UDSS-17

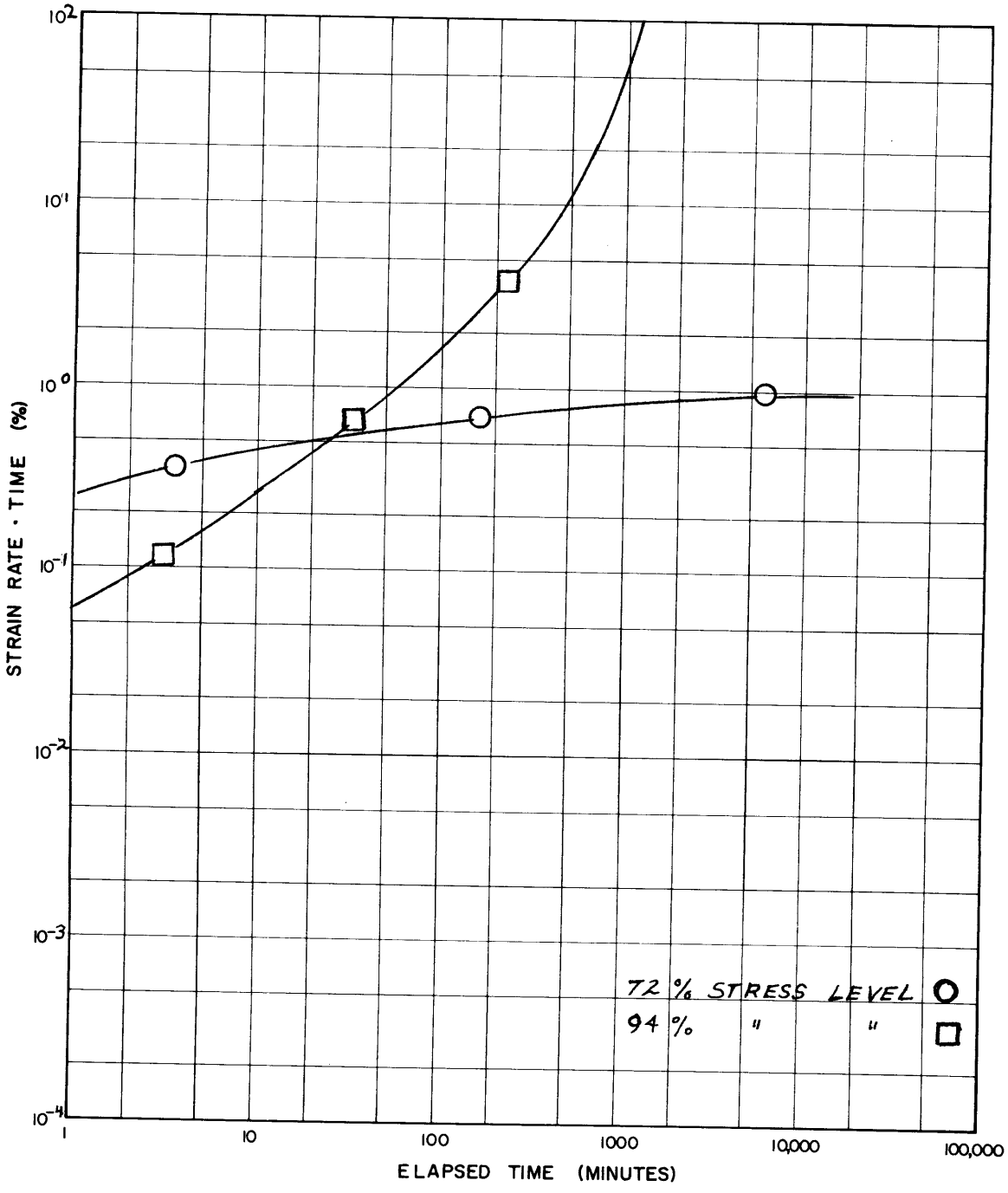

C31: LOG(STRAIN RATE X TIME) VS. LOG TIME, $\overline{CK_o}$UDSS-18

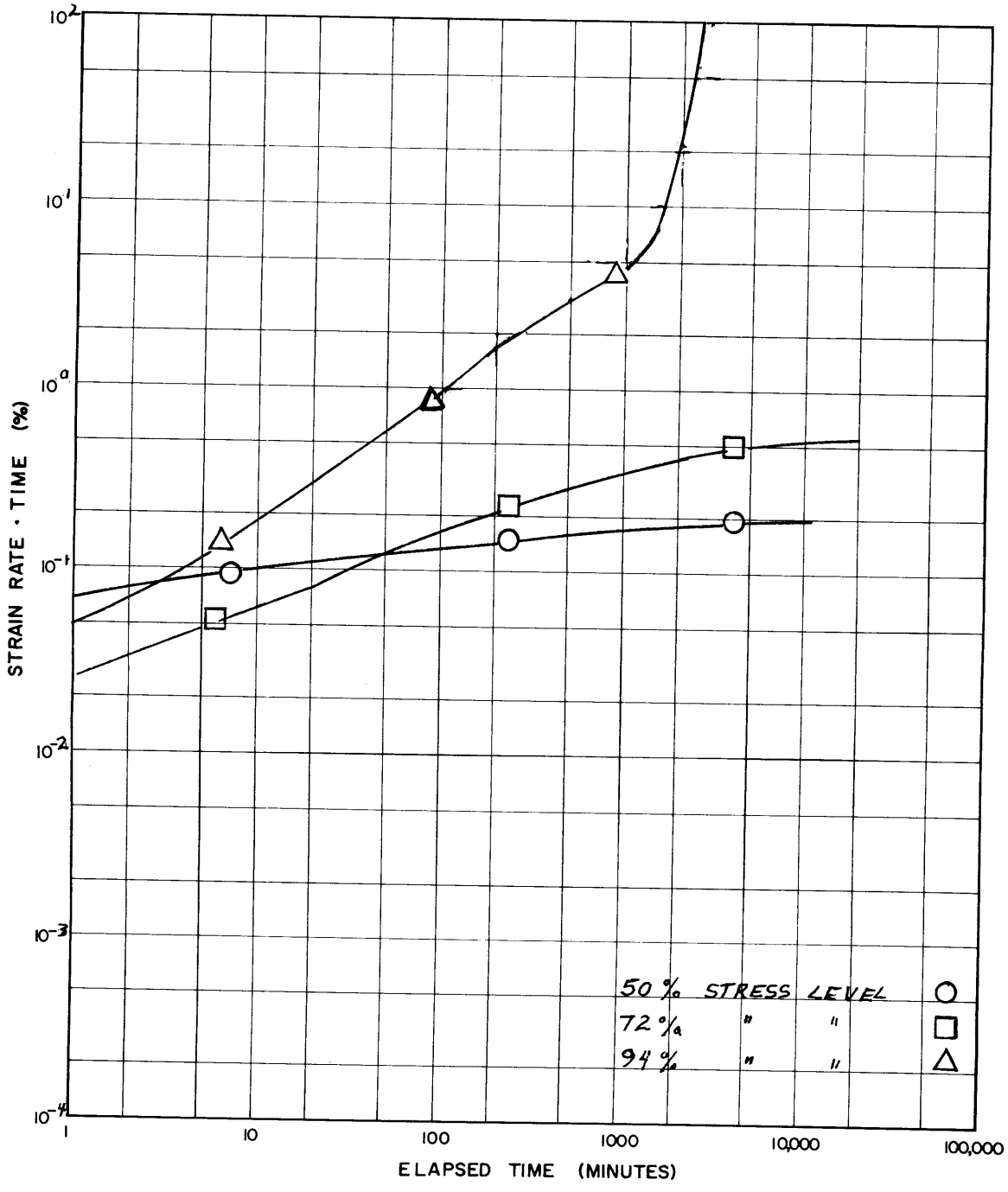

C32: LOG(STRAIN RATE X TIME) VS. LOG TIME, $\overline{CK_oU}$DSS-19

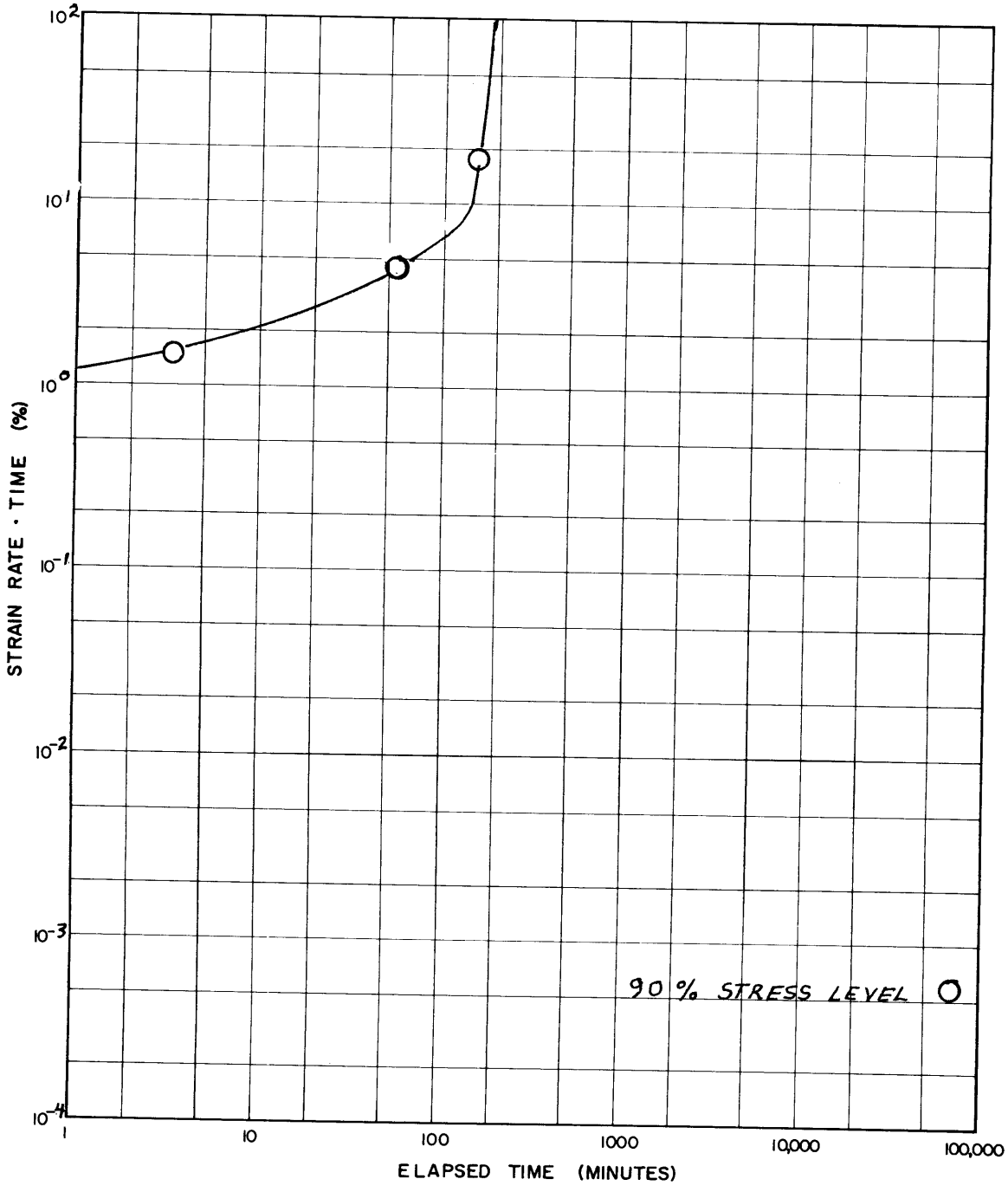

C33: LOG(STRAIN RATE X TIME) VS. LOG TIME, $\overline{CK_o}$UDSS-20

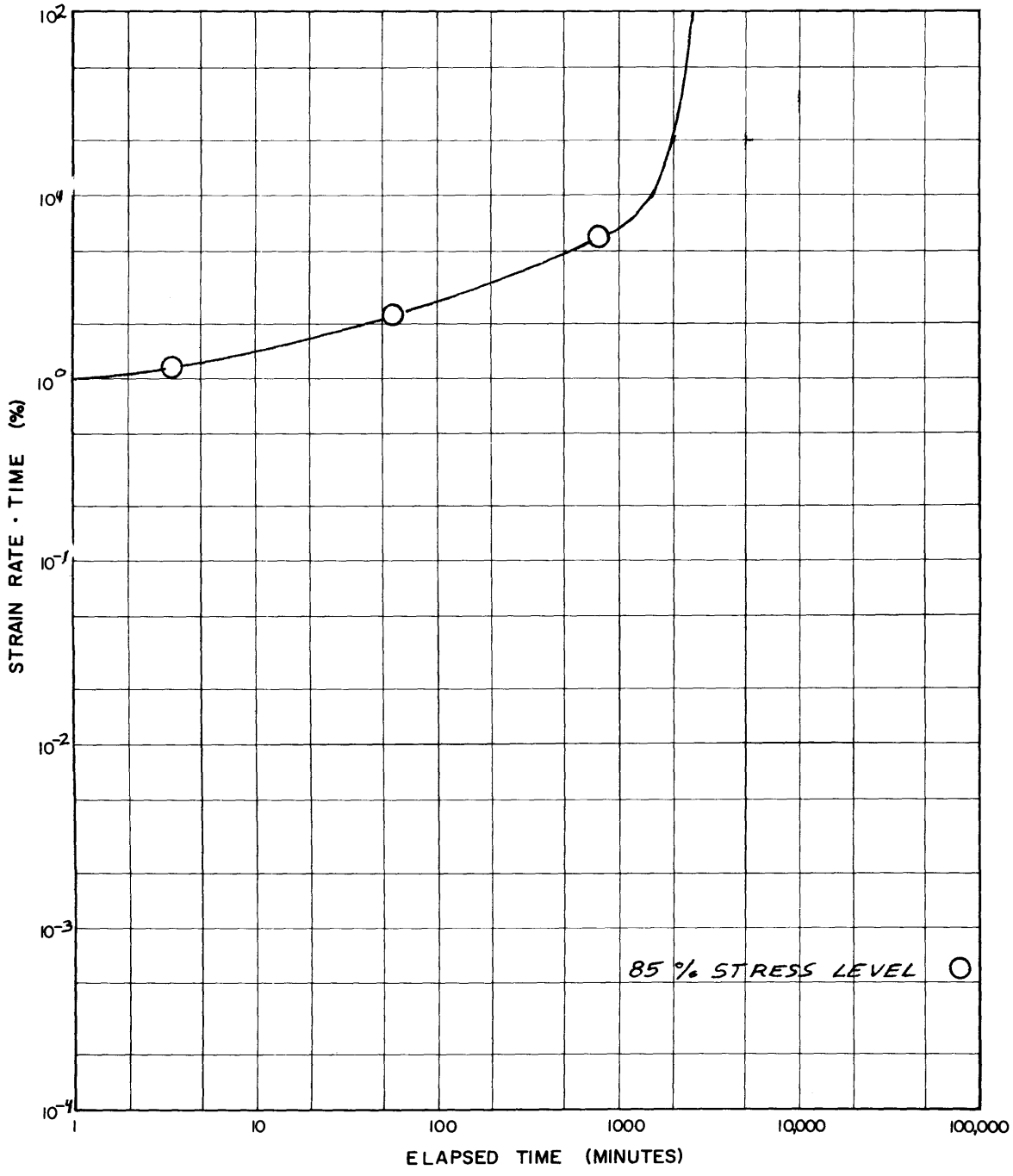

C34: LOG(STRAIN RATE X TIME) VS. LOG TIME, $\overline{CK_o}$UDSS-21

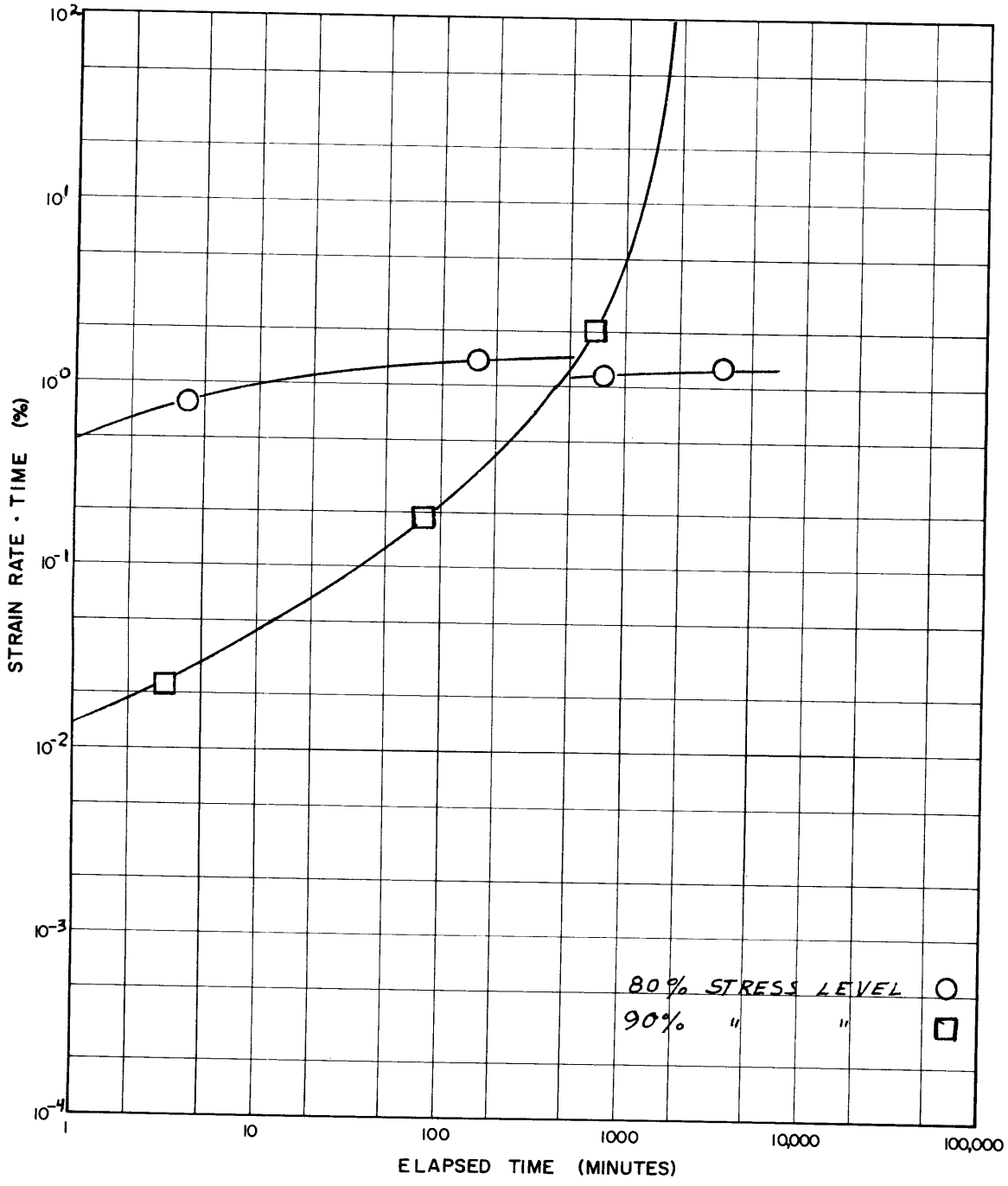

C35: LOG(STRAIN RATE X TIME) VS. LOG TIME, $\overline{CK_oU}$DSS-22

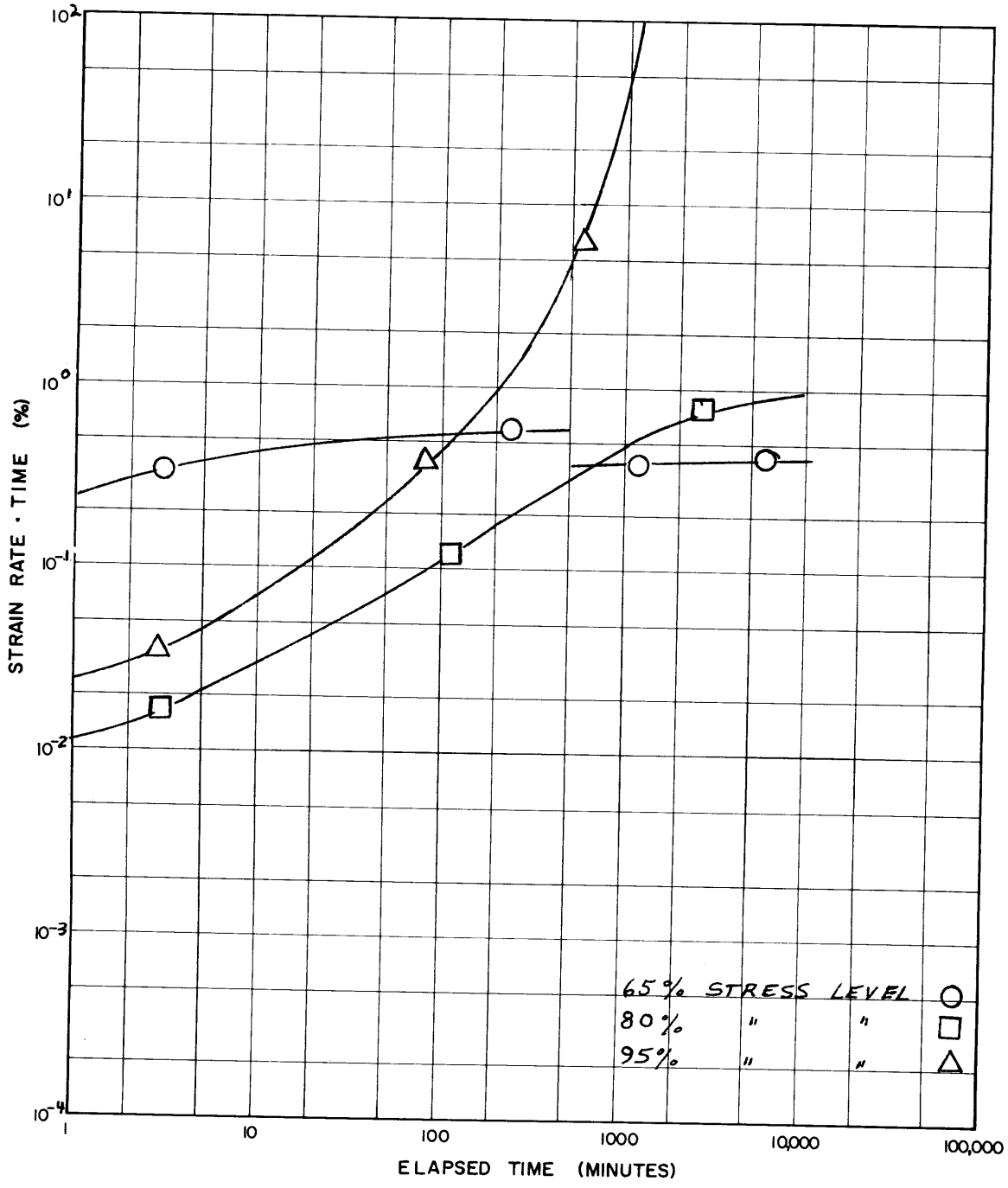

C36: LOG(STRAIN RATE X TIME) VS. LOG TIME, $\overline{CK_o}$UDSS-23

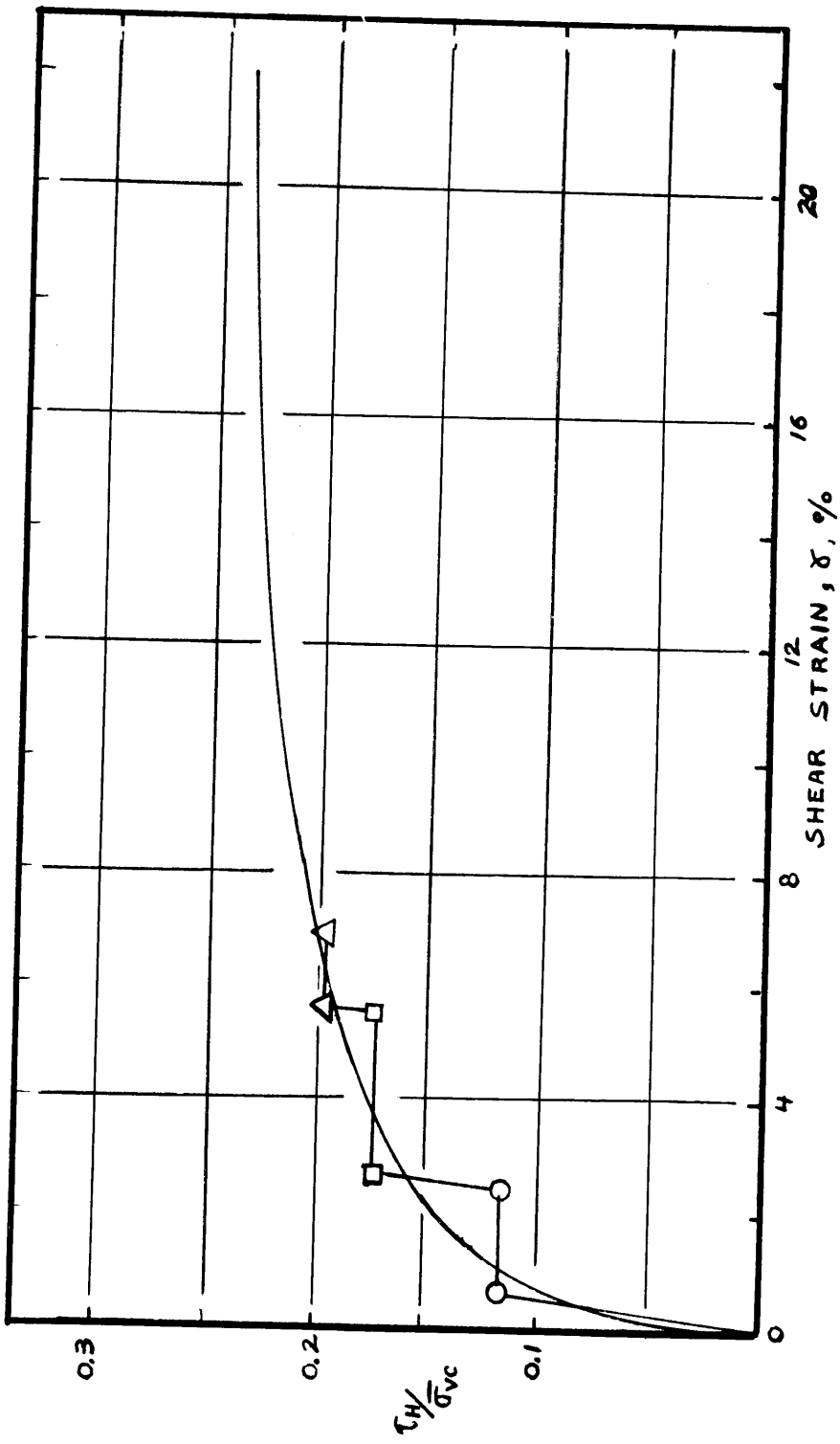

C37: SHEAR STRESS VS. SHEAR STRAIN, $\overline{CK_oUDSS}$-8

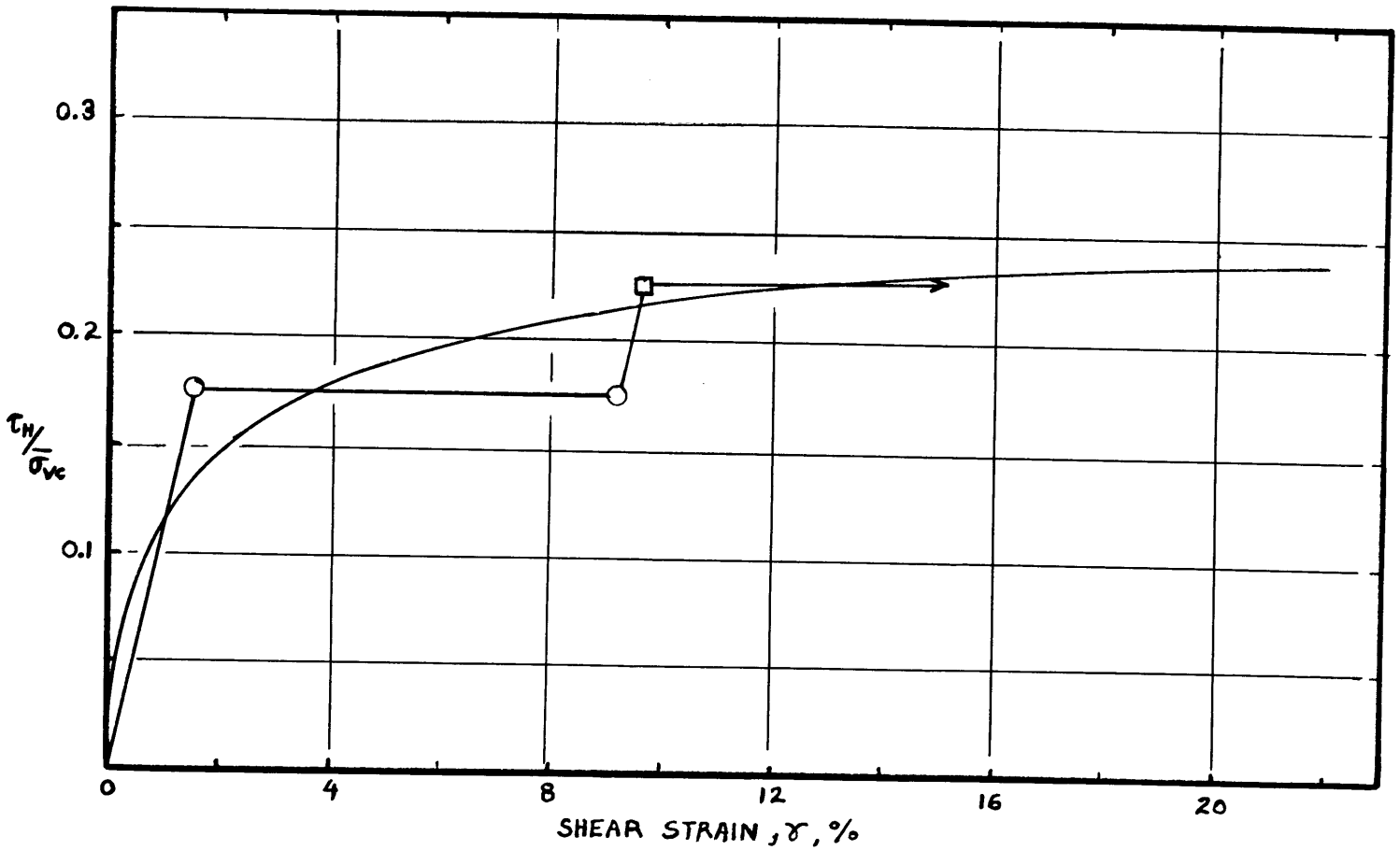

C38: SHEAR STRESS VS. SHEAR STRAIN, $\overline{CK_oU}$DSS-10

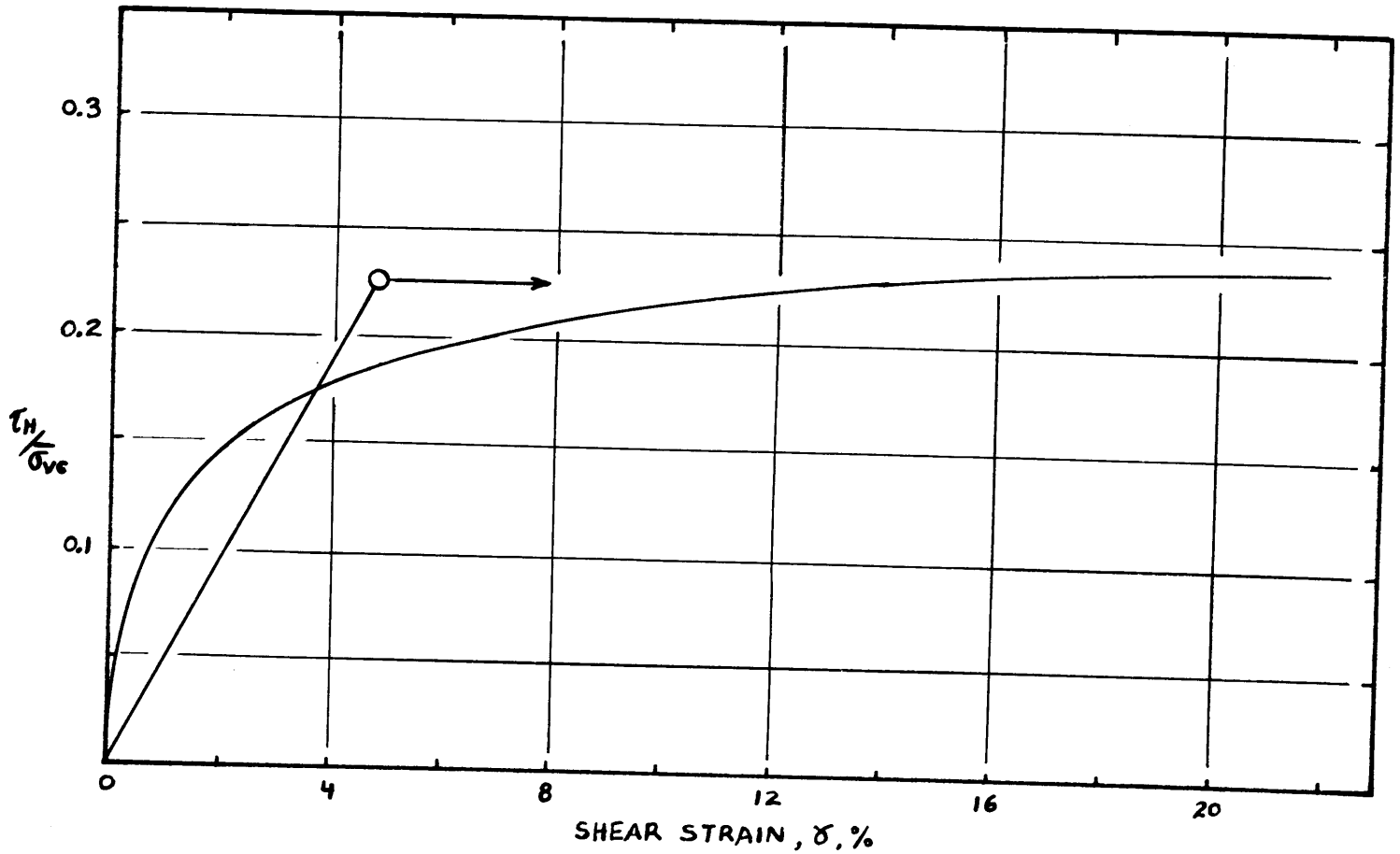

C39: SHEAR STRESS VS. SHEAR STRAIN, $\overline{CK_oU}$DSS-11

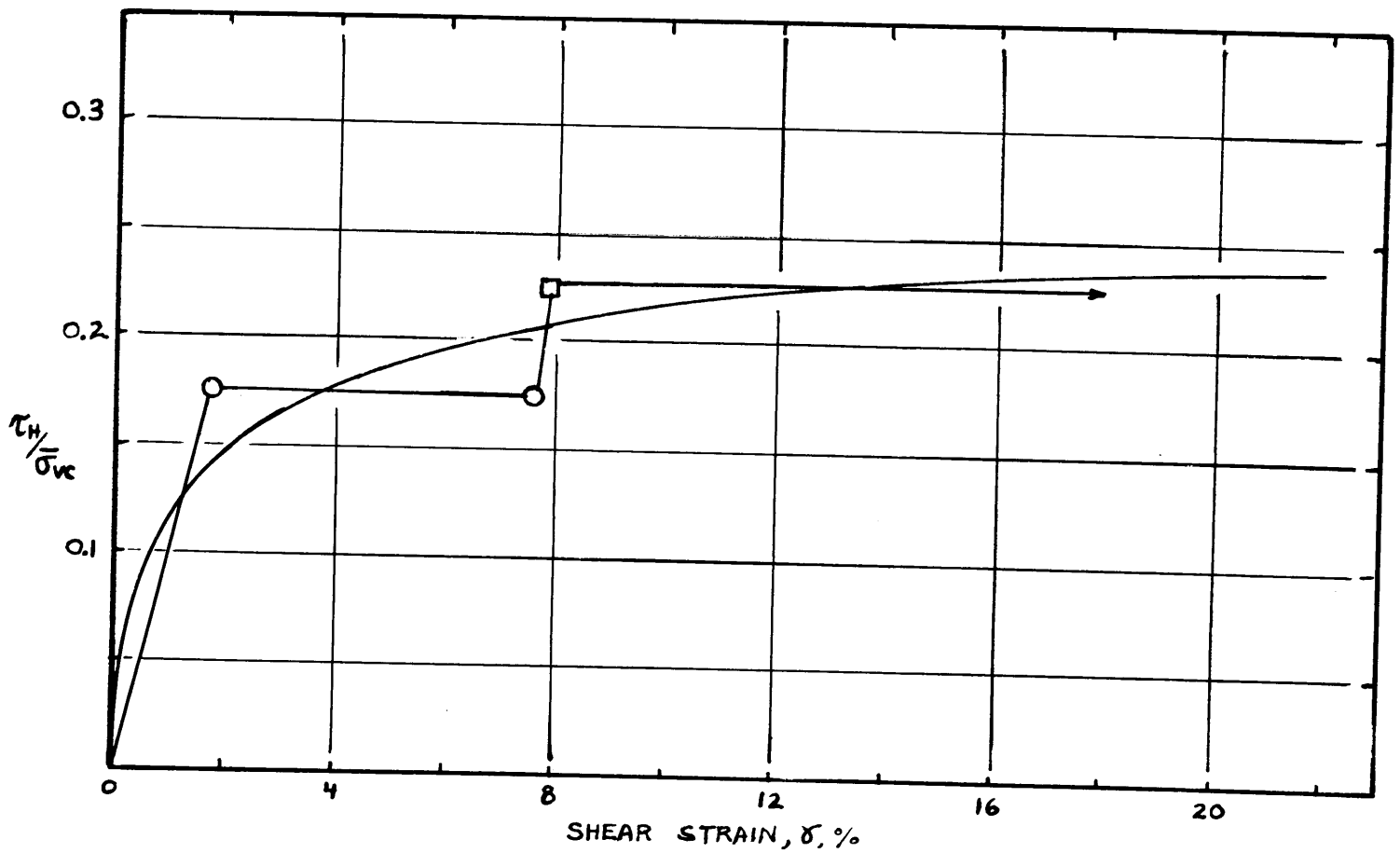

C40: SHEAR STRESS VS. SHEAR STRAIN, $\overline{CK_oU}$DSS-12

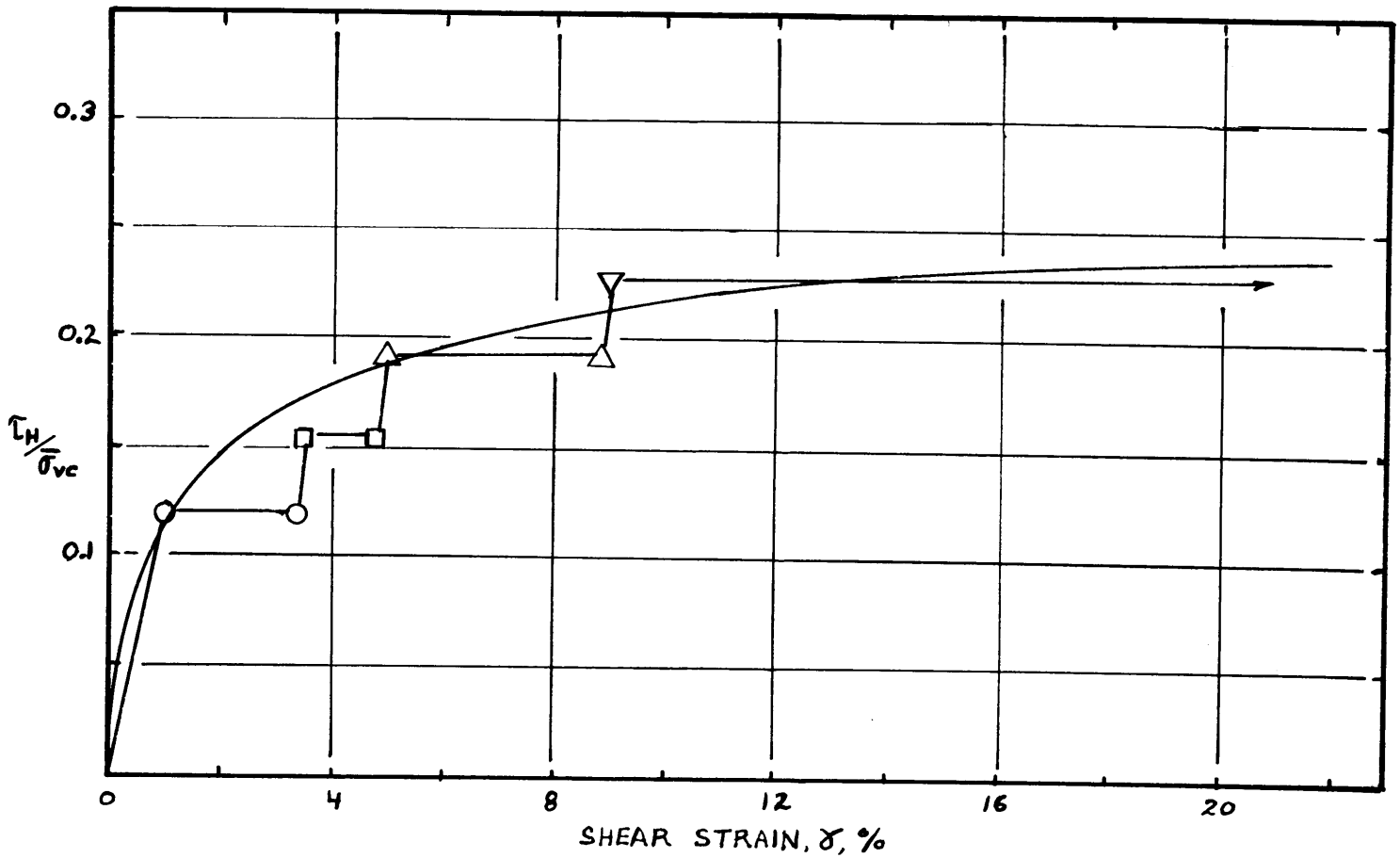

C41: SHEAR STRESS VS. SHEAR STRAIN, $\overline{CK_oU}$DSS-16

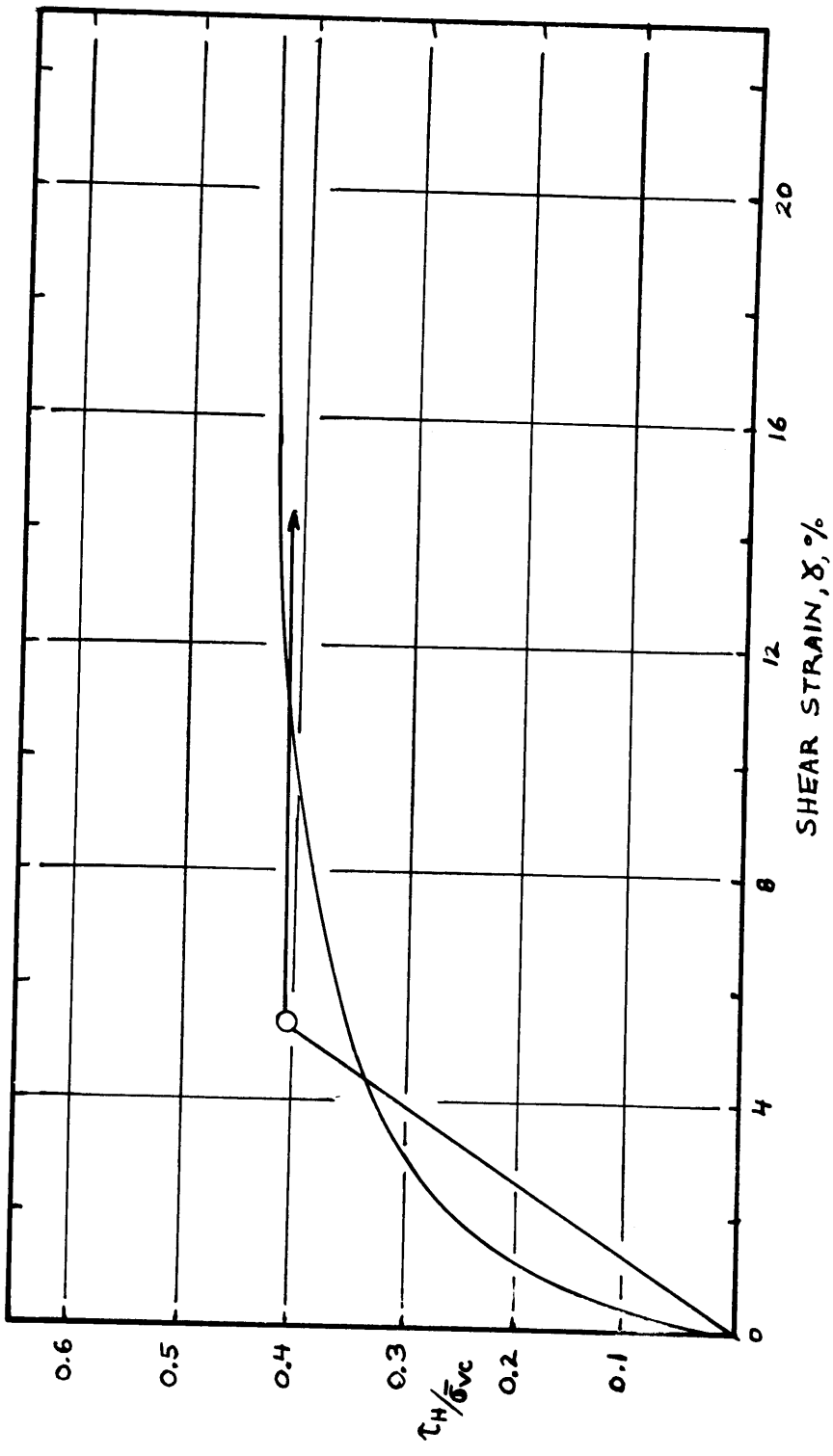

C42: SHEAR STRESS VS. SHEAR STRAIN, $\overline{CK_oU}$DSS-17

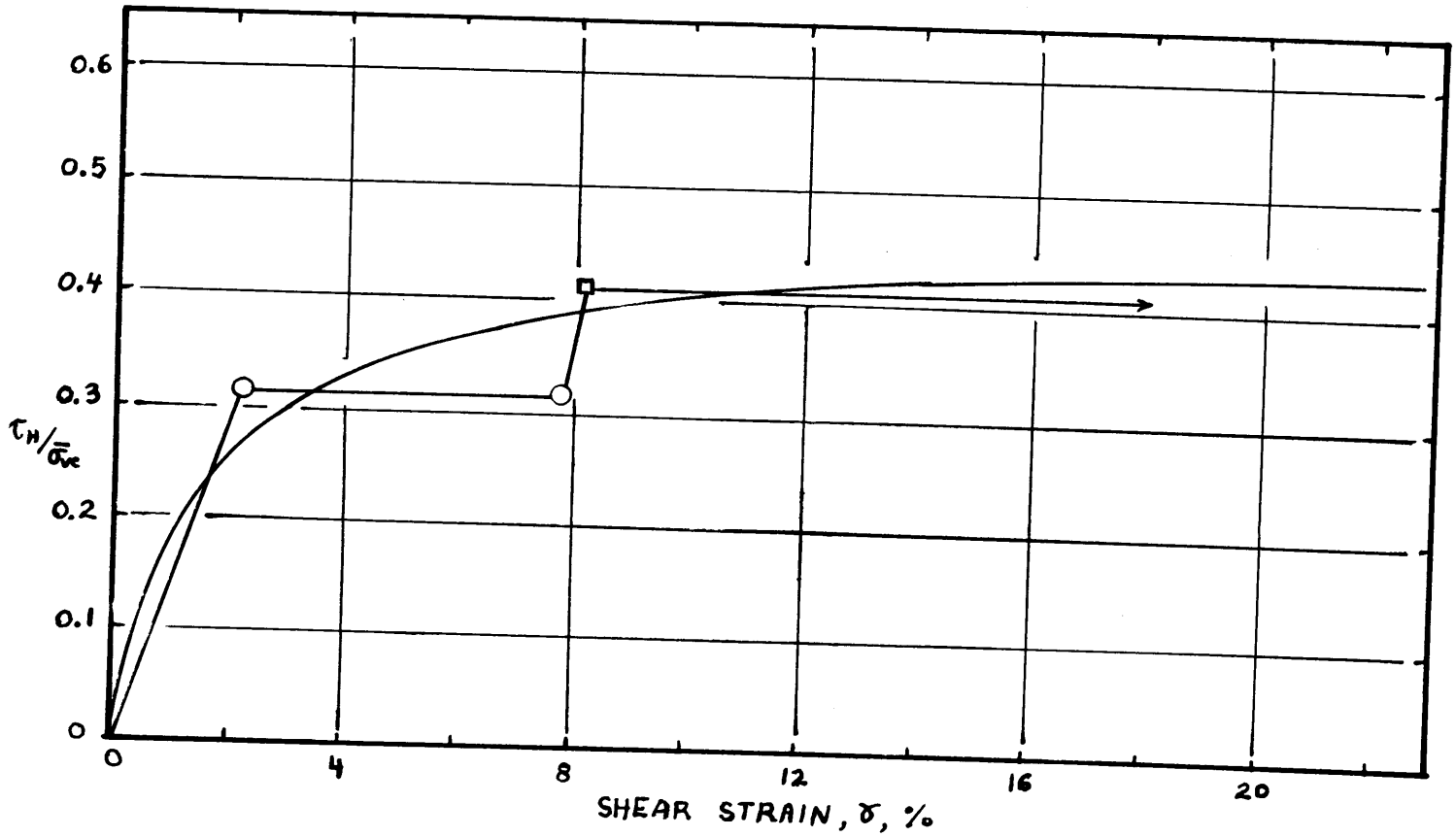

C43: SHEAR STRESS VS. SHEAR STRAIN, $\overline{CK_oU}$DSS-18

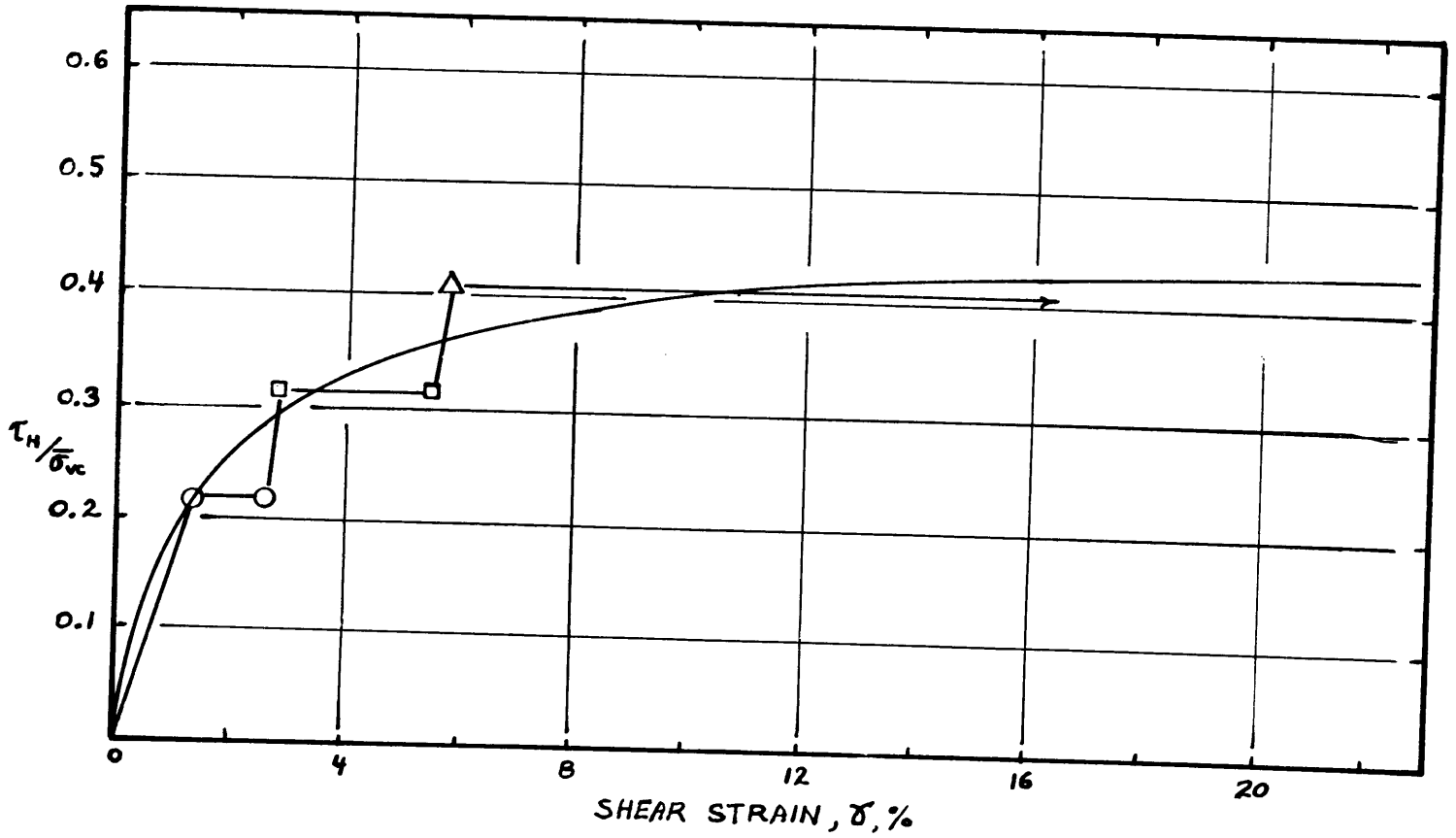

C44: SHEAR STRESS VS. SHEAR STRAIN, $\overline{CK_oU}$DSS-19

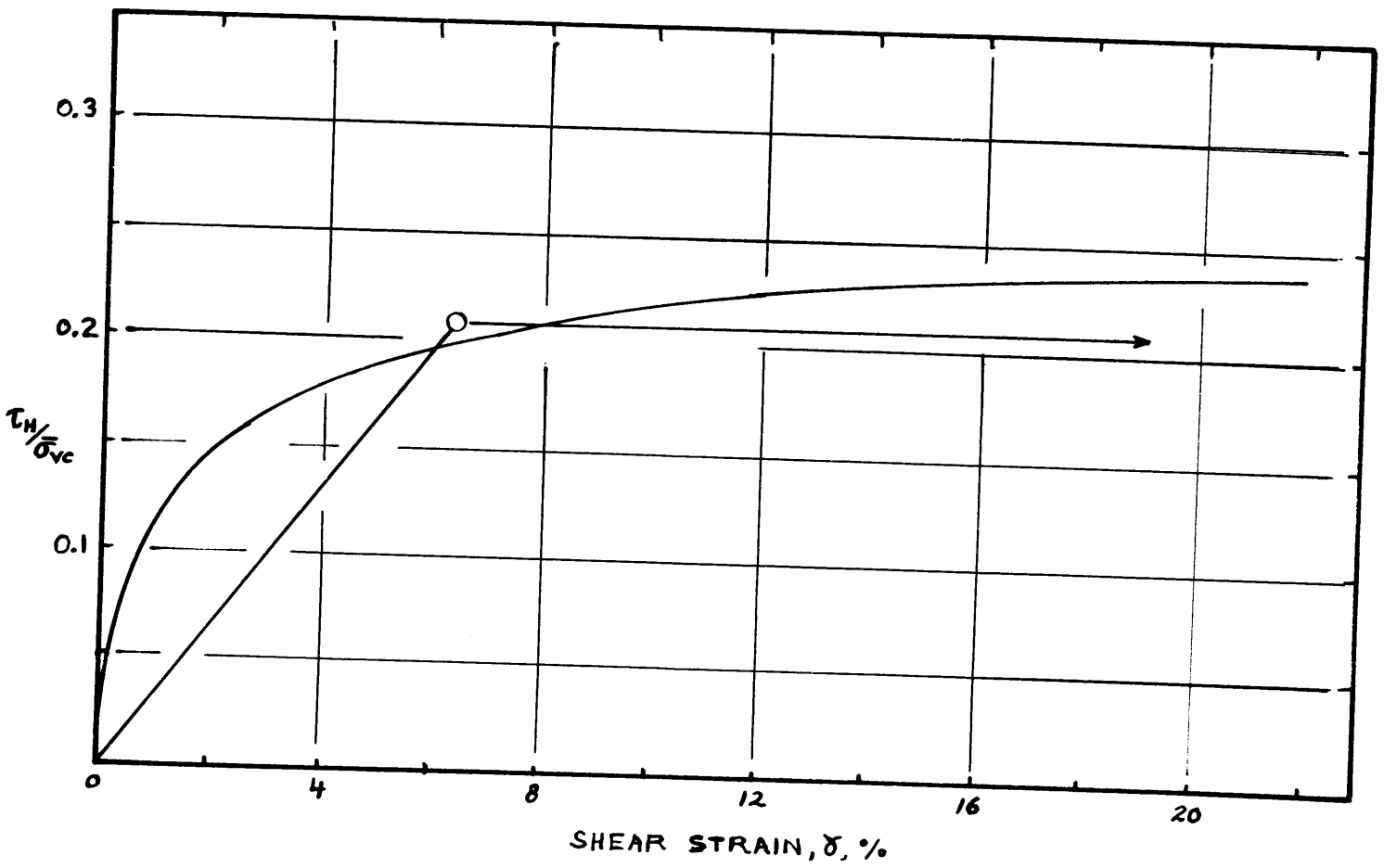

C45: SHEAR STRESS VS. SHEAR STRAIN, $\overline{CK_oU}$DSS-20

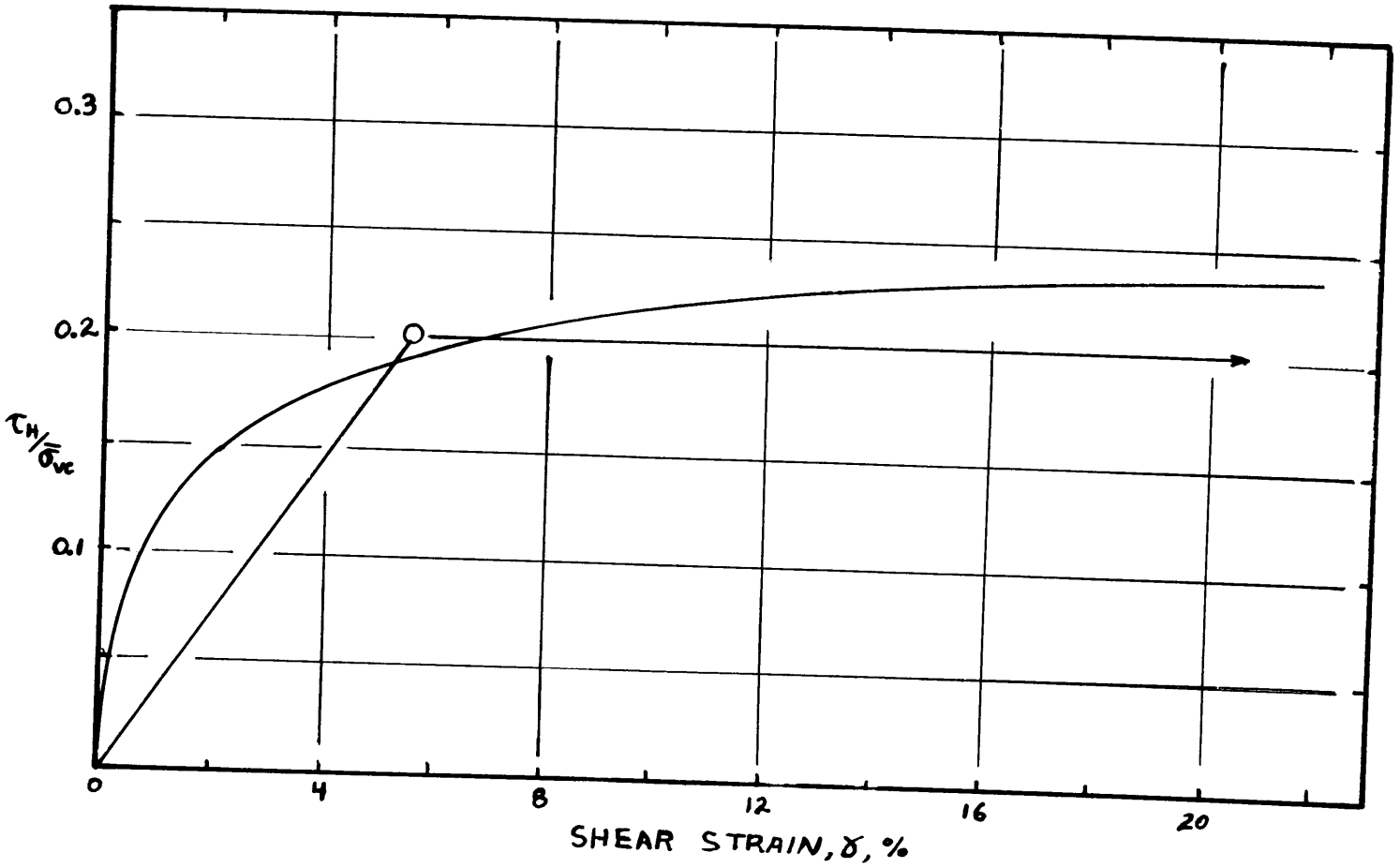

C46: SHEAR STRESS VS. SHEAR STRAIN, $\overline{CK_oU}$DSS-21

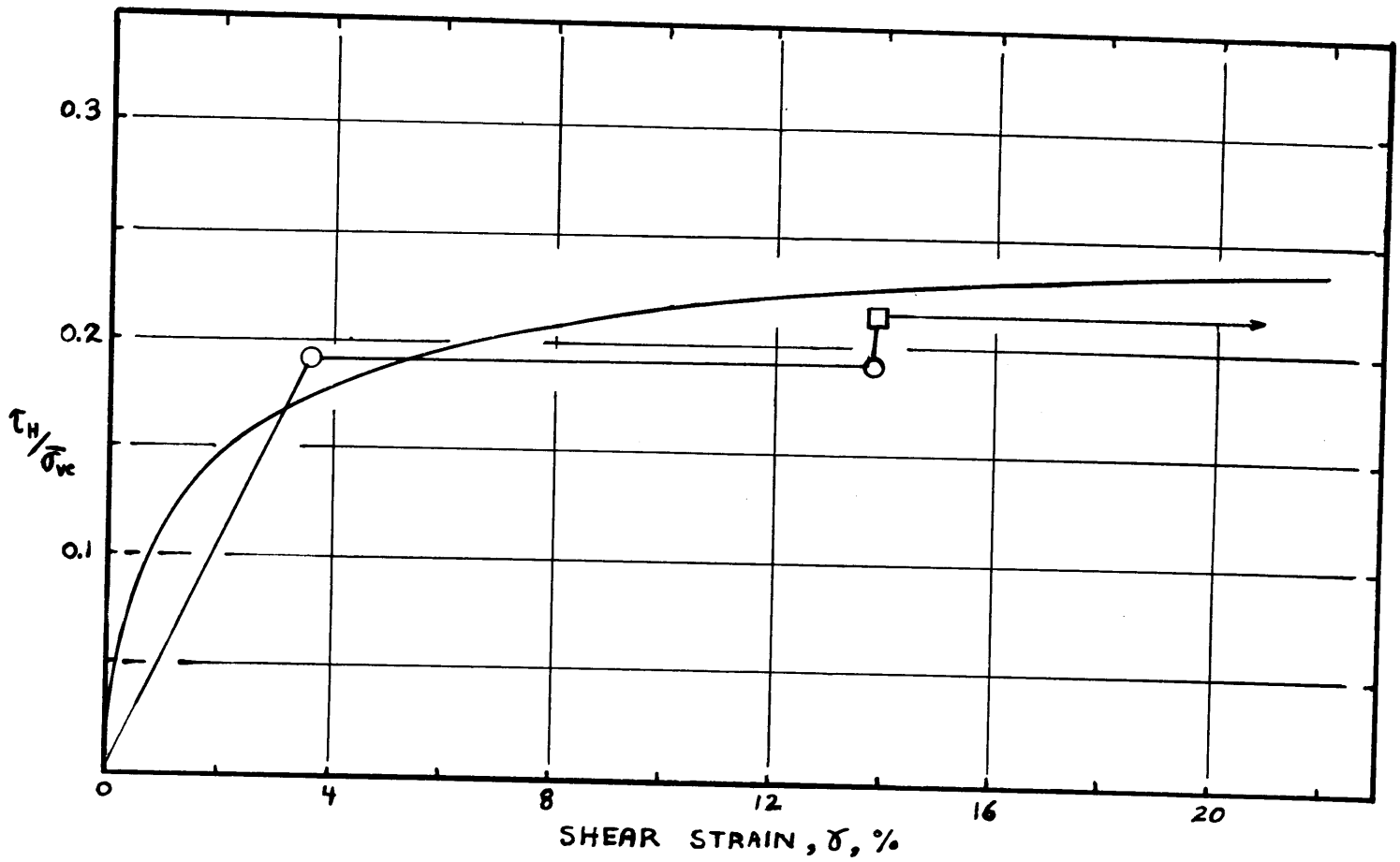

C47: SHEAR STRESS VS. SHEAR STRAIN, $\overline{CK_oU}$DSS-22

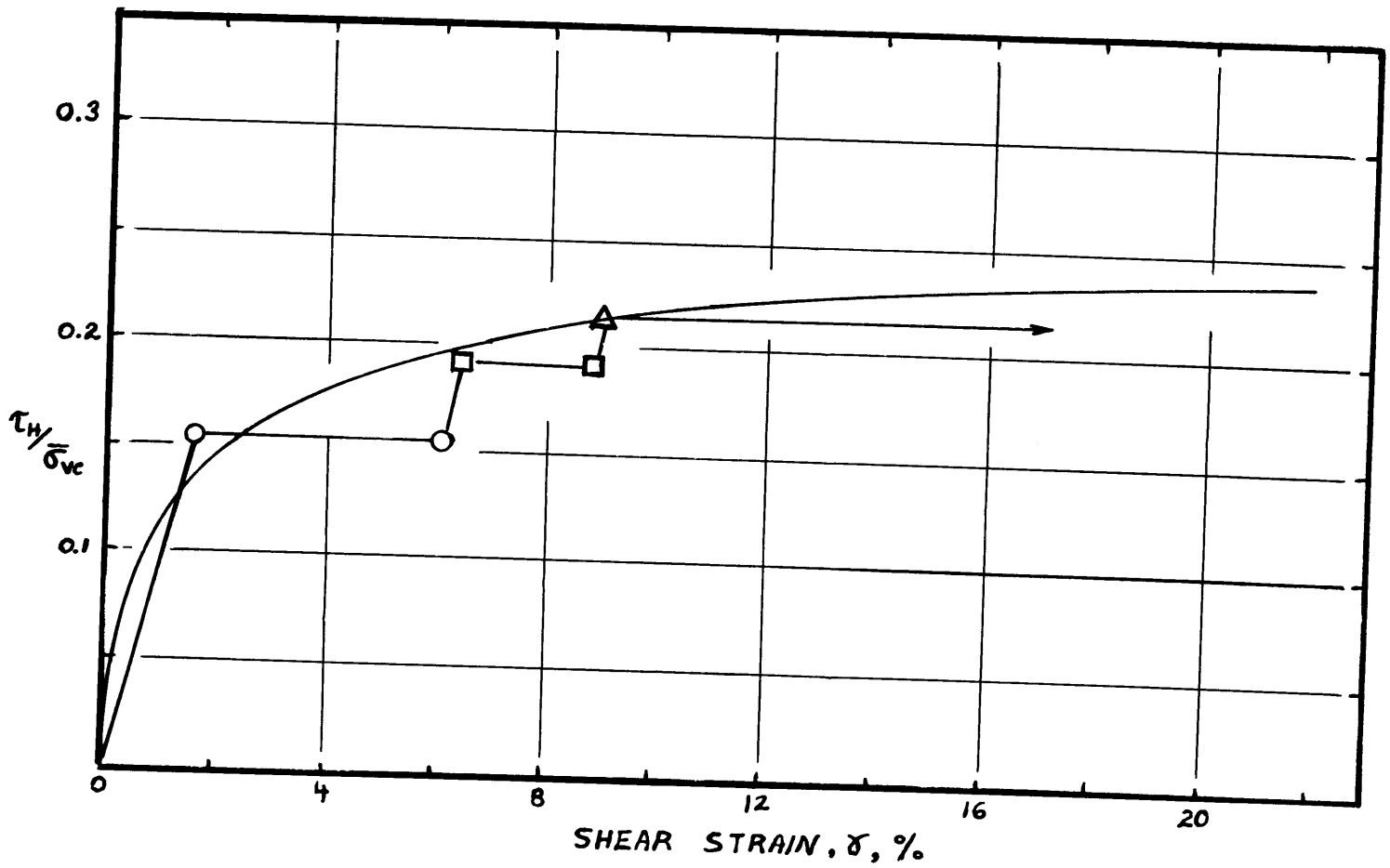

C48: SHEAR STRESS VS. SHEAR STRAIN, CK_oUDSS-23

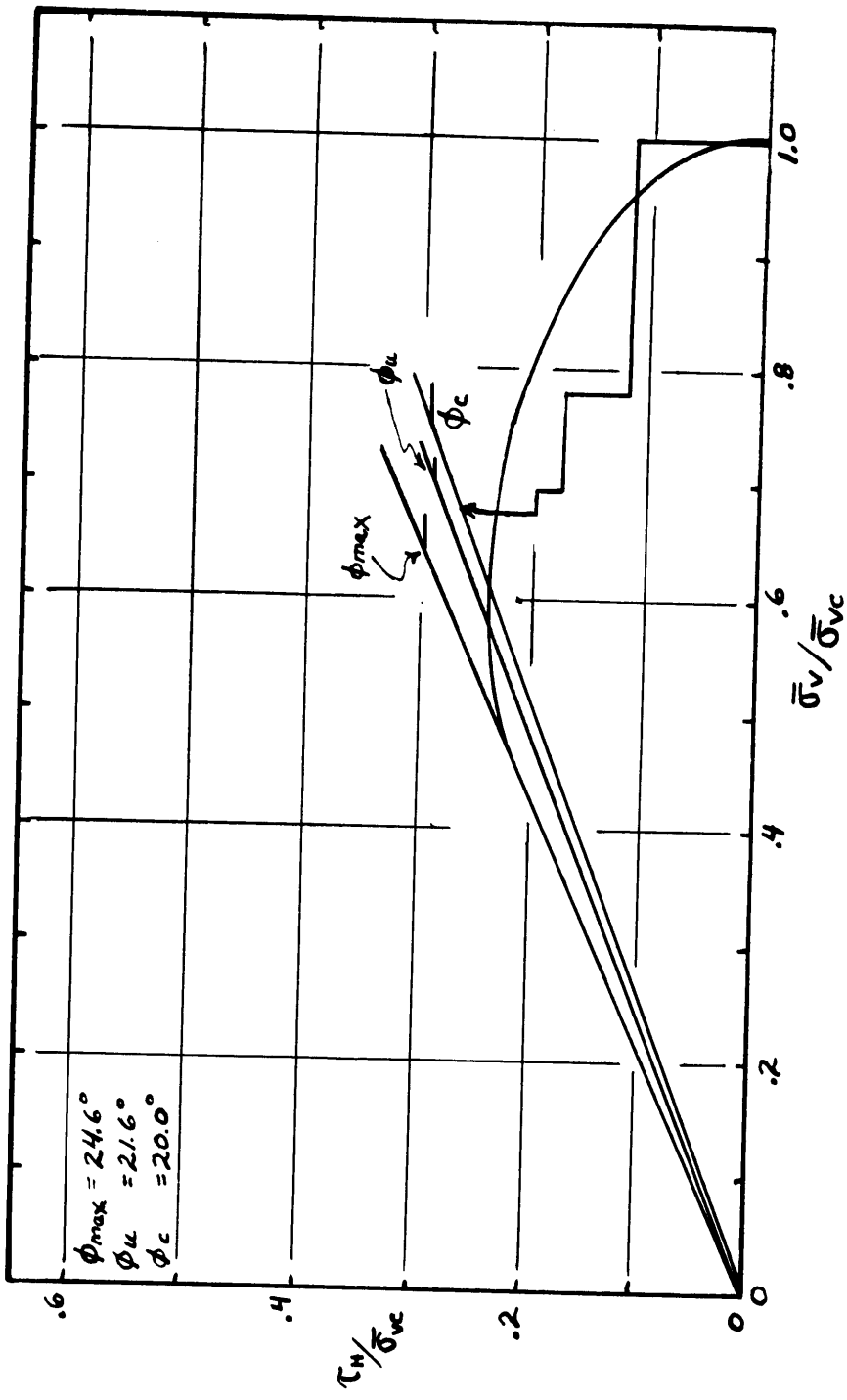

C49: CREEP TEST STRESS PATH, $\overline{CK_oU}$DSS-8

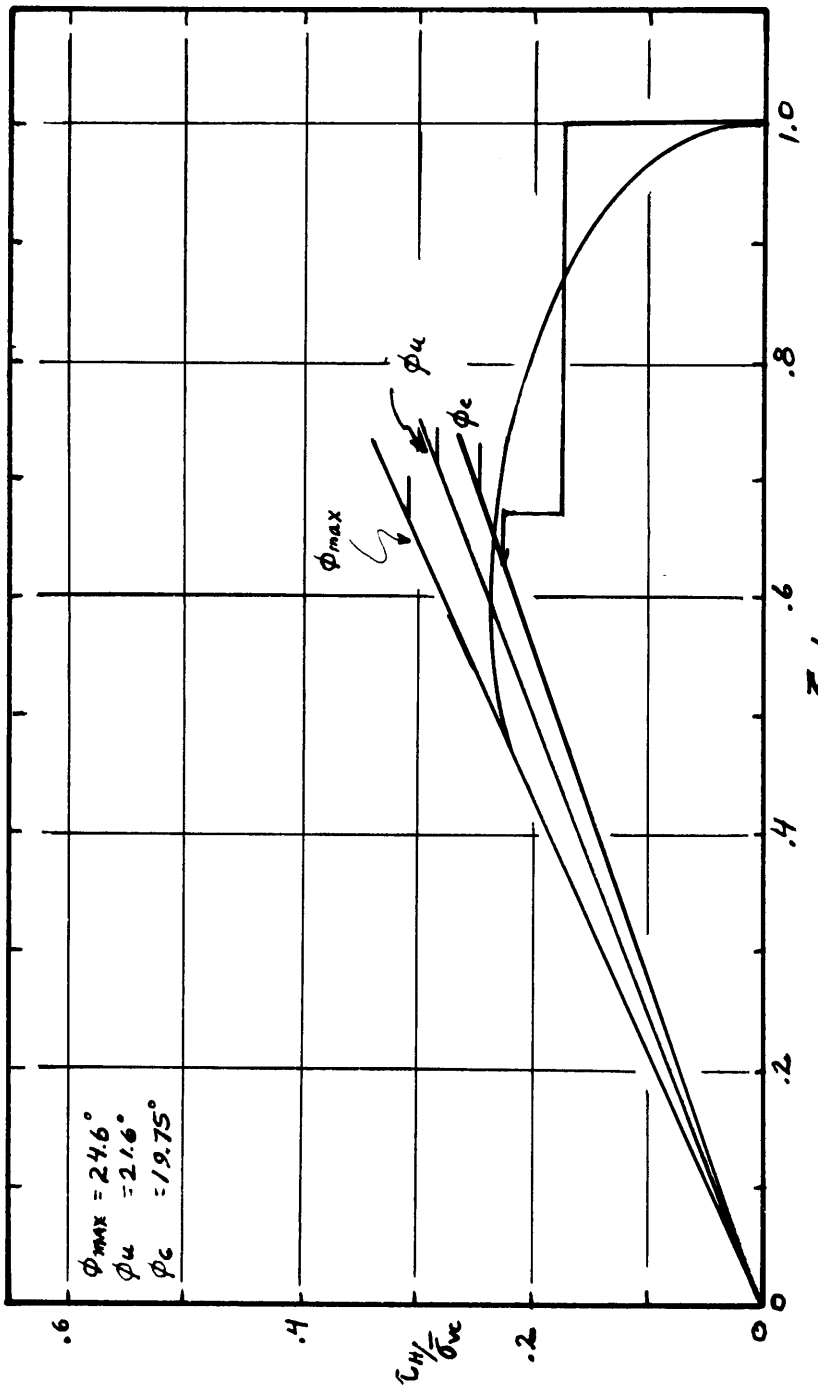

C50: CREEP TEST STRESS PATH, CK_OUDSS-10

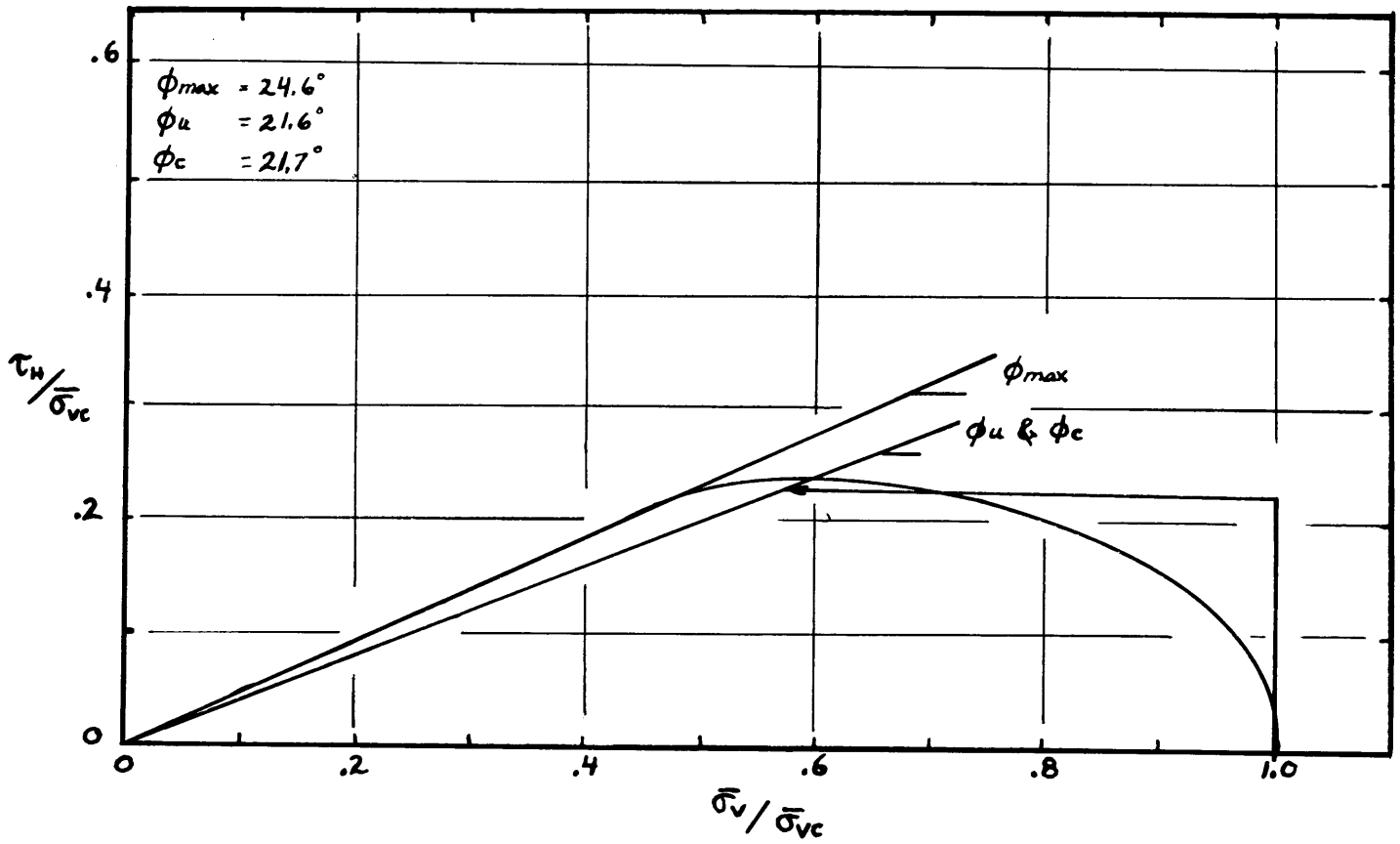

C51: CREEP TEST STRESS PATH, $\overline{CK_oU}$DSS-11

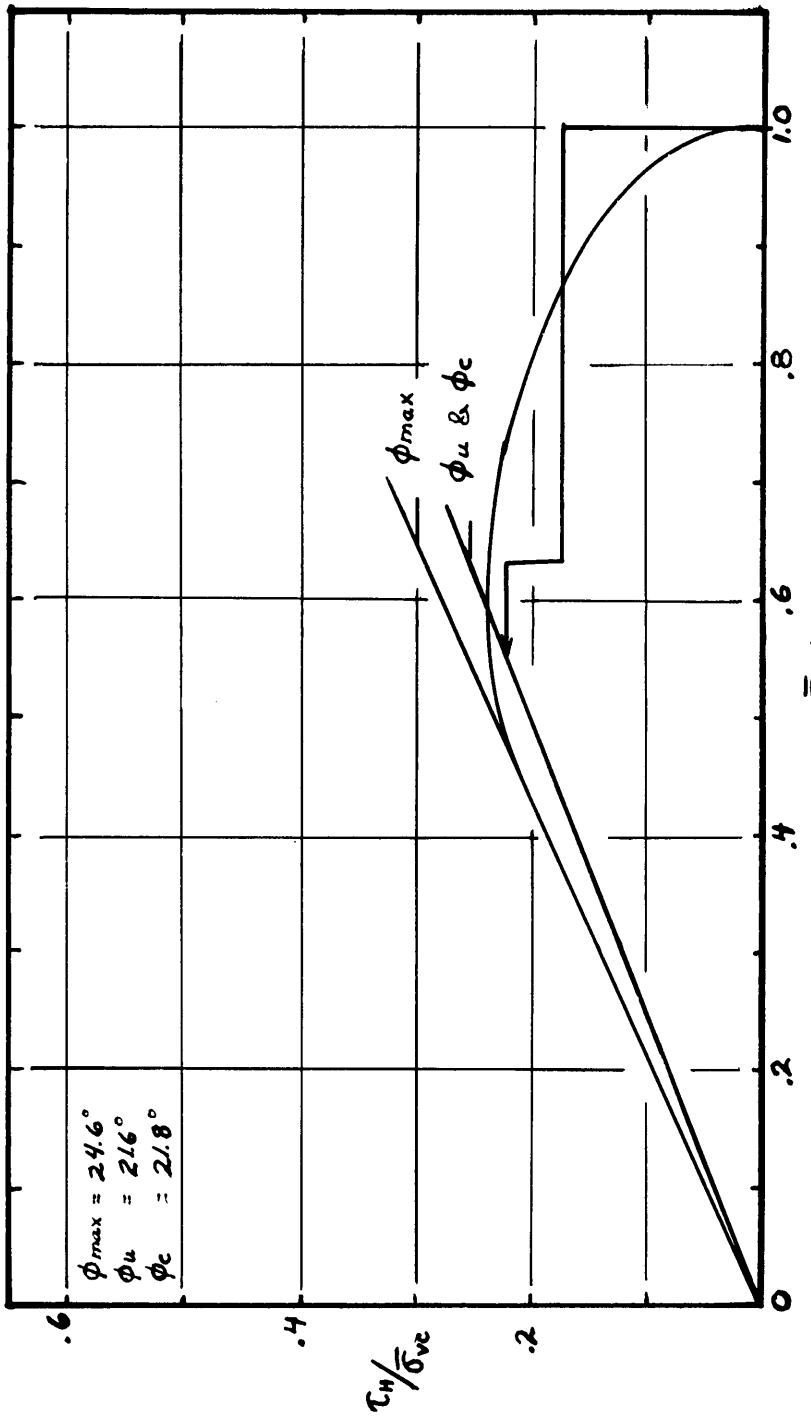

C52: CREEP TEST STRESS PATH, $\overline{CK_o}$UDSS-12

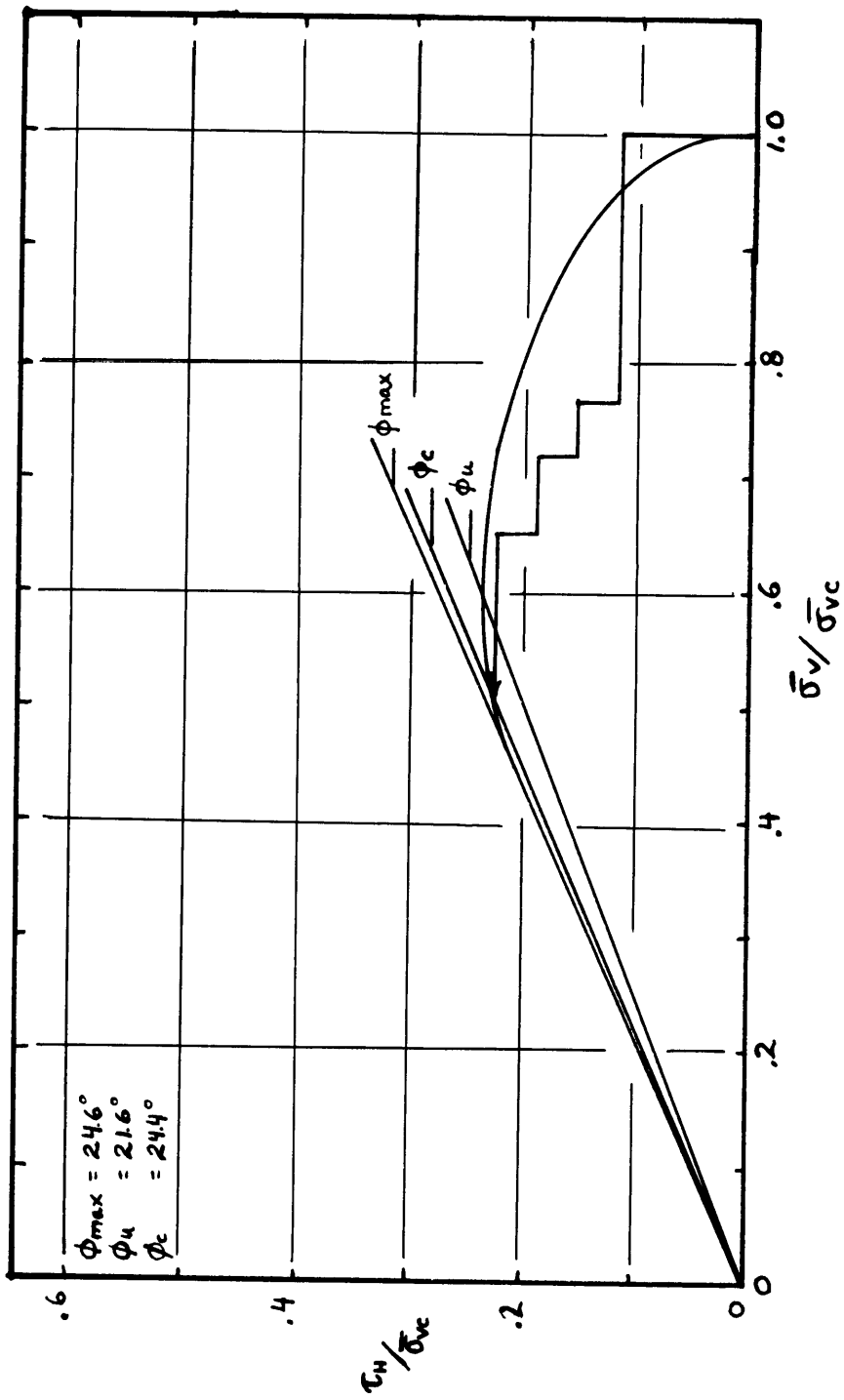

C53: CREEP TEST STRESS PATH, $\overline{CK_o}\overline{UDSS}$-16

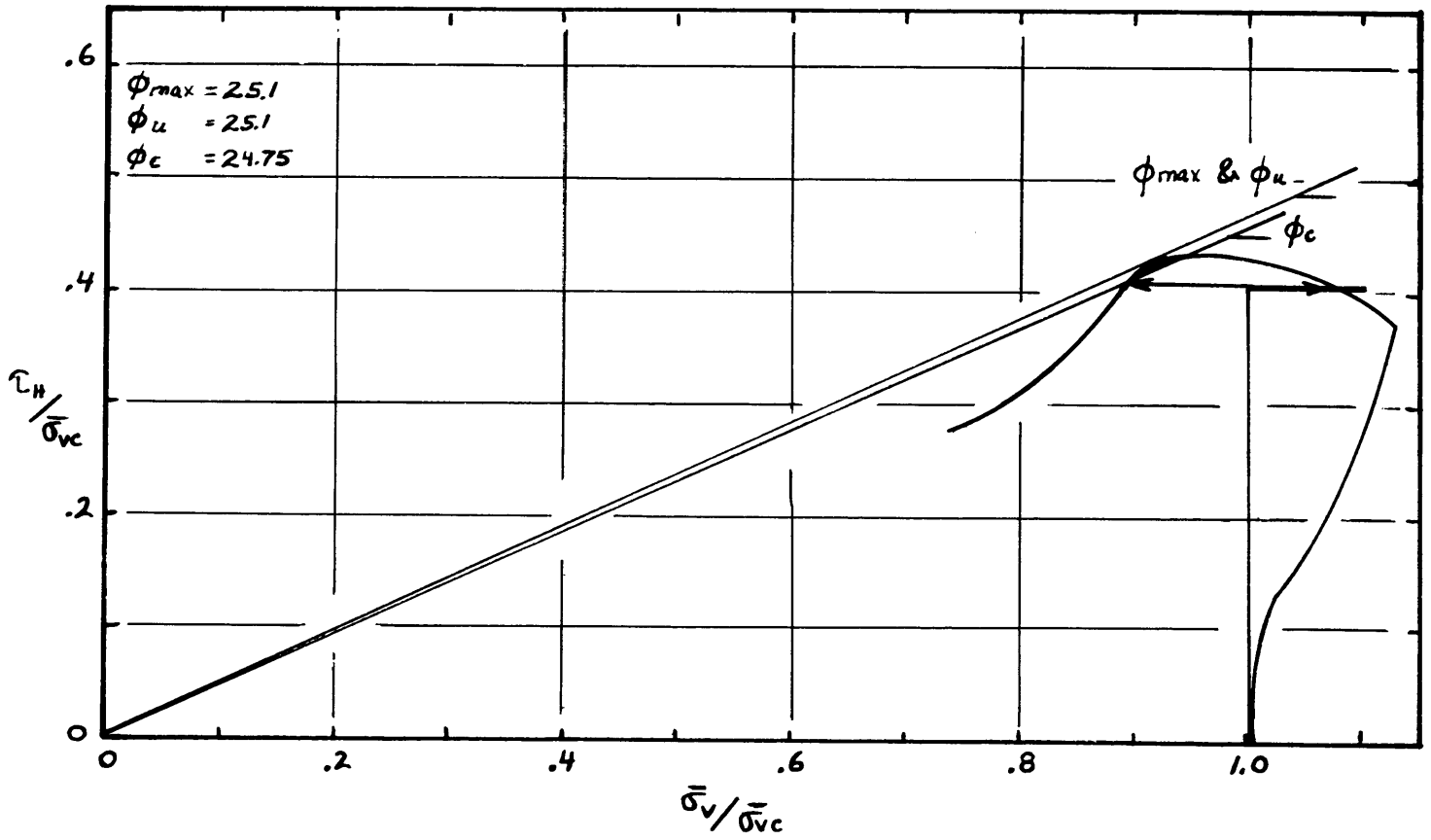

C54: CREEP TEST STRESS PATH, $\overline{CK_oU}$DSS-17

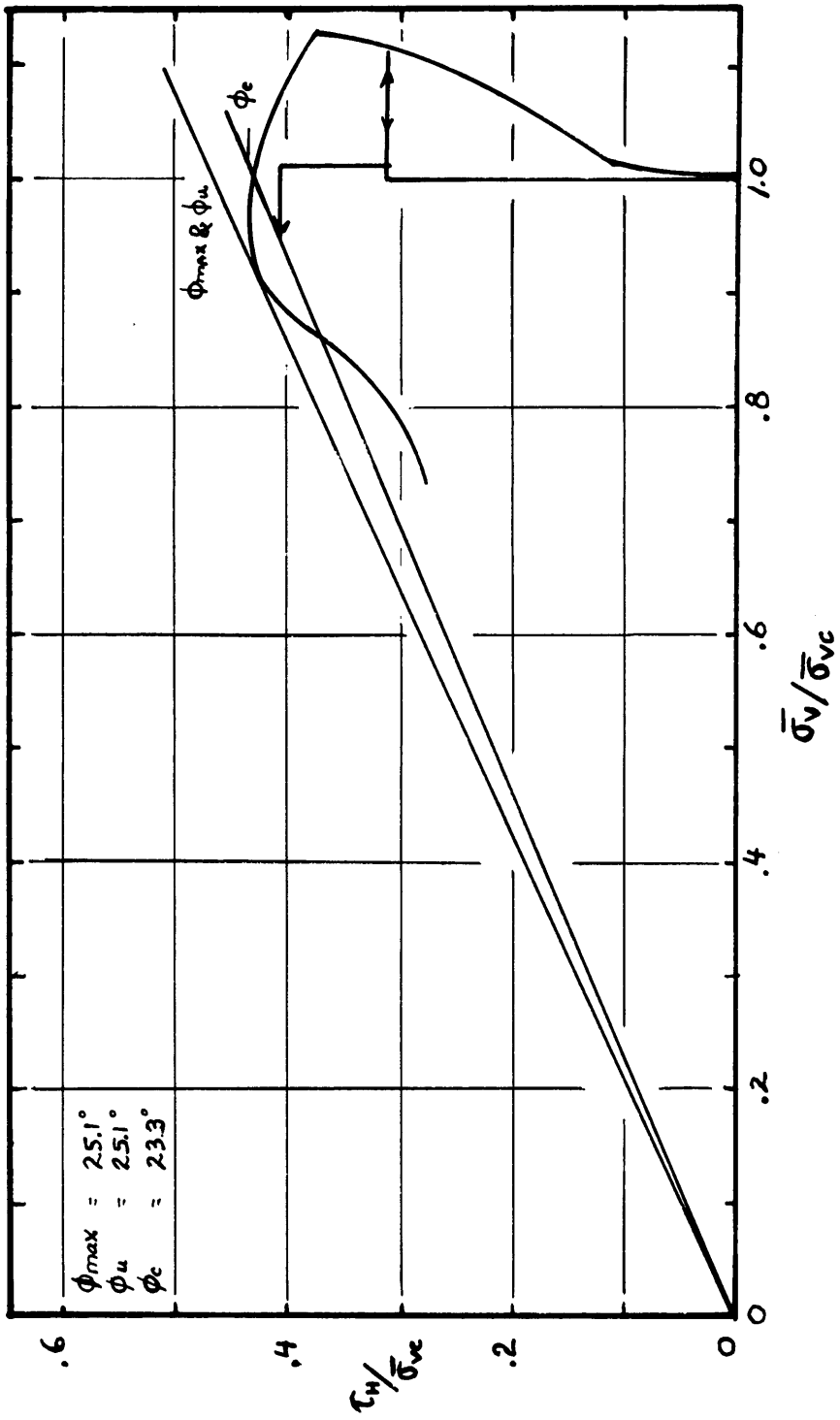

C55: CREEP TEST STRESS PATH, $\overline{CK}_o\overline{U}$DSS-18

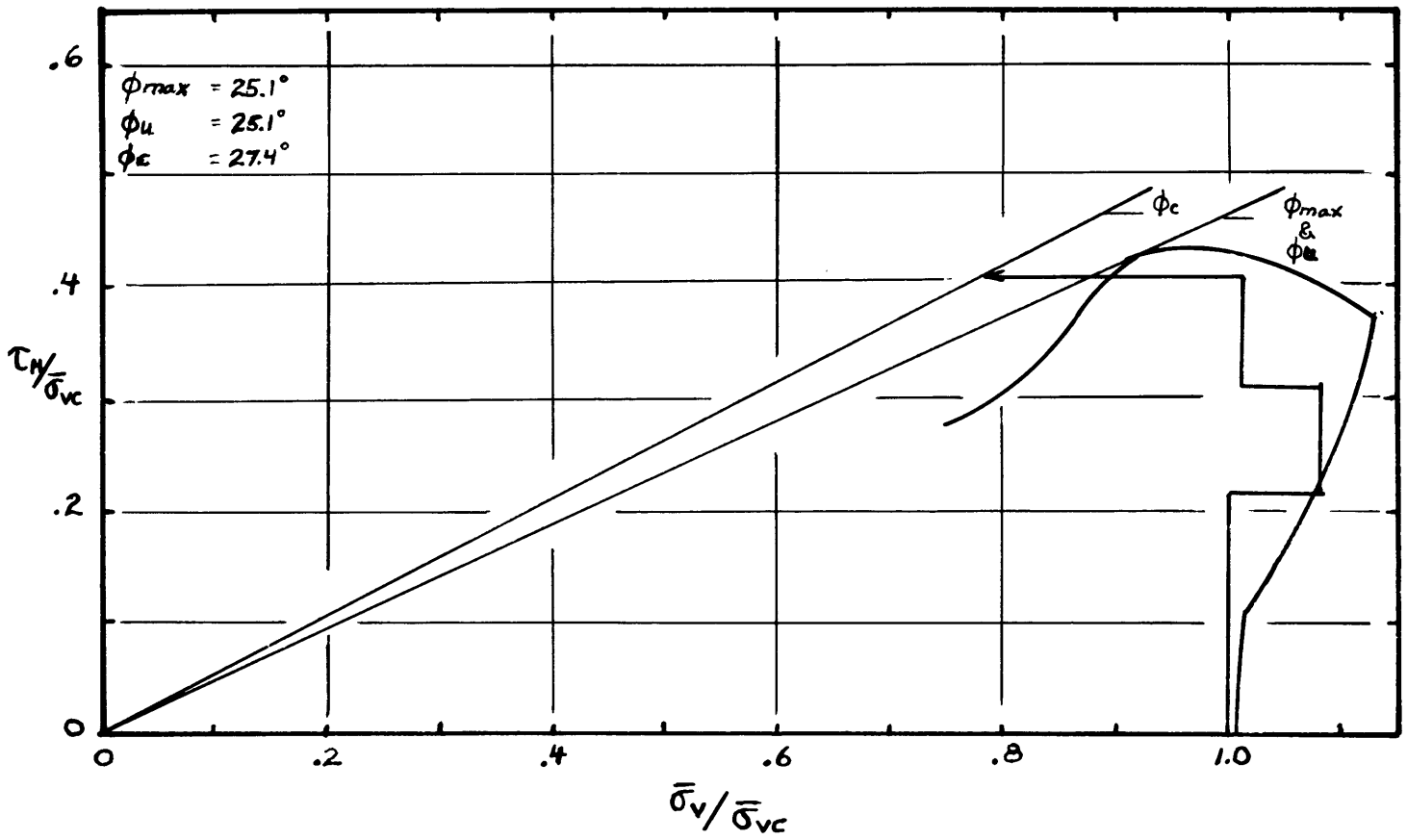

C56: CREEP TEST STRESS PATH, $\overline{CK_oUDSS}$-19

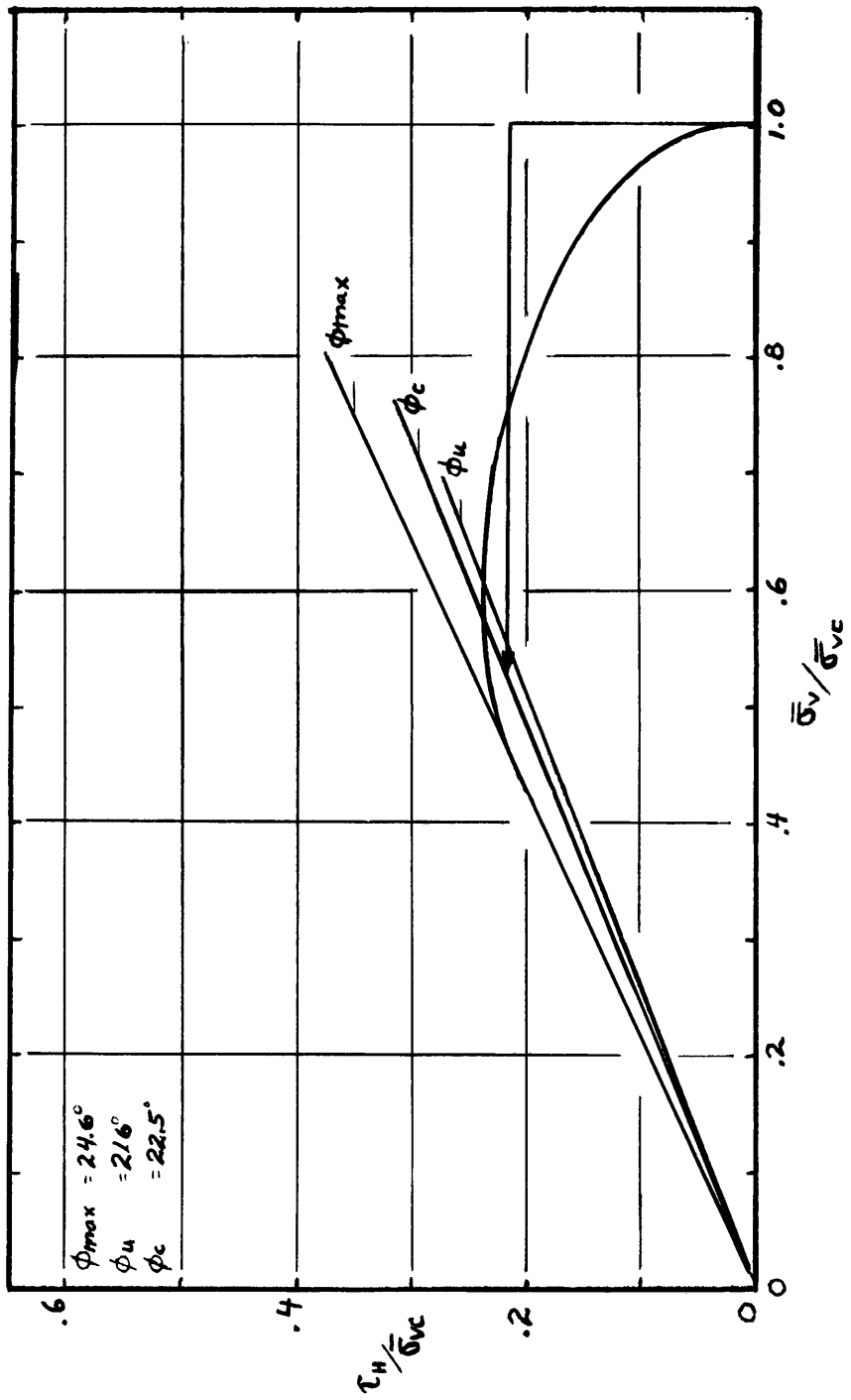

C57: CREEP TEST STRESS PATH, $\overline{CK_o}$UDSS-20

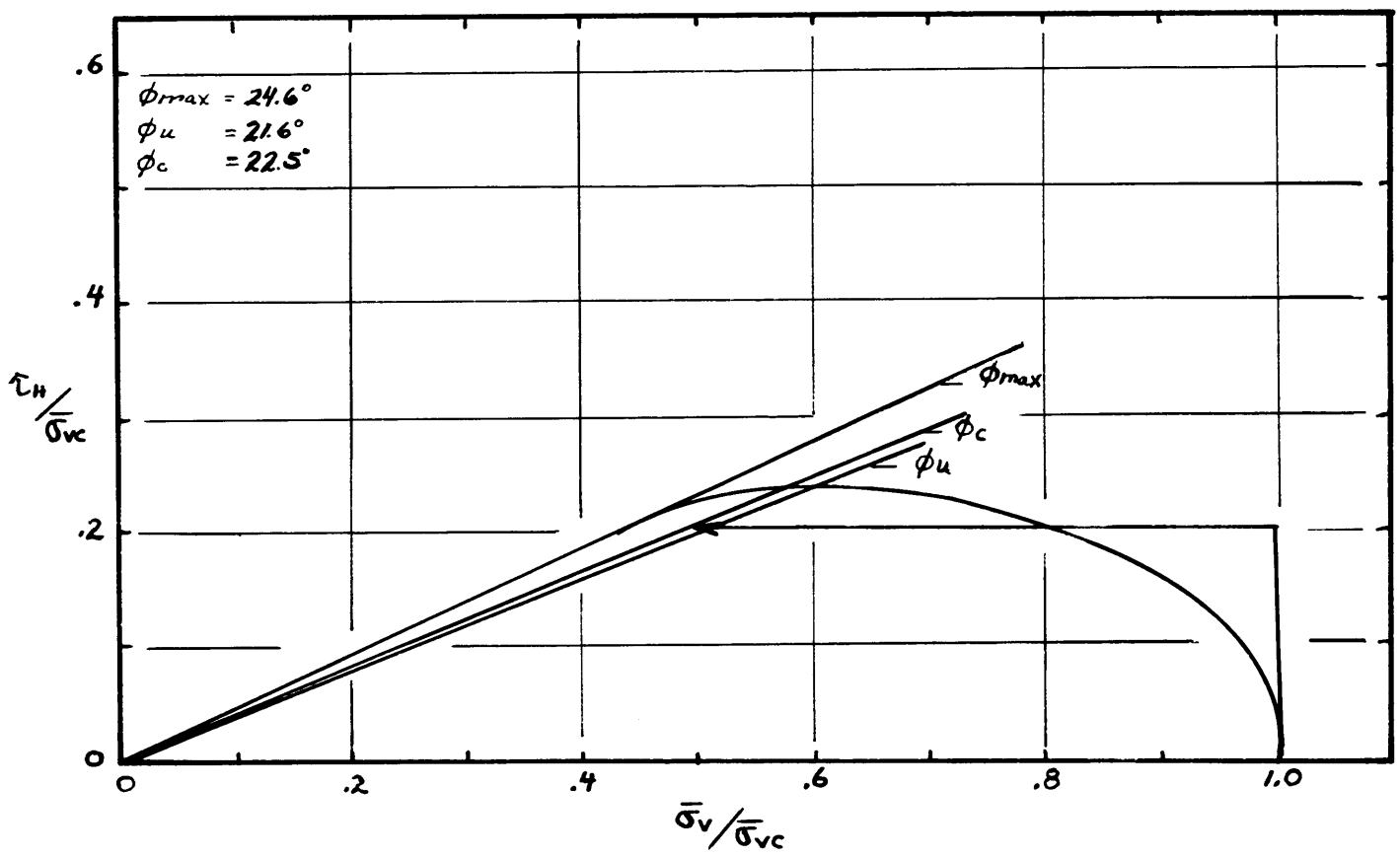

C58: CREEP TEST STRESS PATH, $\overline{CK_oU}$DSS-21

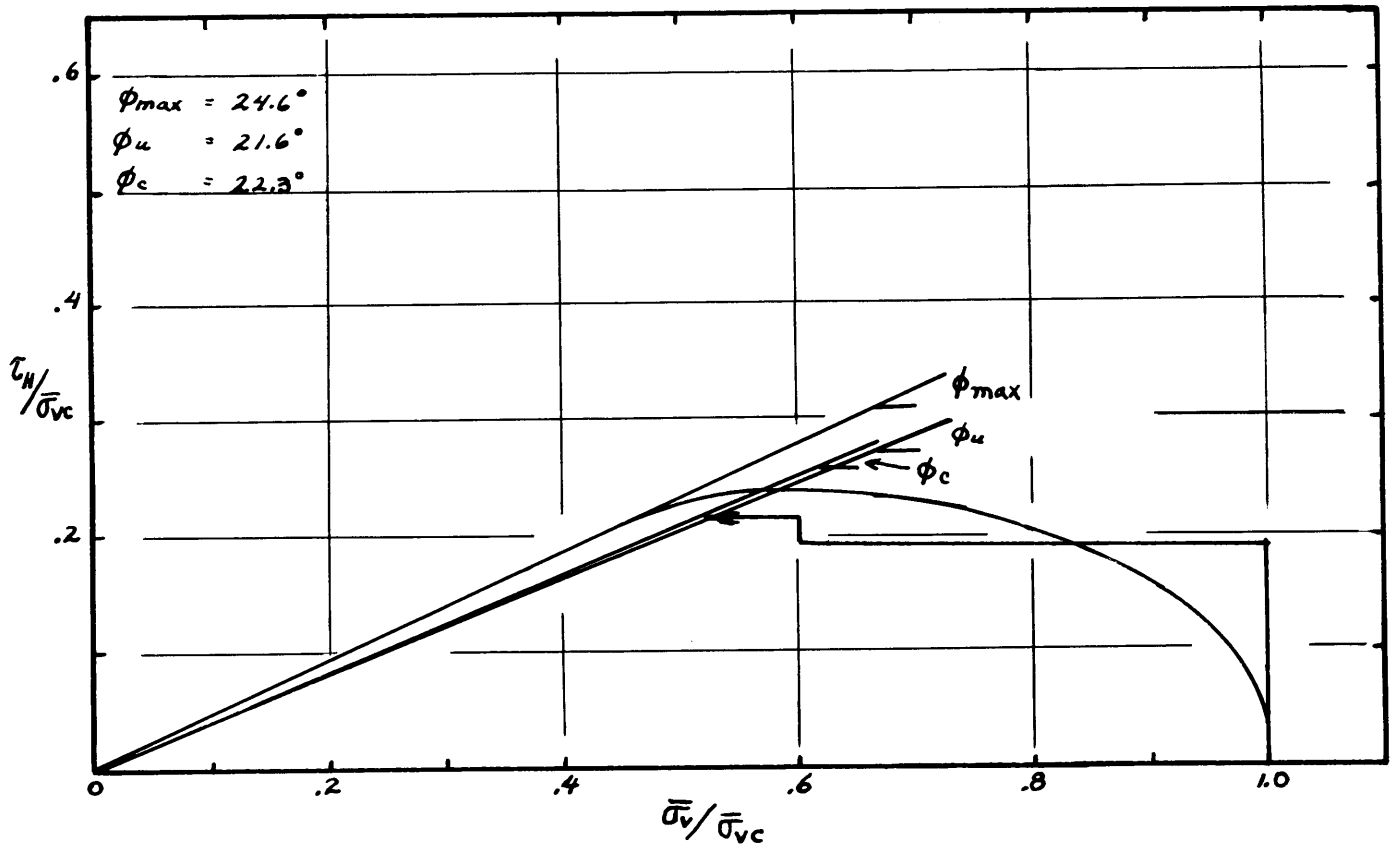

C59: CREEP TEST STRESS PATH, $\overline{CK_oU}$DSS-22

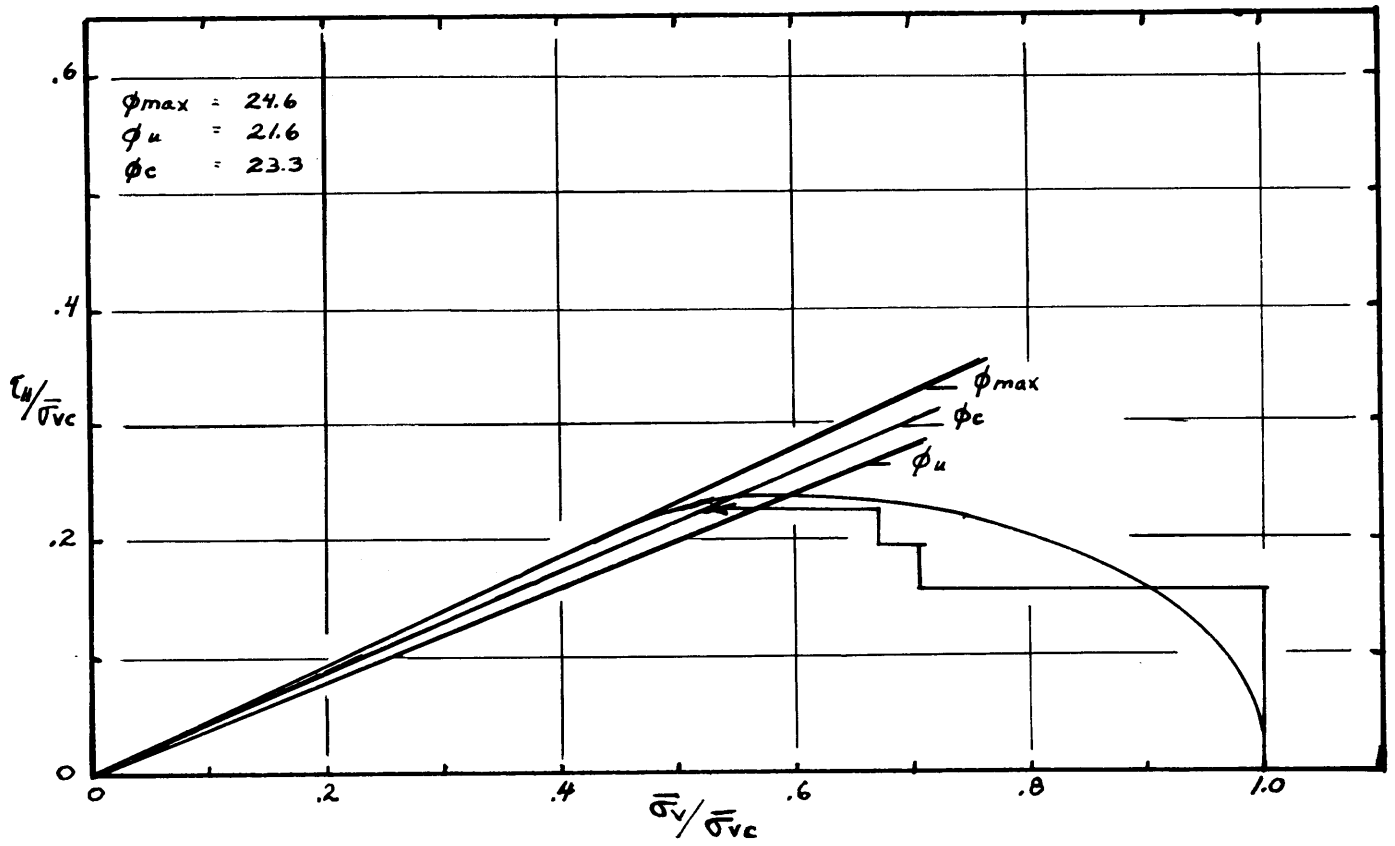

C60: CREEP TEST STRESS PATH, $\overline{CK_oU}$DSS-23